

## University of Southampton Research Repository ePrints Soton

Copyright © and Moral Rights for this thesis are retained by the author and/or other copyright owners. A copy can be downloaded for personal non-commercial research or study, without prior permission or charge. This thesis cannot be reproduced or quoted extensively from without first obtaining permission in writing from the copyright holder/s. The content must not be changed in any way or sold commercially in any format or medium without the formal permission of the copyright holders.

When referring to this work, full bibliographic details including the author, title, awarding institution and date of the thesis must be given e.g.

AUTHOR (year of submission) "Full thesis title", University of Southampton, name of the University School or Department, PhD Thesis, pagination

**UNIVERSITY OF SOUTHAMPTON**

FACULTY OF MEDICINE, HEALTH AND LIFE SCIENCES

School of Medicine

**Induction of protective antigen-specific anti-tumour immunity using vaccines  
incorporating immunoenhancing properties of the coat protein from  
the potato virus X (PVX)**

by

**Jantipa Jobsri**

Thesis for the degree of Doctor of Philosophy

July 2010

UNIVERSITY OF SOUTHAMPTON

ABSTRACT

FACULTY OF MEDICINE, HEALTH AND LIFE SCIENCES

SCHOOL OF MEDICINE

Doctor of Philosophy

INDUCTION OF PROTECTIVE ANTIGEN-SPECIFIC ANTI-TUMOUR IMMUNITY  
USING VACCINES INCORPORATING IMMUNOENHANCING PROPERTIES OF  
THE COAT PROTEIN FROM THE POTATO VIRUS X (PVX)

by Jantipa Jobsri

DNA fusion vaccines encoding the idiotypic (Id) single chain variable fragments of B-cell malignancies fused to the potato virus X coat protein (PVXCP) were shown to enhance anti-Id antibody and T-cell responses which resulted in protection in lymphoma and myeloma models. I further explored the use of PVXCP to enhance induction of anti-tumour immunity. The aims of this study were to generate two types of Id tumour vaccines against the BCL<sub>1</sub> lymphoma, a multimeric Id-PVXCP fusion protein and a PVX particle displaying Id antigen, and to compare their performance with the DNA fusion vaccine.

The multimeric fusion protein vaccine was produced in plants using the HyperTrans expression system. Three constructs which directed expression to the cytoplasm, for retention in the endoplasmic reticulum (ER) and for secretion were tested. The construct that directed the fusion protein to retain in the ER provided high protein expression and was used for further studies. The fusion protein was purified by antibody affinity chromatography and size exclusion. ELISA confirmed the integrity of the expressed protein and protein multimerisation was shown by transmission electron microscopy (TEM). This vaccine induced both anti-Id and anti-PVXCP antibody responses in mice to the levels comparable to the DNA vaccine and it provided protection against the lymphoma challenge.

The plant viral particle (PVP) Id vaccine was produced by linking BCL<sub>1</sub>IgG to PVX via biotin-streptavidin. The PVP vaccine induced both anti-Id and anti-PVXCP antibodies to significantly higher levels than the DNA vaccine. PVP provided protection to the levels comparable to the DNA vaccine. The PVP vaccine also induced cellular responses as high numbers of PVXCP-specific IFN- $\gamma$  and IL-2 secreting cells were detected. *In vivo* PVX bound to CD11c<sup>+</sup> dendritic cells (DCs) and induced activation of all CD11c<sup>+</sup> DC subsets as determined by up-regulation of activation markers. PVX-activated DCs also changed their cytokine, chemokine and chemokine receptor expression profiles toward activated DC phenotypes. These data suggest that PVX enhanced immunity to the linked tumour antigen with the involvement of T cells and DCs.

The feasibility of genetically linking BCL<sub>1</sub> scFv to PVX was also determined. BCL<sub>1</sub> scFv sequence was fused to the N-terminus of PVXCP sequence and inserted into a PVX-based vector to enable expression of the chimeric viral particle (CVP) in plants. CVP was assembled in plants as judged by the ability to infect host plants both locally and systemically. The CVP RNA and proteins (both fusion protein and PVXCP) were detected in all infected leaves. BCL<sub>1</sub> scFv on the CVP surface was detected by TEM with gold-labelled anti-BCL<sub>1</sub> antibody. However, low amount of CVP was obtained and therefore this vaccine production strategy requires further optimisation.

## List of contents

Chapter 1. General Introduction .....	16
1.1 Immune response .....	16
1.1.1 Innate immunity .....	16
1.1.2 Linking innate and adaptive immunity .....	19
1.1.3 Adaptive immunity .....	23
1.1.3.1 Antigen and antigen binding molecules.....	23
1.1.3.1.1 Antibody .....	23
1.1.3.1.2 T-cell receptor.....	24
1.1.3.1.3 MHC molecules and antigen presentation .....	24
1.1.3.2 B lymphocytes .....	25
1.1.3.2.1 B cell maturation.....	25
1.1.3.2.2 B cell activation and antibody production .....	27
1.1.3.2.3 Effector function of antibody.....	29
1.1.3.3 T lymphocytes.....	33
1.1.3.3.1 T cell subsets.....	33
1.1.3.3.1.1 CD4 <sup>+</sup> T cells.....	33
1.1.3.3.1.2 CD8 <sup>+</sup> T cells.....	34
1.1.3.3.1.3 Other T cells.....	34
1.1.3.3.2 T-cell maturation.....	34
1.1.3.3.3 T cell activation.....	35
1.2 Hematologic malignancies: Incidence and therapy .....	36
1.3 Tumour vaccines .....	41
1.3.1 Tumour antigens .....	41
1.3.2 Immunogenicity of tumours and tumour antigens.....	44
1.3.3 Vaccination Strategies .....	45
1.3.3.1 Protein and glycoprotein vaccines .....	45
1.3.3.2. Peptide vaccines.....	45
1.3.3.3 Vaccine adjuvants .....	46
1.3.3.4. DNA vaccines .....	47
1.3.3 Idiotypic vaccines .....	48
1.4 Plant virus-based vaccines .....	51
1.4.1 TMV CVPs .....	51
1.4.2 Cowpea mosaic virus (CPMV) CVPs.....	52
1.4.3 Potato virus X (PVX) CVPs .....	53
1.5 Plant viral vectors for vaccine production in plants.....	56
Chapter 2. Materials and Methods .....	61
2.1 ScFv.BCL <sub>1</sub> -PVXCP fusion protein vaccine expression in plants.....	61
2.1.1 Assembly of Special K.scFv.BCL <sub>1</sub> -PVXCP expression plasmids .....	61
2.1.1.1 Polymerase chain reaction (PCR) .....	63
2.1.1.2 Restriction enzyme digestion.....	64
2.1.1.3 Agarose gel electrophoresis .....	64
2.1.1.4 Gel extraction.....	65
2.1.1.5 Ligations .....	65
2.1.1.6 Transformations .....	65
2.1.1.7 Colony PCR screening.....	66
2.1.1.8 Small scale bacterial culture .....	66
2.1.1.9 Small scale plasmid purification (Miniprep) .....	66
2.1.1.10 DNA sequencing.....	66
2.1.2 Transformation to Agrobacterium tumefaciens.....	67
2.1.3 Agrobacterium infiltration (Agroinfiltration) .....	67
2.1.4 Plant growth conditions .....	68
2.1.5 Detection of scFv.BCL <sub>1</sub> -PVXCP expression.....	68

2.1.5.1 Protein gel electrophoresis .....	68
2.1.5.2 Gel staining to visualise protein bands .....	68
2.1.5.3 Western blot analysis .....	68
2.2 ScFv.BCL <sub>1</sub> -PVXCP purification .....	69
2.2.1 Preparing the anti-BCL <sub>1</sub> antibody affinity column .....	69
2.2.2 Preparing the anti-PVX antibody affinity column .....	70
2.2.3 ScFv.BCL <sub>1</sub> PVXCP purification.....	70
2.2.4 Size exclusion .....	70
2.2.5 Enzyme-linked immunosorbent assay (ELISA) for characterisation of scFv.BCL <sub>1</sub> -PVXCP fusion protein .....	71
2.2.6 Migration of scFv.BCL <sub>1</sub> -PVXCP on native protein gel .....	71
2.3 Protein quantitation .....	72
2.4 BCL <sub>1</sub> -PVP vaccine preparation .....	72
2.4.1 Wildtype PVX purification .....	72
2.4.2 BCL <sub>1</sub> IgG expression and purification.....	73
2.4.3 Biotin labelling of PVX and BCL <sub>1</sub> IgG .....	73
2.4.4 Determination of the level of biotin incorporation .....	73
2.4.5 Linking BCL <sub>1</sub> IgG to PVX .....	73
2.5 Endotoxin test .....	74
2.6 Mouse Experimental Protocol.....	74
2.6.1 Mice .....	74
2.6.2 Vaccination .....	74
2.6.3 Serial blood sampling .....	75
2.6.4 BCL <sub>1</sub> tumour challenge.....	75
2.7 Detection of mouse antibody responses by ELISA .....	75
2.8 Enzyme-linked Immunospot (ELISPOT) .....	76
2.9 In vitro DC activation .....	76
2.9.1 Generation of bone marrow derived dendritic cells (BmDCs) .....	76
2.9.2 BmDC activation and FACS analysis.....	77
2.9.3 Gene expression of bmDCs after PVX activation .....	77
2.9.3.1 DC purification after PVX activation .....	77
2.9.3.2 RNA extraction .....	78
2.9.3.3 DNase I treatment of extracted RNA.....	78
2.9.3.4 cDNA synthesis .....	78
2.9.3.5 Real-time PCR .....	79
2.10 FACS analysis of PVX binding to DCs or B cells in vivo .....	79
2.10.1 Labeling PVX with Alexa <sup>®</sup> Fluor 647 .....	79
2.10.2 In vivo PVX binding.....	79
2.10.3 Splenocytes isolation .....	79
2.10.4 Cell staining and FACS analysis.....	80
2.11 In vivo APCs activation by PVX.....	80
2.11.1 FACS analysis of in vivo activation of DCs and B cells .....	80
2.11.2 Gene expression of in vivo activation of DCs .....	81
2.12 BCL <sub>1</sub> 2APVX expression in plants.....	81
2.12.1 Assembly of pcDNA3.scFv.BCL <sub>1</sub> -2A-PVXCP.....	81
2.12.2 In vitro transcription/translation (IVTT) of pcDNA3.scFv.BCL <sub>1</sub> -2A-PVXCP .....	82
2.12.3 Mammalian cells transfection with pcDNA3.scFv.BCL <sub>1</sub> -2A-PVXCP .....	82
2.12.4 Assembly of pgR107.scFv.BCL <sub>1</sub> -2A-PVXCP .....	82
2.12.5 Expression of BCL <sub>1</sub> 2APVX in plants.....	82
2.12.6 BCL <sub>1</sub> 2APVX RNA detection .....	84
2.12.6.1 RNA extraction .....	84
2.12.6.2 Reverse transcription-polymerase chain reaction (RT-PCR) .....	84
2.13 BCL <sub>1</sub> 2APVX purification.....	84
2.13.1 PEG precipitation and ultracentrifugation .....	84

2.13.2 BCL <sub>1</sub> 2APVX purification using affinity chromatography .....	85
2.14 Transmission electron microscope (TEM).....	85
2.14.1 Negative stain.....	85
2.14.2 Immunosorbent electron microscopy (ISEM) .....	85
2.14.3 Immuno-negative labeling .....	85
Chapter 3. ScFv.BCL <sub>1</sub> -PVXCP fusion protein vaccine.....	87
3.1 Introduction.....	87
3.1.1 BCL <sub>1</sub> model .....	87
3.1.2 Id protein and DNA vaccines.....	87
3.1.3 Expression of recombinant protein in plants .....	89
3.1.3.1 HyperTrans (HT) expression system .....	89
3.1.3.2 <i>Agrobacterium</i> -mediated DNA transfer .....	89
3.1.4 Aims.....	91
3.1.5 Hypotheses.....	91
3.2 Results.....	97
3.2.1 Construction of scFv.BCL <sub>1</sub> -PVXCP expression plasmid .....	97
3.2.2 Expression and purification of scFv.BCL <sub>1</sub> -PVXCP in <i>N. benthamiana</i> .....	102
3.2.3 Characterization of purified scFv.BCL <sub>1</sub> -PVXCP .....	108
3.2.4 Evaluation of scFv.BCL <sub>1</sub> -PVXCP immunogenicity.....	109
3.3 Summary .....	121
3.4 Discussion.....	122
3.4.1 Expression and purification of scFv.BCL <sub>1</sub> -PVXCP .....	122
3.4.2 Characterization of scFv.BCL <sub>1</sub> -PVXCP fusion protein.....	123
3.4.3 Immunogenicity of scFv.BCL <sub>1</sub> -PVXCP vaccine.....	124
Chapter 4. PVX-based PVP vaccine.....	127
4.1 Introduction.....	127
4.1.1 Plant virus-based vaccines .....	127
4.1.2 APC activation by microbes .....	128
4.1.3 Aims.....	130
4.1.4 Hypotheses.....	130
4.2 Results.....	131
4.2.1 PVX-based vaccine induced antibody response to the attached Id antigen.....	131
4.2.2 Role of PVX RNA in induction of anti-BCL <sub>1</sub> antibody response .....	144
4.2.3 BCL <sub>1</sub> -PVP vaccine induced helper T cell responses .....	146
4.2.3 Activation of APCs by PVX.....	150
4.3 Summary .....	161
4.4 Discussion.....	162
Chapter 5. Expression of PVX CVP vaccine in plants.....	166
5.1 Introduction.....	166
5.1.1 Expression of CVP vaccine with genetically fused antigen on the surface.....	166
5.1.2 pgR107 vector.....	166
5.1.3 PVX infection by pgR107.....	168
5.1.4 Aims.....	168
5.1.5 Hypotheses.....	168
5.2. Results.....	169
5.2.1 Construction of BCL <sub>1</sub> 2APVX.....	169
5.2.2 <i>In vitro</i> transcription/translation (IVTT).....	169
5.2.3 scFv.BCL <sub>1</sub> -2A-PVXCP expression in Cos-7 cells .....	170
5.2.4 Propagation of BCL <sub>1</sub> 2APVX in plants .....	175
5.2.4.1 BCL <sub>1</sub> 2APVX infection .....	175
5.2.4.2 BCL <sub>1</sub> 2APVX purification.....	181
5.3 Summary .....	189
5.4 Discussion.....	190
Chapter 6. General conclusion.....	192

6.1 Main findings .....	192
6.1.1 Fusion protein vaccine .....	192
6.1.2 BCL <sub>1</sub> PVP vaccine .....	194
6.1.3 BCL <sub>1</sub> CVP vaccine .....	195
6.2 Optimisation.....	196
6.3 Future use.....	197
Appendix.....	200
References.....	206

## List of figures

Figure 1-1. Hematopoiesis .....	20
Figure 1-2. Cellular locations of pattern recognition receptors .....	21
Figure 1-3. Human Ig heavy chain and light chain gene rearrangements .....	30
Figure 1-4. B-cell activation and selection in germinal centre .....	31
Figure 1-4. Schematic diagram of target tumour antigens.....	43
Figure 1-5. Id vaccine mechanism .....	50
Figure 1-6. Schematic diagram of rod-shaped plant virus.....	54
Figure 1-7. Schematic diagram of TMV CVP production.....	55
Figure 1-8. Expression of foreign protein using a plant virus-based vector.....	59
Figure 2-1. Schematic diagram showing double step cloning of scFv.BCL <sub>1</sub> -PVXCP into Special K plasmid .....	62
Figure 2-2. Schematic diagram of pcDNA3.scFv.BCL <sub>1</sub> -PVXCP and pcDNA3.scFv.BCL <sub>1</sub> -2A-PVXCP vector .....	83
Figure 2-3. Diagram shows pgR107.scFv.BCL <sub>1</sub> -2A-PVXCP.....	83
Figure 3-1. Mechanism of Id fusion vaccine .....	92
Figure 3-2. Schematic diagram of a CPMV RNA-2-based HT expression vector.....	93
Figure 3-3. Schematic diagram of Ti-plasmid .....	94
Figure 3-4. Transferring T-DNA into the plant genome.....	95
Figure 3-5. Schematic diagram of Special K (SK) vector of HT expression system .....	96
Figure 3-6. Schematic diagram of scFv.BCL <sub>1</sub> -PVXCP constructs in SK vector .....	98
Figure 3-7. PCR screening for pM81 containing the scFv.BCL <sub>1</sub> -PVXCP sequence .....	99
Figure 3-8. PCR screening of Special K containing the scFv.BCL <sub>1</sub> -PVXCP sequence.....	100
Figure 3-9. PCR screening for Agrobacterium containing SK-based constructs .....	101
Figure 3-10. Coomassie-stained SDS-PAGE and Western blot analysis of expressed scFv.BCL <sub>1</sub> -PVXCP.....	104
Figure 3-11. Coomassie-stained SDS-PAGE and Western blot analysis of purified scFv.BCL <sub>1</sub> -PVXCP.....	105
Figure 3-12. Size exclusion chromatogram of purified scFv.BCL <sub>1</sub> -PVXCP .....	106
Figure 3-13. SDS-PAGE analysis of fractions after size exclusion chromatography .....	107
Figure 3-15. Native gel Western blot analysis of purified scFv.BCL <sub>1</sub> -PVXCP .....	112
Figure 3-16. ISEM of purified scFv.BCL <sub>1</sub> -PVXCP .....	113
Figure 3-17. DLS data of purified scFv.BCL <sub>1</sub> -PVXCP.....	114
Figure 3-18. Anti-BCL <sub>1</sub> antibody responses after priming.....	115

Figure 3-19. Anti-BCL <sub>1</sub> antibody response after priming/boosting .....	116
Figure 3-20. Anti-PVXCP antibody responses after priming.....	117
Figure 3-21. Anti-PVXCP antibody responses after priming/boosting.....	118
Figure 3-22. IgG subclasses of anti-BCL <sub>1</sub> antibody .....	119
Figure 3-23. Protection of immunized mice after tumour challenge.....	120
Figure 3-24. Proposed mechanism of BCL <sub>1</sub> .scFv-PVXCP fusion protein vaccine.....	126
Figure 4-1. BCL <sub>1</sub> -PVP vaccine design .....	134
Figure 4-2. Antibody responses after PVP vaccination.....	135
Figure 4-3. Protection of BCL <sub>1</sub> -PVP-immunised mice .....	136
Figure 4-4. Comparison of anti-BCL <sub>1</sub> antibody responses induced by BCL <sub>1</sub> -PVP vaccine and by Id Ig without linked PVX.....	137
Figure 4-5. Comparison of antibody responses induced by BCL <sub>1</sub> -PVP and DNA vaccines .....	138
Figure 4-6. Protection of BCL <sub>1</sub> -PVP and DNA vaccine-immunised mice after tumour challenge .....	139
Figure 4-7. Anti-BCL <sub>1</sub> antibody responses after vaccination with different doses of BCL <sub>1</sub> - PVP .....	140
Figure 4-8. Anti-PVXCP antibody responses after vaccination with different doses of BCL <sub>1</sub> - PVP .....	141
Figure 4-9. IgG subclasses of anti-BCL <sub>1</sub> antibody induced by BCL <sub>1</sub> -PVP vaccine .....	142
Figure 4-10. Protection of mice immunised with different doses of BCL <sub>1</sub> -PVP vaccine ..	143
Figure 4-11. Anti-BCL <sub>1</sub> antibody responses after vaccination with BCL <sub>1</sub> -CP mixed with RNA .....	145
Figure 4-12. IFN- $\gamma$ ELISPOT .....	147
Figure 4-13. IL-2 ELISPOT.....	148
Figure 4-14. IL-4 ELISPOT.....	149
Figure 4-15. FACS analysis of DC activation in vitro.....	153
Figure 4-16. Expression of cytokines, chemokines and chemokine receptors after in vitro PVX activation.....	154
Figure 4-17. FACS analysis of PVX binding to B cells and DCs in vivo.....	155
Figure 4-18. FACS analysis of the effect of low amounts of LPS in DC activation in vivo .....	156
Figure 4-19. FACS analysis of PVX induced DC activation in vivo .....	158
Figure 4-20. FACS analysis of PVX induced B-cell activation in vivo .....	159
Figure 4-21. Expression of cytokines, chemokines and chemokine receptors after in vivo PVX activation.....	160

Figure 4-22. Proposed mechanism of BCL <sub>1</sub> -PVP vaccine .....	165
Figure 5-1. Schematic diagram of pgR107 vector .....	167
Figure 5-2. Construction of BCL <sub>1</sub> 2APVX.....	171
Figure 5-3. PCR screening for scFv.BCL <sub>1</sub> -2A-PVXCP positive clones .....	172
Figure 5-4. In vitro transcription/translation (IVTT) of pcDNA3.scFv.BCL <sub>1</sub> -2A-PVXCP .....	173
Figure 5-5. Western blot analysis of transfected Cos-7 cells.....	174
Figure 5-6. Symptoms of plants inoculated with either pgR107 or pgR107.scFv.BCL <sub>1</sub> -2A-PVXCP.....	176
Figure 5-7. Symptoms of plants inoculated with either pgR107 or pgR107.scFv.BCL <sub>1</sub> -2A-PVXCP on day 8 post inoculation .....	177
Figure 5-8. Symptoms of plants inoculated with either pgR107 or pgR107.scFv.BCL <sub>1</sub> -2A-PVXCP on day 20 post inoculation .....	178
Figure 5-9. RT-PCR detection of BCL <sub>1</sub> -2A-PVXCP in infected leaves .....	179
Figure 5-10. Western blot analysis of PVXCP .....	180
Figure 5-11. Diagram of PVX purification method.....	183
Figure 5-12. Detection of BCL <sub>1</sub> 2APVX in various samples obtained from established purification method.....	184
Figure 5-13. Diagram of modified BCL <sub>1</sub> 2APVX purification method .....	185
Figure 5-14. Detection of BCL <sub>1</sub> 2APVX in various samples obtained from modified purification method.....	186
Figure 5-15. TEM images of purified products .....	187
Figure 5-16. Virus particles purified from pgR107.scFv.BCL <sub>1</sub> -2A-PVXCP infected plants incorporated free CPs.....	187
Figure 5-17. BCL <sub>1</sub> 2APVX purified by anti-BCL <sub>1</sub> antibody affinity chromatography.....	188

## List of tables

Table 1-1. Toll-like receptors and their ligands.....	22
Table 1-2. FcγR expression on immune cells .....	32
Table 1-3. The 20 most commonly diagnosed cancer in the UK, 2006.....	39
Table 1-4. The 20 most common causes of death from cancer in the UK, 2007.....	40
Table 1-5. Production of protein vaccine by using plant virus-based vector.....	60
Table 2-1. Cloning primers .....	63
Table 2-2. Restriction enzymes.....	64
Table 2-3. Sequencing primers .....	67
Table 4-1. DC subsets in mouse lymphoid tissues .....	130

## **DECLARATION OF AUTHORSHIP**

I, Jantipa Jobsri, declare that the thesis entitled Induction of protective antigen-specific anti-tumour immunity using vaccines incorporating immunoenhancing properties of the coat protein from the Potato Virus X (PVX) and the work presented in the thesis are both my own and have been generated by me as the result of my own original research. I confirm that:

- this work was done wholly or mainly while in candidature for a research degree at this University;
- where any part of this thesis has previously been submitted for a degree or any other qualification at this University or any other institution, this has been clearly stated;
- where I have quoted from the work of others, the source is always given. With the exception of such quotations, this thesis is entirely my own work;
- I have acknowledged all main sources of help;
- where the thesis is based on work done by myself jointly with others, I have made clearly exactly what was done by others and what I have contributed myself;
- none of this work has been published before submission

**Signed:**.....

**Date:**.....

## ACKNOWLEDGMENTS

First of all, I would like to thank the Faculty of Dentistry, Naresuan University, Thailand and the Royal Thai Government for giving me an opportunity to study for a PhD and for providing the financial support necessary for my study in the UK.

I would like to thank my supervisors Prof Freda Stevenson and Dr Natalia Savelyeva for their supervision and advice. I would like to express my gratitude to Natalia for her support, guidance and encouragement throughout the period of my study. This thesis would not have been possible without her dedicated work.

I would like to extend my gratitude to Dr George Lomonosoff and Dr Frank Sainsbury, our collaborators at John Innes Centre (Norwich), for their help and advice in protein and virus expression in plants.

I am thankful to my colleagues in the Genetic Vaccines Group for teaching me laboratory techniques, listening to my complaints and helping me when I had problems. Thank you Amy and Mike for helping me in some experiments. I would like to thank those who proof read my thesis and transfer thesis, Jason, Nicky, Mike, Hayley, Gavin and Elena.

I am indebted to many of the animal house staff, Richard, Lisa, Mel, Sam, Miriam and Vicky. Without them I could not have done all the mouse experiments. I would like to thank Patrick for his help in protein work especially the size exclusion. I also would like to thank all other staff in Cancer Sciences Division who supported me in any respect during the completion of my project.

I would like to thank all my friends in the UK and Thailand for they have helped me to get through all the hard times and enjoy living in the UK. Thanks to Dao, Suan, Oz, Nu and Kao for listening to all my silly complaints, cheering me up and being nice travelling companions without moaning about my demands. Thanks to friends, especially Ploy, who sent me books, DVDs, MP3s and snacks. Those little things you gave me brought me the warmth of friendship and cheered me up during hard work and loneliness.

Lastly, I owe my deepest gratitude to my parents. They have been unconditionally loving and supportive since the day I was born. They let me come to the UK with understanding and blessing.

## Abbreviations

ADCC	Antibody-dependent cell-mediated cytotoxicity
ALL	Acute lymphocytic leukaemia
APC	Antigen presenting cell
<i>A. tumefaciens</i>	<i>Agrobacterium tumefaciens</i>
BCL <sub>1</sub>	Mouse B cell lymphoma
BCR	B-cell receptor
CaMV	Cauliflower Mosaic Virus
CARD	Caspase activation and recruitment domain
CD	Cluster of differentiation
cDC	Classical dendritic cell
CDC	Complement-dependent cytotoxicity
CFA	Complete Freund's adjuvant
CHO	Chinese hamster ovarian
CLL	Chronic lymphocytic leukaemia
CM	Complete medium
CML	Chronic myeloid leukaemia
CP	Coat protein
CPMV	Cowpea Mosaic Virus
CTL	Cytotoxic T lymphocyte
DAI	DNA-dependent activator of interferon regulatory factor
DC	Dendritic cell
DC-SIGN	DC-specific ICAM3-grabbing non-integrin
DEC-205	Dendritic and thymic epithelial cell 205 kDa protein
dH <sub>2</sub> O	Deionised water
EP	Electroporation
ELISA	Enzyme-linked immunosorbent assay
ELISPOT	Enzyme-linked immunospot
ER	Endoplasmic reticulum
FcγR	Fcγ receptor
FDC	Follicular dendritic cell
FMDV	Foot-and-Mouth Disease Virus
FrC	Fragment C of the tetanus toxin
GFP	<i>Aequorea Victoria</i> green fluorescent protein
GM-CSF	Granulocyte macrophage colony-stimulating factor
h	Hour(s)
HSC	Hematopoietic stem cell
HT	HyperTrans expression system
ICAM	Intracellular adhesion molecule
Id	Idiotypic
IFA	Incomplete Freund's adjuvant
IFN	Interferon
Ig	Immunoglobulin
IKDC	interferon-producing killer DC
IL	Interleukin
i.m.	Intra-muscular (injection)
i.p.	Intra-peritoneal (injection)
ITAM	Immunoreceptor tyrosine-based activation motif
i.v.	Intravenous (injection)
IVTT	In vitro transcription/translation
KLH	Keyhole limpet hemocyanin
KO	Knock-out

LC	Langerhans cell
LPS	Lipopolysaccharide
M	Molar
MAC	Membrane attack complex
MAC1	Macrophage receptor 1
MAIT	Mucosal-associated invariant T cell
MBL	Mannose binding lectin
MDA5	Melanoma differentiation-association gene 5
mDC	Myeloid dendritic cell
µg	microgram(s)
MHC	Major histocompatibility complex
MICA	MHC-I chain-related molecule A
MICB	MHC-I chain-related molecule B
min	Minute(s)
ml	millilitre(s)
µl	microlitre(s)
MR	Mannose receptor
MR1	Major histocompatibility class I-related molecule
MZ	Marginal zone
<i>N. benthamiana</i>	<i>Nicotiana benthamiana</i>
NALP3 or NLRP3	NLR family, pyrin-domain-containing 3
NO	Nitric oxide
NOD	nucleotide-oligomerisation domain
NK	Natural killer
NKG2	NK group 2
NHL	Non-Hodgkin's lymphoma
NLR	NOD-like receptor
NLRP3	NLR family, pyrin-domain-containing 3
NMS	Normal mouse serum
OAS	Oligoadenylate synthetase
OD	Optical density
PAMP	Pathogen-associated molecular pattern
PapMV	Papaya Mosaic Virus
PCD	Program cell death
PCR	Polymerase chain reaction
pDC	Plasmacytoid dendritic cell
PEG	Polyethyleneglycol
p.i.	Post-infiltration
PKR	RNA dependent protein kinase
PRR	Pattern recognition receptor
PVP	Plant virus particle
PVX	Potato Virus X
PVXCP	Potato Virus X coat protein
RAG	Recombination-activating gene
RIG-1	Retinoic acid inducible gene-1
RT-PCR	Reverse transcription-polymerase chain reaction
ROS	Reactive oxygen species
SA	Streptavidin
scFv	Single chain variable fragment
SCS	Subcapsular sinus
sec	Second(s)
SK	Special K plasmid
TAP	Transporter associated with antigen presentation
TCR	T-cell receptor

TD	Thymus-dependent
TdT	Terminal deoxynucleotidyl transferase
T-DNA	Transferred DNA element on <i>Agrobacterium</i> Ti plasmid
TEM	Transmission electron microscope
Tfh	Follicular helper T cell
TGBp	Triple gene block protein
TGF	Transforming growth factor
Th	Helper T cell
TI	Thymus-independent
TLR	Toll-like receptor
TNF	Tumour necrosis factor
TMV	Tobacco Mosaic Virus
Treg	Regulatory T cell
UC	Ultracentrifugation

# Chapter 1. General Introduction

## 1.1 Immune response

The immune system is responsible for recognition and elimination of foreign substances, especially microbes, and transformed host cells. There are two systems of immunity: innate and adaptive. Some of cellular and molecular components of the immune system function in both.

### 1.1.1 Innate immunity

The innate immune system consists of physical barriers, effector cells and molecules that provide defence against infection. Innate immunity distinguishes precisely between self and pathogens. The main physical barriers are skin and mucosal membranes. Effector molecules of innate immunity include acid contents in stomach, enzymes and antimicrobial molecules in saliva and tears.

Important molecules of the innate immune system are proteins of the complement system that recognises and destroys microbes. Complement includes a group of serum proteins that circulate in an inactive state. Inactive complement proteins can be activated by three pathways, alternative, classical and lectin pathways. The alternative pathway is initiated by binding of complement proteins to a microbe. The classical pathway is initiated by binding of antibodies to a microbe followed by binding of complement proteins to the bound antibodies. The lectin pathway is initiated by mannose binding lectins (MBLs) bound to mannose residues on a microbe followed by interaction of MBL-associated serine proteases and complement proteins. All three pathways lead to cleavage of C3, the most abundant complement protein, and other complement proteins which thereby leads to activation of the membrane attack complex (MAC) that causes cell lysis. Moreover, complement cleavage products can activate inflammation that promotes phagocytosis and enhances effector cell activation.

In addition, natural antibody plays a role in innate immunity against microbes. Natural antibodies, mostly are immunoglobulin M (IgM), are produced by subsets of B lymphocytes, a cellular component of adaptive immunity, called B-1 cells and marginal zone B cells. Natural antibodies recognise mainly polysaccharides and lipids, e.g. lipopolysaccharide (LPS), commonly found on many types of bacteria and therefore, function as a defence mechanism against microbes.

Innate immune effector cells include monocytes/macrophages, neutrophils, dendritic cells (DCs) and natural killer (NK) cells which are differentiated from myeloid or lymphoid progenitors during hematopoiesis (figure 1-1). Innate immune cells recognise microbial

substances called pathogen-associated molecular patterns (PAMPs), e.g. microbial cell surface carbohydrates, bacterial LPS, viral RNA and bacterial DNA, through the receptors called pattern recognition receptors (PRRs). Cellular localization of PRRs is shown in figure 1-2. Binding to PAMPs, leads to stimulation of PRRs and activation of downstream signaling pathways which results in the effector functions of innate immunity, including production of cytokines that enhance inflammation and control immune cell function. Some cytokines such as interferon (IFN)- $\alpha$  and IFN- $\beta$  have anti-viral functions.

PRRs include toll-like receptors (TLRs), C-type lectins, scavenger receptors, NOD (nucleotide-oligomerisation domain)-like receptors (NLRs), CARD (caspase activation and recruitment domain)-containing proteins and absent in melanoma 2 (AIM2). C-type lectins are a large group of receptors expressed on cell membranes and bind to carbohydrate structures found on microbial cell surfaces. C-type lectins include mannose receptor (MR) [1], dendritic and thymic epithelial cells 205 kDa-protein (DEC-205) [2-3] and DC-specific ICAM3 (intracellular adhesion molecule3)-grabing non-integrin (DC-SIGN) which bind to high mannose and fucose structures on microbes [4-7]. NLRs include NOD1, NOD2 and NLR family, pyrin-domain-containing 3 (NLRP3 or NALP3) which bind to bacterial peptidoglycans. An example of CARD-containing proteins is retinoic acid inducible gene-1 (RIG-1), a receptor of double-stranded ribonucleic acid (dsRNA). AIM2 is a sensor for cytoplasmic DNA and after binding to DNA it activates the inflammasome to produce pro-inflammatory cytokines IL-1 and IL-18 [8-10]. Cellular locations and ligands of some PRRs are shown in figure 1-2.

TLRs are membrane receptors found on cell membranes and endosomal membranes. In humans, there are 11 TLRs identified (TLR1-10, TLR13). Mice express TLR1-9, 11 and 13 [11]. TLR signaling requires dimerisation of two TLRs which may be homodimerisation or heterodimerisation. The identified ligands for TLRs are shown in table 1-1. Each TLR is responsible for binding to different microbial products. For example, TLR4 is located on cell membranes and is specific for LPS. TLR7/8 and TLR9 are located on endosomal membranes and are responsible for recognition of RNA and DNA inside the endosomes.

Among innate immune cells, neutrophils are the first cells that migrate to the site of infection. They phagocytose microbes and internalise them within phagosomes which will later fuse with granules containing antimicrobial peptides (e.g. defensins and cathelicidins) and enzymes (e.g. protease and lysozyme) which are able to destroy microbes. Neutrophils also produce reactive oxygen species (ROS) and nitric oxide (NO) which are able to kill microbes [12-13].

NK cells are responsible for recognition and elimination of infected or malignant cells. NK cell activation is regulated by the balance between signals generated from

activating receptors and inhibitory receptors. Inhibitory receptors on NK cells recognise class I major histocompatibility complex (MHC-I) molecules which are expressed on normal cells but are not expressed or are reduced in viral infected cells or cancer cells. Some of activating receptors recognise molecules expressed only in infected or cancer cells; the example is NK receptor called NK group 2-D (NKG2D) which recognises MHC-I like proteins such as MHC-I chain-related molecule A and B (MICA and MICB) [14-15]. Some activating receptors recognise molecules expressed by both abnormal and healthy cells, e.g. CD94/NKG2C receptor can bind to MHC-I molecules but with lower affinities than inhibitory receptors. Thus, the inhibitory signals from MHC-I binding prevent NK from killing normal cells. The effector functions of NK cells are the killing of infected or cancer cells and activating macrophages to destroy ingested microbes by IFN- $\gamma$  secretion. NK cells kill the target cells by releasing granules containing cytotoxic proteins (e.g. perforin and granzymes) which mediate killing.

Macrophages are differentiated from monocytes circulating in the blood and reside in the tissues. Some macrophages can move throughout the tissues and some are fixed in the tissue, e.g. Kupffer cells in the liver, intestinal macrophages in the gut, and mesangial cells in the kidney. Macrophages phagocytose microbes and their phagocytic activity is increased by cytokines produced by activated helper T (Th) cells. Th cells also stimulate macrophages to destroy ingested microbes. Upon activation, phagosomes containing microbes fuse with lysosomes to form phagolysosomes. Lysosomes contain enzymes such as proteases and lysozyme which are able to destroy microbes. Macrophages also produce ROS and NO inside phagolysosomes to kill microbes. Ingested microbes are also killed by antimicrobial molecules in phagosomes similar to the mechanism found in neutrophils. In addition, macrophages express higher level of MHC-II molecules, which present peptide antigens to Th cells, and secrete cytokines including interleukin-1 (IL-1), tumour necrosis factor- $\alpha$  (TNF- $\alpha$ ), IL-6 and IL-12. IL-1 and TNF- $\alpha$  function in recruitment of leukocytes to the site of infection while IL-12 stimulate NK and T cells to produce IFN- $\gamma$  which in turn activate macrophages to kill ingested microbes. IL-6 is involved in B and T-cell differentiation [16].

DCs have long membranous projections, a characteristic of these cells. They may be divided into four major types, Langerhans cells (LCs) found in epidermal layers of skin, interstitial DCs found in the interstitial spaces, myeloid DCs (mDCs) or also called classical DCs (cDCs) and plasmacytoid DCs (pDCs). LCs are differentiated from embryonic precursors that colonise the epidermis before birth and they are self-renewing cells [17]. Other DCs are derived from haemopoietic stem cells via different pathways and are found in different locations [18]. Myeloid DCs reside in lymphoid organs and peripheral tissues. From peripheral tissues, mDCs migrate to lymphoid organs via afferent lymphatics and via

high endothelial venules. Plasmacytoid DCs are present in bone marrow and peripheral tissues and are specialized to respond to viral infection. They produce type I interferons which have potent antiviral activities.

DCs express various receptors, including Fc $\gamma$  receptors, Fc $\epsilon$  receptor, and many PRRs, which allow DCs to recognise diverse antigen molecules. PRRs expressed by DCs include NLRs, TLRs, C-type lectin receptors (e.g. MR, DC-SIGN and DEC-205). DCs serve a critical function in linking innate and adaptive immunity by capturing microbial antigens and displaying them to T lymphocytes of the adaptive immune response.

### **1.1.2 Linking innate and adaptive immunity**

In tissues, DCs are in an immature form capable of capturing antigen by phagocytosis, receptor-mediated endocytosis and pinocytosis. Upon activation through PRRs, immature DCs undergo maturation, a process whereby they shift from an antigen-capturing phenotype to an antigen-presenting phenotype. DC activation is also mediated by various factors including CD40L from T cells and balance between pro-inflammatory cytokines (e.g. TNF, IL-1, IL-6) and anti-inflammatory cytokines (IL-10 and transforming growth factor- $\beta$  [TGF- $\beta$ ]).

Mature DCs express chemokine receptor CCR7, the molecule required for migration to the T cell zone in the secondary lymphoid organs. Mature DCs lose the capacity for antigen capture but the surface expression of CD40, MHC-II and costimulatory (B7-1 and B7-2) molecules is increased. MHC molecules are required for antigen presentation to T cells. Interaction of B7 molecules to their receptor CD28 on T cells leads to stimulation of T-cell differentiation into effector T cells. CD40 binding to CD40L on T cells enhances expression of the costimulatory molecules. Activated DCs also produce cytokines (e.g. IL-12) for T-cell proliferation and differentiation. DCs can polarise differentiation of CD4<sup>+</sup> T cells into different subsets. Binding of naïve T cells to peptide-MHC-presenting DCs with no costimulator expression may lead to T-cell anergy or tolerance [19].

Among antigen-presenting cells (APCs), DCs are the most effective APCs as they expresses both MHC and costimulatory molecules at high levels upon activation. In addition, DCs are the most potent cells in the ability to present exogenous antigen to both CD4<sup>+</sup> and CD8<sup>+</sup> T cells.

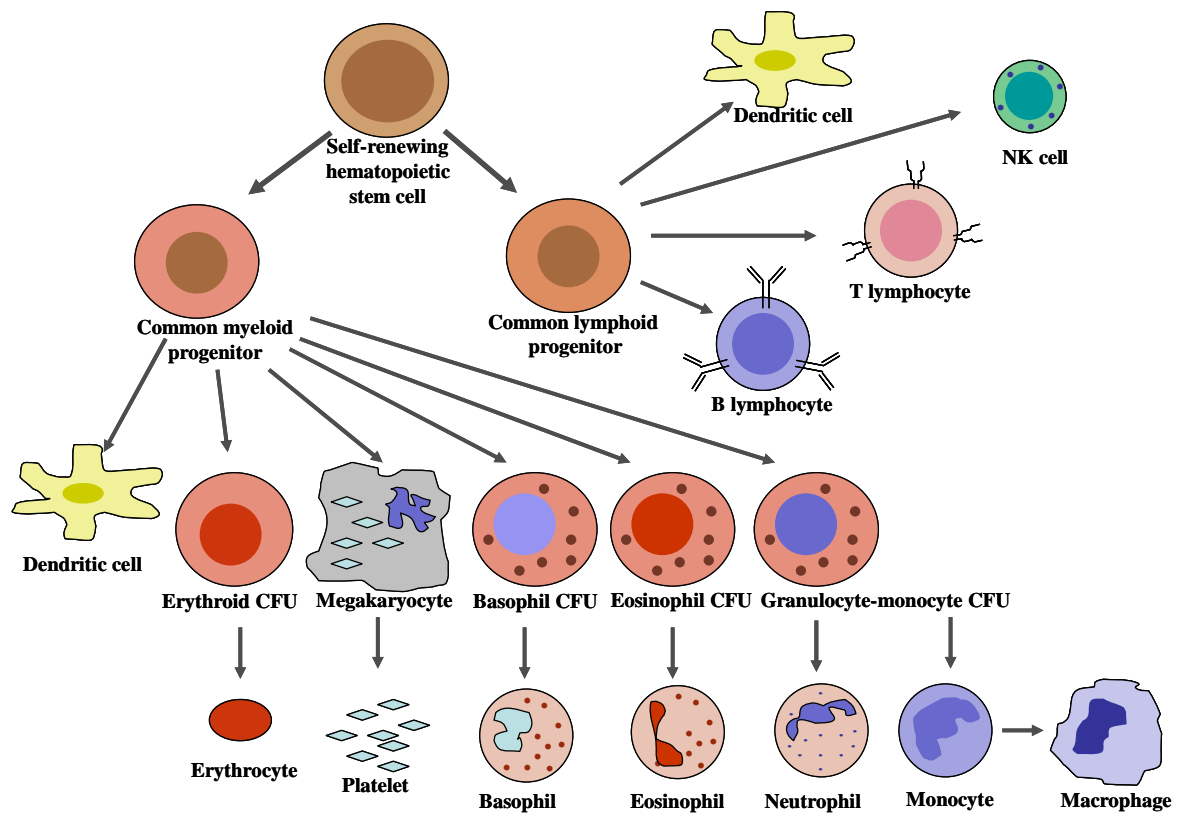


**Figure 1-1. Hematopoiesis**

Self-renewing hematopoietic stem cells give rise to common lymphoid and myeloid progenitor. T cells, B cells and NK cells are differentiated from the lymphoid progenitor. Cells of myeloid lineage, i.e. basophils, eosinophils, neutrophils, monocytes/macrophages, arise from the myeloid progenitor. Dendritic cells are differentiated from both lymphoid and myeloid progenitors. CFU, colony-forming unit; NK cells, natural killer cells [20-21]

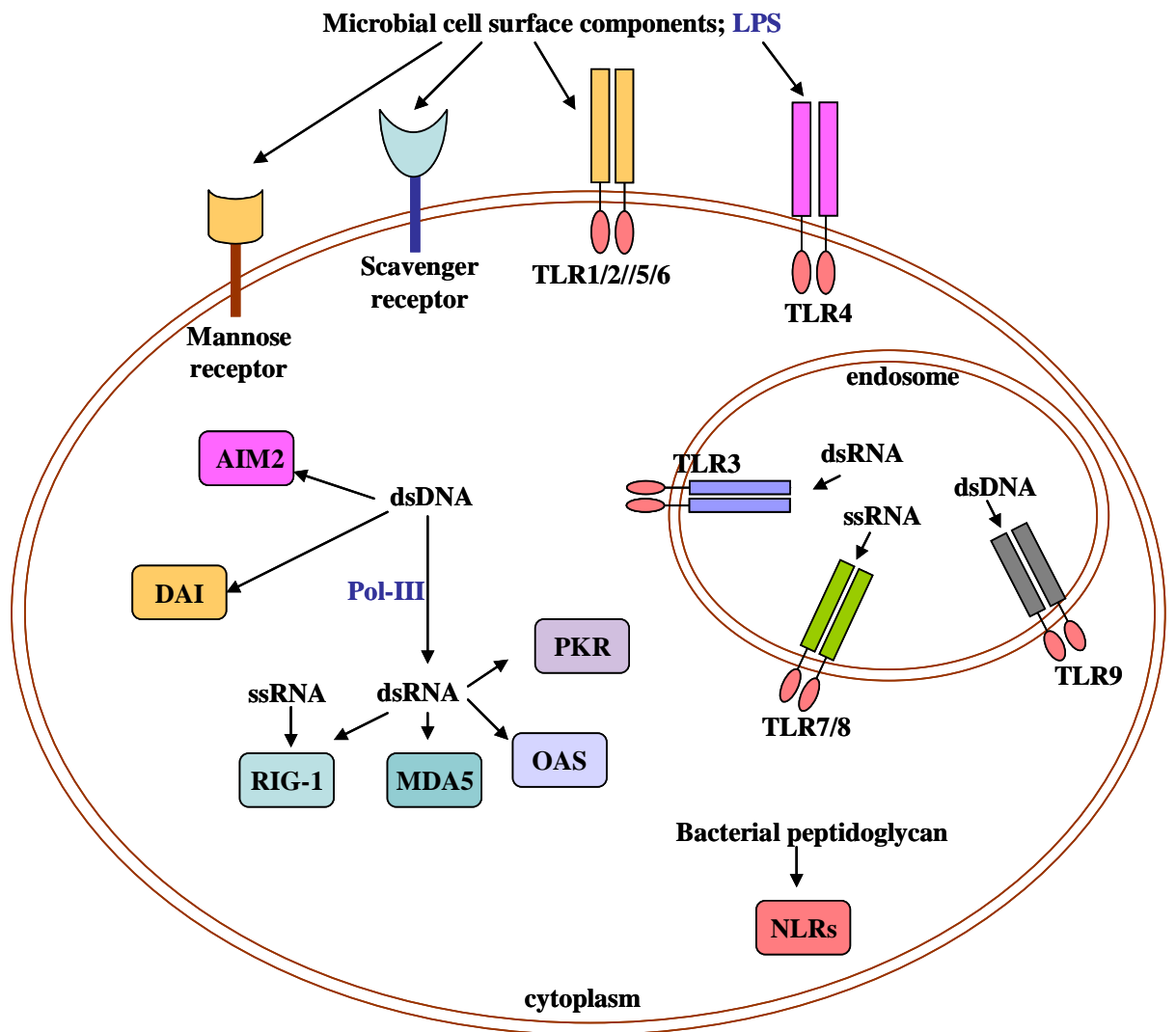


**Figure 1-2. Cellular locations of pattern recognition receptors**

PRRs and their ligands are shown in this figure. TLR, Toll-like receptor; RIG-1, retinoic acid-inducible gene 1; OAS, oligoadenylate synthetase; MDA5, melanoma differentiation-association gene 5; PKR, RNA dependent protein kinase; DAI, DNA-dependent activator of IRF (interferon regulatory factor); NLR, NOD (nucleotide-oligomerisation domain)-like receptor; Pol-III, RNA polymerase III [10, 21-24]

<b>TLR</b>	<b>TLR ligand</b>	<b>references</b>
TLR1:TLR2	Tri-acyl lipopeptides	[25]
TLR2	Lipoprotein, zymosan, peptidoglycan, glycolipid	[25-26]
TLR3	dsRNA, poly (I:C), poly (A:U)	[25, 27-28]
TLR4	Gram negative bacterial LPS Host HSP60, HSP70	[25] [29-30]
TLR5	Bacterial flagellin	[25]
TLR2:TLR6	di-actyl lipopeptides	[25]
TLR7	Imiquimod, R-848 imidazoquinoline synthetic compounds, ssRNA, poly (A:U)	[22, 25, 28, 31-32]
TLR8	ssRNA	[22, 32]
TLR 9	CpG motifs of synthetic DNA Natural DNA	[33] [34-35]
TLR11	<i>Toxoplasma gondii</i> profilin	[36]

**Table 1-1. Toll-like receptors and their ligands**

Toll-like receptors and their ligands are summarized in this table; ligands for TLR1-9 and 11 have been identified. TLR1 or TLR6 form dimer with TLR2 (TLR1:TLR2 or TLR6:TLR2 indicated in the table) to bind to the identified ligands. Other TLRs form homodimer. Poly (I:C), polyinosinic:polycytidylic acids; Poly (A:U), polyadenylic:polyuridylic acids.

### **1.1.3 Adaptive immunity**

Adaptive immunity develops in response to infection and adapts to recognise, eliminate and remember the invading pathogen. Adaptive immunity begins a few days after the initial infection. An important consequence of an adaptive immune response is memory. If the same, or a closely related, pathogen infects the body, memory cells provide means to make a rapid and often highly effective attack on the invading pathogen. Cells of the adaptive immune system are antigen-specific B and T lymphocytes. APCs display antigen to and activate T cells. Pathogens or antigens are eliminated by effector cells upon activation of T cells. Antibodies produced by B cells (plasma cells) bind to antigens and facilitate elimination of antigen by the immune system.

#### **1.1.3.1 Antigen and antigen binding molecules**

Antigens are substances recognised by antibodies, which appear as free antibodies or membrane bound antibodies on B cells. Antigens are also recognised by T-cell receptors (TCRs). Antibody binds to intact antigens but TCR recognise an antigen in a form of a peptide of processed antigen; and peptide antigens need to bind to MHC molecules to be recognised by TCRs.

Most antigenic molecules are proteins. Some lipids, carbohydrates and nucleic acids also exhibit antigenic properties but they are not generally recognised by TCRs. From the whole antigen molecule, only specific regions on antigen are recognised by antibodies and TCRs. Those specific regions are called antigenic determinants or epitopes.

##### **1.1.3.1.1 Antibody**

Antibodies are immunoglobulins (Ig). The Ig molecule has two identical light chains and two identical heavy chains. Both light chains and heavy chains consist of amino-terminal variable (V) regions and carboxy-terminal constant (C) regions. The V regions of each light chain and heavy chain form an antigen-binding site. The variety of amino acid sequences in this region makes Ig produced by one B cell different from those produced by other B cells. The C regions of heavy chains are responsible for mediation of the effector function. Both light chain and heavy chain contain Ig domains, the globular motif characteristic of Ig superfamily molecules. V and C regions of a light chain contain one Ig domain. A heavy chain has one Ig domain in the V region and three or four Ig domains in the C region, depending on the Ig isotype.

Igs are divided into 5 classes (isotypes) according to structure of their heavy chain;  $\alpha$ ,  $\delta$ ,  $\epsilon$ ,  $\gamma$ , and  $\mu$  heavy chain for IgA, IgD, IgG, IgE and IgM isotypes, respectively. In humans, there are two subclasses of IgA, IgA1 and IgA2. Human IgG is divided into 4

subclasses, IgG1, IgG2, IgG3 and IgG4; mouse IgG is divided into IgG1, IgG2a, IgG2b and IgG3, according to the subclasses of the  $\gamma$  chains. Ig can exist on the surface of B cells (IgD and IgM) which function as antigen receptors or as secretory Igs in the circulation, tissues, and mucosal sites. IgE and IgG are secreted in a monomeric form, IgA can exist as a monomer, a dimer (dominant form) or a trimer, and secretory IgM is a pentamer. Multimeric Ig contains joining (J) chain that binds to tail pieces of Ig via disulfide bonds.

#### **1.1.3.1.2 T-cell receptor**

A TCR consists of two transmembrane polypeptide chains covalently linked to each other by a disulfide bond. Most T cells express  $\alpha$  and  $\beta$  chains which form  $\alpha\beta$  TCR. The small subset of T cells express  $\gamma\delta$  TCR composed of  $\gamma$  and  $\delta$  chains. Each chain consists of an Ig-like N-terminal variable (V) domain, an Ig-like constant (C) domain, a hydrophobic transmembrane region, and a short cytoplasmic region. TCR V domains form peptide-MHC complex binding site similar to the antigen-binding site of Ig molecule.

#### **1.1.3.1.3 MHC molecules and antigen presentation**

MHC molecules are membrane-bound glycoproteins that form complexes with peptides derived from processed protein antigens and present them to T cells. MHC molecules are called H-2 (histocompatibility-2) molecules in mice and HLA (human leukocyte antigen) molecules in humans. MHC molecules that form complexes with peptide antigens are divided into two classes, class I and class II MHC molecules.

Class I MHC molecules are expressed in most nucleated cells and they are composed of  $\alpha$  chain transmembrane glycoprotein associated with  $\beta_2$ -microglobulin molecule. The peptide-binding cleft of a MHC-I molecule can bind a peptide of eight to ten amino acids. MHC-I molecules bind to processed cytosolic antigens. Cytosolic proteins, e.g. viral derived proteins, are degraded into peptides by the proteasome, transported to the endoplasmic reticulum (ER) by TAP (transporter associated with antigen processing) proteins and assembled with MHC molecules before being presented on the cell membrane for T-cell recognition. MHC-I molecules in humans are HLA-A, HLA-B and HLA-C; MHC-I molecules in mice are H-2K, H-2D and H-2L.

Class II MHC molecules contain two transmembrane glycoproteins,  $\alpha$  and  $\beta$  chains. The peptide-binding cleft of a class II MHC molecule can bind a peptide of thirteen to eighteen amino acids. Class II MHC molecules are expressed only in APCs, i.e. macrophages, DCs and B cells, and the level of expression is increased when the cells are activated. Exogenous proteins internalised by APCs are degraded within the phagosomes or endosomes and the peptides are later associated with MHC class II molecules transported to

the vesicles. The peptide-MHC complexes are thereafter expressed on the cell surface for T cell recognition. MHC-II molecules in humans are HLA-DR, HLA-DQ and HLA-DP; MHC-II molecules in mice are I-A and I-E.

As mentioned earlier, endogenous antigens are processed and presented by MHC class I molecules, whereas exogenous proteins are subjected to the MHC class II pathway. However, exogenous proteins may also access the class I presentation pathway in professional APCs via a process called cross-presentation. In mice the major APCs capable of cross-presentation are CD8<sup>+</sup> DCs which are efficient in phagocytic uptake of blood-borne dead cells [37-38]. In addition, CD8<sup>+</sup> DCs can uptake antigen transferred from tissue DCs migrating into the secondary lymphoid organs [39] or from marginal zone macrophages [40]. The mechanism of cross-presentation is not clear but can be distinguished into TAP-dependent and TAP-independent pathways [41]. In the TAP-dependent pathway, the phagocytosed antigens are transported from phagosomes to the cytosol and the antigens enter class I presentation pathway [41-43]. The TAP-independent pathway includes the exchange within the endosome of an exogenous peptide antigen with the already loaded peptide present on class I MHC molecule [41, 44-45].

### **1.1.3.2 B lymphocytes**

Before birth, B cells develop in the fetal liver while after birth B cells are generated in the bone marrow. Fetal liver-derived hematopoietic stem cells (HSCs) differentiate into the B-1 B subset which resides in peritoneum and at mucosal sites. Bone marrow-derived HSCs are the precursors of B-2 B cells which further differentiate into follicular B cells and marginal zone B cells. Follicular B cells are the majority of B cells and they are circulating B cells. Marginal zone B cells are located in the marginal sinus of the spleen. Marginal zone B cells and B-1 B cells share some characteristics; they both have limited Ig sequence diversity in the variable regions and they both produce natural antibodies.

#### **1.1.3.2.1 B cell maturation**

In the bone marrow, progenitor B cells (pro-B cells) proliferate and differentiate into precursor B cells (pre-B cells) which thereafter differentiate into immature B cells. Immature B cells develop into mature B cells in the bone marrow or leave the bone marrow and further mature in spleen.

Proliferation and differentiation of pro-B cells into pre-B cells require the microenvironment in the bone marrow. Direct contact of pro-B cells with bone marrow stromal cells activates pro-B cell proliferation and differentiation. The bone marrow stromal cells also secrete IL-7 required for development into pre-B cells. Pro-B cells express

enzymes, including the recombination-activating gene 1 and 2 (*Rag-1/-2*) and the terminal deoxynucleotidyl transferase (TdT), required for V(D)J recombination, a process of Ig gene rearrangement. Ig gene rearrangement is a key event in B-cell development and B-cell diversity.

In human, a locus of Ig heavy chain consists of Ig V genes (approximately 100 genes of which 51 are potentially functional) cluster on the 5' end, with a leader sequence upstream of each V gene, following with 23 diversity (D) segments, 6 joining (J) segments, and 9 C genes. Similarly, human  $\lambda$  and  $\kappa$  light chain loci contain multiple V genes and J segments. V(D)J segment encodes for the variable region and C genes encode for constant regions of the Ig molecule.

Gene rearrangement occurs on the heavy chain locus first. The recombination brings one D and one J segment together followed by joining of a V gene to the DJ segment (figure 1-3). Several enzymes are involved in this process. Rag-1/2 recognises the DNA sequence at the junction of each gene and cleaves it. The resulting fragments are joined by the function of several enzymes including Artemis, exonucleases and TdT. As part of Artemis and TdT function during V and D, D and J, or V and J joining in the light chain loci, some nucleotides are added and some are lost, resulting in variability at the junctions of V, D and J segments (called junctional diversity).

After V(D)J recombination, the first transcript contains rearranged V(D)J, J segments and C $\mu$  exons. RNA processing further splices off unjoined J segments and introns, resulting in  $\mu$  heavy chain transcript. The  $\mu$  heavy chain associates with the  $\lambda 5$  and VpreB proteins (surrogate light chains) and forms pre-B cell receptor (pre-BCR) with Ig $\alpha$  and Ig $\beta$  signal transducing proteins. At this stage the developing B cells are called pre-B cells and they are no longer attached to bone marrow stromal cells. Pre-BCR signals mediate survival, proliferation and maturation of pre-B cells. In addition, pre-BCR signaling is also required for stimulation of the light chain rearrangement.

In the next stage of development, the  $\kappa$  or  $\lambda$  light chain is rearranged. The light chain is then associated with the previously synthesised  $\mu$  chain to form IgM protein. At this stage the developing B cells are immature B cells which express cell surface IgM in association with Ig $\alpha$  and Ig $\beta$  and function as an antigen receptor (BCR). Immature B cells developed from different precursors respond to the strength of a self antigen signalling differently [46-47]. For bone marrow-derived B cells, self antigens provide a weak BCR signal allow positive selection. In contrast, interaction with a high avidity self antigen can lead to cell death (negative selection) or receptor editing. Receptor editing is the process when

additional light chain V-J rearrangements occur and a new light chain is produced, resulting in a different BCR which is not self-reactive.

Immature B cells undergo further maturation into naïve mature B cells. Follicular B cells express both surface IgM and IgD. The coexpression of IgM and IgD is a result of an alternative RNA splicing. The primary heavy chain transcript containing the rearranged VDJ following with  $C_{\mu}$  and  $C_{\delta}$  is spliced in the way that VDJ joined to either  $C_{\mu}$  or  $C_{\delta}$ . The synthesised  $\mu$  and  $\delta$  heavy chain associate with the same light chains, thereby the resulting Igs have the same antigen specificity. Mature naïve B cells die within a few months if they do not encounter antigens they recognise with high affinity.

#### **1.1.3.2.2 B cell activation and antibody production**

When a mature naïve B cell first encounters the antigen that matches its membrane-bound antibody, the binding of the antigen to the antibody causes the cell to divide rapidly and its progeny to differentiate into antibody-secreting plasma cells. B-cell activation may occur in a thymus-dependent (TD) or thymus-independent (TI) manner.

Antigens (protein antigens) that induce antibody responses only in the presence of antigen-specific Th cells are called TD antigens. The B-cell response to TD antigens requires direct contact with Th cells and cytokines produced by T cells. Th cells stimulate B cell clonal expansion, isotype switching, affinity maturation, and differentiation to plasma and memory cells.

Multivalent polysaccharides induce antibody responses without T-cell requirement. These antigens are called TI antigens. These antigens cannot be processed and presented with MHC molecules; therefore Th cells cannot be engaged. The antibodies produced against TI antigens are of low affinity and mostly of the IgM form. MZ and B1-B cells are B cell subsets that respond to TI antigens.

In secondary lymphoid organs (lymph nodes and spleen), antigen activated B cells, T cells and APCs work together to initiate antibody responses. B cells are initially activated by binding to antigen and subsequent BCR cross-linking. B cells can encounter free antigens diffused into follicles or intact antigens bound to receptors on the cell surface of macrophages, DCs, and follicular DCs (FDCs) [48].

Macrophages residing at subcapsular sinus (SCS) can bind to antigen through several receptors. Macrophage receptor 1 (MAC1) binds to complement-coated antigen and the bound antigen remain on the cell surface. Fc $\gamma$  receptor-IIB (Fc $\gamma$ RIIB) and DC-specific intercellular adhesion molecule 3 (ICAM3)-grabbing non-integrin (DC-SIGN) have been shown to be involved in antigen presentation to B cells. Fc $\gamma$ RIIB binds to IgG-coated antigens while DC-SIGN binds to carbohydrate-containing antigens. The proposed

mechanism of antigen presentation by Fc $\gamma$ RIIB and DC-SIGN is that the receptors mediate internalisation of the antigens into non-degradative endosomes and the antigens are recycled to the cell surface. Intact antigens bound to receptors on macrophage cell surfaces then can be recognised by the neighbouring B cells. DCs also bear Fc $\gamma$ RIIB and DC-SIGN thus DCs residing around high endothelial venule supplying the lymph node can bind to antigens and present them to migrating B cells in the T-cell zone. FDCs express complement receptors thus can bind to complement-coated immune complex on MZ B cells which migrate into the follicle and follicular B cells which receive the immune complex from SCS macrophages [48].

B cells recognise and internalise antigens that they are specific for. The antigens are processed and expressed as peptide-MHC-II complexes on the cell surface for Th cell recognition. Antigen-activated B cells also increase expression of MHC-II molecules, cytokine (IL-2 and IL-4) receptors and receptor for CC chemokine (CCR) 7. Activated B cells move toward the T cell zone to interact with T cells that are activated by antigen presenting APCs, especially DCs. Interaction with Th cells results in further activation of B cells by CD40L and T cell-derived cytokines. Thereafter, some activated B cells form extrafollicular foci and differentiate into short-lived plasma cells with some isotype switching and Ig secretion occurring. The rest of activated B cells move back into the follicle where germinal centres are formed and are the site of extensive isotype switching, somatic mutation, and generation of long-lived plasma cells and memory B cells (figure 1-4).

In the germinal centre, activated B cells proliferate rapidly within the dark zone. The proliferating B cells are centroblasts. During cell proliferation, IgV genes undergo somatic hypermutation resulting in some mutated genes having high-affinity Igs and some producing Igs with lower antigen-binding affinity. Progeny of centroblasts are centrocytes which move to the light zone along the network of FDCs. Binding of antigen displayed by FDCs provides a survival signal for B cells. Therefore, only high affinity B cells are selected as antigen is decreased overtime. In addition, high-affinity cells are more efficient in binding the antigen and displaying the peptide-MHC to follicular helper T (Tfh) cells, thus they are better recipients for T-cell help. Cytokines produced by T cells and interactions of CD40 and OX40L on B cells to CD40L and OX40, respectively, on T cells stimulate B-cell proliferation and isotype switching. Various cytokines induce switching to different isotypes, e.g. IFN- $\gamma$  induces switching to IgG2a and IgG2b isotypes in mouse. After differentiation and selection, the cells exit the germinal centre and develop into memory B cells or long-lived antibody-secreting plasma cells.

### 1.1.3.2.3 Effector function of antibody

Antibody functions as the effector of the humoral response by binding to antigen and facilitating its elimination. Antigens coated with antibody are eliminated in several ways. For example, antibody can cross-link several antigens, forming clusters that are more readily ingested by phagocytic cells. Binding of antibody to antigen on a microorganism can also activate the complement system, resulting in lysis of the foreign organism; the process is called complement-dependent cytotoxicity (CDC). Cells coated by antibody also activate phagocytes and NK cell killing; the process is called antibody-dependent cell-mediated cytotoxicity (ADCC). In addition, antibody can neutralise toxins or viral particles by coating them, which prevents them from binding to host cells.

ADCC is a process where Fc receptor (FcR)-bearing innate immune effector cells (monocytes/macrophages, neutrophils, NK cells and dendritic cells) bind to antibody-coated cells by FcRs and destroy these cells [21]. Fc $\gamma$ R expression on immune cells is listed in table1-2. FcRs are divided broadly into the activating and the inhibitory receptors. In mice, activating Fc $\gamma$ R are Fc $\gamma$ RI, Fc $\gamma$ RIII and Fc $\gamma$ RIV. In humans, activating receptors are Fc $\gamma$ RI, Fc $\gamma$ RIIA, Fc $\gamma$ RIIC, Fc $\gamma$ RIIIA and Fc $\gamma$ RIIIB, in which human Fc $\gamma$ RIIA and Fc $\gamma$ RIIIA are closely related to mouse Fc $\gamma$ RIII and Fc $\gamma$ RIV, respectively. Inhibitory receptor Fc $\gamma$ RIIB is conserved in mice and human and is the only inhibitory receptor identified so far [49]. Each IgG subclass has different affinity to Fc $\gamma$ Rs. For example, in mice, IgG1 binds to Fc $\gamma$ RIIB more strongly than to Fc $\gamma$ RIII; IgG2a binds to Fc $\gamma$ RIV more strongly than to Fc $\gamma$ RIIB and Fc $\gamma$ RIII, but it has the highest affinity to Fc $\gamma$ RI; IgG2b binds to Fc $\gamma$ Rs as does IgG2a but it does not bind to Fc $\gamma$ RI [49]. Therefore, the activity of each IgG isotype depends on the ratio of binding to activating and inhibitory receptors and also depends on the ratio of those receptors expressed on the effector cell surface [50-51]. Binding of immune complexes to activating receptors leads to activation of the immunoreceptor tyrosine-based activation motif (ITAM) on the cytosolic domain of receptors, which thereby initiate activation of a series of signalling pathways leads to phagocytosis and release of immune modulators such as cytokines, chemokines, proteases and reactive oxygen species.

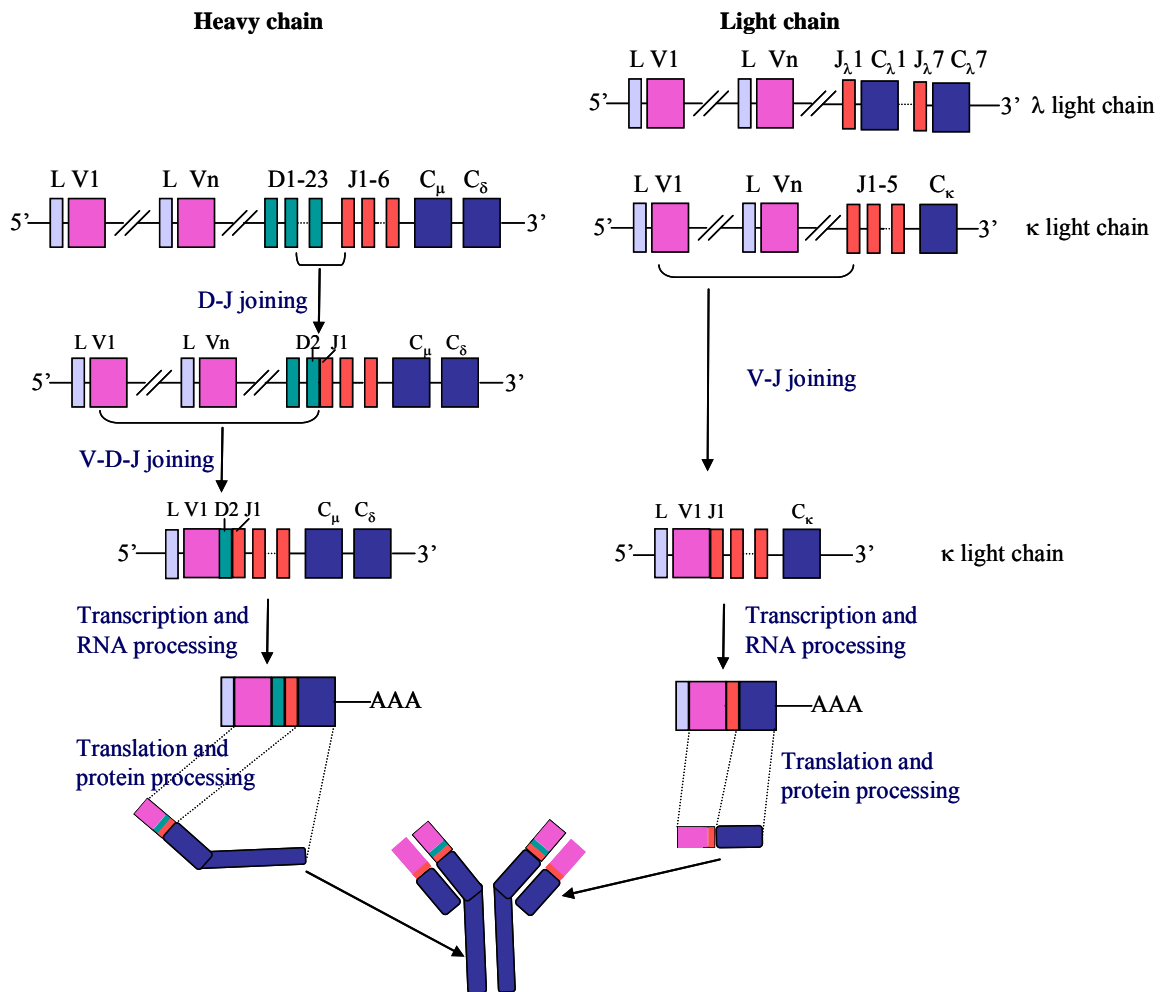


**Figure 1-3. Human Ig heavy chain and light chain gene rearrangements**

Schematic diagram of Ig heavy chain and light chain germ line genes are shown on the top of the figure, each gene is not drawn to scale. In heavy chain loci, only C<sub>μ</sub> and C<sub>δ</sub> are shown, the rest of constant region genes are not indicated. D and J gene segments recombine first, followed with joining of V gene to D-J fragment. The rearranged DNA composes of a leader sequence following with recombined V-D-J, J segments and C genes. The non-combined J segments and sequence downstream C<sub>μ</sub> are spliced during transcription and RNA processing. The leader sequence is cleaved off after the translated protein enters the ER. The synthesised heavy chain consists of a variable region (composed of joined V-D-J) and a constant region. In the light chain, rearrangement of κ chain is shown. V and J segments are joined; the processed RNA consists of a leader sequence, V, J and C genes. V and J segment form V region, and C gene encodes C region of the Ig light chain.

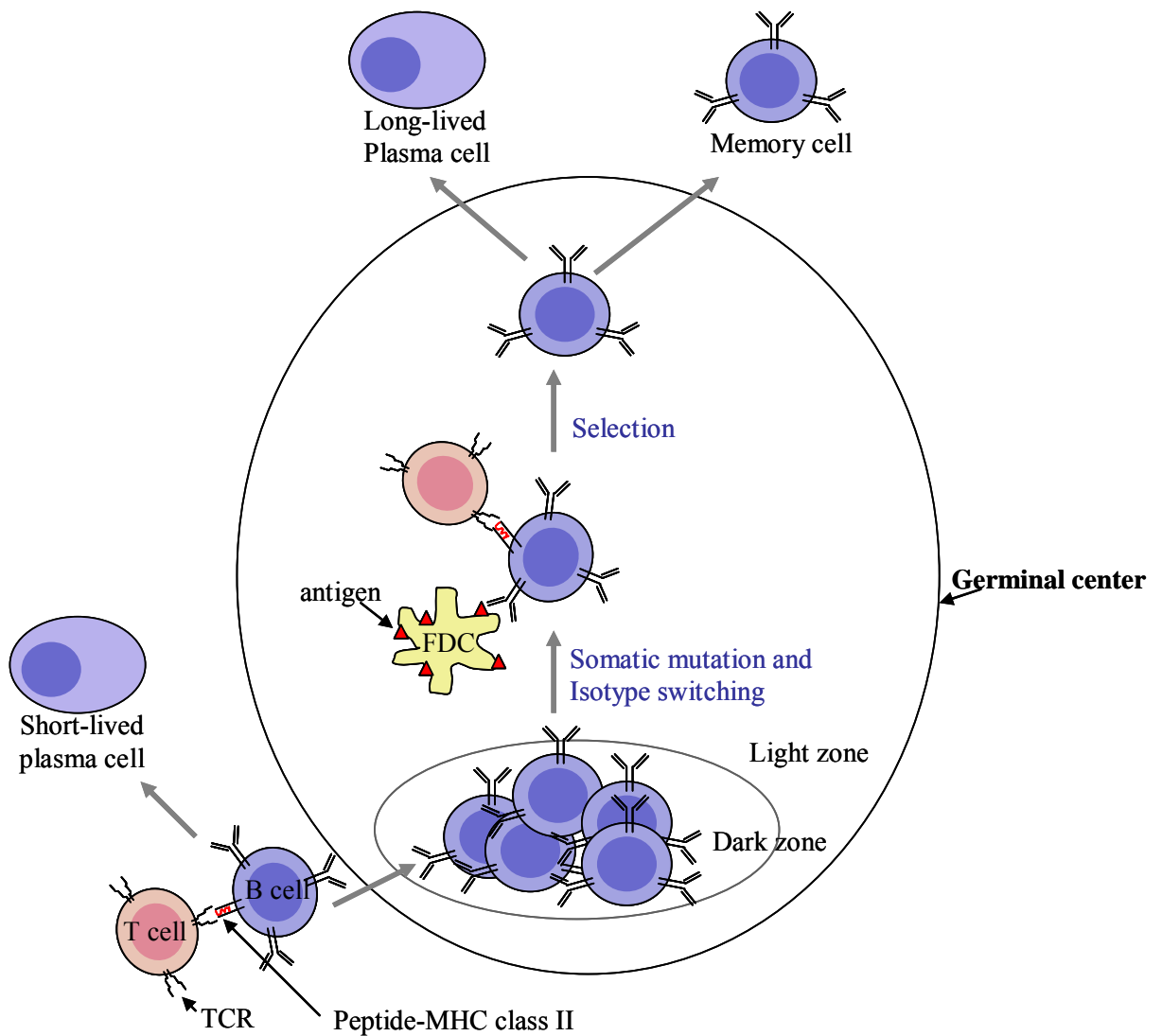


**Figure 1-4. B-cell activation and selection in germinal centre**

Antigen-activated B cells interact with activated T cells and thereafter some of T cell-activated B cells differentiate into short-lived plasma cells in the extrafollicular loci. Some of activated B cells migrate to the germinal centre where they proliferate and undergo somatic mutation. The B-cell progeny (centrocytes) migrate from dark zone to the light zone where they interact with follicular DCs (FDCs). Centrocytes that express high affinity surface Ig are able to bind to antigen presented on FDCs and receive help from antigen-specific follicular helper T (T<sub>fh</sub>) cells. Those interactions with FDCs and T<sub>fh</sub> cells provide survival signals for B cells. As antigen is decreased overtime, only high affinity B cells are selected and differentiated into memory cells or plasma cells.

	<b>Human FcγRs</b>					
	FcγRI	FcγRIIA	FcγRIIB	FcγRIIC	FcγRIIIA	FcγRIIIB
Monocytes/macrophages	+	+	+	-	+	-
NK cells	-	-	-	+	+	-
Neutrophils	+	+	-	-	-	+
B lymphocytes	-	-	+	-	-	-
Dendritic cells	+	+	+	-	+	-

	<b>Mouse FcγRs</b>			
	FcγRI	FcγRIIB	FcγRIII	FcγRIV
Monocytes/macrophages	+	+	+	+
NK cells	-	-	+	-
Neutrophils	-	+	+	+
B lymphocytes	-	+	-	-
Dendritic cells	+	+	+	+

**Table 1-2. FcγR expression on immune cells**

Expression of FcγRs on immune cells is shown. +: FcγR is found on the indicated cell type; -: the FcγR is not found on the indicated cell type [49, 51-53]

### **1.1.3.3 T lymphocytes**

T lymphocytes arise in the bone marrow but migrate to and mature in the thymus. Maturing T cells express unique antigen-binding molecules, T-cell receptors (TCRs), on their membranes. TCR genes undergo rearrangement during T-cell development resulting in generation of a diverse repertoire. After maturation, they enter peripheral lymphoid tissues where they respond to foreign antigens.

#### **1.1.3.3.1 T cell subsets**

##### **1.1.3.3.1.1 CD4<sup>+</sup> T cells**

CD4<sup>+</sup> T cells express cell surface CD4 coreceptor protein and respond to antigens that are processed and displayed as peptide-MHC II complexes by APCs. Naïve CD4<sup>+</sup> T cells differentiate into various subsets upon signals they receive during initial interaction with antigens. They may be divided into five major subsets, Th1, Th2, Th17, Tfh and regulatory T (Treg) subsets, by the pattern of cytokine production and their role in the immune response.

Th1 cells mediate an immune response against intracellular pathogens. Th1 cells produce IFN- $\gamma$  cytokine which together with CD40L-CD40 interaction stimulates phagocytes to destroy ingested microbes. IFN- $\gamma$  also promotes production of opsonising Ig, e.g. IgG2a isotype in mice. Another cytokine produced by Th1 is IL-2 which plays a role in differentiation of memory CD4<sup>+</sup> and CD8<sup>+</sup> T cells [54]. Th2 cells produce IL-4, IL-5, IL-13 and IL-25 cytokines which play a role in clearance of extracellular parasites. For example, IL-4 induces production of IgE, and IgG1 in mouse [51, 54] and IL-5 plays a role in an eosinophil recruitment [55]. Tfh cells express high levels of CXC chemokine receptor (CXCR) 5 and low CCR7, the phenotypes required to migrate to and remain in follicle/germinal centre. Tfh functions are to provide help for somatic hypermutation and isotype switching [56-58].

Th17 cells involve in the induction of many organ-specific autoimmune diseases [54]. Th17 cells produce IL-17, IL-21 and IL-22 which induce autoimmunity by stimulating fibroblasts, endothelial cells and macrophages to produce cytokines, chemokines and matrix metalloproteinases which subsequently recruit polymorphonuclear leukocytes [59]. IL-17 also plays a role in protection against extracellular microbes by recruitment and activation of neutrophils [54]. Regulatory T (Treg) cells are CD4<sup>+</sup>CD25<sup>+</sup>Foxp3<sup>+</sup> T cells. Tregs function in regulation of immune response and self-tolerance. Tregs suppress immune responses by mechanisms including production of suppressive cytokines TGF- $\beta$ , IL-10 and IL-35. Tregs also suppress function of other T cells by direct cell-cell contact; binding of

Tregs to DCs results in down-regulation of CD80 and CD86 on DCs and blocks the binding of responder T cells and thus inhibits immune responses [60].

#### **1.1.3.3.1.2 CD8<sup>+</sup> T cells**

CD8<sup>+</sup> T cells express cell surface CD8 coreceptor protein and are MHC-I restricted since they bind to peptide-MHC-I complexes. The effector function of this T cell type is to kill infected cells or tumour cells, hence the name cytotoxic T cell (CTL). Similar to NK cells, CTLs release granules containing perforin and granzymes upon binding to target cells and activation signals from DCs. Perforin, either released from the granule outside the target cell or from granules endocytosed by target cell, form pores in the target cell membrane/endosome membrane and allow delivery of granzymes to the cytosol of the target cell. Granzymes are able to cleave a wide range of substrates inside the cell and therefore lead to cell apoptosis [61].

#### **1.1.3.3.1.3 Other T cells**

$\gamma\delta$  T cells express the  $\gamma\delta$  TCR instead of the  $\alpha\beta$  TCR expressed by other T cells.  $\gamma\delta$  T cells have limited diversity and are responsible for defence against microbes which commonly invade at the epithelial barrier. The nature of  $\gamma\delta$  TCR antigen recognition is not fully identified but it is suggested that  $\gamma\delta$  TCR recognises the conformational shape of intact antigen [62].

Another T-cell subset is NKT cells which share some characteristics with NK cells. NKT cells express NK1.1, a C-type lectin expressed by NK cells, and  $\alpha\beta$  TCRs that are not MHC-restricted but CD1 restricted and bind to glycolipid antigens [62-64]. An NKT cell-like subset, a mucosal-associated invariant T cell (MAIT), has been identified. MAIT is MR1 (major histocompatibility class I-related molecule) restricted but their natural ligand is unknown [64-66].

#### **1.1.3.3.2 T-cell maturation**

T-cell progenitors migrate to the thymus and the developing T cells (thymocytes) proliferate and differentiate into mature T cells. The maturation processes involves the rearrangement of TCR genes (similar to Ig genes rearrangement of B cells) and expression of membrane markers. The early thymocytes lack both CD4 and CD8, and are called double-negative (DN) cells. DN cells rearrange TCR  $\gamma$ ,  $\delta$  and  $\beta$  genes first. Cells destined for  $\gamma\delta$  T cells diverge at this stage and mature with few changes in the surface phenotype. In cells destined for  $\alpha\beta$  TCR expression, synthesised TCR $\beta$  combines with pre-T $\alpha$  chain and associates with CD3 to form the pre-T-cell receptor (pre-TCR). Formation of the pre-TCR

stimulates cell proliferation and induces progression to CD4<sup>+</sup>CD8<sup>+</sup> double-positive (DP) stage. Each DP cell can rearrange different TCR $\alpha$  gene, therefore generating diversity of the T-cell population. Immature thymocytes expressing  $\alpha\beta$ TCR-CD3 complex undergo thymic selection for MHC-restricted and self-tolerant cells. The surviving cells develop into single positive CD4<sup>+</sup> or CD8<sup>+</sup> T cells. Mature T cells migrate to the circulatory system to enter secondary lymphoid organs. If the naïve mature T cells do not encounter the antigen that they are specific for, they enter circulatory system again to migrate to other secondary lymphoid organs.

#### **1.1.3.3.3 T cell activation**

Activation of naïve T cells is initiated by interaction of the TCR-CD3 complex with a processed antigen peptide-MHC complex on the surface of DCs. Antigen recognition provides signal 1 for T-cell activation. The complete activation requires a second signal provided by interaction with costimulatory molecules on activated DCs.

CD4<sup>+</sup> T cells recognise peptides bound to class II molecules and the activation depends on the second signal from interaction of CD28 on T cells with B7 (B7-1 or B7-2) on DCs. Activated T cells produce IL-2, the cytokines required for T-cell clonal expansion. Some proliferating T cells differentiate into effector T cells and some of them differentiate into memory T cells. Some effector Th cells reside in the secondary lymphoid organ to help B-cell maturation; some of them leave the secondary lymphoid organ to the infected tissue to help other effector cells, e.g. Th cells secrete several cytokines that have diverse activity. Differentiation into a particular subset of Th cell depends on cytokines secreted from activated DCs.

CD8<sup>+</sup> T cells recognise peptides bound to class I MHC molecules. T-cell activation signal 2 may be received from an interaction with a DC either activated directly or through CD4<sup>+</sup> T-cell help. In the response to antigens that induce a strong innate immune response (for example, when DCs are infected with microbes) CD4<sup>+</sup> T-cell help may not be required. CD4<sup>+</sup> T-cell help is required in the response to weak immunogens such as tumour antigens. CD4<sup>+</sup> T cells provide help by secreting cytokines that stimulate CD8<sup>+</sup> T cell differentiation and enhancing the ability of DC (via CD40-CD40L interaction) to stimulate cell differentiation. Activated CD8<sup>+</sup> T cells proliferate and differentiate into effector cells (CTL) and memory cells.

## 1.2 Hematologic malignancies: Incidence and therapy

Tumours occur in various haematopoietic cell lineages and stages. The World Health Organisation (WHO) classifies the tumours of haematopoietic and lymphoid tissues according to the lineage of the neoplastic cells (e.g. myeloid and lymphoid) [67]. Neoplasms of precursor cells (e.g. acute myeloid leukaemia) are separated from neoplasms comprised of more mature cells (e.g. mature B-cell and T/NK-cell lymphoma, Hodgkin's lymphoma). For the mature neoplasms, further sub-classification is based on variety of features including the stage of differentiation as compared to a normal counterpart, morphology, or the combination of morphologic, immunophenotypic and/or genetic parameters [67].

Leukaemia and lymphoma are large groups of hematologic malignancies comprised of more than 30 different diseases classified by the WHO. In the UK, leukaemia was the twelfth most commonly diagnosed cancer (table 1-3), in 2006, and the tenth most common cause of cancer deaths in 2007 (table 1-4) (27% of all deaths are caused by cancer) [68]. Lymphoma is broadly divided into Hodgkin's lymphoma, a disease described since 1865, and non-Hodgkin's lymphoma (NHL) [69]. In 2006, NHL was the fifth most commonly diagnosed cancer in the UK [68]. In 2007, NHL was the ninth cause of cancer death [68].

Treatment of leukaemia and NHL patients depends on the type and stage of cancer, patients' age and general health. The current treatments are chemotherapy, radiotherapy, bone marrow/stem cell transplant and biological therapy including immunotherapy.

Chemotherapy and radiotherapy are generally used in many types of hematologic tumours especially in acute leukaemias and NHL to eliminate leukaemia cells or affected lymph nodes or other tissues. Chemotherapeutic drugs include nucleoside analogues which after intracellular phosphorylation become cytotoxic and inhibit DNA synthesis [70-71]. Chemotherapeutic drugs have been approved for use and have shown efficacy in hematologic malignancies [70, 72-73]. However, patients which received chemotherapy suffer from side effects such as hematologic effects, neurotoxicity, infection, autoimmune complications, liver and renal dysfunction, skin rash, mucositis and hand-foot syndrome [70, 72], the symptoms include erythemas, blistering and ulceration of palms and soles [74].

After intensive chemotherapy or radiotherapy, patients may receive bone marrow/stem cell transplants to restore immune function. Patients who do not respond to other therapies may also receive bone marrow/stem cell transplants. An allogeneic transplant is a potentially curative for patient younger than 60. However, in some diseases such as chronic myeloid leukaemia (CML), most patients are too old to be treated by transplants. Moreover, patients receiving a transplant are at risk of bleeding, infection and graft versus host disease [71, 75].

Biological therapies, including immunotherapy, have been used in leukaemias and advanced NHL. Tyrosine kinase inhibitors have been used in CML and Philadelphia-chromosome positive acute lymphocytic leukaemia (ALL). Philadelphia-chromosome results from reciprocal translocation between long arms of chromosome 9 and 22 creating a hybrid *Bcr-Abl* gene [76]. BCR-ABL protein is a constitutively active tyrosine kinase that activates many signal transduction pathway leading to uncontrolled cell proliferation and reduced apoptosis [76]. Tyrosine kinase inhibitors such as imatinib (Glivec) and dasatinib are potent inhibitors of BCR-ABL oncoprotein, thereby they can inhibit phosphorylation and activation of BCR-ABL downstream protein signalling [77-78]. Common adverse effects from tyrosine kinase inhibitor drugs include nausea, diarrhea, edema, muscle cramps and skin rash [78-79]. Even though imatinib and dasatinib show efficacy in treatment of patients with *Bcr-Abl* mutations, patients with the T315I mutation type develop resistance to both drugs. Other kinase inhibitors are currently under clinical development [77].

Another successful biological therapy is monoclonal antibodies (mAb) rituximab and ofatumumab against CD20, a cell surface marker expressed on most normal and malignant B cells. Rituximab is a chimeric mouse Fab/human Fc monoclonal antibody while ofatumumab is a second generation of anti-CD20 mAb which is fully human IgG1. Rituximab has been used since 1997 and provides a clinical efficacy, especially when used in combination with chemotherapy, such as CHOP (cyclophosphamide, doxorubicin, vincristine and prednisone), in the treatment of B-cell NHL such as diffuse B cell lymphoma and follicular lymphoma [80] and more recently in chronic lymphocytic leukaemia (CLL)[71].

The proposed mechanism of anti-CD20 mAb includes complement-dependent cytotoxicity (CDC), ADCC and programmed cell death (PCD) induction [50]. CD20 is usually expressed at high levels on B cells and therefore the high density of CD20 provides a good target for complement activation via mAb. Anti-CD20 mAb contains a human IgG1 Fc which is a potent activator of the complement system. ADCC activity of the mAb appears to be mediated through Fc $\gamma$ RIIA and Fc $\gamma$ RIIIA as patients with Fc $\gamma$ RIIA or Fc $\gamma$ RIIIA alleles which have higher binding affinity for the mAb Fc showed significantly improved clinical responses to rituximab [81-83]. Moreover, it is proposed that mAb therapy may also exhibit delayed vaccine-like therapeutic effect through generation of specific CTL responses [84].

Despite the evidence showing efficacy of anti-CD20 mAb therapy, resistance to rituximab is observed in about half of the patients in the course of prolonged treatment. Resistance may be related to the lower number of CD20 molecules per cell [85]. Moreover, the immune effector functions become saturated after mAb therapy. The high concentration

of immune complexes leads to the depletion of complement molecules and the exhaustion of effector cells which require a long period of time to restore [50]. The administration of more mAb will not help improve clinical response and therefore limits usage of mAb in tumour therapy.

In an attempt to improve effectiveness of antibody therapy, bispecific antibody has been produced. Bispecific antibodies contain one specificity for a tumour antigen and another for Fc receptor on cytotoxic effector cells or CD3 on T cells [86-87]. Thereby, bispecific antibodies can selectively engage cytotoxic cells and CD3<sup>+</sup> effector T cells to interact with tumour cells. *In vitro* and animal studies have shown the therapeutic potential of this antibody. However, the clinical trial results were less promising and the antibody has a short plasma half-life [86].

Although the treatments mentioned earlier improve survival rates, a proportion of patients die of progressive or relapsed disease. Therefore, the novel treatments are needed to improve the clinical outcome in these diseases. Active immunotherapy or vaccination is one another promising option which provides benefit of long term tumour elimination as it raises memory response against specific tumour. Vaccination against idiotypic (Id) antigen expressed on the surface of tumour B cells has been developed. BiovaxID<sup>TM</sup> is an example of personalised therapeutic NHL vaccine that provides benefit for patients with follicular lymphoma [88].

<b>Persons top 20 UK</b>	<b>Gender</b>		<b>Persons</b>	<b>% of total</b>
	<b>Male</b>	<b>Female</b>		
<b>Cancer site</b>				
<b>Breast</b>	314	45508	45,822	15.61%
<b>Lung</b>	22381	16646	39,027	13.29%
<b>Colorectal</b>	20430	17084	37,514	12.78%
<b>Prostate</b>	35515	0	35,515	12.10%
<b>N-H-L</b>	5658	4911	10,569	3.60%
<b>Melanoma</b>	4803	5607	10,410	3.55%
<b>Bladder</b>	7307	2957	10,264	3.50%
<b>Kidney</b>	4879	2961	7,840	2.67%
<b>Oesophagus</b>	5034	2790	7,824	2.66%
<b>Stomach</b>	4970	2743	7,713	2.63%
<b>Pancreas</b>	3731	3929	7,660	2.61%
<b>Leukaemias</b>	4229	3008	7,237	2.46%
<b>Uterus</b>	0	7045	7,045	2.40%
<b>Ovary</b>	0	6596	6,596	2.25%
<b>Oral</b>	3540	1785	5,325	1.81%
<b>Brain with CNS</b>	1921	2611	4,532	1.54%
<b>Multiple myeloma</b>	2174	1813	3,987	1.36%
<b>Liver</b>	2015	1178	3,193	1.09%
<b>Cervix</b>	0	2873	2,873	0.98%
<b>Mesothelioma</b>	1942	385	2,327	0.79%
<b>Other</b>	16,380	13948	30,328	10.33%
<b>all exc NMSC</b>	147223	146378	293,601	

**Table 1-3. The 20 most commonly diagnosed cancer in the UK, 2006**

Adapted from the Cancer Research UK (CRUK) cancer incidence statistic report, [68]. NMSC : non-melanoma skin cancer.

Persons top 20 UK Cancer site	Gender		Persons	% of total
	Male	Female		
Lung	19637	14,872	34,509	22.19
Colorectal	8474	7,533	16,007	10.29
Breast	92	11,990	12,082	7.77
Prostate	10,239	0	10,239	6.59
Oesophagus	4,805	2,548	7,353	4.73
Pancreas	3,610	3,705	7,315	4.70
Stomach	3,267	1,969	5,236	3.37
Bladder	3,177	1,636	4,813	3.10
NHL	2,443	2,090	4,533	2.92
All leukaemias	2492	1,858	4,350	2.80
Ovary	0	4,317	4,317	2.78
Kidney	2,299	1,453	3,752	2.41
Brain with CNS	2,065	1,546	3,611	2.32
Liver	1,921	1,281	3,202	2.06
Multiple myeloma	1,374	1,321	2,695	1.73
Malignant melanoma	1,104	938	2,042	1.31
Mesothelioma	1,700	321	2,021	1.30
Oral	1259	592	1,851	1.19
Uterus	0	1,659	1,659	1.07
Bone and connective tissue	589	502	1,091	0.70
Other cancers	29,997	27,318	57,315	36.86
<b>All</b>	<b>80,907</b>	<b>74,577</b>	<b>155,484</b>	

**Table 1-4. The 20 most common causes of death from cancer in the UK, 2007**

Adapted from the CRUK mortality report [68].

## 1.3 Tumour vaccines

### 1.3.1 Tumour antigens

10 – 20% of cancers are known to be associated with infectious organisms, usually viruses. It is clearly possible to vaccinate against those organisms and thereby prevent the associated cancer. A dramatic example is the success of the recombinant virus-like particle preventive vaccine against human papillomavirus (HPV) [89-90]. In addition, tumour antigens include proteins, commonly as glycoproteins at cell surfaces, peptides, carbohydrates, and glycolipids, expressed by tumour cells.

Glycoprotein antigens may be expressed at the surface of the tumour cell, or be secreted, while the peptides will be bound to either the MHC class I or class II molecules (figure 1-4) (reviewed in [91]). Cell surface glycoproteins are potentially accessible to antibody attack, e.g. clone-specific idiotypic (Id) Ig of B-cell neoplasms and clonotypic T-cell receptors of T-cell tumours. Cell surface glycoproteins may also be expressed as MHC-associated peptides and therefore could also be susceptible to T-cell attack [91]. Tumour antigens vary in expression level and specificity, from those detected only on tumour cells to those that are also expressed by normal cells, but that may be up-regulated in tumour cells.

Unique tumour antigens are products of mutations in genes that create new gene products that may give rise to new antigenic epitopes. Typical examples include proto-oncogenes that are involved in normal cell division and differentiation. A single point mutation may activate an oncogene (e.g. ras, b-raf) or inactivate tumour suppressor genes (e.g. CDK4, p53) causing increased signal transduction and uncontrolled cell division (reviewed in [92]). Point mutations in p53 are seen in about 50% of human malignancies. Antibodies to mutated p53 correlate with poor prognosis and can be associated with either undetected malignancy or a pre-malignant state (reviewed in [92]). In melanoma patients, mutation in  $\beta$ -catenin, a protein involved in cell adhesion and signalling regulation, resulted in epitopes that induced a HLA-A\* 24 restricted CD8<sup>+</sup> T-cell response [93]. Another mutation in melanoma, in CDC27 (a protein involved in cell cycle regulation), led to altered protein trafficking into the endosomal compartment. The epitope presented with MHC class II is recognised by CD4<sup>+</sup> T cells [94].

Tissue-specific differentiation antigens are molecules present on tumour cells and their normal cell counterparts. The lineage-specific proteins are expressed by tumour cells of prostate, breast, melanocytes and other cancers. These proteins can be targeted by vaccination with minimal side effects anticipated. For melanoma, vaccines were successful in inducing antitumour immunity but also attacked normal melanocytes [95]. Haematological malignancies express clonally restricted products of the specialized cells of

origin, including Id Ig of B-cell neoplasms or clonal T-cell receptors of T cell tumours [91]. These are perfect tumour-specific antigens with no autoimmune outcome expected. However, a disadvantage of clone-specific targets is that vaccines have to be individual for each patient.

Overexpressed antigens on cancers represent attractive targets as an immune response to tumours can be elicited. *Her2/neu* (HER-2) is a proto-oncogene which shares homology with other members of the HER family of tyrosine kinase receptors and epidermal growth factor. It is overexpressed in around 30% of breast cancers associated with disease aggression and poor prognosis. Anti-tumour effects of Trastuzumab (Herceptin<sup>®</sup>, a humanized monoclonal antibody) in breast cancer are mediated by either inducing apoptosis (reviewed in [92]) or Fc receptor-mediated ADCC [96]. CD20 (described previously) is a differentiation antigen that is overexpressed in lymphomas and is also a target for passive antibody immunotherapy.

Some tumour antigens are expressed by a wide range of tumours. Cancer-testis antigens are found on male germ cells and are silent on healthy somatic cells, but expressed on a variety of tumours. They include the MAGE, BAGE, GAGE, RAGE and LAGE families, NY-ESO, PRAME and PASD1 [97-102]. Peptides associated with several human MHC class I haplotypes have been identified and clinical trials of vaccines against them are in progress (reviewed in [91]). Another example of a tumour antigen expressed by a wide range of tumours is MUC1, a transmembrane type I molecule found on almost all human epithelial adenocarcinomas. Some tumour cells express high levels of MUC1, with changes in glycosylation patterns that reveal core protein epitopes, masked in normal mucin. Cytotoxic T cells specific for the mucin have been detected in cancer patients, and can apparently act in an MHC-unrestricted manner [103].

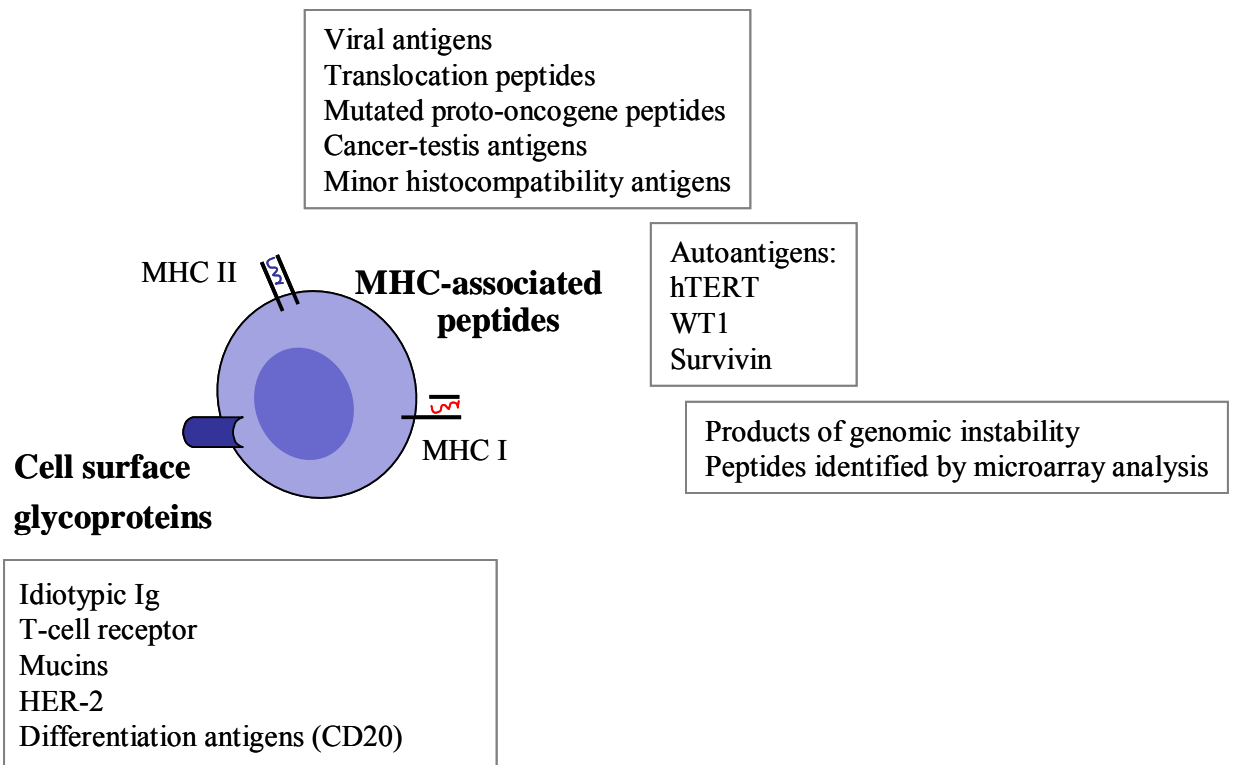


**Figure 1-4. Schematic diagram of target tumour antigens**

### 1.3.2 Immunogenicity of tumours and tumour antigens

The immune system can eliminate a tumour or suppress tumour growth by recognising tumour antigens and attacking the transformed cells. Spontaneous tumours express weak immunogens but the evidence of immune cells in control of tumour growth was shown in some tumours; the presence of some tumour infiltrating lymphocytes (e.g. CTLs and Th1 cells) correlates with good prognosis in colon cancer [104-105]. The tumour elimination may be complete or partial. If the immune system fails to completely eliminate tumour cells, tumour variants that can resist or suppress anti-tumour immune response then escape and emerge [106].

Tumours can escape detection and elimination by immune system by many ways. Tumours can induce T-cell tolerance, both central and peripheral. Central tolerance is achieved by the deletion of T cells with high affinity for tumour antigens during selection in the thymus. Tumour antigens that are not present in the thymus may induce peripheral tolerance by induction of antigen unresponsiveness (anergy), deletion of T cells that are chronically stimulated by antigen, and skewing of T-cell functional responses (reviewed in [106]). Tregs are involved in suppression of anti-tumour immunity. Tregs infiltrate many tumours, and the number of Tregs is increased in the blood and draining lymph nodes in patients with many different cancers (reviewed in [107]). Tregs inhibit tumour-specific CD4<sup>+</sup> and CD8<sup>+</sup> T-cell effector function by cell-cell contact or the production of suppressive cytokines, IL-10 and TGF- $\beta$  (reviewed in [107-108]).

T cells will fail to detect tumour if the tumour loses or down-regulates MHC molecules [109]. Tumours can further inhibit immune responses by producing immune suppressive factors (e.g. TGF- $\beta$  and IL-10) and express T-cell inhibitory molecules (e.g. B7H-1) [106, 110]. Some tumours can resist cytotoxic pathways; for example, tumour with mutations in death receptor Fas can resist Fas inducing apoptosis by T cells. In addition, tumour can induce and recruit host immune cells that suppress anti-tumour responses, such as tumour-associated macrophages and myeloid-derived suppressor cells (MDSCs) [111-112]. These suppressor cells express amino acid metabolising enzymes which affect T-cell activation. MDSCs express arginase 1 (ARG1) that cause L-arginine depletion and production of urea [112]. DCs and macrophages can be induced to express indoleamin 2,3-dioxygenase (IDO) which metabolises L-tryptophan and produces kinurenine. Expression of ARG1 and IDO suppresses a T-cell response by mechanisms including down-regulation of CD3  $\zeta$  chain expression, thus compromising TCR signalling [112].

As most tumours are weakly immunogenic and able to escape immune response, successful tumour vaccination must be able to break tolerance and induce effective anti-

tumour immunity. In many vaccination studies where both innate and adaptive immunity are activated, the ability to induce specific anti-tumour responses has been shown.

### **1.3.3 Vaccination Strategies**

#### **1.3.3.1 Protein and glycoprotein vaccines**

Exogenous protein or carbohydrate vaccines are expected to induce antibody responses. From clinical application in passive immunotherapy using monoclonal antibodies, antibody appears to play an important role in attacking tumour cells via surface molecules. examples include anti-CD20 against B cell tumours [113] and Herceptin, a monoclonal antibody against HER-2 [114]. In a clinical trial study using Id-Ig protein vaccine against B-cell tumours coupled to keyhole limpet hemocyanin (KLH), the vaccine can induce protective and therapeutic immunity, with the protection mediated largely by antibody [115]. In the mouse model, HER-2 protein vaccination in combination with an adjuvant also resulted in specific antibody production and this antibody mediated protection from the tumour challenge [116].

Adjuvants are important for immune induction by protein vaccines. Induction of CD4<sup>+</sup> or CD8<sup>+</sup> T-cell responses by protein vaccines may be achievable using appropriate adjuvants (reviewed in [91]). One example is the vaccination of Id-Ig KLH protein vaccine with granulocyte macrophage colony-stimulating factor (GM-CSF) adjuvant in follicular lymphoma patients where the vaccine induced both Id specific CD4<sup>+</sup> and CD8<sup>+</sup> T-cell responses [117].

The mechanism of tumour attack mediated by antibody has been studied using anti-CD20 monoclonal antibodies [50]. Binding of antibody to CD20 on the malignant B cell surface allows antibody to deliver an immunological attack from complement and FcR-expressing innate effectors such as macrophages [50]. In addition, there is evidence for a direct inhibitory signal via the B cell receptor [118]. An anti-Id antibody may dislodge tumour cells from the site in the germinal centre where maintenance signaling via the B cell receptor is occurring [119].

#### **1.3.2.2. Peptide vaccines**

Peptides bind to MHC molecules and then can induce a CTL response. The problems of peptide vaccines are that they lack immunogenicity and may be subjected to degradation. However, vaccination of melanoma patients with only MAGE-3A1 peptide led to a significant tumour regression in 7 out of 25 patients [120].

Immunogenicity of peptide vaccines can be enhanced to induce more CTL responses by amino acid modification at the MHC-binding residues [121], by inclusion of T-helper

epitopes [121], and by increasing peptide length. The advantage of using a long peptide is that it will be only taken up, processed and presented by dendritic cells (DCs) which then activate T cells. The presentation of CTL epitopes on B cells can induce a transient CTL response and subsequently deletion of these cells [121]. In addition, adjuvants could be included in peptide vaccination to improve immune induction and polarisation of T-cell immunity by DCs. Alternatively, specific peptides can be loaded onto DCs *in vitro* and cells reinfused (reviewed in [91]).

### **1.3.2.3 Vaccine adjuvants**

Adjuvants are compounds that enhance the specific immune response against co-inoculated antigen. Alum is the adjuvant most commonly used in human subjects and has been used for longer than 80 years [122-124]. The first evidence showing adjuvant activity of alum for the co-inoculated diphtheria toxoid was published in 1926 by Glenny *et al* (cited in [122] and [123]). In a study in melanoma patients, injection of melanoma peptide gp100, MART-1 and tyrosinase with adjuvant Montanide ISA 51 and alum with IL-2 induced higher levels of immune response to the peptides than injection without alum. Patients who responded to the peptides had lower risk of relapsing than those who did not have an immune response to the peptides [125].

Alum salts are aluminium-based compounds, principally aluminium phosphate or hydroxide. Studies suggest that alum works by causing the formation of an antigen depot at the inoculation site from where antigen is released slowly. The trapping of soluble antigen in the alum may also increase the duration of antigen interaction with the immune system (reviewed in [122]). Despite the long term use of alum and the knowledge that alum induces Th2 response, its adjuvanticity mechanism had not been revealed until a few years ago. Intraperitoneal injection of alum induces the local recruitment of monocytes, which migrate to the draining lymph nodes and differentiate into inflammatory DCs [126]. Cells damaged by alum release uric acid, the endogenous danger signal which known to trigger NALP3 inflammasome [127]. It has been shown that NALP3, ASC (apoptosis-associated speck-like protein containing a caspase recruitment domain) or caspase-1 (components of NALP3 inflammasome) knock-out (KO) mice failed to mount an antibody response to antigen administered with alum [128]. Therefore, alum adjuvanticity seems to act through NALP3 inflammasome. Activation of the NALP3 inflammasome induces transcriptional up-regulation of the pro-inflammatory cytokines IL-1 $\beta$  and IL-18 (reviewed in [129]) which thereafter enhances antibody production. However, the inflammasome may or may not be crucial for adjuvanticity of alum since there are evidences that Ig production against antigen administered with alum was not impaired in mice deficient in NALP3 [130-131].

The most potent adjuvant known is complete Freund's adjuvant (CFA), an emulsion of water and mineral oil containing killed mycobacteria (reviewed in [122]). The major active components of CFA are bacterial peptidoglycan (muramyl dipeptide) and bacterial DNA. These bacterial components are potent immune activators. They activate immune cells through several receptors including NLRs, receptors of bacterial peptidoglycan, and TLR9, DAI and AIM2, receptors of dsDNA. CFA is highly efficient in stimulating immune responses but it is not appropriate for application in humans, due to its damaging inflammatory effect (reviewed in [122]).

Incomplete Freund's adjuvant (IFA) has the same emulsion mixture as CFA but does not contain mycobacteria. Therefore, IFA is less toxic and has been used in human vaccine formulation ([132] and reviewed in [122]). Montanide ISA adjuvants are water-in-oil emulsions similar to IFA. Montanide adjuvants induce a similar antibody response to that of CFA and IFA with less inflammatory response (reviewed in [133])

#### **1.3.2.4. DNA vaccines**

In a DNA vaccine, the gene encoding a tumour antigen is incorporated into a plasmid backbone and then expressed by transfected cells *in vivo*. Although the transfection process is inefficient and varies with the target tissue and means of delivery, sufficient DNA is generally taken up to prime the immune response (reviewed in [134]). A leader sequence can be added in order to target a translated polypeptide to the endoplasmic reticulum, where post-translational modifications including glycosylation occur. Antigens produced and secreted by this route are efficient in inducing antibody response. For antigens aimed for CTL responses, antigens should be released to the cytosol where they will access the proteasomal degradation pathway for induction of peptide-specific CD8<sup>+</sup> T cell responses. Since vaccines containing a leader sequence also induce CD8<sup>+</sup> T cells, a leader sequence can be incorporated in all vaccine constructs (reviewed in [134]).

As plasmid DNA, DNA vaccines can stimulate innate immunity and then trigger the adaptive immune response. DNA vaccines can stimulate immune cells through TLR9, the first receptor identified for DNA. However, TLR9 KO mice are capable of responding to DNA vaccines (reviewed in [135]) as DNA can activate cells through other receptors, DAI and AIM2. In addition, RNA polymerase III transcription can yield dsRNA which can be recognised by RIG-1 [10, 135]. Activation of TLR9, DAI and RIG-1 results in secretion of pro-inflammatory cytokines and interferon type-I. Binding of dsDNA to AIM2 leads to formation of the AIM2 inflammasome which results in IL-1 $\beta$  and IL-18 secretion and pyroptosis [10, 135]. Therefore, DNA vaccines can activate innate immunity by many pathways.

The common method of DNA vaccine delivery is an intramuscular injection. It is likely that the encoded antigens expressed by transfected cells are presented to antigen presenting cells (APCs) by cross-presentation. Although at the skin sites, DNA can be delivered to Langerhans cells directly by using a gene gun; cross-presentation from keratinocytes might still be a major route. Host immune responses to the antigen incorporated in the vaccine consist of specific antibody and CD4<sup>+</sup> and CD8<sup>+</sup> T cells.

CD4<sup>+</sup> T cells play many roles in the immune system; they have a major role in helping B cells to produce antibody, in controlling induction of CD8<sup>+</sup> T cells and helping other CD4<sup>+</sup> T cells. Therefore, it is important to activate Th cells to amplify and maintain anti-tumour immunity. Tumour antigens themselves generally do not induce significant T-cell help. Microbial protein sequences fused to the tumour antigen sequence help to overcome this problem as they engage an available large Th cell repertoire (reviewed in [91, 134]). The fusion partners that have been used in our laboratory are fragment C of the tetanus toxin (FrC) and Potato Virus X coat protein (PVXCP) ([136] and are reviewed in [134]). Both of them induced specific immune responses to the fused Id B cell lymphoma single chain variable fragment (scFv) and protected mice from the tumour challenge.

FrC contains two linked domains (DOM1 and DOM2). The full-length FrC fused to the 3' end of the tumour antigen induced antibody and/or CD4<sup>+</sup> T-cell responses against the tumour. For induction of CD8<sup>+</sup> T cells, only DOM1, containing a MHC-II-binding peptide (p30), has been fused to the tumour antigen (reviewed in [134]). Interaction to FrC-specific Th cells is expected to licence the DCs presenting peptides from both FrC and tumour antigen to induce anti-tumour CD8<sup>+</sup> and CD4<sup>+</sup> T cells. The licensed DCs can survive in an active state and resist attack by CTL, maintaining a memory population to prevent tumour emergence (reviewed in [134]).

Clinical trials using DNA vaccines have been performed and showed encouraging clinical responses (reviewed in [135]). The vaccine design and delivery need to be optimized to achieve an effective immune outcome. The strategy of DNA priming and electroporation (EP) after DNA injection at boosting was proved to increase DNA vaccine efficiency [137]. In clinical trial, EP induced DNA vaccine-specific immune response (reviewed in [135]). DNA vaccination with EP is therefore a potential strategy for clinical vaccination.

### **1.3.3 Idiotypic vaccines**

For each malignant B-cell clone, Id Ig expressed on its surface is a tumour-specific antigen for that tumour. Therefore, the Id Ig can be used in tumour vaccination. The early Id vaccinations were performed in mouse B cell tumour models; the purified Id proteins co-

administered with CFA [138-139] or Id Ig coupled to KLH with or without adjuvant [140-142] induced anti-Id antibody and protected animals from tumour. Id Ig coupled to KLH in CFA was effective in therapy against the tumour [143]. In humans, anti-tumour immunity was observed from vaccination with Id Ig rescued from tumour cells which was coupled to KLH and injected with GM-CSF into patients [117]. In these experiments, cell surface Id Ig from lymphoma cells was rescued by fusion with a myeloma cell line. However, this vaccine production method requires long period of time, 3-6 months [144], and therefore is a hurdle in practical use.

The later molecular technology allows production of Id DNA vaccine encoding for Id single chain variable fragments (scFv). Since the idiotopes are in the variable domain of the Id Ig, only Id scFv has been used to raise immune response against the tumour. The idiotypic antigen alone may not be able to break tolerance and induce effective immunity against the tumours and addition of an immunogenic molecule into idiotypic vaccine is necessary. Id scFv DNA vaccines incorporated immuno-enhancing molecules such as FrC or PVXCP exhibited protective immunity against tumours [137, 145].

The developed molecular cloning technology also provides a faster way to produce Id Ig or scFv. The cloned Id genes can be expressed in bacteria, insect cells, mammalian cells, and plants, the vaccine yield is better than hybridoma technology mentioned earlier [144, 146]. However, the protein vaccine requires co-administration with other substances to enhance the Id immunogenicity. The immunogenicity of the Id antigen can be enhanced by chemical conjugation to powerful immunogenic carrier KLH, co-administration with granulocyte-monocyte colony-stimulating factor (GM-CSF) and/or adjuvant [144, 146-147].

The mechanism of Id vaccination appears to involve both humoral and cellular immunity, in which induced anti-Id antibodies or possibly Id specific CTLs are able to destroy tumour cells (figure 1-5). In many models, Id vaccines can induce both humoral and cellular immune responses against tumour. As mentioned earlier, DNA vaccines are able to induce antibody production and specific T cells [134]. Id protein vaccines (Id Ig-KLH with GM-CSF [117, 144], Id Ig with CFA[138], Id scFv with GM-CSF [146]) also induced Id-specific antibody and T cells with some studies [117, 138] showed detection of Id-specific CTLs. Anti-Id antibody was shown to play an important role in protection against lymphoma [138, 148]. One possible mechanism by which anti-Id antibody destroys tumour cells is via ADCC as the patients with the Fc $\gamma$ RIIIA genotype that is predicted to bind more strongly to Fc responded to the vaccine better than patients with different genotypes [81].

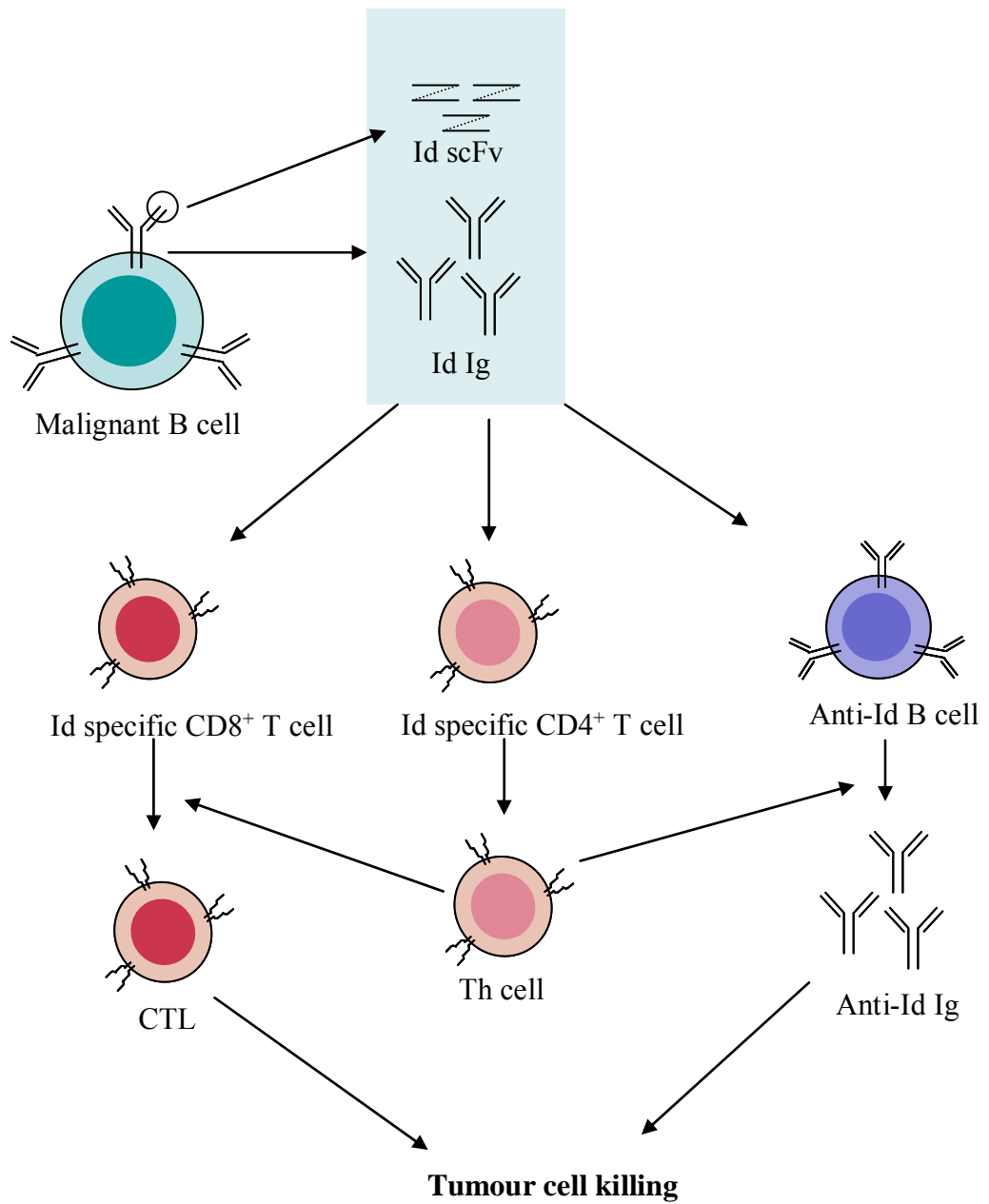


**Figure 1-5. Id vaccine mechanism**

Id Ig or Id scFv vaccine induces anti-Id antibody production and activates T cells. Activated Th cells provide help to antibody production by B cells and CTLs. Anti-Id antibody is likely to be the main mechanism for tumour elimination.

## **1.4 Plant virus-based vaccines**

Plant viruses are becoming increasingly popular as carrier molecules in vaccine preparation. However their usage for vaccines against cancer has been very limited. Plant viruses have multiple, thousands in some viruses, coat protein (CP) subunits that encapsidate the RNA genome (figure 1-6). Linking of antigenic peptide to the viral CP will lead to display of the antigen on the plant viral particle (PVP). This therefore provides benefit of concentrating and aggregating the antigen and together with a carrier effect provided by virus. RNA could potentially contribute to immunogenicity by activating innate immunity through TLR signalling.

Plant virus particles have been used to display various peptide antigens derived from animal pathogens and these used as vaccines showed ability to induce both humoral and cellular immunity [149]. Papaya mosaic virus (PapMV) displaying a lymphocytic choriomeningitis virus (LCMV) CTL epitope is an example of the plant virus-based vaccine that successfully induced immune response. Vaccination of the PapMV-based vaccine without adjuvant was able to induce specific CTLs and provided protection against the viral infection [150]. In the tumour model, chemically or genetically linking of tumour derived T-cell epitope to tobacco mosaic virus (TMV) induced IFN- $\gamma$  producing T cells and prolonged survival of tumour challenged mice [151-152].

By using genetic engineering technology, the plant virus-based vaccine can be expressed in the host plants. The target antigenic peptides are expressed as in-frame fusions with the viral CP and the antigens are displayed on the surface of the viral particle without interfering with the ability of the modified CP to assemble into particles. These chimeric virus particle (CVP) coated with antigenic peptides can be further purified and used for vaccination.

### **1.4.1 TMV CVPs**

TMV is a rod-shaped virus containing a monopartite 6.4 kb genome encoding up to five proteins, including a movement protein and a CP which are both translated from subgenomic RNAs (reviewed in [149]). TMV wild-type virus particle contains 2,130 copies of the CP display. Initial chimeric TMV production by fusion of the foreign epitope to the C-terminus of CP was unsuccessful because the recombinant coat protein subunits did not assemble into stable virus particles [153]. This problem was addressed by developing a system in which both the wild-type and epitope-containing CPs combined to form heteromeric virus particles. This was achieved through the introduction of a leaky termination codon (reviewed in [149]). Fusion of a peptide to the C-terminus of TMV resulted in up to 5% of the foreign peptide displayed (figure 1-7, C). In addition, it has

proved possible to produce CVPs in which all the CP subunits carry peptides by insertion of peptide at other positions. Insertion after residue 154 (figure 1-7, B) and between residue 63 and 66 (figure 1-7, A) of CP provide 100% of foreign peptide displayed. In all identified insertion sites, only small peptides (up to 13 amino acids) can be displayed on TMV.

Fitchen *et al.* published in 1995 the first analysis of the immunogenicity of chimeric TMV particles. Thirteen amino acids from the glycoprotein ZP3 from the murine zona pellucida were fused to TMVCP. Mice immunized parenterally with chimeric TMV in the presence of monophosphoryl-lipid A-Trehalose dicorynomycolate (MPL-TDM) adjuvant produced serum antibody to the ZP3 epitope [154]. Using the vector developed by Fitchen *et al.*; Koo *et al.* were able to produce chimeric TMV presenting 10 and 15 amino acids epitopes from mouse hepatitis virus (MHV) [155]. Mice immunized with purified CVPs produced antibodies against the MHV epitope, and those with high antibody titers were protected against challenge with the virus.

#### **1.4.2 Cowpea mosaic virus (CPMV) CVPs**

CPMV structure is very well characterized. Sixty copies each of two CP subunits (L and S) are arranged to form an icosahedral capsid surrounding a bipartite RNA genome. The CPMV genome is composed of bipartite RNA, RNA1 and RNA2. RNA1 contains genes for a protease cofactor, helicase, protease and replicase. RNA2 contains the movement protein gene and genes for CP L and CP S subunits. For the aim of epitope display on the viral particle, in most cases, the sequence of interest can be inserted in both CP S and L genes. Upon viral assembly, the epitope would be displayed on the outer surface of viral particles (reviewed in [149] and [156]).

CPMV was used to display a 17 amino acid epitope from the VP2 capsid protein of canine parvovirus (CPV) in which the sequence is identical in mink enteritis virus (MEV), and feline panleukopenia virus (FPLV), the viruses that infect cats, dogs, mink and raccoons. Immunization with the CVP protected minks and dogs from the viral disease ([157] [158]). In mice, the vaccine induced Th1 responses as determined by IgG2a predominance, and the release of IFN- $\gamma$  but not IL-4 and IL-5. Immunised mice produced both anti-viral and anti-peptide IgA and serum antibody showed neutralising activity against CPV in vitro [159]. Mice and rats immunised with CPMV CVP displayed the D2 peptide derived from an *S. aureus* fibronectin-binding protein (FnBP) produced high titers of specific antibody of IgG2a and IgG2b isotypes in mice. Rat sera against the CVP were able to block adherence of *S. aureus* to fibronectin, indicating the potential to neutralise the infection [160].

### 1.4.3 Potato virus X (PVX) CVPs

PVX is a filamentous (modal length of about 515 nm and 13.5 nm in diameter) plant virus infecting many *solanaceous* species. PVX is classified into Potexvirus genus, Flexiviridae family [161]. About 1300 identical protein subunits form a helical array with the 6.4 kb viral RNA packed between the turns of the helix. There are 8.9 subunits per turn of a primary helix. The RNA genome of PVX contains five open reading frames (ORFs) [162]. They encoded a replicase, three movement proteins referred to as TGBp1 (Triple-gene block protein 1), TGBp2 and TGBp3, and a 236-residue CP. The method of thermally activated tritium atoms and immunoassay revealed that the N-terminus of the CP (residues 1 to 56) was exposed on the virus surface, and this region forms a highly immunogenic virus-specific antigenic region [163].

Work on another member of the Potexvirus family, the papaya mosaic virus (PapMV), gives insight into assembly of the virus. Individual CP subunits self-assemble first into helical discs and then into virus particles [164-165]. Packaging occurs when these discs bind RNA and then assemble along the central RNA into full-length virions [165]. Virion assembly is triggered when cells contain a sufficient supply of discs and viral RNA in a cell.

One advantage of the PVX over other plant viruses is that a large protein can be fused to the N-terminus of PVXCP to produce CVPs displaying the antigen of interest. In order to produce CVP displaying long polypeptide, a mixed population of free wild-type CPs and fused CPs is required. The 2A peptide of the aphthovirus Foot-and-Mouth Disease Virus (FMDV) sequence was used for this purpose. The FMDV2A peptide occasionally mediates a ribosomal skip from one codon to the next without the formation of a peptide bond [166]. Therefore, when FMDV2A sequence is inserted between the foreign gene and the PVXCP gene, some foreign protein-FMDV2A portions and free PVXCPs are produced apart of the full length fusion proteins. Using this strategy, it was shown that a modified form of PVX, PVX.GFP-CP which expressed a chimeric gene encoding a fusion between the 27-kDa *Aequorea Victoria* green fluorescent protein (GFP) and the amino terminus of the 25-kDa PVXCP, assembled into virions and moved both locally and systemically [167]. Other examples are the fusion of 397 amino acid of Rotavirus VP6 [168] or a scFv against the herbicide diuron to PVXCP [169]. In each case, the fusion protein is successfully assembled into CVPs. However, the immunological properties of purified CVPs have not been studied.

In 2001, Marusic *et al.* showed that CVPs which incorporate the human immunodeficiency virus type 1 (HIV-1) ELDKWA epitope from glycoprotein 41 were able to elicit high levels of HIV-1 specific immunoglobulin G (IgG) and IgA antibodies [170]. In

severe combined immunodeficient mice reconstituted with human peripheral blood lymphocytes (hu-PBL-SCID), the CVPs were used to pulse autologous dendritic cells and then to immunise mice. The immunised mice were able to produce a human antibody specific to the HIV-1 epitope. Moreover, sera from both normal mice and hu-PBL-SCID mice showed an anti-HIV-1 neutralising activity.

PVX has been also utilised to present multiple small epitopes [171]. Two different 7 amino acid epitopes, ep4 and ep6, from the beet necrotic yellow vein virus (BNYVV) were able to express as N-terminal CP fusions and were displayed on the surface of PVX particles. And the mixed infection with PVX vectors containing the individual ep4 and ep6 sequences resulted in the formation of PVX particles displaying ep4 alone, ep6 alone, or both epitopes.

Moreover, PVX was able to display a 38 amino acid long peptide, D2 peptide derived from an *S. aureus* fibronectin-binding protein (FnBP). The CVP induced IgG2a and IgG2b antibody specific to FnBP in mice and the mouse serum was shown to inhibit the binding of fibronectin to the immobilised FnBP [160]. Recently, the vaccine of PVX displaying CTL epitope of influenza virus was produced and it showed ability to activate specific CD8<sup>+</sup> T cells [172].

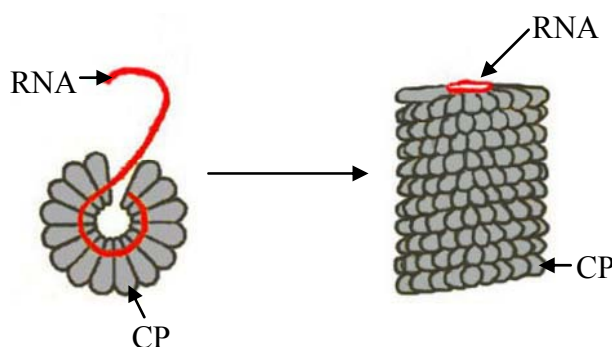


**Figure 1-6. Schematic diagram of rod-shaped plant virus**

Plant viral genome is shown in red and encapsidated by multiple copies of coat protein (CP). Viral CPs are arranged along the viral RNA (left) to form a rod-shaped particle (right).

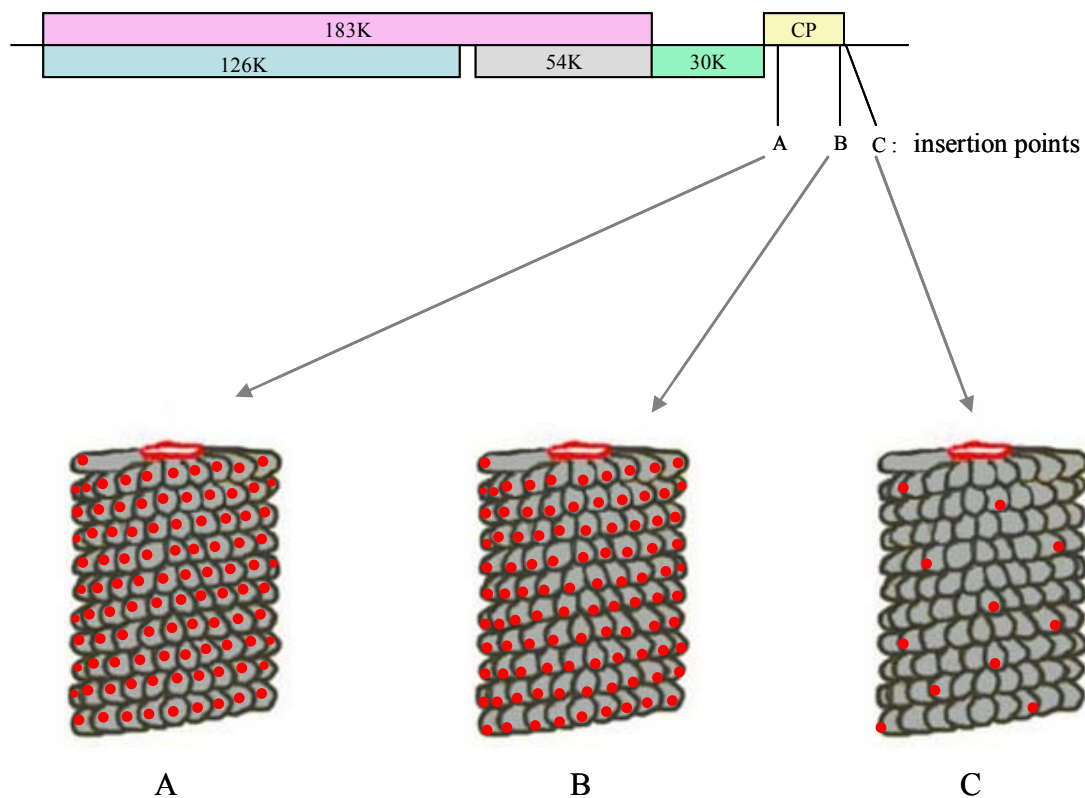


**Figure 1-7. Schematic diagram of TMV CVP production**

Foreign oligonucleotide sequences are inserted at one of three positions, labeled A, B and C, in the gene of the TMV coat protein. The resulting chimeric TMV virus particle with inserted peptide (red dot) displaying on the CVP is shown.

## 1.5 Plant viral vectors for vaccine production in plants

Historically, bacteria were often the protein expression system of choice and yeast cells or baculovirus-infected insect cell systems were of minor importance (reviewed in [173]). A classic example is the expression of recombinant insulin in bacteria using the advantage that human insulin is a small polypeptide requiring only minimal post-translational processing to become functional (reviewed in [173]). While the bacteria are an inexpensive and convenient production system, they are incapable of most of the post-translational modifications necessary for the activity of many mammalian proteins [174]. In addition, recombinant protein produced in bacteria requires efficient elimination of bacterial endotoxin. Mammalian cell culture provides the benefit of correct post-translational modification but this system requires expensive media and supplements and animal pathogen contamination is possible (reviewed in [173] and [175]).

Plants become an attractive expression system because they offer high yield of protein with low cost of production. The amount of specific protein produced in plants can go up to several hundred micrograms per gram fresh weight of plant tissue [176]. In addition, protein preparations from plant cells are not subject to contamination with animal pathogens. Moreover, plant cells carry out higher eukaryotic post-translational modification that allows proper folding, disulfide bond formation and glycosylation of proteins. Although plant glycosylation pattern is different from mammalian cells (reviewed in [175] and [177]), many publications show that protein vaccines produced in plants are able to induce protective immune responses in animal models (reviewed in [178]).

The first strategy for expressing foreign proteins in plants is stable genetic transformation by integration of the gene of interest into the plant genome. The establishment of a permanent transgenic plant requires a long period of time as it involves transformation and several generations of breeding to achieve a suitable number of plants for production. Other drawbacks of protein production in a transgenic plant are the low yield of required proteins and concerns about transgene escape into the environment (reviewed in [178]).

Another approach is the use of plant virus-based vectors. This strategy provides an advantage since the viral genome is small and therefore easy to manipulate (reviewed in [149, 178]). The infection of plants with recombinant viruses is simple and a large scale production can be developed in a short period of time. The protein expressed from a viral vector is processed in the same manner as endogenous plant proteins. Therefore, appropriate folding, targeting and post-translational modification of the protein is possible.

The vaccine could be produced by two major strategies of foreign protein production using plant virus-based vectors. In the first strategy, the target antigen is engineered as a

discrete reading frame in the viral genome and expression is directed by a subgenomic RNA promoter, giving soluble heterologous protein product. In the second strategy, the target antigen is expressed as in-frame fusion with the viral CP, resulting in the display of heterologous epitopes on the surface of CVP (figure 1-8).

The soluble heterologous protein expressed in plants can be purified, usually by affinity chromatography, from plant endogenous proteins and viral particles. Examples of protein vaccines produced in plants using plant virus-based vector are shown in table 1-5. The earlier plant virus expression systems were based on the DNA virus, Cauliflower Mosaic Virus (CaMV). However, CaMV-based system has limited packaging capacity and a restricted amount of viral DNA that can be removed without affecting essential functions.

The most widely used vectors are derived from RNA viruses including TMV, PVX and CPMV. TMV and PVX contain single RNA genomes and are rod-shaped particles which provide fewer constraints on the amount of the inserted nucleic acid [179]. TMV and PVX-based vectors have duplicated subgenomic promoter placed upstream of a cloning site, between the movement protein and CP genes (figure 1-8A), for transgene insertion. The virus is able to replicate and assemble correctly, and produce soluble heterologous protein [178]. Recently, a high yield of IgG (0.5g/kg fresh plant tissue) was produced in plants using an expression system of mixed vectors derived from non-competing viruses, TMV- and PVX-based vectors [180]. One vector expressed the heavy chain and the other expressed the light chain; the assembled IgG was functional and the first gram of IgG could be obtained within two weeks.

CPMV contains two RNA genomes, RNA-1 and RNA-2. While RNA-1 is encoded for proteins involved in replication, RNA-2 is encoded for the movement and structural proteins. The gene of interest can be inserted into RNA-2 with the addition of FMDV2A inserted between the target protein and the viral CP [181]. As mentioned earlier, the FMDV2A peptide occasionally mediates a ribosomal skip from one codon to the next without the formation of a peptide bond. Therefore, when FMDV2A sequence is inserted between the foreign and the viral genes, free foreign proteins are released from time to time. Recently, the high expression system, named HyperTrans, with the expression vector based on deleted version of CPMV RNA-2 was developed [182]. In this approach, the majority of the coding region of RNA-2 was replaced by a gene of interest. Therefore, a large protein sequence could be inserted and the virus particles were not produced, this prevents possible environment containment concerns. This newly developed vector provided a high level of heterologous protein expression; approximately 1 g protein/kg of plant tissue was produced in the host plants.

Many publications showed successful heterologous protein production in plants, some examples are shown in table 4. Most of the proteins produced in plants are derived from pathogens of infectious diseases with some examples of anti-pathogen antibody. One example is the production of virus-associated tumour antigen, human papillomavirus (type16) E7 protein, from the PVX-based vector. The protein was able to induce humoral and cellular responses, and protected vaccinated mice from tumour development after challenge with the E7-expressing C3 tumour cell line [183]. IgA against transmissible gastroenteritis coronavirus (TGEV) is an example of antibody production in plants. It was produced with the strategy that individual light and heavy chains were inserted into separate PVX constructs. Plants co-infected with both constructs produced full size IgA which protected piglets against challenge with TGEV [184].

The data on the production of antigen expressed by tumour cells are limited. The examples are production of the Id single-chain variable fragment (scFv) expressed by 38C13 mouse B-cell lymphoma and human non-Hodgkin's lymphoma. Mice vaccinated with purified 38C13 scFv generated anti-Id IgG and were protected from tumour challenge [185]. Similarly, Id scFv specific for individual Non-Hodgkin's lymphoma patients was successfully produced in plants. In a clinical trial, patients immunized with Id scFv by subcutaneous injection in conjunction with GM-CSF generated humoral and cellular responses [146].

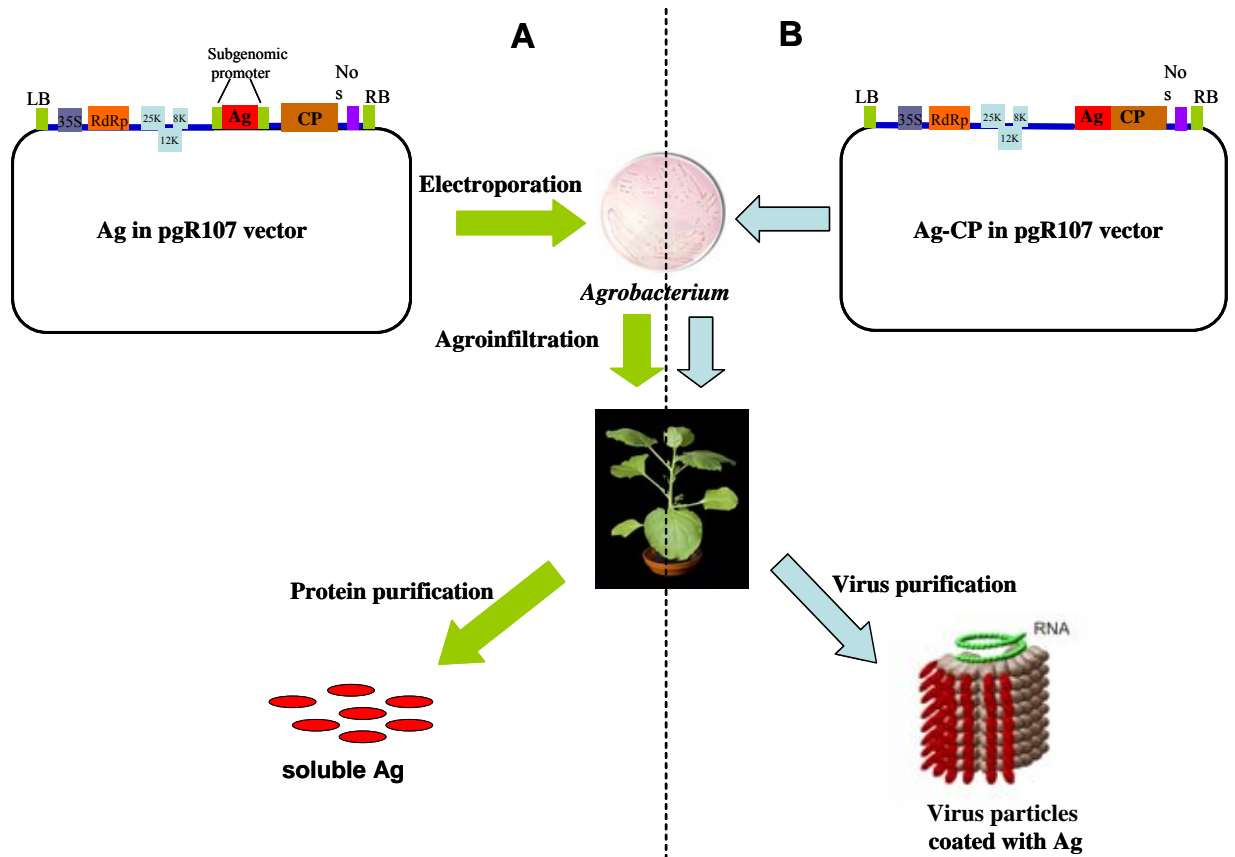


**Figure 1-8. Expression of foreign protein using a plant virus-based vector**

A. Production of target antigen as soluble protein. The antigen gene is expressed under the control of subgenomic promoters. Therefore, antigen protein is produced as free soluble protein in the plant tissue.

B. Production of CVP incorporating target antigen. The target antigen (Ag) gene is fused in-frame with the viral CP gene in the viral vector. The CVP coated with target antigen is accumulated in plant tissue and can be purified by established virus purification methods.

In both A and B, the vector is transformed into *Agrobacterium tumefaciens* which is then used to infiltrate young plants. *Agrobacterium* facilitates targeting the vector to plant cell nucleus where the vector will start expressing viral genes including the antigen gene or the fusion antigen-coat protein gene.

LB and RB represent left and right border of *Agrobacterium* T-DNA, respectively. 35S: the 35S RNA promoter, RdRp: the virus RNA-dependent RNA polymerase gene, 25 K, 12 K and 8K: Movement protein genes, CP: the PVXCP gene, Nos: the transcriptional terminator of the nopaline synthase gene of *A. tumefaciens*.

vector	polypeptide	Immune outcome	reference
TMV	Foot and mouth disease virus VP1	Mice protected against virus challenge after vaccination with VP1 in the presence of CFA	[186]
	Betv ( pollen antigen)	Injection with crude leaf extracts generated specific IgE and IgG1 antibody, and positive skin test reaction	[187]
	Norwalk virus	Partially purified Norwalk virus-like particles induced specific serum IgG and vaginal IgA	[188]
	Cottontail rabbit papillomavirus (CRPV) L1 capsid protein	Vaccinated rabbits produced CRPV-specific antibody and the rabbits were protected from wart development	[189]
	<i>Plasmodium yoelii</i> merozoite surface protein 4/5 (PyMSP4/5)	Vaccinated mice produced PyMSP4/5-specific antibody	[190]
	38C13 scFv specific to the 38C13 mouse B-cell lymphoma	Mice vaccinated with purified 38C13 scFv generated anti-Id immunoglobulins and were protected from challenge by a lethal dose of the syngeneic 38C13 tumour.	[185]
	Idiotypic Non-Hodgkin's lymphoma ScFv	Patients immunized in conjunction with GM-CSF developed cellular response and humoral response	[146, 191]
CPMV	Anti-coronavirus antibody	No data	[184]
	Nucleocapsid protein (HBcAg) of hepatitis B virus	No data	[176, 182]
PVX	Human papillomavirus (type16) E7 protein	Vaccinated mice generated humoral and cellular responses, and were protected from tumour development after challenge with the E7-expressing C3 tumour cell line	[183]
	ScFv against tospoviruses	No data	[192]
	Anti-coronavirus antibody	The TGEV titer in piglets was reduced after administration of the antibody	[184]
	Tuberculosis antigen ESAT-6	No data	[193]

**Table 1-5. Production of protein vaccine by using plant virus-based vector**

## Chapter 2. Materials and Methods

### 2.1 ScFv.BCL<sub>1</sub>-PVXCP fusion protein vaccine expression in plants

#### 2.1.1 Assembly of Special K.scFv.BCL<sub>1</sub>-PVXCP expression plasmids

In order to express scFv.BCL<sub>1</sub>-PVXCP fusion protein in plants, recombinant scFv.BCL<sub>1</sub>-PVXCP was constructed in 3 different contexts (figure 2-1), scFv.BCL<sub>1</sub>-PVXCP, Leader-scFv.BCL<sub>1</sub>-PVXCP or Leader-scFv.BCL<sub>1</sub>-PVXCP-HDEL, within the Special K (SK) plasmid provided by Dr. George Lomonosoff (John Innes Centre (JIC), Norwich) [194]. Cloning of a fusion gene into the SK plasmid requires 2 steps. First, the fusion gene was inserted into pM81-FSC2-GFP-HT cloning vector via the *NruI* and *XhoI* sites. The next step was insertion of the *AscI*, *PacI* digested fragment containing fusion gene into SK plasmid.

The fusion genes were amplified by polymerase chain reaction (PCR) using primers listed in table 2-1. The DNA vaccine pcDNA3.scFv.BCL<sub>1</sub>-PVXCP was used as the template. ScFv.BCL<sub>1</sub>-PVXCP sequence was amplified by PCR with *NruI* BCL<sub>1</sub> FWD and PVX REV primers. Leader-scFv.BCL<sub>1</sub>-PVXCP was amplified with *NruI* L FWD and PVX REV primers. Leader-scFv.BCL<sub>1</sub>-PVXCP-HDEL was amplified with *NruI* L FWD and HDEL PVX REV primers. The respective PCR product was inserted into *NruI* and *XhoI* linearised pM81.FSC2-GFP-HT. JM109 competent cells were transformed with the recombinant plasmids and the bacterial colonies that grew on Luria agar plates with 100 µg/ml ampicillin (Sigma-Aldrich Company Ltd, Gillingham, UK) were screened by PCR using cloning primers and the DNA sequence was verified.

In the second cloning step, the DNA fragment containing each recombinant scFv.BCL<sub>1</sub>-PVXCP sequence was separated from pM81 plasmid by *PacI* and *AscI* digestion and ligated to *PacI* and *AscI* linearised SK plasmid. JM109 competent cells were transformed with the ligated plasmid and the bacteria were plated out on agar with 50 µg/ml kanamycin (Sigma-Aldrich); colonies were subjected to PCR screening and subsequently DNA sequence analysis was performed.

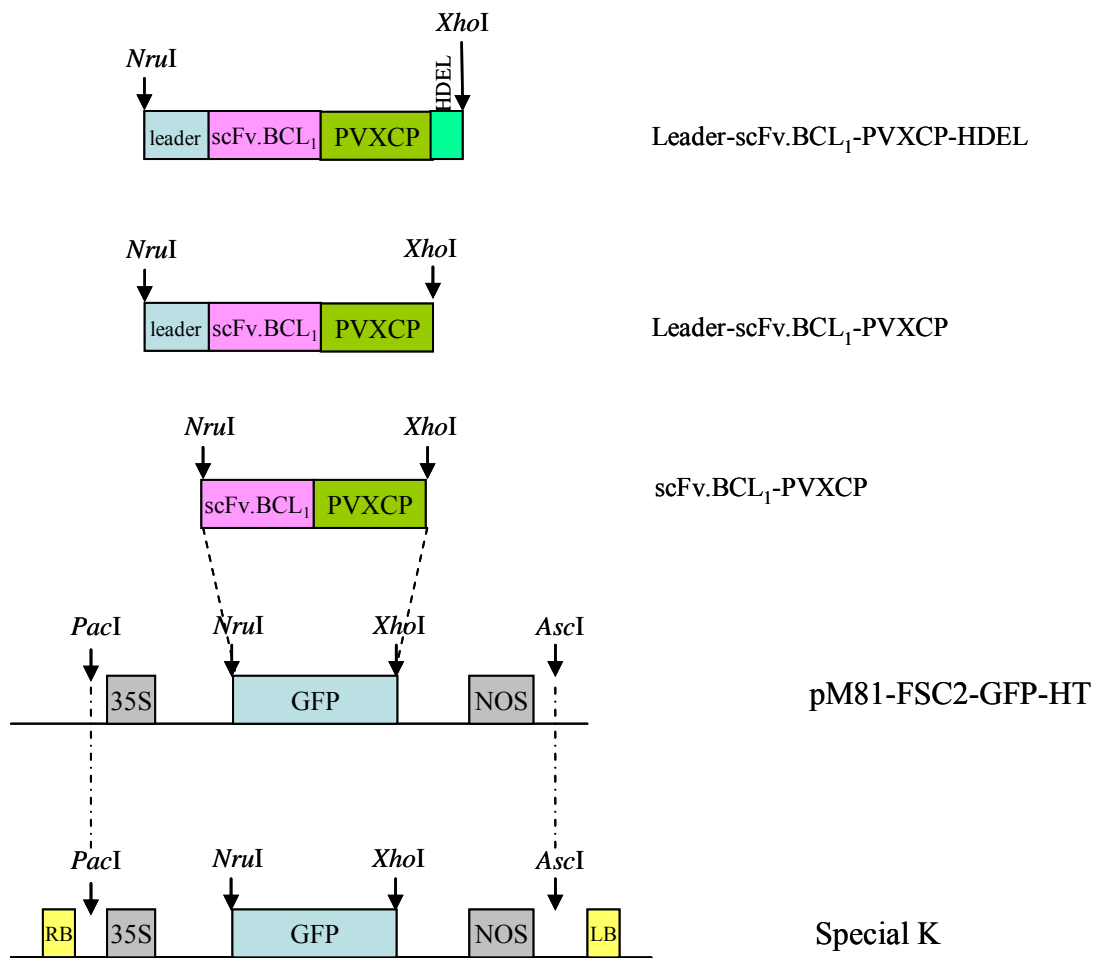


**Figure 2-1. Schematic diagram showing double step cloning of scFv.BCL<sub>1</sub>-PVXCP into Special K plasmid**

The scFv.BCL<sub>1</sub>-PVXCP, Leader-scFv.BCL<sub>1</sub>-PVXCP or Leader-scFv.BCL<sub>1</sub>-PVXCP-HDEL fragment was amplified by PCR and initially inserted into *Nru*I/*Xho*I linearized pM81-FSC2-GFP-HT. The *Pac*I/*Asc*I fragment containing each recombinant scFv.BCL<sub>1</sub>-PVXCP was subsequently ligated into *Pac*I/*Asc*I linearized Special K plasmid.

### 2.1.1.1 Polymerase chain reaction (PCR)

All PCRs were carried out with HotStart Taq® (QIAGEN, Crawley, UK). The cloning primers used in this work are listed in table 2-1; all primers were ordered from Sigma-Aldrich Company Ltd. PCR reactions were performed in a total volume of 50 µl and contained 2.5 Units of HotStarTaq™ DNA polymerase, 0.1 mM dNTP, 0.4 µM of each primer and 1X buffer (containing Tris-Cl, KCl, (NH<sub>4</sub>)<sub>2</sub>SO<sub>4</sub>, 1.5 mM MgCl<sub>2</sub>, pH 8.7). All PCR reactions were set up in a laminar flow cabinet to minimize the risk of contamination.

The PCR cycle conditions were 95°C for 15 min followed by 30 cycles of denaturing at 95 °C for 45 sec, annealing at 51°C for 45 sec, and extension at 72°C for 1 min and 30 sec. A final step was carried out at 72°C for 7 min.

primer	Sequence 5' to 3'
PVX FWD	AT <u>TCCGGA</u> <u>AATTTTGACCTTCTTAAGCTTGCGGGAGACGTCGAGTCCA</u> <i>BspEI</i> <i>FMDV2A</i> <u>ACCCTGGG</u> <u>CCAGCCAACAACACTCAA</u> <i>PVXCP4</i>
PVX REV	AC <u>CTCGAG</u> <u>TTATGGTGGGGGTAGTGA</u> <i>XhoI</i> <i>PVXCP4</i>
BCL FWD	GCATCA <u>ATCGAT</u> <u>GCCACC</u> ATG <u>CAGGCTGTTGTGACTCAG</u> <i>ClaI</i> <i>KOSAK</i> <i>BCL</i>
<i>NruI</i> L FWD	CATTTA <u>TCGCGA</u> <u>TGGGCTGGAGCCTGATC</u> <i>NruI</i> <i>Leader sequence</i>
<i>NruI</i> BCL FWD	CATTTA <u>TCGCGA</u> <u>TGCAGGCTGTTGTGACTCAG</u> <i>NruI</i> <i>BCL</i>
HDEL PVX REV	AC <u>CTCGAG</u> <u>TTA</u> <u>AAGTTCATCATG</u> <u>TGGTGGGGGTAGTGAAAC</u> <i>XhoI</i> <i>Stop</i> <i>HDEL</i> <i>PVXCP4</i>

**Table 2-1. Cloning primers**

### 2.1.1.2 Restriction enzyme digestion

PCR products or plasmids were double digested by using enzymes and recommended buffers (listed in table 2-2) containing 0.1 mg/ml BSA, according to the manufacturer's instructions (New England Biolabs (UK) Ltd, Hitchin, UK). The reactions were performed at 37°C for 1 h and enzymes were heat inactivated at the temperature indicated in table 2-2. After restriction enzyme digestion, the large plasmid backbone was separated from the small DNA fragment by agarose gel electrophoresis and then extracted from the agarose gel for further ligation.

<b>Enzymes</b>	<b>Buffer</b>	<b>Heat inactivation</b>
<i>Nru</i> I and <i>Xho</i> I	Buffer 3	65 °C
<i>Pac</i> I and <i>Asc</i> I	Buffer 4	65 °C
<i>Bsp</i> EI and <i>Xho</i> I	Buffer 3	80 °C
<i>Cla</i> I and <i>Xho</i> I	Buffer 4	65 °C

**Table 2-2. Restriction enzymes**

### 2.1.1.3 Agarose gel electrophoresis

A PCR product or a digested plasmid was separated on an agarose gel prepared from 1% agarose in TAE buffer (4.84 g of Tris, 1.14 ml of acetic acid, 2 ml of 0.5M EDTA in 1 L dH<sub>2</sub>O) plus ethidium bromide. The electrophoresis was performed at constant 100 V for approximately 40 min. The DNA was visualized using either the Gel Doc It™ Imaging System (UVP, Cambridge, UK) or the Chemi Doc (Bio-Rad, Hemel Hempstead, UK). The Hyperladder I marker (Bioline, London, UK) was used to estimate the size of PCR products or linearised plasmids.

#### **2.1.1.4 Gel extraction**

After gel electrophoresis PCR products or linearised plasmids of the correct size were cut out and purified with the QIAquick<sup>®</sup> Gel Extraction Kit (QIAGEN) following the manufacturer's guideline. Briefly, the agarose gel piece containing the desired PCR product or plasmid fragment was melted at 50°C for approximately 10 min in QC buffer (the volume required was 3 times the weight of the gel piece). Once the gel was dissolved, one time the gel weight of isopropanol was added and then placed onto spin columns. DNA within the solution bound to the silica membrane and the loaded columns were centrifuged at 14,000 rpm using the Eppendorf Centrifuge 5417R (Eppendorf AG, Hamburg, Germany) to remove the waste gel solution. The column was washed with 750 µl of PE buffer before DNA elution with 30 µl of the elution buffer.

#### **2.1.1.5 Ligations**

All ligation reactions were performed in a 10 µl reaction volume with T4 DNA ligase (Promega, Southampton, UK). The molar ratios of the insert to the vector varied from 3:1 to 5:1 but 100 ng of vector was always used per reaction. The ligation reactions were incubated overnight at 4°C. The reactions were inactivated at 70°C for 10 min prior to JM109 cell transformation.

#### **2.1.1.6 Transformations**

Ten microlitres of a ligation reaction was transformed into 100 µl of JM109 competent *E. coli* cells (Promega). The cells were incubated on ice for 30 min before being subjected to a heat shock at 42°C for 45 sec. They were then incubated on ice for a further 2 min before the addition of 900 µl of Luria Broth (LB) (Sigma-Aldrich). The transformed cells were then incubated at 37°C for 1 h. The cells were pelleted by centrifugation at 1,000 x g for 10 min, then 900 µl of LB was discarded using a pipette. The cell pellet was resuspended in the remaining media and spread on a Luria agar plate containing 100 µg/ml of ampicillin (Sigma-Aldrich) for bacteria transformed with pM81-based constructs, or 50 µg/ml of kanamycin (Sigma-Aldrich) for bacteria transformed with SK-based constructs. Plates were incubated at 37°C overnight to allow bacterial growth. Bacterial colonies were further screened by PCR.

### **2.1.1.7 Colony PCR screening**

After overnight growth on a Luria agar plate containing a selective antibiotic, individual bacterial colonies were picked and resuspended in 50 µl LB containing the same antibiotic. Ten µl of the suspension was used as a template in a PCR screening reaction. The PCR products were subjected to an agarose gel electrophoresis to verify the size of the expected PCR product.

### **2.1.1.8 Small scale bacterial culture**

Following PCR screening, positive bacterial colonies were seeded into a universal tube containing 5 ml of LB containing selective antibiotic. The bacterial cultures were incubated at 37°C overnight. The overnight cultures were subjected to small scale plasmid purification.

### **2.1.1.9 Small scale plasmid purification (Miniprep)**

Plasmid DNA was purified from a small scale bacterial culture by using QIAprep® Spin Miniprep Kit (QIAGEN) following the manufacturer's protocol. Briefly, 5 ml of each culture was centrifuged at 10,000 x g for 5 min and resuspended in 250 µl of P1 resuspension buffer. The bacterial cells were lysed with 250 µl of P2 lysis buffer followed by neutralization with 350 µl of N3 buffer. The lysate was centrifuged at 15,000 x g for 10 min and the plasmid-containing supernatant was loaded onto a spin column for the DNA to be adsorbed to the silica membrane. The columns were centrifuged and washed in PB binding buffer and PE washing buffer before DNA elution into 100 µl of the elution buffer.

### **2.1.1.10 DNA sequencing**

DNA sequencing was performed using the ABI Prism Big Dye Terminator v1.1 Cycle Sequencing Kit (Applied Biosystems, Warrington, UK). Reactions used 2 µl BigDye Terminator Ready Reaction Mix (A-dye, C-dye, G-dye and T-dye terminators labeled with dichloro[R6G],[ROX],[R110], and [TAMRA] respectively; dNTPs [dATP], [dCTP], [dGTP], and [dTTP]; AmpliTaq DNA polymerase), 1X sequencing buffer (80 mM Tris-HCL, pH 9.0; 2 mM MgCl<sub>2</sub>), 1 µl of DNA from Miniprep, 1 µl of 20 µM primer (table 2-3) and were made up to a 10 µl volume with water. Cycling conditions were denaturation at 94 °C for 10 sec, primer annealing at 50 °C for 50 sec and extension at 60 °C for 4 min, for 25 cycles. The sequencing reactions were precipitated by mixing with 2 µl of 3M sodium acetate pH 5.3 and 30 µl of absolute ethanol, incubating on ice for 10 min and centrifuging at 14,000 rpm with Eppendorf Centrifuge 5417R (Eppendorf AG) for 30 min at 4°C. The DNA pellet was washed with 200 µl of 70% ethanol and centrifuged for another 5 min. The

ethanol was discarded and the DNA pellet was air-dried and then resuspended in 10 µl of formamide. The DNA sequencing reaction was run on the 3130xl Genetic Analyzer (Applied Biosystems). The DNA sequences were analyzed with MacVector™ 7.2.3 software.

<b>Primer</b>	<b>Sequence 5' to 3'</b>	<b>Supplier</b>
BCL FWD	GCATCAATCGATGCCACCATGCAGGCTGTTG TGACTCAG	Sigma-Aldrich
BCLlinkrev	GTCTCCGGAACCTAGGACAGTGACCTT	MWG-Biotech AG
VHF	TGAGCAGACTGTGAGAGTGGT	Sigma-Aldrich
ScPVXJ	CACAGCCTTCGCGGTGCT	MWG-Biotech AG
PVXseqf	GCTCAGGCAGCTTGGGACTTA	MWG-Biotech AG
PVXseqr	AGCTGCAGGATTGGTGACTCC	Sigma-Aldrich
pgR107 seqf	TGCAAACCTAGATGCAGAAACCATAAGG	Sigma-Aldrich

**Table 2-3. Sequencing primers**

### **2.1.2 Transformation to *Agrobacterium tumefaciens***

The SK-based constructs were transformed into *Agrobacterium* strain LBA4404 provided by Dr George Lomonosoff. Plasmid (100 ng) was mixed with 50 µl of *Agrobacterium* competent cells and transferred into pre-cooled 2 mm Gene Pulser® Cuvette (Bio-Rad). The cuvette was inserted into the Gene Pulser® II electroporator (Bio-Rad) and a pulse of 25 µF was applied. The cells were resuspended in 750 µl of LB and incubated at 28°C with shaking at 200-220 rpm for 1 h. The cell suspension (10 or 100 µl) was then spreaded on LB agar with 50 µg/ml each of kanamycin, rifampicin, and streptomycin (all three antibiotics were purchased from Sigma-Aldrich). The plates were incubated at 28°C for 3 days. The colonies were screened by PCR.

### **2.1.3 *Agrobacterium* infiltration (Agroinfiltration)**

The *Agrobacterium* containing a desired plasmid was inoculated into 5 ml of LB with 50 µg/ml each of kanamycin, rifampicin and streptomycin and incubated at 28°C overnight. The culture was spun down at 2000 x g for 20 min at 4°C and resuspended in the

desired volume of MMA solution (10 mM MgCl<sub>2</sub>, 10 mM MES pH 5.6 and 100 μM acetosyringone). The suspension was incubated at room temperature for 2 h and applied with a syringe to *Nicotiana benthamiana* leaves that were wounded with a pipette tip.

#### **2.1.4 Plant growth conditions**

*N. benthamiana* plants were grown in green houses at the John Innes Centre, Norwich. The temperature was maintained at 23°C to 25°C with 16 h of supplementary light per day.

#### **2.1.5 Detection of scFv.BCL<sub>1</sub>-PVXCP expression**

Infiltrated leaves were collected 7 days post-infiltration (p.i.). They were either used immediately or stored at -80°C.

##### **2.1.5.1 Protein gel electrophoresis**

A small disc was cut from a fresh infiltrated leaf using the large end of 1 ml pipette tip, the plant material was dry ice-frozen and grounded into a fine powder. The plant tissue powder was boiled in NuPAGE<sup>®</sup> LDS sample buffer (Invitrogen, Paisley, UK) containing 0.2 M DTT at 100°C for 5 min. The denatured protein samples were separated by sodium dodecyl sulfate polyacrylamide gel electrophoresis (SDS-PAGE). The protein samples were loaded onto the NuPAGE<sup>®</sup> NOVEX<sup>®</sup> Bis-Tris 4-12% gradient gel (Invitrogen). The electrophoresis was run using NuPAGE<sup>®</sup> MES SDS running buffer (Invitrogen) at 180 constant V for approximately 45 min. Full-Range Rainbow<sup>™</sup> Molecular Weight Markers (GE Healthcare, Little Chalfont, UK) or Broad-Range NEB Prestained Marker (New England Biolabs (UK) Ltd) was used to estimate the size of the proteins.

##### **2.1.5.2 Gel staining to visualise protein bands**

After protein gel electrophoresis the gel was washed three times in deionised water (dH<sub>2</sub>O) for 5 min and stained with SimplyBlue<sup>™</sup> SafeStain (Invitrogen) for 1 h. The gel was washed with dH<sub>2</sub>O for 1 h or longer if a clearer background was required.

##### **2.1.5.3 Western blot analysis**

After protein gel electrophoresis the gel was subsequently placed into a protein transfer cassette. All filter papers (Whatman plc, Kent, UK) were soaked in NuPAGE<sup>®</sup> transfer buffer (Invitrogen) containing 20% methanol. PVDF membrane (GE Healthcare) was dipped in methanol and then soaked in transfer buffer. For semi-dry blotting system

(Bio-Rad), the sandwich was assembled in the following order from the anode side: two filter papers, a PVDF membrane, protein gel, and two filter papers. The transfer was performed at constant 300 mA for 1.5 h. For XCell SureLock system (Invitrogen), the sandwich was composed of three gauzes, a filter paper, a PVDF membrane, protein gel, a filter paper and two gauzes. The transfer was performed at constant 30 V for 1.5 h.

After protein transfer the membrane was washed in PBS-0.1% Tween-20 and blocked in blocking buffer (PBS, 0.1% Tween-20, 5% w/v skim milk) with rotating for 1 h at room temperature or overnight at 4°C. The membrane was incubated with anti-PVXCP mouse antiserum diluted in blocking buffer (1/500 dilution) for 2 h at room temperature and washed three times with PBS containing 0.1 % Tween for 15 min at room temperature. The membrane was then incubated with horseradish peroxidase (HRP)-conjugated anti-mouse IgG secondary antibody diluted 1/1000 in blocking buffer for 1.5 h at room temperature. The membrane was washed three times and placed on Syran wrap film. ECL Plus substrate (Amersham GE healthcare) was added onto the membrane and incubated for 5 min at room temperature. The chemiluminescence signal was captured using either Fluor-S™ MultiImager or Chemi Doc (both were purchased from Bio-Rad).

## **2.2 ScFv.BCL<sub>1</sub>-PVXCP purification**

ScFv.BCL<sub>1</sub>-PVXCP fusion protein was purified by anti-BCL<sub>1</sub> or anti-PVX antibody affinity chromatography.

### **2.2.1 Preparing the anti-BCL<sub>1</sub> antibody affinity column**

Three milligrams each of AT65, MC106A5, and MC104A12 anti-BCL<sub>1</sub> idiotypic monoclonal antibodies were dissolved in 2.85 ml of coupling buffer (0.1 M NaHCO<sub>3</sub>, pH 8.3 containing 0.5 M NaCl). A 2 ml volume of CNBr-activated sepharose 4B (GE Healthcare), suspended and washed with 1mM HCl, was added to the monoclonal antibody solution. The mixture was rotated end-over-end for 1 h at room temperature. The excess ligand was washed away with 5 medium (gel) volumes of coupling buffer. The remaining reactive groups on sepharose 4B were blocked with 0.1 M Tris-HCl pH 8.0 for 2 h at room temperature. The coupled sepharose was washed with 5 medium volumes of 0.1M acetic acid/sodium acetate pH 4.0 containing 0.5 M NaCl followed by 5 medium volumes of 0.1 M Tris-HCl pH 8.0 containing 0.5 M NaCl. This washing step was repeated 3 times. The anti-BCL<sub>1</sub> antibody-coupled sepharose 4B was packed on the top of a glass wool base in a 25 ml glass column with a stopcock at the bottom. The packed column was kept in binding buffer (0.1 M Tris-HCL pH 8.0, 0.5 M NaCl, 5 mM Na<sub>2</sub>EDTA).

### **2.2.2 Preparing the anti-PVX antibody affinity column**

Rabbit anti-PVX antibody (aluminium sulphate precipitated IgG fraction) was purchased from Yorkshire Bioscience Ltd, York, UK. One-hundred milligrams of the anti-PVX IgG was coupled to 10 ml of sepharose 4B following the protocol described in section 2.2.1.

### **2.2.3 ScFv.BCL<sub>1</sub>PVXCP purification**

*N. benthamiana* leaves infiltrated with *Agrobacterium* containing recombinant SK plasmid were frozen in liquid nitrogen and grounded into a fine powder using a mortar and a pestle. Protein was extracted with 1 ml of 0.1 M phosphate buffer pH 8.0 containing protease inhibitor cocktail (Roche, Burgess Hill, UK) per 1 g of leaves. Plant debris was eliminated by centrifugation at 3,000 rpm for 20 min at 4°C (Sorvall<sup>®</sup> Legend RT, Kendro Laboratory Products Ltd, Bishop's Stortford, UK). Supernatant was filtered through 0.22 µm Millex<sup>®</sup> GP filter (Millipore, Durham, UK) and applied to antibody affinity column. The unbound materials were washed away with five column volume of binding buffer. The bound proteins were eluted with one column volume of elution buffer (1 M potassium thiocyanate, 4% ammonia) followed with two column volumes of binding buffer. Immediately after elution the eluent pH was adjusted to neutral with 1 volume of 1 M Tris-HCL pH 7 and dialyzed into PBS containing protease inhibitor. Purified proteins were stored at 4°C.

### **2.2.4 Size exclusion**

ScFv.BCL<sub>1</sub>PVXCP purified by affinity chromatography was further purified by size exclusion using an ÄKTA prime FPLC (GE Healthcare). The gel filtration column (Superdex 200 10/300 GL, GE Healthcare) was equilibrated in PBS and 500 µl of sample was applied at a flow rate of 0.6 ml/min. Sample passed through the column was collected every 2 ml for the first 3 fractions, 1 ml for the following 2 fractions, and every 0.5 ml were collected until the end of running.

The collected fractions were analysed by protein gel electrophoresis following with silver staining using SilverSNAP<sup>®</sup> Stain Kit II (Fisher Scientific, Loughborough, UK). Protein gel was washed twice in dH<sub>2</sub>O for 5 min. Gel was fixed in fixing solution (30% ethanol, 10% acetic acid) for 15 min. Fixation was repeated once. The fixed gel was washed twice with 10% ethanol for 5 min following with 2 wash of dH<sub>2</sub>O 2 for 5 min. Gel was then soaked in Sensitizer Working Solution (50 µl of SilverSNAP<sup>®</sup> Sensitizer in 25 ml of dH<sub>2</sub>O) for 1 min and washed twice in dH<sub>2</sub>O for 1 min. Gel was stained with Stain Working Solution (0.5 ml of SilverSNAP<sup>®</sup> enhancer in 25 ml of SilverSNAP<sup>®</sup> Stain) for 30 min and

wash twice in dH<sub>2</sub>O for 20 sec. The protein bands were visualised in Developer Working Solution (0.5 ml of SilverSNAP<sup>®</sup> enhancer in 25 ml of SilverSNAP<sup>®</sup> Developer) and the reaction was stopped by soaking the gel in 5% acetic acid for 10 min.

### **2.2.5 Enzyme-linked immunosorbent assay (ELISA) for characterisation of scFv.BCL<sub>1</sub>-PVXCP fusion protein**

96-well flat-bottomed Nunc Immunos<sup>™</sup> ELISA plates (Nunc, Roskilde, Denmark) were coated with 200 µl of 1 µg/ml each of MC106A5 and MC104A12 anti-BCL<sub>1</sub> idiotypic monoclonal antibodies diluted in coating buffer (1.53 g of Na<sub>2</sub>CO<sub>3</sub> anhydrous, 2.92 g of NaHCO<sub>3</sub> in 1 litre of dH<sub>2</sub>O, pH 9.5) at 4°C overnight. The plates were washed three times with 200 µl/well PBS-0.1% Tween-20 prior to blocking with 200 µl/well 0.5% BSA in PBS at 37°C for 1 h. Another three washes were carried out before the addition of purified protein samples or plant extracts diluted in PBS-0.1% Tween-20 (two-time serial dilutions starting from 2 µg/ml). Following a 90 min incubation with samples, the plate was washed three times before the addition of 200 µl/well of 2 µg/ml of rabbit anti-PVX IgG (Yorkshire Bioscience) in PBS-0.1% Tween-20. The plate was incubated with the antibody for 90 min, then washed three times before addition of 1/1,000 dilution of HRP-conjugated anti-rabbit IgG antibody (Cell Signal Technology<sup>®</sup>, New England Biolabs (UK) Ltd) and incubation for a further 90 min. Another three washes were carried out prior to addition of the substrate. One o-phenylenediamine (OPD) tablet (Sigma-Aldrich) and a 1/1,000 dilution of H<sub>2</sub>O<sub>2</sub> were added to 50 ml of substrate buffer (4.68g anhydrous citric acid, 7.3g Na<sub>2</sub>HPO<sub>4</sub> in 1 litre dH<sub>2</sub>O, pH 5.5). Two-hundred microlitres of this substrate was added to the plate and the reaction was quenched with 80 µl/well of 2.5M H<sub>2</sub>SO<sub>4</sub> when the colour had developed sufficiently. The optical densities were measured at 490 nm using a Dynex MRX Platereader (Dynex Technologies Ltd, Billingshurst, UK).

### **2.2.6 Migration of scFv.BCL<sub>1</sub>-PVXCP on native protein gel**

The purified scFv.BCL<sub>1</sub>-PVXCP protein was mixed with Novex<sup>®</sup> Native Tris-Glycine sample buffer (Invitrogen) and loaded onto 12% Novex<sup>®</sup> Tris-Glycine Gel. PVX and 5T33-FrC proteins were used as a positive control and a negative control for protein multimerization, respectively. The denatured forms of proteins were also loaded on the same gel and the denatured samples were prepared by mixing with Tris-Glycine SDS sample buffer (Invitrogen) containing 0.2 M DTT and boiling at 100°C for 5 min. The electrophoresis was run in Native Tris-Glycine running buffer (Invitrogen) at 125 constant V for 1.5 h. Full-Range Rainbow<sup>™</sup> Molecular Weight Markers was loaded in parallel with the protein samples. After electrophoresis, proteins were transferred to PVDF membrane

using Novex<sup>®</sup> Tris-Glycine transfer buffer (Invitrogen). Western blot analysis using anti-PVXCP mouse antiserum was performed as previously described in section 2.1.5.3.

### **2.3 Protein quantitation**

Proteins were quantified using the Pierce<sup>®</sup> BCA protein assay kit (Thermo Fisher Scientific, Cramlington, UK). Two hundred  $\mu$ l of working reagent (BCA reagent A: BCA reagent B, 50:1) was added into microplate wells followed by the addition of 10  $\mu$ l of albumin standard (range from 25 – 2000  $\mu$ g/ml) or test sample. The plate was incubated at 37°C for 45 min. The optical density of the developed colour was measured at 570 nm wavelength using a Dynex MRX Platerreader (Dynex Technologies Ltd).

### **2.4 BCL<sub>1</sub>-PVP vaccine preparation**

PVP vaccine of PVX displaying BCL<sub>1</sub> Id antigen on its surface was made by linking BCL<sub>1</sub> IgG to the PVX particle using biotin-streptavidin binding reaction. The generated vaccine is named BCL<sub>1</sub>-PVP.

#### **2.4.1 Wildtype PVX purification**

*N. benthamiana* leaves infected with PVX were ground into fine powder and mixed with 3 volumes of sodium borate (NaBr) buffer (0.5 M boric acid, pH was adjusted with NaOH to 8.2) containing a protease inhibitor cocktail (Roche). The suspension was filtered through a 70  $\mu$ m cell strainer, transferred into a 50 ml Falcon tube and mixed with an equal volume of chloroform. The mixture was centrifuged at 4000 rpm for 20 min (Sorvall<sup>®</sup> Legend RT, Kendro Laboratory Products Ltd). The clear top layer of the supernatant was transferred to a 100 ml bottle and then 0.25 ml of 20% PEG-8000 and 0.5 ml of 20% NaCl per 1 ml of the supernatant were added. The mixture was stirred in a cold room (4°C) for 2 h and then centrifuged at 10,000 rpm for 10 min at 4°C (Sorvall<sup>®</sup> Discovery<sup>™</sup> 100S, Kendro Laboratory Products Ltd). The pellet was resuspended in ¼ volume of the starting supernatant. The suspension was centrifuged at 12,000 rpm for 10 min at 4°C. The pellet was discarded. PEG was added to the supernatant at 10% of final concentration and left on a magnetic stirrer in a cold room overnight. The mixture was centrifuged at 12,000 rpm for 10 min at 4°C. The purified PVX pellet was resuspended in 1 ml of NaBr buffer containing protease inhibitors. The purified virus was stored at 4°C.

#### 2.4.2 BCL<sub>1</sub>IgG expression and purification

BCL<sub>1</sub>IgG (BCL<sub>1</sub> V<sub>H</sub> and V<sub>L</sub> linked to human C<sub>γ</sub>1 and C<sub>κ</sub>) was expressed and secreted by Chinese hamster ovarian (CHO) cells. The CHO cells were maintained in Glasgow's modified Eagle's medium (GMEM) (First Link UK Ltd, Birmingham, UK) supplemented with 10% dialysed FCS (First Link UK Ltd) and 50 μM L-Methionine sulfoximine (Sigma-Aldrich). BCL<sub>1</sub> IgG was purified from the culture medium using protein-A column (Thermo Fisher Scientific). Cell supernatant containing the IgG was mixed with 1 volume of PBS and loaded onto the column. BCL<sub>1</sub> IgG bound to the column was eluted using elution buffer (0.1 M glycine, 2 mM EDTA, pH 2.8). The collected IgG solution was neutralised with 1 M Tris buffer and dialysed to PBS.

#### 2.4.3 Biotin labelling of PVX and BCL<sub>1</sub>IgG

PVX particles or BCL<sub>1</sub>IgG was conjugated with biotin using BiotinTag<sup>TM</sup> (Sigma-Aldrich) or EZ-link<sup>®</sup> NHS-Biotin Reagents (Pierce). One to ten milligrams of PVX or BCL<sub>1</sub>IgG was dissolved in 0.5 to 2 ml of PBS and incubated with 20-fold molar excess of biotin at room temperature for 30 min. The non-reacted biotin was removed by dialysis.

#### 2.4.4 Determination of the level of biotin incorporation

The level of biotin incorporation was determined by using the Pierce<sup>®</sup> Biotin Quantitation Kit (Thermo Fisher Scientific). One hundred and sixty μl of PBS and 20 μl of HABA/Avidin Premix solution was added into microplate wells and mixed well. The absorbance of the mixture was measured at 490 nm as the value of A<sub>490</sub> HABA/avidin. Twenty microlitres of biotinylated PVX or biotinylated BCL<sub>1</sub> IgG or biotinylated HRP (positive control) was added to the well containing the HABA/avidin reaction mixture. The absorbance of the solution was recorded as the value of A<sub>490</sub> HABA/avidin/biotin sample. Biotin incorporation (mmol incorporated biotin per mmol protein) was calculated from the following equation.

$$\text{mmol biotin/ml} = (A_{490} \text{ HABA/avidin} - A_{490} \text{ HABA/avidin/biotin sample}) / 34,000 \times 0.5$$

$$\text{mmol biotin/ mmol protein} = (\text{mmol biotin per ml} \times 10) / \text{mmol protein per ml}$$

In which 34,000 = extinction coefficient of HABA/avidin pH 7.0 at 500 nm, 0.5 is the height (depth) of the solution, 10 is a dilution factor.

#### 2.4.5 Linking BCL<sub>1</sub>IgG to PVX

Streptavidin (Invitrogen) was left overnight to bind to biotinylated BCL<sub>1</sub>IgG at a 1:3 (mole:mole) ratio at 4°C. Streptavidin-BCL<sub>1</sub>IgG was added to biotinylated PVX at a 1:1 (μg of BCL<sub>1</sub>IgG:μg of PVX) ratio and incubated at 4°C overnight to generate BCL<sub>1</sub>-PVP

vaccine. The linking of BCL<sub>1</sub> IgG to PVX was examined by ELISA described earlier in section 2.2.5.

## **2.5 Endotoxin test**

The amount of endotoxin in the purified PVX sample was determined by Limulus Amebocyte Lysate (LAL) test (Charles River Laboratories, Margate, UK) using LPS as a standard. Fifty microlitres of PVX or LPS solution was added into microplate wells and incubated at 37°C for 5 min before mixing with 50 µl of LAL reagent and incubating at 37°C for further 7 min. One-hundred microlitres of 0.69 mg/ml S-2423 substrate (diluted in 0.025 M Tris, pH 9.0) was added to the mixture and the reaction was quenched (after the colour was developed sufficiently) by addition of 100 µl of 20% acetic acid. The optical density was measured at 405 nm using Dynex MRX Platereader.

## **2.6 Mouse Experimental Protocol**

### **2.6.1 Mice**

BALB/c and C57BL/6 mice, aged between 6 and 12 weeks at the beginning of procedures, were kept in accordance with the Home Office Guidelines. Experiments were performed under Project Licence JR 70/6401 and Personal Licence PIL 70/20084.

### **2.6.2 Vaccination**

BALB/c mice were immunized with DNA vaccines prepared at 0.5 mg/ml in sterile saline. A 50 µl volume of vaccine was injected into each rear quadriceps muscle (total 50 µg of DNA vaccine per mouse). For BCL<sub>1</sub>PVXCP vaccine, 100 µg of purified protein was diluted in 100 µl of PBS and 1 volume of alum (Pierce) was added and mixed end-over-end for 1 h and the mixture was given by intra peritoneal (i.p.) injection. Fifty µg of PVXCP mixed with alum was injected i.p. as a control.

For the BCL<sub>1</sub>-PVP vaccine, mice were vaccinated i.p. with the vaccine alone or with the vaccine mixed with 1 volume of alum. BCL<sub>1</sub>-PVP vaccine containing 20 µg of BCL<sub>1</sub>IgG was used except in the dose-response experiment where the other amount was also applied. In some experiments, 20 µg of PVX or BCL<sub>1</sub>IgG (20 µg) linked to streptavidin was injected i.p. into mice.

### **2.6.3 Serial blood sampling**

To detect vaccine-induced antibody responses, blood samples were taken from vaccinated mice by tail bleeding. Local anaesthetic (Instillagal® , FARCO-PHARMA GmbH, Cologne, Germany) was applied to the tip of the tails and mice were warmed at 37°C for 5 min. A 1-2 mm section of the tip of the tail was cut with a scalpel and up to 200 µl of blood was removed per mouse. After clotting, whole blood was spun at 10,000 rpm for 10 min and the serum was collected. Serum samples were preserved by the addition of 1 µl of 1mM sodium azide and store at -20°C.

### **2.6.4 BCL<sub>1</sub> tumour challenge**

The BCL<sub>1</sub> cells for tumour challenge were routinely passaged through BALB/c mice. On the day of tumour challenge, animals exhibiting a terminal splenic tumour burden were culled and splenocytes were isolated as described in section 2.10.3. Cells were resuspended at  $2.5 \times 10^5$  cells/ml in RPMI 1640. Mice received 200 µl of the cell suspension injected into the tail vein and were culled when splenomegaly became apparent to the trained animal technicians. Statistical analysis to compare groups injected with different vaccines was performed using the Logrank test.

### **2.7 Detection of mouse antibody responses by ELISA**

A 96-well flat-bottomed Nunc Immunos<sup>TM</sup> ELISA plate (Nunc) was coated with 200 µl of 1 µg/ml of PVXCP or 2 µg/ml of BCL<sub>1</sub> humanized IgG or 1.5 µg/ml of BCL<sub>1</sub> F(ab')<sub>2</sub> diluted in coating buffer at 4°C overnight. Plates were washed three times with 200 µl/well PBS-0.1% Tween-20 prior to blocking with 200 µl/well of 1% BSA in PBS at 37°C for 1 h. Another three washes were carried out before the addition of standard sera or each sera sample diluted in PBS-0.1% Tween (four times serial dilution started from 1/20 dilution). Following a 90 min incubation with the sera, plates were washed three times before the addition of 200 µl/well of a 1/1,000 dilution of the secondary HRP conjugated anti-mouse IgG (The Binding Site, Birmingham, UK) or IgG1 (Oxford Biotechnology Ltd, Kidlington, UK) or IgG2a (Harlan Sera-Lab Ltd., Loughborough, UK) or IgG2a (Harlan Sera-Lab Ltd.) or IgG3 (Harlan Sera-Lab Ltd.) antibody and incubated for a further 90 min. Another three washes were carried out prior to addition of the substrate and the enzymatic activity was measured at 490 nm wavelength using a Dynex MRX Platerreader. The serum antibody levels (units/ml) were calculated from a standard curve and analyzed by Graphpad PRISM 4.03 software. Statistical analysis to compare groups injected with different vaccines was performed using the Mann-Whitney test for non-parametric data.

## **2.8 Enzyme-linked Immunospot (ELISPOT)**

All reagents for ELISPOT assay were purchased from BD Biosciences otherwise indicated. BD™ ELISOPT Plates were coated with 100 µl of 1/200 dilution of anti-mouse IFN-γ or anti-mouse IL-2 or anti-mouse IL-4 antibody in sterile PBS overnight at 4°C. Coated plates were then washed once with 200 µl of RPMI 1640 complete medium and then blocked with 200 µl of RPMI 1640 complete medium (CM: RPMI 1640 containing 10% FCS, 2-ME, glutamine, nonessential amino acids, penicillin, streptomycin) for 2 h at RT. Splens were collected from mice two weeks after vaccination and cells were prepared as described in section 2.10.3. Splenocytes were plated at  $2.5 \times 10^5$  cells per well in 200 µl of complete media containing desired antigen and were incubated at 37°C for 42 h. All variables were repeated in triplicate.

After the incubation period, the cells on the plate were first lysed by two 5 min washes with 200 µl of milliQ water. The plates were then washed three times with PBS containing 0.05% Tween-20. One hundred µl of 1/250 dilution of biotinylated anti-mouse IFN-γ or anti-mouse IL-2 or anti-mouse IL-4 in PBS containing 10% FBS was added to each well and incubated for 2 h at RT. Unbound antibody solution was discarded and the plates were washed three times with 200 µl of PBS containing 0.05% Tween-20. One hundred µl of 1/500 dilution of streptavidin-ALP (MABtech, Nack a Strand, Sweden) in PBS containing 10% FBS was added and the plates were incubated for 1 h at RT. Plates were then washed 4 times with PBS containing 0.05% Tween-20 and were further washed twice with 200 µl of 1X PBS. The complex was finally developed using the BCIP/NBT substrate kit (Invitrogen) to reveal a purple precipitate resulting from the enzymatic reaction.

## **2.9 *In vitro* DC activation**

### **2.9.1 Generation of bone marrow derived dendritic cells (BmDCs)**

Bone marrow cells were collected from tibias and femurs of 6-8 week old C57BL/6 mice, and passed through a nylon mesh to remove small pieces of bone and debris. Cells were prepared at density of  $1 \times 10^6$  cells/ml in CM containing 20 ng/ml GM-CSF, and  $3 \times 10^6$  cells/well were cultured in 6-well culture plates. After 2 days, nonadherent cells were discarded by gently swirling the plates, aspirating the entire medium, adding 3 ml of prewarmed RPMI 1640, aspirating all of RPMI 1640, and adding back fresh CM containing GM-CSF. Cells were cultured for further 4 days.

## **2.9.2 BmDC activation and FACS analysis**

BmDCs were treated with 10 µg/ml of PVX or 1 µg/ml of LPS or left untreated for 48 h. Cells were collected by centrifugation at 1,350 rpm for 5 min and the cell pellet was resuspended in 500 µl FACS buffer (PBS, 1% BSA, 1 mM sodium azide). An aliquot of 10 µl of cell suspension was mixed with 1 volume of Trypan Blue. The mixture was loaded onto a haemocytometer and the number of cells was counted using a microscope. Cell concentration was calculated and diluted to  $1 \times 10^7$  cells/ml using FACS buffer. One hundred microlitres of cell suspension ( $1 \times 10^6$  cells) was transferred into FACS tube and cells were incubated with 1 µg of anti-CD16/32 Fc blocker (clone 93, eBioscience, Hatfield, UK) for 20 min on ice before staining with with 1 µg of PE-labeled anti-CD11C (clone N418, Caltag Laboratories, Invitrogen, Paisley, UK), biotinylated anti-CCR7 (clone 4B12, Biolegend, Cambridge, UK) or anti-CD40 (clone 3/23) or anti-CD80 (clone 16-10A1) or anti-CD86 (clone GL1) or FITC-labeled anti-I-A/I-E antibodies (clone 2G9) (the latter 4 antibodies were BD Pharmingen™ purchased from BD Bioscience, Erembodegem, Belgium). The unbound antibody was removed by three washes with 4 ml of FACS buffer and resuspended in 100 µl of FACS buffer. Cells stained with biotinylated antibody were incubated with 0.1 µg of APC-conjugated streptavidin for 20 min on ice; cells were resuspended in 100 µl of FACS buffer after three washes. Cells were also stained with isotype control antibody that had been conjugated with matched fluorochrome. The cell suspensions were analyzed by FACSCalibur with Cell Quest Pro software (BD Bioscience). Fifty thousand events were acquired for analysis.

## **2.9.3 Gene expression of bmDCs after PVX activation**

### **2.9.3.1 DC purification after PVX activation**

BmDCs were treated with 10 µg/ml of PVX or 1 µg/ml of LPS for 15 h or left untreated. Cells were collected by centrifugation at 1,350 rpm for 5 min and the cell pellet was resuspended in buffer (PBS containing 0.5% BSA) at  $10^7$  cells/ 100 µl buffer. Ten µl of PE-anti CD11c (clone N418, Caltag Laboratories) per 100 µl of cell suspension was added and incubated at 4°C for 10 min. Unbound antibody was washed out by adding 2 ml of buffer per  $10^7$  cells and centrifuging at 300 x g for 10 min. The cell pellet was resuspended in 80 µl of buffer per  $10^7$  cells. Twenty µl of anti-PE MicroBeads (Miltenyi Biotec, Surrey, UK) was added and the mixture was incubated at 4°C for 15 min. Cells were washed with 2 ml of buffer per  $10^7$  cells and centrifuged at 300 x g for 10 min. Cells were resuspended in 500 µl of buffer and loaded on LS column placed in the magnetic field. Unlabeled cells were washed with 3 ml of buffer three times. Column was removed from the magnet and placed

on 15 ml collection tube. Five ml of buffer was added and the labeled cells were immediately flushed out by firmly pushing the plunger into the column. The purity of the eluted cells was determined by FACS analysis.

### **2.9.3.2 RNA extraction**

RNA from purified DC was extracted by using RNeasy kit (QIAGEN) according to the manufacturer's manual. DCs up to  $5 \times 10^6$  cells were lysed with 350  $\mu$ l of buffer RLT and homogenized by five times passing through 20-gauge needle. The homogenized lysate was mixed with 1 volume of 70% ethanol and transferred to the spin column placed on the collection tube before 8000 x g centrifugation for 15 sec. The spin column was washed by adding 700  $\mu$ l of buffer RW1 and spinning for 15 sec. The column membrane was further washed with 500  $\mu$ l of buffer RPE with 15 sec spinning and another 500 ml of buffer RPE with 2 min spinning. The column was transferred to a new collection tube and centrifugation for additional 1 min was performed to eliminate the residual buffer. The column was transferred to an RNA collection tube, 30  $\mu$ l of RNase-free water was added to the column and RNA was eluted by centrifugation for 1 min. The concentration and purity of RNA samples was examined by measuring their absorbance at 260 and 280 nm using Eppendorf BioPhotometer (Eppendorf AG). To ensure that the final RNA preparation was free of protein a 260/280 nm absorbance ratio of 1.8 was desired. The integrity of RNA samples was confirmed by an agarose gel electrophoresis.

### **2.9.3.3 DNase I treatment of extracted RNA**

The extracted RNA was further treated with DNase I (Invitrogen) to eliminate contaminated genomic DNA. One  $\mu$ g of RNA was mixed with 1  $\mu$ l of 10x reaction buffer [200 mM Tris-HCL (pH 8.4), 500 mM KCl, 20 mM MgCl<sub>2</sub>], 1  $\mu$ l of DNase I and RNase-free water was added to final volume of 10  $\mu$ l. The reaction mixture was incubated at RT for 15 min. The reaction was inactivated by addition of 1  $\mu$ l of 25 mM EDTA and incubation at 65°C for 15 min.

### **2.9.3.4 cDNA synthesis**

DNase treated total RNA was reversetranscribed to cDNA using SuperScript™ First-Strand Synthesis System for RT-PCR (Invitrogen). DNase treated RNA was mixed with 1  $\mu$ l of Oligo(dT) (500 ng/ $\mu$ l) and 1  $\mu$ l of 10 mM dNTP mix and incubated at 65°C for 5 min. The reaction mixture was then mixed with 1  $\mu$ l of 10 x reaction buffer [200 mM Tris-HCL (pH 8.4), 500 mM KCl], 3  $\mu$ l of 25 mM MgCl<sub>2</sub>, 2  $\mu$ l of 0.1 M DTT and 1  $\mu$ l of RNase out. The mixture was incubated at 42°C for 2 min before mixing with 1  $\mu$ l (50 units)

of SuperScript<sup>™</sup> II RT. The reaction was incubated at 42°C for 50 min and terminated at 70°C for 15 min. Finally, RNA was eliminated by mixing with 1 ml of RNase H and incubation at 37°C for 20 min.

### **2.9.3.5 Real-time PCR**

All real-time PCR reagents were purchased from Tebu-Bio, Peterborough, UK. One µl of cDNA was mixed with 1 µl of 10 mM PCR primer pair, 12.5 µl of RT<sup>2</sup> Real-Time<sup>™</sup> SYBR Green/ ROX PCR master mix and 10.5 µl of H<sub>2</sub>O. The reaction mixture was added to MicroAmp<sup>™</sup> Optical 96-Well Reaction Plate (Applied Biosystems). The thermal cycle was 95°C, 10 min, following with 40 cycles of 95°C, 30 sec; 55°C, 30 sec; 72°C, 30 sec. The real-time PCR reaction was performed using 7500 Real Time PCR System in connection with 7500 software version 2.0.1 (Applied Biosystems). Gene expression changes in treated cell samples were analysed by  $\Delta\Delta C_t$  method compare to non-activated cell control and  $\beta$ -actin was used as the reference gene.

## **2.10 FACS analysis of PVX binding to DCs or B cells in vivo**

### **2.10.1 Labeling PVX with Alexa<sup>®</sup> Fluor 647**

Five-hundred µl of 2 mg/ml of PVX in PBS was mixed with 50 µl of 1 M sodium bicarbonate. PVX solution was added to a vial of Alexa Fluor<sup>®</sup> 647 reactive dye (Molecular Probes, Invitrogen) containing a magnetic flea. The reaction mixture was stirred at room temperature for 1 h. The excess of an unbound dye was removed by dialysis to PBS using Vivaspin column (Sartorius AG, Goettingen, Germany).

### **2.10.2 In vivo PVX binding**

Two hours after 100 µg/200 µl of Alexa Fluor 647-labeled PVX or 200 µl of saline was injected intra venously (i.v.) into C57BL/6 mice, spleens were collected and incubated with 0.06% w/v Collagenase type IV in Hank's balance salt solution without Ca<sup>2+</sup> and Mg<sup>2+</sup> containing 0.5 mM EDTA for 30 min at 37°C (all reagents were purchased from Sigma-Aldrich Company Ltd). Splenocytes were isolated as described in the next section.

### **2.10.3 Splenocytes isolation**

Splenocytes were isolated by grinding a spleen in complete media and the cell suspension was passed through a 70 µm BD Falcon<sup>™</sup> cell strainer (BD Bioscience), layered over 1 volume of lymphoprep<sup>™</sup> (Axis-Shield PoC AS, Oslo, Norway) and spun at 2,100 rpm for 20 min. The cell layer at the interphase was collected and washed with 50 ml of

RPMI 1640 (Invitrogen). The cell suspension was spun at 1,600 rpm for 5 min and the cell pellet was resuspended in 1 ml FACS buffer. Cells were counted and diluted into a desired concentration using FACS buffer or RPMI 1640.

#### **2.10.4 Cell staining and FACS analysis**

One-million cells in 100  $\mu$ l of FACS buffer were stained with 1  $\mu$ g of PE-labeled anti-CD11c (clone N418, Caltag Laboratories) or anti-CD19 antibody (clone 1D3, BD Pharmingen<sup>TM</sup>, BD Bioscience) or isotype control antibody labeled with a matched fluorochrome for 30 min on ice. The unbound antibody was removed by three washes with 4 ml of FACS buffer. After final wash, cells were resuspended in 100  $\mu$ l of FACS buffer. Antibody fluorescence was detected by FACSCalibur; 300,000 events were acquired and analyzed using CellQuest Pro software (BD Bioscience).

### **2.11 In vivo APCs activation by PVX**

#### **2.11.1 FACS analysis of in vivo activation of DCs and B cells**

C57BL/6 mice were injected i.v. with 100  $\mu$ g of PVX or 250  $\mu$ g of LPS or 25  $\mu$ g of LPS or saline. Twenty hours after injection, spleens were collected and cells were prepared as described in section 2.10.3. Splenic cells,  $2 \times 10^6$  cells/100  $\mu$ l, were incubated with 1  $\mu$ g of anti-CD16/32 Fc blocker (clone 93, eBioscience) for 20 min on ice before staining with 1  $\mu$ g of PE-labeled anti-CD11c and biotinylated anti-CCR7 (clone 4B12, Biolegend) or anti-CD40 (clone 3/23) or anti-CD80 (clone 16-10A1) or anti-CD86 (clone GL1) or anti-I-A/I-E (clone 2G9) antibodies (the latter 4 antibodies were BD Pharmingen<sup>TM</sup> purchased from BD Bioscience). Cells were washed three times and resuspended in 100  $\mu$ l of FACS buffer before incubating with 0.1  $\mu$ g of APC conjugated streptavidin for 20 min on ice. In the experiment investigating activation of DC subsets, 1  $\mu$ g each of APC-labeled anti-CD8 $\alpha$  (clone 53-6.7, BD Pharmingen<sup>TM</sup>) and FITC-labeled anti-CD4 antibodies (clone RM4-4, BD Pharmingen<sup>TM</sup>) were added in combination with the previously mentioned anti-CD11c and biotinylated anti-CCR7 or anti-CD40 or anti-CD80 or anti-CD86 or anti-I-A/I-E antibodies. Cells were washed three times and resuspended in 100  $\mu$ l of FACS buffer before incubating with 0.1  $\mu$ g of PerCP-Cy5.5 conjugated streptavidin for 20 min on ice. Cells were also stained with isotype control antibodies that had been conjugated with the matched fluorochrome. Cells were resuspended in 100  $\mu$ l of FACS buffer after three washes and analyzed by FACSCalibur using Cell Quest Pro software. Five hundred thousand events were acquired for analysis.

In order to determine B cell activation, cells were stained with PE-labeled anti-CD19 (clone 1D3, BD Pharmingen™), and biotinylated CD40 (clone 3/23, BD Pharmingen™) or I-A/I-E (clone 2G9, BD Pharmingen™) for 30 min on ice. In the experiment investigating B cell subset activation, cells were stained with APC-labeled anti-CD19 (clone 1D3, BD Pharmingen™), FITC-labeled anti-CD21 (clone 7G6, BD Pharmingen™), PE-labeled anti-CD23 (clone B3B4, BD Pharmingen™) and biotinylated anti-CD86 (clone GL1, BD Pharmingen™) for 30 min on ice. Cells were washed three times, resuspended, and incubated with 0.1 mg of PerCP-Cy5.5 conjugated streptavidin for 20 min on ice. Separated cell suspensions were stained with isotype control antibody labeled with the matched fluorochrome. After three washes and resuspending, cells were analyzed by FACSCalibur using Cell Quest Pro software. One hundred thousand events were acquired for analysis.

### **2.11.2 Gene expression of in vivo activation of DCs**

Mice were injected with 100 µg of PVX or 25 µg of LPS in 200 µl of saline or saline alone into the tail vein. Six hours after injection, spleens were collected and splenocytes were isolated. DCs were purified as described in section 2.9.3.1 and RNA of purified DCs was extracted for real-time RT-PCR as described in section 2.9.3.2 – 2.9.3.5.

## **2.12 BCL<sub>1</sub>2APVX expression in plants**

### **2.12.1 Assembly of pcDNA3.scFv.BCL<sub>1</sub>-2A-PVXCP**

The scFv.BCL<sub>1</sub>-FMDV2A-PVXCP4 (scFv.BCL<sub>1</sub>-2A-PVXCP) fusion gene was assembled using the previously constructed pcDNA3.scFv.BCL<sub>1</sub>-PVXCP as a template. The plasmid contains *BspEI* and *XhoI* sites at the end of scFv.BCL<sub>1</sub> sequence and PVXCP4 sequence, respectively (figure 2-2). A DNA fragment encoding FMDV2A-PVXCP4 fusion protein was amplified by PCR from PVXCP4 with PVX FWD primer containing the *BspEI* site and FMDV2A sequence, and PVX REV primer containing the *XhoI* site (table 1). The FMDV2A-PVXCP4 fragment replaced original PVXCP4 by inserting it into pcDNA3.scFv.BCL<sub>1</sub>-PVXCP, yielding pcDNA3.scFv.BCL<sub>1</sub>-2A-PVXCP plasmid (figure 2-2). JM109 competent cells were transformed with the recombinant plasmids and the bacterial colonies that grew on Luria agar plates with 100 ng/ml ampicillin (Sigma) were screened with the PCR primers used for the cloning. The positive clones were subjected to DNA sequencing using AB3130xl Genetic Analyzer.

### **2.12.2 In vitro transcription/translation (IVTT) of pcDNA3.scFv.BCL<sub>1</sub>-2A-PVXCP**

Five-hundred nanograms of recombinant pcDNA3 plasmid DNA was mixed with 20 µl of TNT master mix (Promega, Southampton, UK), 1 µl of <sup>35</sup>S Methionine in 25 µl reaction. The mixture was incubated at 30°C for 90 min and then run on NuPAGE<sup>®</sup> NOVEX<sup>®</sup> Bis-Tris 4 – 12 % gradient gel (Invitrogen, Paisley, UK). The gel was dried and exposed to autoradiography film, Hyperfilm (GE Healthcare), overnight or at desired period of time. The film was developed manually with a developer (Kodak, Sigma-Aldrich Company Ltd) and a fixer solution (Kodak, Sigma-Aldrich Company Ltd) to visualize protein fragments.

### **2.12.3 Mammalian cells transfection with pcDNA3.scFv.BCL<sub>1</sub>-2A-PVXCP**

Two µg of recombinant pcDNA3 plasmid was mixed with 5 µl of Fugene (Roche) in 100 µl of Opti-Mem<sup>®</sup> (Invitrogen). The mixture was left at room temperature for 30 min and then added drop wise to 5x10<sup>5</sup> COS-7 cells cultured in 3 ml of Opti-Mem<sup>®</sup>. After 48 h, the culture medium was collected. Cells were lysed with 85°C pre-warmed protein loading buffer and cell debris was eliminated by centrifugation at 10,000 x g for 10 min at 4°C. Culture medium and cell lysates were subjected to SDS-PAGE and Western blot analysis.

### **2.12.4 Assembly of pgR107.scFv.BCL<sub>1</sub>-2A-PVXCP**

The pgR107 plasmid, provided by Dr. David Baulcombe (JIC, Norwich), was used to construct pgR107.scFv.BCL<sub>1</sub>-2A-PVXCP vector. ScFv.BCL<sub>1</sub>-2A-PVXCP was amplified using BCL FWD primer containing the *Cla*I site and PVX REV primer containing the *Xho*I site (table 2-1). The respective PCR products were gel-purified, digested with the *Cla*I and *Xho*I enzymes and ligated into the *Cla*I and *Xho*I linearized pgR107, yielding pgR107.scFv.BCL<sub>1</sub>-2A-PVXCP vector (figure 2-3). JM109 competent cells were transformed with the recombinant plasmids and the bacterial colonies that grew on Luria agar plates with 50 ng/ml kanamycin were screened by PCR and the positive clones were subjected to DNA sequencing.

### **2.12.5 Expression of BCL<sub>1</sub>2APVX in plants**

pgR107.scFv.BCL<sub>1</sub>-2A-PVXCP was transformed into *Agrobacterium* strain GV3101 containing pSoup (a plasmid essential for the replication of pgR107 vector) provided by Dr. George Lomonosoff. The *Agrobacterium* culture was infiltrated into *N. benthamiana* plants. The details of *Agrobacterium* transformation, Agroinfiltration, and plant growing condition were previously described in section 2.1.2, 2.1.3, and 2.1.4, respectively. Infection symptoms were observed and photographed with a Nikon D1x

digital camera under visible light. CVP proteins were analyzed by SDS-PAGE and Western blot analysis with anti-PVXCP mouse antiserum as previously described in section 2.1.5.1 – 2.1.5.3.

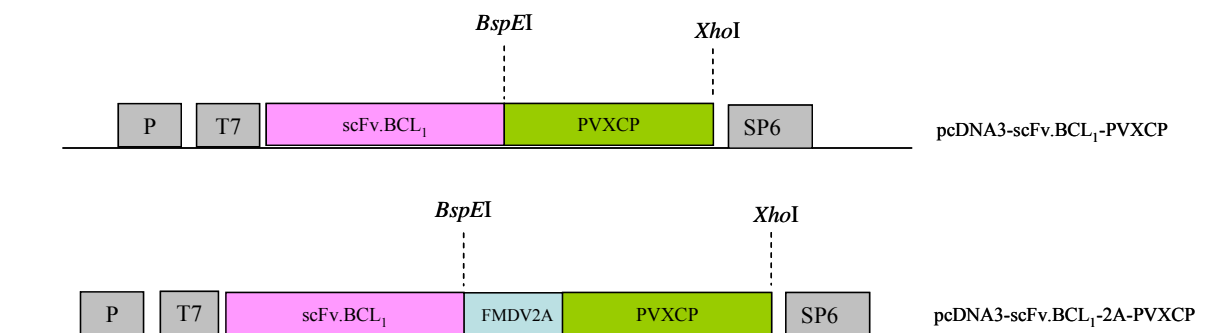


**Figure 2-2. Schematic diagram of pcDNA3.scFv.BCL<sub>1</sub>-PVXCP and pcDNA3.scFv.BCL<sub>1</sub>-2A-PVXCP vector**

P : CMV promoter, T7 : T7 promoter

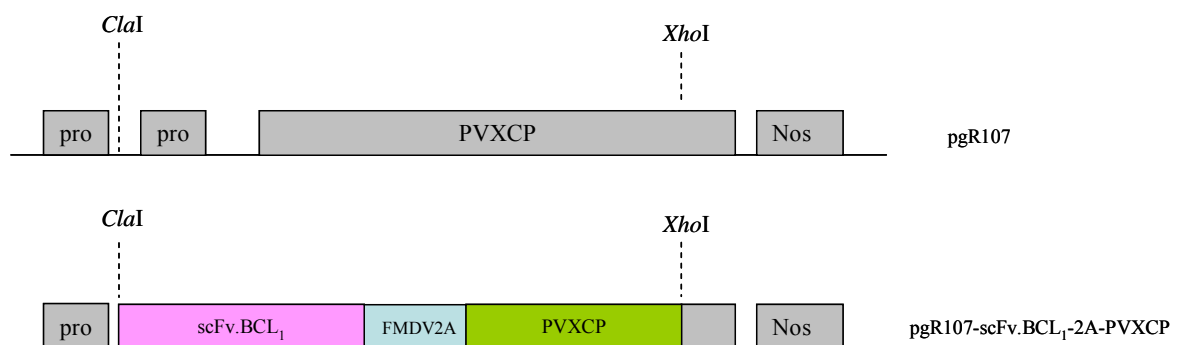


**Figure 2-3. Diagram shows pgR107.scFv.BCL<sub>1</sub>-2A-PVXCP**

## **2.12.6 BCL<sub>1</sub>2APVX RNA detection**

### **2.12.6.1 RNA extraction**

RNA was extracted from the plant leaf using TRI reagent (Sigma-Aldrich). Approximately 1 x 1 cm<sup>2</sup> of the dry ice-frozen plant tissue was grounded into fine powder and resuspended in 1 ml of TRI-reagent. Two-hundred microlitres of chloroform was added and mixed by vigorous shaking. The mixture was left to stand for 2-15 min before spinning down at 12,000 x g for 15 min at 4°C. The upper phase containing RNA was transferred to the new tube and mixed with 500 µl of isopropanol by inverting 4-6 times. The RNA was precipitated by centrifugation at 12,000 x g for 10 min at 4°C. The supernatant was carefully removed. One ml of 70% ethanol was added following with centrifugation at 12,000 x g for 5 min at 4°C. The ethanol solution was carefully removed and the RNA pellet was left to dry and then resuspended in 20 µl of water. RNA concentration was measured using Eppendorf BioPhotometer (Eppendorf AG).

### **2.12.6.2 Reverse transcription-polymerase chain reaction (RT-PCR)**

One microgram of DNaseI treated RNA in a final volume of 20 µl was reverse transcribed using an oligo-dT primer as described in section 2.6.3.2. Two microlitres of cDNA was used to amplify scFv.BCL<sub>1</sub>-2A-PVXCP fusion gene with HotStarTaq<sup>®</sup> (QIAGEN) and cloning primers. The PCR cycle conditions were explained in section 2.1.1.1. The PCR products were separated by agarose gel electrophoresis as described in section 2.1.1.3.

## **2.13 BCL<sub>1</sub>2APVX purification**

### **2.13.1 PEG precipitation and ultracentrifugation**

Purification of BCL<sub>1</sub>2APVX was modified from the wild-type PVX purification method described in section 2.4.1. BCL<sub>1</sub>2APVX infected tissues were grounded in liquid nitrogen, extracted with 3 volume of NaBr buffer containing protease inhibitor cocktail, filtered through a nylon mesh, and clarified with 1 volume of chloroform. The virus particles were precipitated with PEG and the resuspended pellet was further purified by ultracentrifugation (UC) or a second PEG precipitation. For UC method, the resuspended pellet was spun at 40,000 rpm for 2 h and the resulted pellet was resuspended in NaBr buffer. For second PEG precipitation method, the resuspended pellet was incubated in the presence of 10% PEG and left on a magnetic stirrer in a cold room for 2 h following by centrifugation at 12,000 rpm for 10 min at 4°C. The pellet was resuspended in NaBr buffer.

### **2.13.2 BCL<sub>1</sub>2APVX purification using affinity chromatography**

The plant extract in NaBr buffer was diluted in 1 volume of binding buffer and applied to anti-BCL<sub>1</sub> antibody column. The unbound material was washed away with 10 column volumes of binding buffer. The bound BCL<sub>1</sub>2APVX was eluted with 1 column volume of elution buffer (1 M Potassium thiocyanate containing 4% Ammonia) following with 2 column volume of binding buffer. Immediately after elution, the eluent pH was adjusted to neutral with 1 volume of 1 M Tris-HCL pH 7 and dialyzed to PBS.

## **2.14 Transmission electron microscope (TEM)**

### **2.14.1 Negative stain**

Five µl of the virus sample was dropped on a carbon coated copper grid and incubated for 5 min. The excess sample was carefully blotted off with a corner of a paper towel and then the sample was stained with 5 µl of 1% ammonium molybdate in 0.1 M ammonium acetate buffer pH 7.0 for 10 sec. The excess solution was carefully blotted and the grid was left to air-dry before analyzed under a transmission electron microscope (Hitachi H-600).

### **2.14.2 Immunosorbent electron microscopy (ISEM)**

Five µl of anti-BCL<sub>1</sub> or anti-PVXCP mouse antiserum or normal mouse serum (NMS) diluted in PBS containing 0.1% Tween-20 was dropped on a carbon coated copper grid and incubated for 1.5 h. The antibody was blotted off and the grid was blocked with 5 µl of 1% BSA in PBS for 30 min. The blocking solution was gently blotted off and the grid was washed by adding 5 µl of washing buffer (0.1 M phosphate buffer containing 1% BSA and 0.1% Tween-20), incubating for 5 min and blotting the buffer off. The grid was washed three times. The grid was subsequently incubated with purified scFv.BCL<sub>1</sub>-PVXCP protein for 1.5 h. The grid was washed with 20 drops of dH<sub>2</sub>O before negative stain and then was observed under TEM.

### **2.14.3 Immuno-negative labeling**

Five µl of the virus sample was dropped on a carbon coated copper grid and incubated for 30 min. The excess sample was blotted off and the sample on the grid was blocked with 5 µl of 1% BSA in PBS for 10 min. The blocking solution was gently blotted and the grid was washed with 5 µl of washing buffer for 1 min, three times. The grid was subsequently incubated with anti-BCL<sub>1</sub> serum diluted 1 in 100 in washing buffer for 1 h and then washed three times before incubating with 15 nm gold-conjugated goat anti-mouse IgG

(Abcam) diluted 1/50 in washing buffer for another 1 h. The grid was washed for 1 min three times with washing buffer, subsequently washed for 5 min with 0.1 M phosphate buffer and then fixed for 5 min with 3% glutaraldehyde. The grid was incubated in distilled water for 2 min twice before negative staining and then was observed under TEM.

## Chapter 3. ScFv.BCL<sub>1</sub>-PVXCP fusion protein vaccine

### 3.1 Introduction

#### 3.1.1 BCL<sub>1</sub> model

Mouse B cell lymphoma BCL<sub>1</sub>, a well defined spontaneous tumour of BALB/c origin, has been used as a model for tumour immunotherapy. The BCL<sub>1</sub> tumour closely resembles human prolymphocytic leukemia in which the clinical and laboratory features are massive enlargement of the spleen (spleens of BCL<sub>1</sub> tumour-bearing mice weigh approximately 3 g compared to the usual 0.2 g in normal mice), minimal lymph node enlargement, and blood contains circulating lymphocytes of more than 10<sup>8</sup> cells/ml (compared to normal 5 x 10<sup>6</sup> cells/ml of normal mice) [195-196]. The tumour can be transferred by intravenous (i.v.) injection of tumour cells into syngeneic mice. BCL<sub>1</sub> cells multiply and differentiate in the spleen and then migrate to the blood. 87% of cells in the spleen, 85% of nucleated cells in the blood and 10-15% of bone marrow cells were found to be BCL<sub>1</sub> cells [195].

BCL<sub>1</sub> cells express cell-surface idiotypic (Id) IgM and IgD [197]. BCL<sub>1</sub> cells maintained in our institute express Id IgM strongly but weakly express IgD [138]. This specific molecule on tumour cells provides an ideal target for tumour immunotherapy. In the early BCL<sub>1</sub> tumour immunotherapy experiment, Krolick *et al* (1982) used immunotoxin-conjugated anti-Id to treat tumour bearing mice after total lymphoid irradiation. The anti-Id immunotoxin delayed the appearance of tumour cells but did not protect mice from relapse [198]. In 1998, Tutt AL *et al* treated tumour challenged mice with anti-Id mAb and found that the mAb appeared to prevent tumour cell growth. Even though the mice died eventually, the mAb prolonged survival significantly compared to non-treated mice [199].

#### 3.1.2 Id protein and DNA vaccines

Vaccination against BCL<sub>1</sub> Id was initially done by injection of 50 µg of Id IgM mixed with CFA into two subcutaneous sites [138]. The vaccinated mice were challenged with a lethal dose of the tumour after two boosts. At day 20 after tumour challenging, spleen weight and surface and cytoplasmic Id Ig levels of immunized mice were dramatically lower than the control mice. The immunized mice survived longer than 100 days, compared to control mice that died within 38 days. In addition, cytotoxic anti-idiotypic antibody and splenic T cells specific to Id IgM were induced in immunized mice; and passive transfer of anti-Id antibody provided protection against the tumour. This evidence proves the principle that the Id Ig is a good target for vaccination against lymphoma. In the therapy experiment,

vaccination was performed after inoculation of BCL<sub>1</sub> cells [143]. The tumour passage was performed 3 days before vaccination; the time expected that the tumour is established in the spleen. The Id IgM with CFA could not treat the tumour-bearing mice. KLH conjugation to Id IgM improved the efficiency of the vaccine as the Id-KLH in combination with CFA provided protection against the inoculated tumour.

An alternative way of vaccination is the use of a DNA vaccine. DNA fusion vaccines including tumour-derived Id have been developed in our laboratory. The V<sub>L</sub> and V<sub>H</sub> sequences of Id Ig could be assembled with a flexible linker sequence to encode scFv, a minimal polypeptide sequence able to fold as idiotypic determinants [200]. DNA vaccine encoding scFv alone was a poor immunogen, but fusion with the sequence from tetanus toxin fragment C (FrC) promoted anti-Id antibody responses and led to protective immunity [201]. The mechanism of the fusion DNA vaccine is to engage the non-deleted wide T-cell repertoire available for the microbe (figure 3-1). DNA vaccine fusion of BCL<sub>1</sub> scFv and FrC induced antibody and the antibody response was improved by electroporation immediately after DNA injection during boosting [137].

In the study of the BCL<sub>1</sub> model by Benvenuti *et al* (2000), mice were protected from tumour challenge only when vaccinated with plasmid DNA encoding a Id V<sub>L</sub>/V<sub>H</sub> conformational epitope, but not when vaccinated with a combination of plasmids encoding V<sub>H</sub> or V<sub>L</sub> separately [202]. In addition, the anti-Id antibody caused tumour cell apoptosis and cell cycle arrest *in vitro* [203]. In this study, the Id-specific T cell responses were not detected.

The PVXCP is another fusion partner used in our laboratory. It was chosen because of the lack of pre-existing immunity in human individuals and its good immunogenicity. DNA vaccines encoding scFv Id Ig from B-cell malignancies fused with PVXCP were developed and they were shown to generate protection against the B-cell tumours [136]. The DNA fusion vaccine encoding scFv from the mouse A31 lymphoma or 5T33 myeloma induced antibodies that specifically recognised both the tumour antigen and PVXCP. In addition, the vaccine provided protection against the tumours and the protection appeared to involve CD4<sup>+</sup> T cells [136]. Since the tumour antigen itself is a weak immunogen, T-cell help is important to produce an effective vaccine. A fusion of PVXCP provided T-cell help which has been proven to be a crucial factor for both induction and maintenance of antibody responses to tumour antigens [145]. An additional property of PVXCP fusion proteins is the ability to form aggregates [136], a feature which could further enhance immunogenicity. Moreover, performance of PVXCP fusion vaccines will be in a setting of no pre-existing immunity. This is potentially beneficial as there is a known potential neutralizing effect of pre-existing antibody. In this chapter, I transferred the established principle of the DNA

fusion vaccine to PVXCP fusion protein vaccine and chose a plant expression system for vaccine preparation.

### **3.1.3 Expression of recombinant protein in plants**

#### **3.1.3.1 HyperTrans (HT) expression system**

The recently-developed HT expression system which utilises a plant viral-based vector was developed from the deleted version of the CPMV RNA-2 (delRNA-2) expression system [204]. In the CPMV delRNA-2 vector, the majority of encoding region could be replaced by the gene of interest, GFP in 1-GFP construct (figure 3-2) [204]. Sainsbury *et al* (2008) modified further the 1-GFP construct by deleting one or both of the two additional AUG codons (position 115 and 161) upstream of AUG position 512 (the translation initiation codon of the inserted gene) on RNA-2 (figure 3-2,  $\Delta$ 115,  $\Delta$ 161 and  $\Delta$ 115/161)[182]. The level of GFP expression in the host plant was examined under UV light and by SDS-PAGE. They found that removal of AUG161 with or without removal of AUG115 was critical for the increasing of the expression levels of the gene of interest. They referred to the viral RNA-2 leader sequence lacking AUG161 as the hypertranslatable (HT) leader. By using this system, the Hepatitis B core antigen (HBcAg) was expressed at high levels (approximately 1 g/kg of fresh-weight tissue) at 6 day postinfiltration (p.i.) with the viral construct and the HBcAg was shown to be assembled into the virus core protein [182].

In addition to the rapidly achieved high expression levels, further advantages of this novel expression system are low level of plant tissue necrosis and absence of infectious CPMV particles [182]. As the majority of the encoding region of RNA-2 was deleted, the infectious CPMV particles are not produced and could not be released to the environment. This provides the solution for the biocontainment problem. The HT system provides the expression system without major damage to the host plant, thus results in high expression levels of the protein of interest. The modified HT expression cassette can be introduced into the host plant by *Agrobacterium* infection.

#### **3.1.3.2 *Agrobacterium*-mediated DNA transfer**

The introduction of an expression vector, including a vector of the HT system, into the host plant cell utilizes the benefit of an *Agrobacterium* infection. *A. tumefaciens* is a pathogenic bacterium that causes a crown gall disease in plant species. *Agrobacterium* transfers a portion of its DNA to plant cells and transforms the plant cells to overproduce phytohormone, causing cell proliferation, which results in the growth of tumours (crown galls). The ability of *Agrobacterium* to transfer a fragment of its own DNA on tumour-

inducing (Ti) plasmid to the plant cell provides a powerful tool for plant biotechnology and therefore *Agrobacterium*-mediated DNA transfer is one of the most commonly used techniques of plant transformation.

The *Agrobacterium* transfers its transferred DNA (T-DNA) on the Ti-plasmid to the plant cells. T-DNA contains genes encoded for phytohormone producing enzymes that stimulate growth of tumours and metabolic enzymes responsible for synthesis of opine, the nutrient required by the colonizing bacteria [205-206]. The elements of Ti vector required for DNA transfer include *vir* genes and the T-DNA 25 bp imperfect repeat boundaries, known as the right and left borders, RB and LB, respectively (figure 3-3) [207]. The Vir proteins function in producing a single-stranded T-DNA from the Ti plasmid, facilitating delivery of the T-DNA into the nucleus of a plant cell, and involved in T-DNA integration into plant genome (figure 3-4). Subsequently, genes on T-DNA are expressed under the plant protein expression machinery [205].

In the development of Ti as a gene expression plasmid, it was found that *vir* genes and T-DNA could be located in 2 separate plasmids, so-called Ti binary vector [208]. This reduces the size of the expression plasmid and leads to ease of recombinant gene manipulation. In addition, removal of all the genes in T-DNA, but not RB and LB, does not impede the ability of *Agrobacterium* to transfer the DNA [207-208]. Therefore, in Ti vectors, T-DNA genes could be removed and replaced by the expression cassette. Similarly, in the SK plasmid, an expression vector of the HT system, the expression cassette with the inserted foreign gene replaces the T-DNA genes (figure 3-5). The recombinant plasmid would be transformed into *Agrobacterium* containing suitable *vir* genes before inoculation into a host plant [208]. Thereafter, the expression cassette would be transferred to the plant nucleus and the inserted gene would be expressed by the plant protein translational machinery.

### **3.1.4 Aims**

In this section, the aim is to produce multimeric fusion protein specific to BCL<sub>1</sub> Id in form of BCL<sub>1</sub> scFv fused to PVXCP (scFv.BCL<sub>1</sub>-PVXCP). The fusion protein is aimed to be produced in plants and the purified protein is expected to be able to induce immunity against the tumour.

### **3.1.5 Hypotheses**

1. The constructed scFv.BCL<sub>1</sub>-PVXCP expression cassette can drive expression of the fusion protein in plants.
3. ScFv.BCL<sub>1</sub>-PVXCP can be purified from plant tissue by antibody affinity chromatography.
2. ScFv.BCL<sub>1</sub>-PVXCP expressed in plants appears in a multimeric form based on the ability of PVXCP to form disc-like structure.
4. ScFv.BCL<sub>1</sub>-PVXCP is able to induce antibody against BCL<sub>1</sub> and provide protection against tumour challenge at levels comparable to the DNA vaccine.

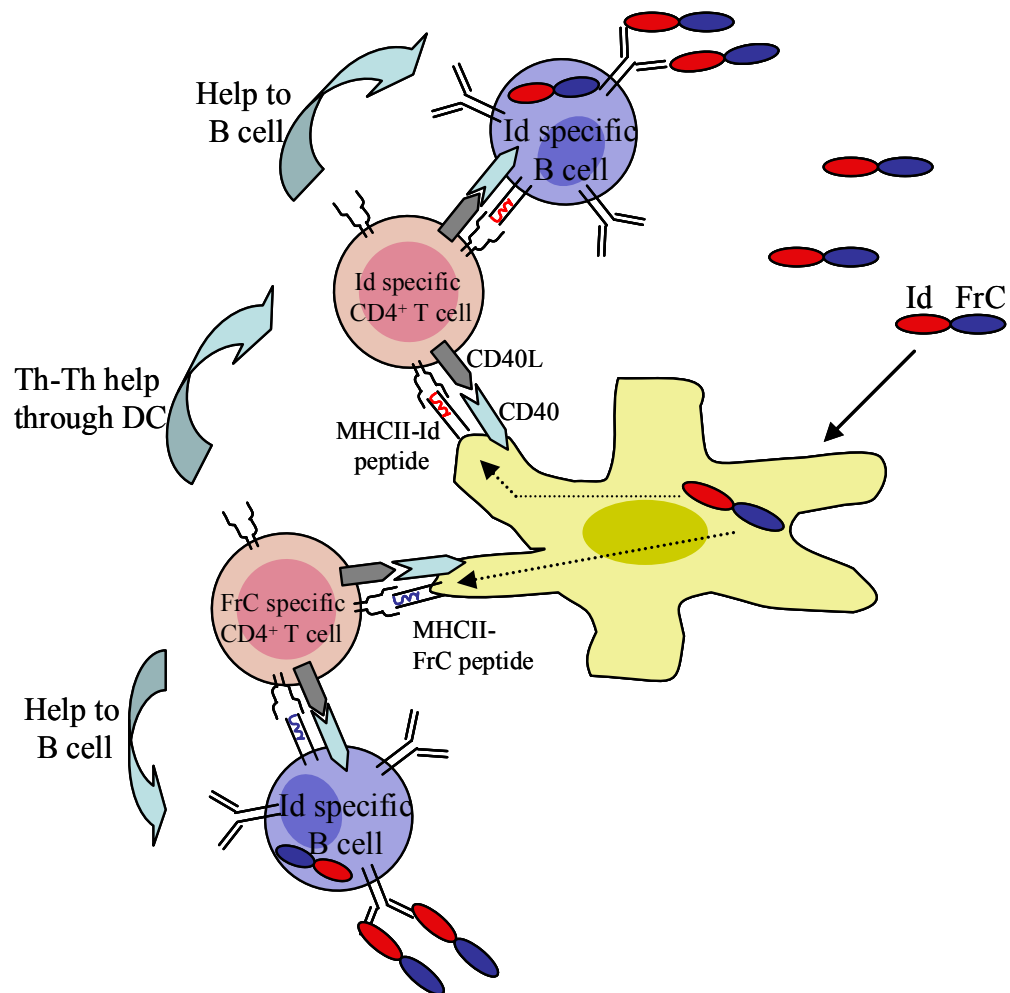


**Figure 3-1. Mechanism of Id fusion vaccine**

Id fusion vaccine such as Id-FrC protein is internalised by DCs and B cells which later process the vaccine into Id peptide and FrC peptide and present them as complexes with MHC II molecules. Id or FrC-specific CD4<sup>+</sup> T cells bind to their specific peptide-MHCII complex on DCs and are activated. The activated T cells then provide help to Id-specific B cells via interaction to Id or FrC peptide-MHC II on B cells with FrC playing the major role. In addition, FrC specific CD4<sup>+</sup> T cells can provide help to Id specific CD4<sup>+</sup> T cells through DC licensing.

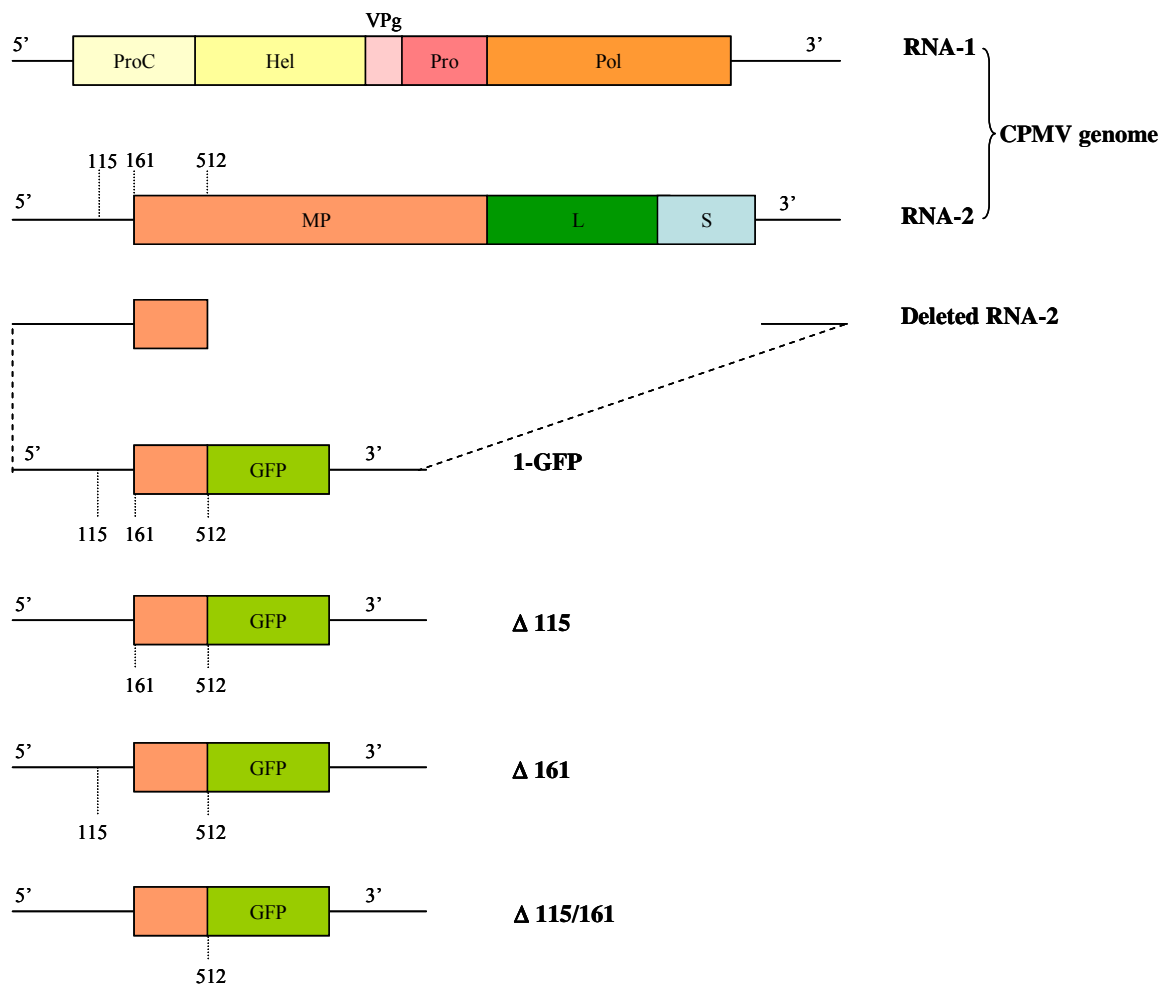


**Figure 3-2. Schematic diagram of a CPMV RNA-2-based HT expression vector**

In the CPMV delRNA-2 expression system, the majority of RNA-2 coding region was replaced by the GFP gene, resulting in 1-GFP expression vector [204]. The viral 5' sequence of 1-GFP was modified by deletion of AUG at position 115 ( $\Delta 115$ ) or 161 ( $\Delta 161$ ) or both positions ( $\Delta 115/161$ ) which are upstream of AUG position 512 (the translation initiation codon of the inserted gene). The viral RNA-2 leader containing the deleted AUG161 provided high levels of protein expression and was therefore referred to as the HT leader [182]. The positions of AUG codons are indicated by numbers. ProC: proteinase cofactor, Hel: Helicase, VPg: virus protein genome-linked, Pro: proteinase, Pol: polymerase, MP: movement protein, L: large coat protein subunit, S: small coat protein subunit.

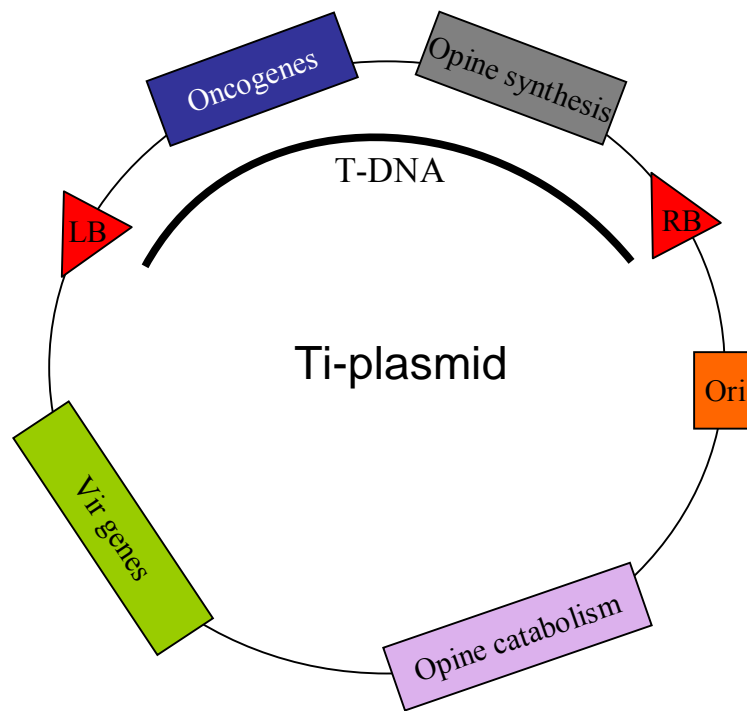


**Figure 3-3. Schematic diagram of Ti-plasmid**

Ti plasmid contains transferred DNA element (T-DNA), *vir* genes, opine catabolism genes, and origin of replication (Ori). The T-DNA contains right border (RB), opine synthesis genes, oncogenes, and left border (LB).

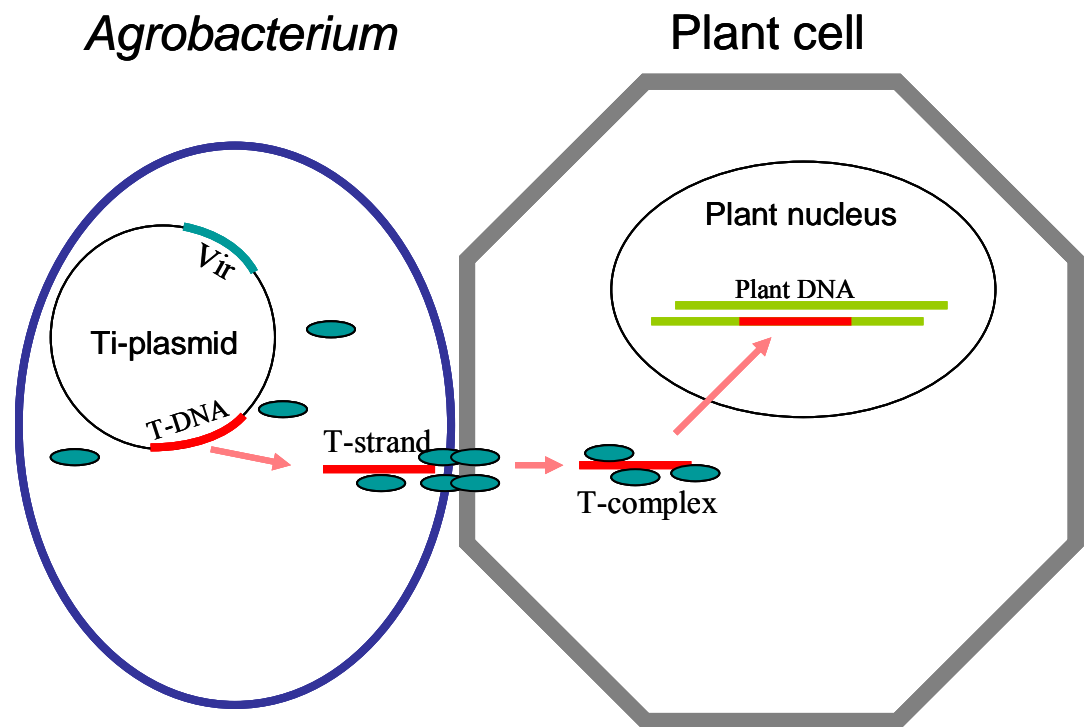


**Figure 3-4. Transferring T-DNA into the plant genome**

The virulence (*Vir*) proteins produce the T-strand from T-DNA of the Ti-plasmid. After the bacterium attaches to a plant cell, the T-strand and several types of *Vir* proteins are transferred to the plant cell and form the T-complex. This complex targets the nucleus, allowing the T-DNA to integrate into the plant genome and express the encoded genes.

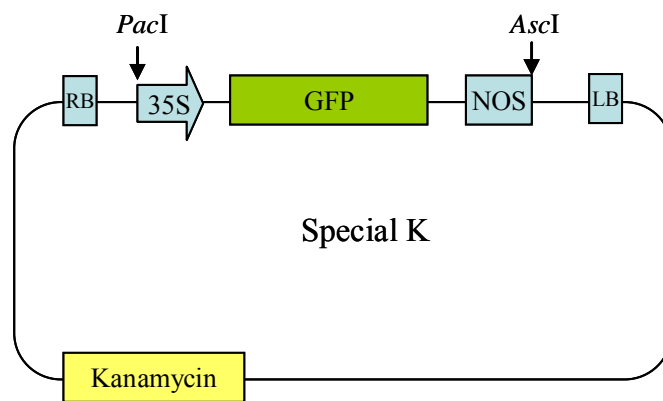


**Figure 3-5. Schematic diagram of Special K (SK) vector of HT expression system**

LB and RB represent left and right border of *Agrobacterium* T-DNA, respectively. 35S: the 35S RNA promoter; *GFP*: the green fluorescence protein (GFP) gene; *Nos*: the transcriptional terminator of the nopaline synthase gene of *Agrobacterium tumefaciens*. *Kanamycin*: Kanamycin resistant gene. *PacI* and *AscI* are the restriction sites.

## 3.2 Results

### 3.2.1 Construction of scFv.BCL<sub>1</sub>-PVXCP expression plasmid

The scFv.BCL<sub>1</sub>-PVXCP fusion protein was expressed in *Nicotiana benthamiana* host plants using the SK expression vector of the HT system. Recombinant scFv.BCL<sub>1</sub>-PVXCP was constructed in three different contexts within the SK plasmid (figure 3-6); the first construct was a fusion of scFv.BCL<sub>1</sub> and PVXCP (SK-B) aimed for expression of the protein in the cytosol; the second construct contained the leader sequence at the N-terminus of scFv.BCL<sub>1</sub> (SK-L) to direct the protein to the ER and subsequently to target to a secretory pathway; the final construct (SK-LH) contained the leader sequence and HDEL, the ER retention signal, added for protein accumulation in the ER.

Introduction of the recombinant genes into the SK plasmid required two-step cloning to prevent SK backbone digestion by *NruI* and *XhoI*, the two enzymes required for restriction digestion and subsequently insertion of the recombinant gene into the expression cassette. The recombinant gene was amplified from pcDNA3.scFv.BCL<sub>1</sub>-PVXCP (the DNA vaccine) and inserted into pM81 cloning vector at *NruI/XhoI* cloning sites to obtain the in-frame fusion with the HT leader sequence. The expression cassette was then isolated from pM81 by *PacI/AscI* digestion and subsequently inserted into *PacI/AscI* digested SK plasmid for further transformation to *Agrobacterium*.

The three sequences for each constructs were obtained by PCR and inserted into the pM81 plasmid. The clones containing recombinant plasmid were screened by PCR using the cloning primers. The plasmid pcDNA3.scFv.BCL<sub>1</sub>-PVXCP was used as a positive control for PCR. *E. coli* colonies containing the inserted sequence with the expected size of 1.5 kb were detected in all 3 constructs (figure 3-7). The correct recombinant sequences were confirmed by DNA sequencing analysis.

The correct DNA fragments were then isolated from pM81 by *PacI/AscI* digestion and ligated to digested SK plasmid. The ligated plasmids were transformed to *E. coli* and the clones containing recombinant sequences were screened by PCR (figure 3-8). The inserts were analyzed by DNA sequencing. The correct recombinant plasmids were transferred to *Agrobacterium*. The *Agrobacterium* clones were screened by PCR to confirm the presence of recombinant SK (figure 3-9).

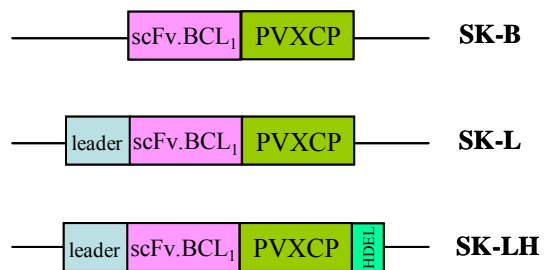


**Figure 3-6. Schematic diagram of scFv.BCL<sub>1</sub>-PVXCP constructs in SK vector**

The fusion BCL<sub>1</sub>-PVXCP gene was introduced into Special K (SK) vector in 3 different contexts; SK-B construct contained only the scFv.BCL<sub>1</sub>-PVXCP fusion sequence; SK-L construct contained an additional leader sequence at the N-terminus of the scFv.BCL<sub>1</sub> sequence; SK-LH contained a leader sequence and HDEL, the ER retention signal.

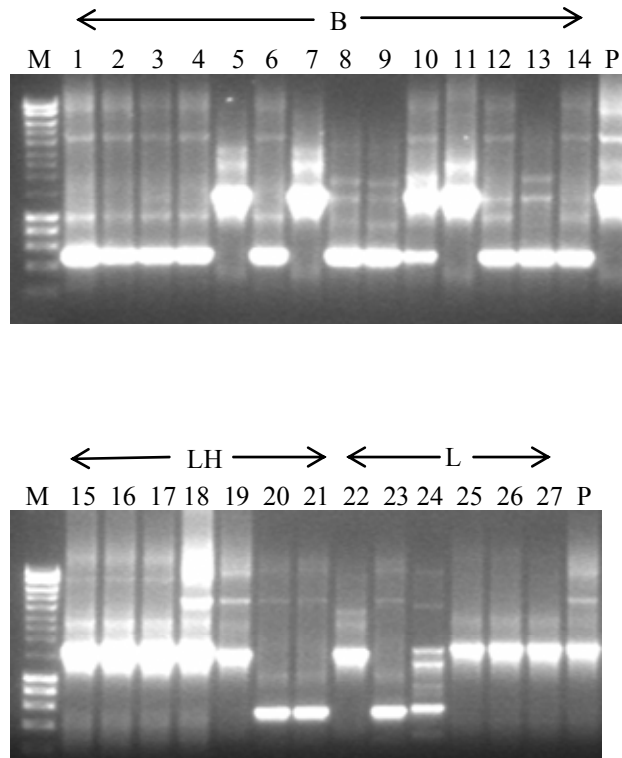


**Figure 3-7. PCR screening for pM81 containing the scFv.BCL<sub>1</sub>-PVXCP sequence**

Bacteria containing recombinant pM81 were screened by PCR with the cloning primers. Numbers represent each colony screened for pM81.scFv.BCL<sub>1</sub>-PVXCP (B), pM81.Leader-scFv.BCL<sub>1</sub>-PVXCP (L) or pM81.Leader-scFv.BCL<sub>1</sub>-PVXCP-HDEL (LH). *M* represents Hyper ladder I marker. *P* represents PCR product from pcDNA3.scFv.BCL<sub>1</sub>-PVXCP as a positive control for PCR.

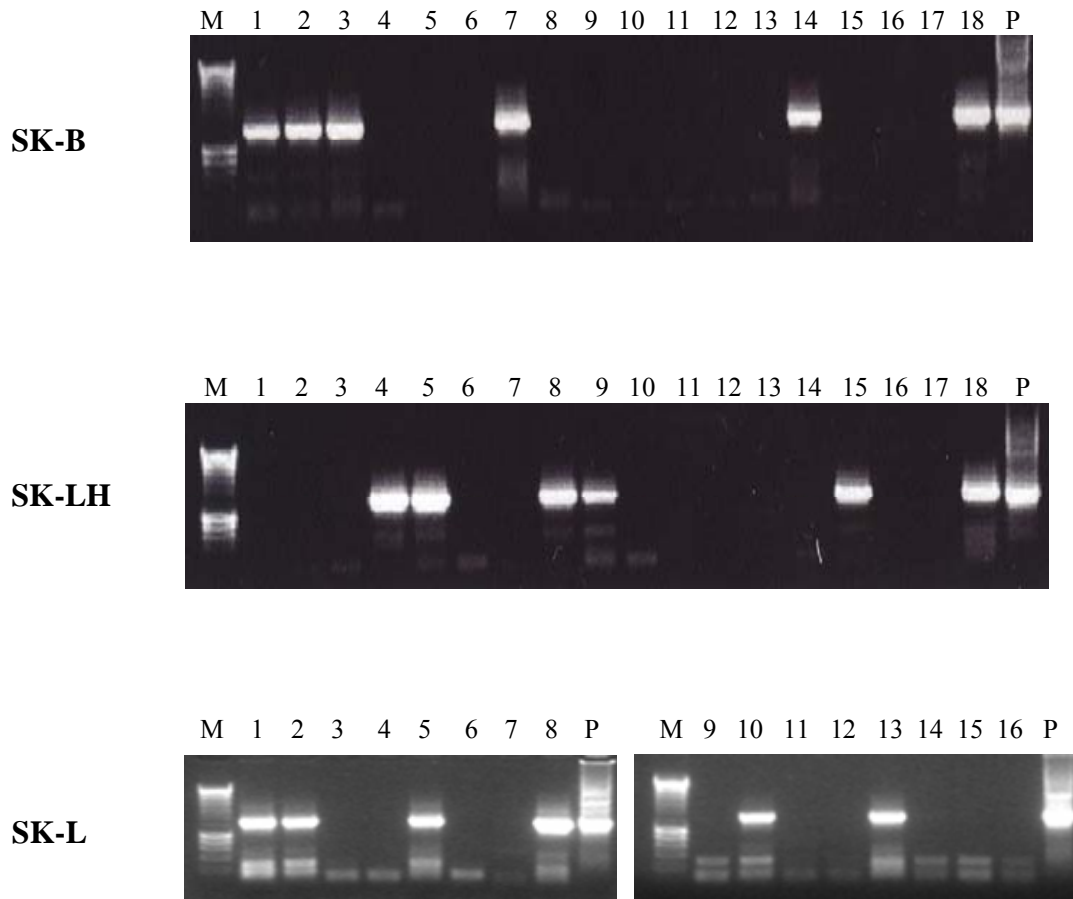


**Figure 3-8. PCR screening of Special K containing the scFv.BCL<sub>1</sub>-PVXCP sequence**

Bacteria containing recombinant Special K (SK) were screened by PCR with the cloning primers. Numbers represent each colony screened for SK.scFv.BCL<sub>1</sub>-PVXCP (SK-B), SK.Leader-scFv.BCL<sub>1</sub>-PVXCP (SK-L) or SK.Leader-scFv.BCL<sub>1</sub>-PVXCP-HDEL (SK-LH). *M* represents Hyper ladder I marker. *P* represents the PCR product from pcDNA3.scFv.BCL<sub>1</sub>-PVXCP as a positive control for PCR.

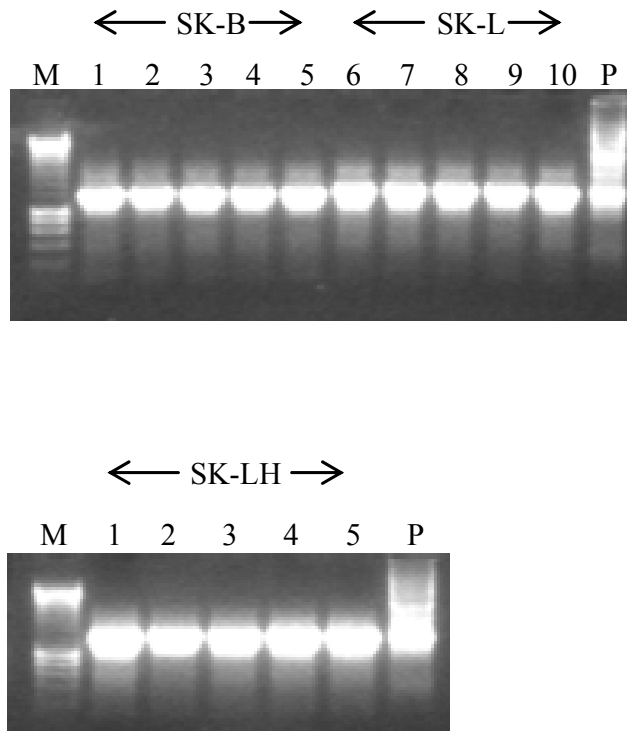


**Figure 3-9. PCR screening for *Agrobacterium* containing SK-based constructs**

*Agrobacterium* colonies containing recombinant SK were screened by PCR with the cloning primers. Numbers represent each colony screened for SK.scFv.BCL<sub>1</sub>-PVXCP (SK-B), SK.Leader-scFv.BCL<sub>1</sub>-PVXCP (SK-L) or SK.Leader-scFv.BCL<sub>1</sub>-PVXCP-HDEL (SK-LH). *M* represents Hyper ladder I marker. *P* represents a PCR product from pcDNA3.scFv.BCL<sub>1</sub>-PVXCP plasmid as a positive control for PCR.

### 3.2.2 Expression and purification of scFv.BCL<sub>1</sub>-PVXCP in *N. benthamiana*

The *Agrobacterium* culture containing the scFv.BCL<sub>1</sub>-PVXCP expression plasmid was infiltrated into host plants and the inoculated leaves were harvested at day 7 p.i. Initially, the expression of the fusion protein was analyzed. The whole protein extracted from the leaf infiltrated with either SK-B or SK-L or SK-LH was separated by SDS-PAGE and visualized by Coomassie staining (figure 3-10A). The expected size of recombinant scFv.BCL<sub>1</sub>-PVXCP is approximately 50 kDa which appeared to migrate to the same position as the large subunit of plant RuBisCO protein (figure 3-10A). In addition, the extract from the SK-L-inoculated leaf contained protein size approximately 30 kDa and 15 kDa (circle red in figure 3-10A lane L). These 2 proteins were suspected to be degraded products of scFv.BCL<sub>1</sub>-PVXCP. Subsequently, a Western blot analysis with anti-PVXCP mouse antiserum confirmed that the fusion protein was present in SK-L and SK-LH but not in SK-B-inoculated plants (figure 3-10B). Therefore, out of three constructs tested, two constructs (SK-L and SK-LH) expressed the fusion protein and the one targeted to the cytoplasm resulted in no expression of the protein. The SK-LH construct was chosen for further expression of the fusion protein as it provided high level of protein expression with minimal protein degradation.

Two types of affinity chromatography were developed to purify scFv.BCL<sub>1</sub>-PVXCP, an anti-PVX and an anti-BCL<sub>1</sub> antibody affinity column. Rabbit anti-PVX polyclonal antibody or the mixture of three anti-BCL<sub>1</sub> monoclonal antibodies was coupled to CnBr-activated sepharose 4B supporting beads. The anti-PVX affinity column was proposed to be a generic method of purification for all PVXCP fusion proteins; the anti-BCL<sub>1</sub> affinity column was aimed at selection of a folded BCL<sub>1</sub> antigen. Purification using the anti-BCL<sub>1</sub> column provided up to 200 µg per g fresh weight of plant per 1 ml of the anti-BCL<sub>1</sub> matrix. While purified protein up to 40 µg per g plant fresh weight per 1 ml of the matrix was obtained from the anti-PVX column. The purified product was further analyzed by SDS-PAGE. The protein purified from the anti-BCL<sub>1</sub> column contained protein of the size of the fusion protein and other 4 smaller proteins (figure 3-11A, lane α-B). The Western analysis revealed that apart from the fusion protein, 2 smaller proteins also reacted with anti-PVXCP mouse antiserum (figure 3-11B, lane α-B). The smaller proteins were then suspected to be degraded products of the fusion protein which underwent degradation during the purification process. In contrast, the protein purified from anti-PVX column contained fusion protein with lower amounts of degraded products (figure 3-11, lane α-P).

The protein was further purified by size exclusion, based on the principle that large proteins will emerge from the column before small proteins. The anti-PVX affinity

chromatography purified protein (400 µg in 500 µl) was applied onto a PBS-equilibrated size exclusion column (Sephadex 200 10/300 GL) at a flow rate of 0.6 ml/min. The sample that passed through the column was collected every 2 ml for the first 3 fractions, 1 ml for the following 2 fractions, and then collected every 0.5 ml from fraction 6 until the end of running. As shown in figure 3-12, the chromatogram appeared to be divided into 5 peaks; the first peak was composed of fraction 7 and 8, the second peak was from fraction 9 to 13, the third peak started from fraction 15 to 17, the fourth peak was from fraction 18 to 21, and the last peak was from fraction 22 to 24. The initial study showed that scFv.BCL<sub>1</sub>-PVXCP and lower molecular weight protein appeared between fraction 15 and 25. Therefore, the detailed analysis of fractionated sample was applied to the last three peaks. The selected fractions were further analyzed by SDS-PAGE following with silver staining (figure 3-13). The results showed that the first 2 peaks of the chromatogram consisted of very high molecular weight proteins. ScFv.BCL<sub>1</sub>-PVXCP without degraded products appeared in the fraction 15 – 18 with the intensity of the fusion protein band increasing in the later fractions. Fraction 19 and 20 contained the highest amount of the fusion protein with the contamination of some degraded products. The last peak of the chromatogram contained all degraded products with a very faint band of the fusion protein was observed. Therefore, size exclusion successfully separated the intact fusion protein from contaminating high molecular weight proteins as well as the products of degradation and therefore is promising method for obtaining highly purified fusion protein. After pooling highly pure fractions (fraction 15-18) and concentrating the protein with a concentrating column, a yield of approximately 5 µg (from 400 µg starting material) was obtained. This purified protein was further used in experiments involved characterisation of the fusion protein while the vaccine immunogenicity study was carried out using protein purified by affinity chromatography.

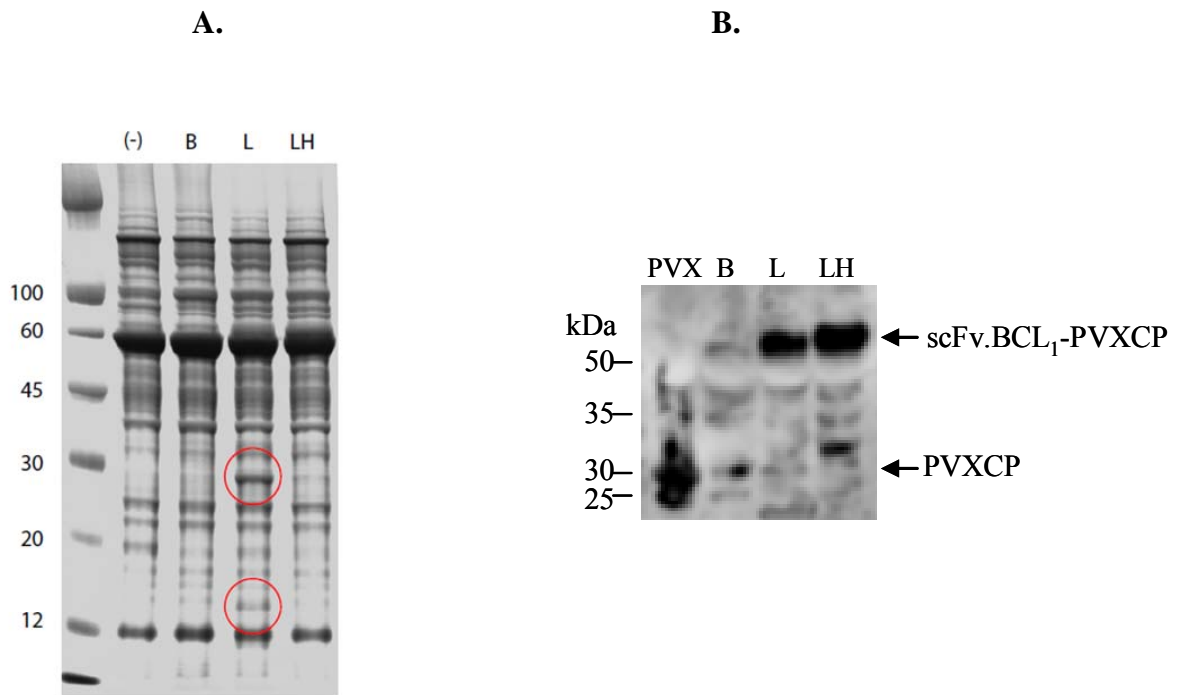


**Figure 3-10. Coomassie-stained SDS-PAGE and Western blot analysis of expressed scFv.BCL<sub>1</sub>-PVXCP**

Extracts from plant tissues infiltrated with SK-B (B) or SK-L (L) or SK-LH (LH) were made and run on SDS-PAGE in parallel with an extract from a plant infiltrated with SK empty vector (-) and either visualised by Coomassie staining (A.) or analysed by Western blot analysis (B.) with anti-PVXCP mouse antiserum in comparison with wild-type PVX. In red circles are proteins found only in SK-L infiltrated tissue. The protein size markers are indicated.

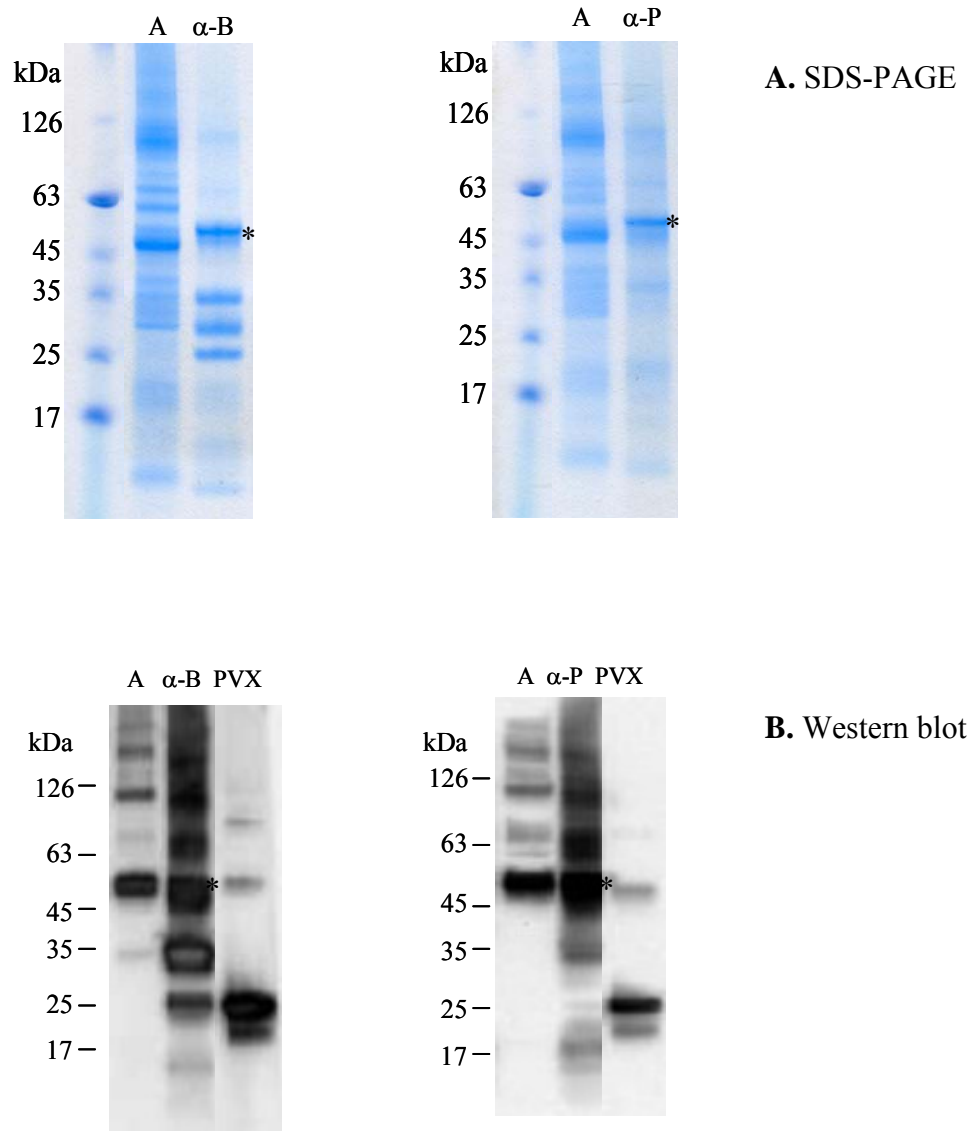


**Figure 3-11. Coomassie-stained SDS-PAGE and Western blot analysis of purified scFv.BCL<sub>1</sub>-PVXCP**

Crude protein extract from SK-LH infiltrating leaves (A) was purified by anti-BCL<sub>1</sub> (α-B) or anti-PVX (α-P) antibody affinity column. The purified protein was analyzed by Coomassie-stained SDS-PAGE (A.) and Western blot analysis with anti-PVXCP mouse antiserum (B.). Asterisks (\*) indicate expected size of scFv.BCL<sub>1</sub>-PVXCP.

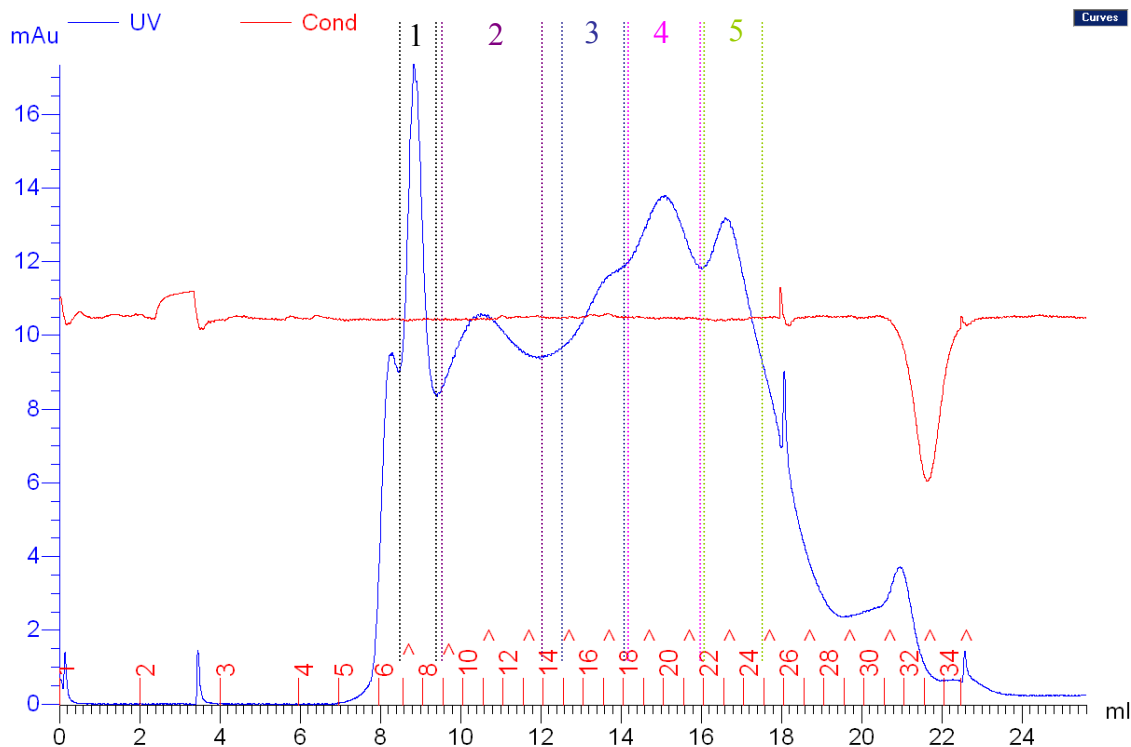


**Figure 3-12. Size exclusion chromatogram of purified scFv.BCL<sub>1</sub>-PVXCP**

Anti-PVX affinity chromatography-purified scFv.BCL<sub>1</sub>-PVXCP (400 µg in 500 µl PBS) was applied onto PBS-equilibrated size exclusion column at a flow rate of 0.6 ml/min. The fractionated samples were collected every 2 ml for the first 3 fractions, 1 ml for the following 2 fractions, and then collected every 0.5 ml from fraction 6 until the end of running, as shown by drop peak of system conductivity (red line in chromatogram). Fraction numbers are shown in red. Numbers on the top of chromatogram represent peak number observed from the chromatogram. The blue line represents UV (280nm) absorbance in milli-arbitrary unit (mAu) of the sample during the chromatography.

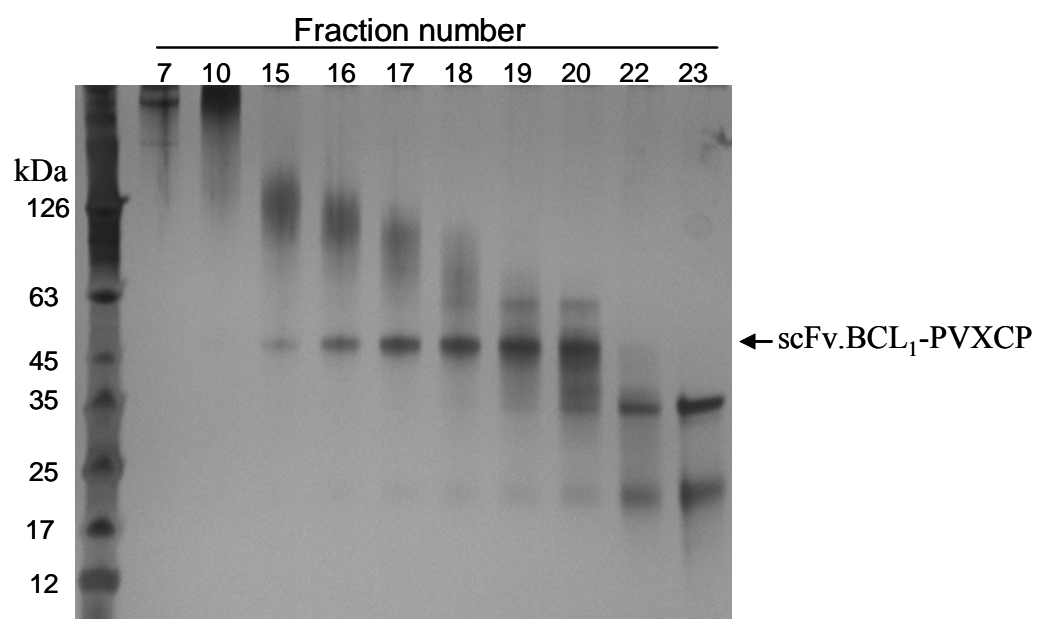


**Figure 3-13. SDS-PAGE analysis of fractions after size exclusion chromatography**

After size exclusion, fractions corresponding to the peaks of UV absorbance value (shown in figure 3-11) were analyzed by SDS-PAGE following with silver staining. Fraction numbers of interest are indicated.

### 3.2.3 Characterization of purified scFv.BCL<sub>1</sub>-PVXCP

As proper folding of the Id is crucial for induction of anti-Id antibody, the integrity of the purified fusion protein was evaluated. The proteins were examined by ELISA in comparison with a crude extract from the SK-LH-infiltrated leaf. BCL<sub>1</sub> IgM and purified PVXCP were included as negative controls. The proteins were incubated with a plate coated with the mixture of anti-BCL<sub>1</sub> monoclonal antibodies and subsequently detected by anti-PVX rabbit antiserum followed by HRP-conjugated anti-rabbit IgG. The optical density (OD) of the enzymatic reaction after substrate addition was measured at 490 nm. As expected, OD<sub>490</sub> was low when BCL<sub>1</sub> IgM and PVXCP were used because they were not able to react with both antibodies (figure 3-14). The fusion protein purified with both the anti-BCL<sub>1</sub> and the anti-PVX columns were positive in ELISA, with the anti-BCL<sub>1</sub> purified protein giving a higher OD value indicating that anti-BCL<sub>1</sub> column probably selected for better folded fusion protein.

The fact that in size exclusion chromatography the fusion protein was detected in five different fractions (figure 3-13), suggesting that the fusion protein forms multimers with variation in size. The protein multimerisation was initially investigated by a native non-denaturing protein gel electrophoresis with a subsequent Western blot analysis looking for slower migration of aggregated protein versus non-aggregated. PVX viral particle was included as a positive control for PVXCP mediated aggregation. The protein sample was kept in a multimeric form by loading with native loading buffer and run in comparison with the sample denatured by boiling in SDS loading buffer containing 0.2 M DTT. Because BCL<sub>1</sub> scFv contains disulfide bonds, it was necessary to include DTT to obtain the denatured form of this protein. In contrast, it is known that SDS alone could destroy the multimeric structure of PVX particle into monomeric CP. The same denaturing loading buffer was used for consistency of the protein denaturing condition. After electrophoresis, the protein was transferred to a PVDF membrane using the native buffer system and was detected by anti-PVXCP mouse antiserum. The Western blot analysis showed that non-denatured scFv.BCL<sub>1</sub>-PVXCP migrated slower than the denatured protein (figure 3-15). The native fusion protein migrated to the position between 160 kDa to the top of the gel above the size marker range, while the denatured protein migrated faster and was between 160 – 250 kDa. This was similar to the PVX particle control where the particle migrated slower than the single CP disrupted by denaturing condition. The negative control did not show any bands. In conclusion, purified scFv.BCL<sub>1</sub>-PVXCP showed a high degree of aggregation. This provided initial data on scFv.BCL<sub>1</sub>-PVXCP aggregation.

Multimerization of scFv.BCL<sub>1</sub>-PVXCP was then further investigated using ISEM. The purified protein was incubated with an anti-BCL<sub>1</sub> or an anti-PVXCP mouse antiserum

or NMS coated grid, followed by excessive washing to remove unbound protein. The grid was further negatively stained and investigated by EM. On both the anti-BCL<sub>1</sub> and anti-PVXCP antiserum coated grid, some particles of approximately 10 nm were observed (figure 3-16). The majority of particles observed were larger than 10 nm, appeared in irregular shapes, and seemed to consist of several 10 nm particles. In contrast, those particles were not observed on an NMS-coated grid suggesting that scFv.BCL<sub>1</sub>-PVXCP which specifically bound to either anti-BCL<sub>1</sub> and anti-PVXCP antiserum appeared in multimeric forms. In addition, the highly pure protein (combined fraction 18-19 after size exclusion) was analysed by dynamic light scattering (DLS) by Dr. G Lomonossoff and colleagues in JIC, Norwich. DLS is the technique used for determination of size of a molecule dissolved in a liquid. A diameter of a molecule is determined by intensity of scattering of a given light [209]. It was found that 97% of the protein were larger than 5.5 nm (size range from 5.5 – 3619.4 nm) with the majority (70%) was 5.5 – 13.1 nm (figure 3-17) which corresponded to the size of between half a PVX disk and two disks stacked together. Taken together, it appeared that the fusion protein formed multimers.

#### **3.2.4 Evaluation of scFv.BCL<sub>1</sub>-PVXCP immunogenicity**

To evaluate the immunogenicity of the fusion protein vaccine, BALB/c mice were vaccinated with purified scFv.BCL<sub>1</sub>-PVXCP. A group of 10 mice was vaccinated with anti-BCL<sub>1</sub> purified protein and a group of 8 mice was vaccinated with anti-PVX purified protein. A separate group of 10 mice vaccinated with the DNA vaccine pcDNA3.scFv.BCL<sub>1</sub>-PVXCP was included as a positive control. The DNA vaccine was chosen for comparison because it was previously found to induce high levels of anti-BCL<sub>1</sub> antibody and protection against the BCL<sub>1</sub> tumour. Another group of 8 mice was vaccinated with purified PVXCP as a negative control. DNA vaccine (50 µg) was injected i.m. whereas PVXCP (50 µg) or anti-BCL<sub>1</sub> or anti-PVX antibody affinity chromatography-purified scFv.BCL<sub>1</sub>-PVXCP (100 µg) was mixed with alum and injected i.p. Alum was the adjuvant of choice because it enhances immunogenicity of a vaccine and is widely used in humans (reviewed in [122]). Blood was collected from a tail tip 3 weeks after priming. Mice were boosted with scFv.BCL<sub>1</sub>-PVXCP in alum on day 35 after priming and blood was collected 2 weeks after. Serum antibody was detected by ELISA using chimeric BCL<sub>1</sub>hIgG or PVXCP as a coating protein.

After priming, the median value of anti-BCL<sub>1</sub> antibody induced in DNA-vaccinated mice was higher than in mice vaccinated with either of scFv.BCL<sub>1</sub>-PVXCP protein vaccines but the difference was not statistically significant (figure 3-18). PVXCP did not induce anti-BCL<sub>1</sub> antibody response and sera from non-immune mice did not react to BCL<sub>1</sub> IgG as

expected. After boosting, anti-BCL<sub>1</sub> antibody levels dramatically increased in all three vaccine groups (figure 3-19). The antibody responses induced by the two protein vaccines were not significantly different between the two groups. The antibody levels induced by anti-PVX purified vaccine were significantly higher than the levels induced by DNA vaccine ( $p = 0.027$ ) while antibody levels induced by anti-BCL<sub>1</sub> purified protein and DNA vaccine were not different. Mice boosted with PVXCP also did not produce antibody to BCL<sub>1</sub> as expected.

Anti-PVXCP antibody was induced by both protein and DNA vaccines after priming (figure 3-20). DNA vaccine induced anti-PVXCP antibody levels which were not significantly different to the antibody levels induced by both protein vaccines. Anti-BCL<sub>1</sub> purified vaccine induced significantly higher anti-PVXCP antibody responses than anti-PVX purified vaccine ( $p = 0.0062$ ). Levels of anti-PVXCP antibody were increased by boosting in all groups (figure 3-21). Protein vaccine purified by anti-BCL<sub>1</sub> affinity chromatography induced anti-PVXCP antibody responses higher than DNA vaccine ( $p = 0.0021$ ) and anti-PVX purified protein vaccine ( $p = 0.0062$ ). The antibody levels induced by DNA vaccine and anti-PVX purified protein vaccine were comparable. Anti-PVXCP antibody responses induced by PVXCP were very high after both priming and boosting and higher than in other groups. Sera from naïve mice were negative for antibody reacting with PVXCP.

Subclasses of anti-BCL<sub>1</sub> IgG produced by scFv.BCL<sub>1</sub>-PVXCP and DNA vaccines were also determined as they are good indicators of the type of Th response induced by a vaccine as well as the ability of the antibody to engage antibody-dependent cell-mediated cytotoxicity (ADCC). In each group, sera from four mice with highest responses were used. Both DNA and protein vaccines appeared to induce mixed Th1/Th2 responses as in all groups IgG1, IgG2a and IgG2b subclasses were induced (figure 3-22). The IgG1 subclass was induced to higher levels than IgG2a and IgG2b in all groups. In the anti-BCL<sub>1</sub> purified protein vaccine group, IgG1 was dominant with the median ratio of IgG1/IgG2a 76 and IgG1/IgG2b 164. In the DNA vaccine and anti-PVX purified protein vaccine groups, the ratio of IgG1 to IgG2 was not as high as in the anti-BCL<sub>1</sub> purified protein group (IgG1/IgG2a ratios were 2 and 8, IgG1/IgG2b ratios were 7.27 and 15.33 in the DNA vaccine and anti-PVX purified protein groups, respectively). The IgG3 subclass was detected in only one mouse of the anti-BCL<sub>1</sub> purified protein vaccine group.

To evaluate if the induced response was protective, the vaccinated mice together with naïve controls were challenged with the BCL<sub>1</sub> tumour. Naïve mice that received the lethal dose of the tumour died within 24 days after challenge (figure 3-23). PVXCP-vaccinated mice died within 22 days after as they were not immune against BCL<sub>1</sub> and

therefore were not protected from the lethal dose of tumour, as expected. All BCL<sub>1</sub> vaccines protected mice against the tumour challenge; anti-PVX purified protein vaccine prolonged survival of tumour-challenged mice with the median survival of 55 days (Logrank test showed significantly different survival in comparison with naïve mice), mice vaccinated with the DNA vaccine and anti-BCL<sub>1</sub> purified protein vaccine were protected with 60% of mice in both groups surviving with no splenomegaly until day 125 after challenge when they were terminated. The data indicate that the fusion protein vaccines protected mice against the tumour, with the anti-BCL<sub>1</sub> purified protein being superior to anti-PVX purified protein and comparable to DNA vaccine. The anti-PVX purified vaccine induced less efficient protection than other vaccines even though it induced high anti-Id antibody levels, as previously determined by ELISA.

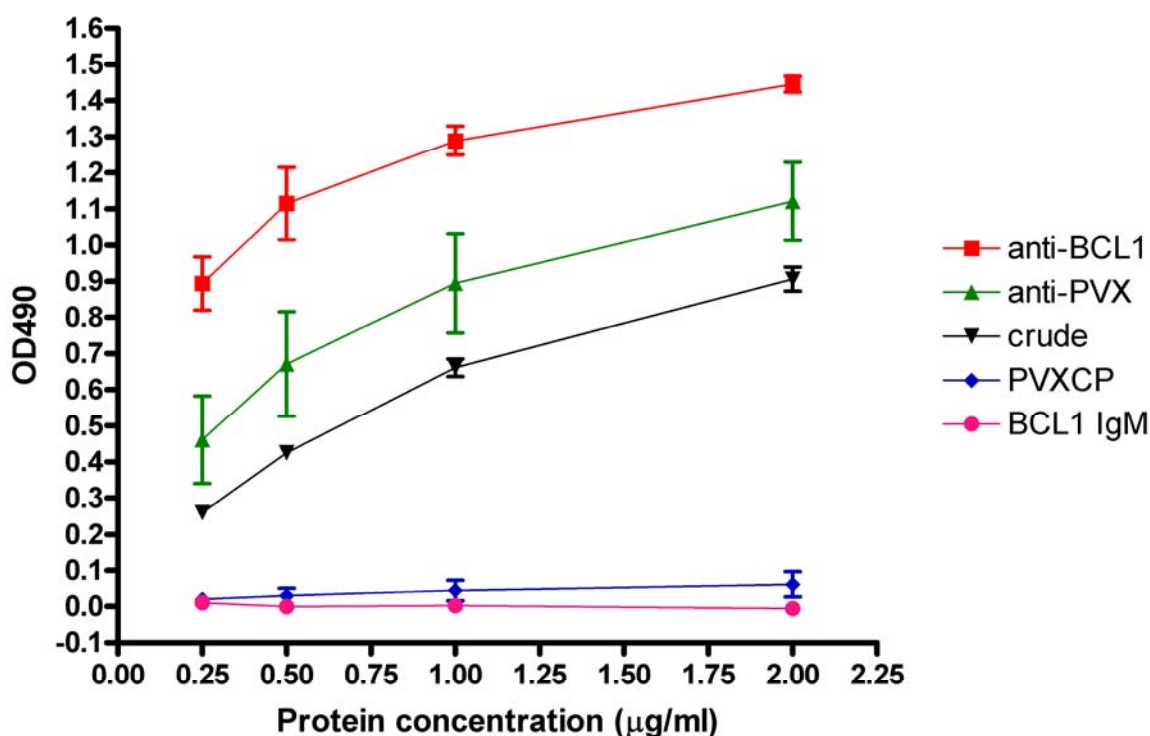


**Figure 3-14. Evaluation of scFv.BCL<sub>1</sub>-PVXCP by ELISA**

ScFv.BCL<sub>1</sub>-PVXCP purified by using an anti-BCL<sub>1</sub> or anti-PVX affinity column was incubated with a plate coated with anti-BCL<sub>1</sub> monoclonal antibodies and subsequently detected with HRP conjugated anti-PVX rabbit antiserum. Total protein extracted from a SK-LH infiltrated leaf (crude), PVXCP and BCL<sub>1</sub> IgM were included. The optical density of the reaction was measured at 490 nm. The concentration of protein is indicated.

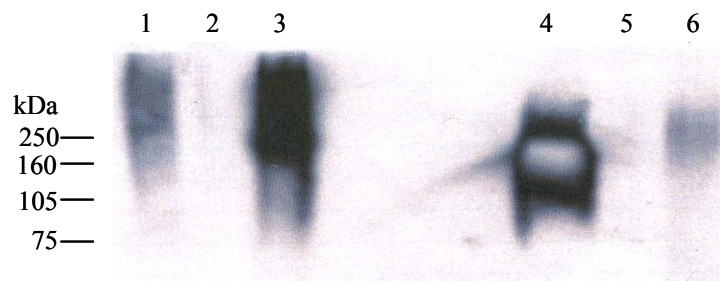
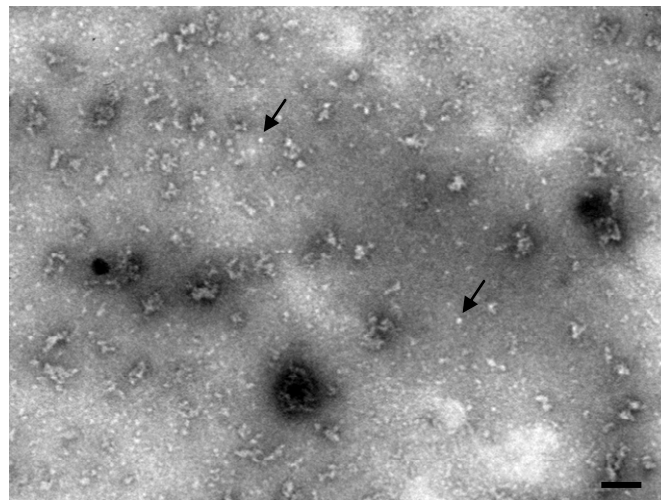
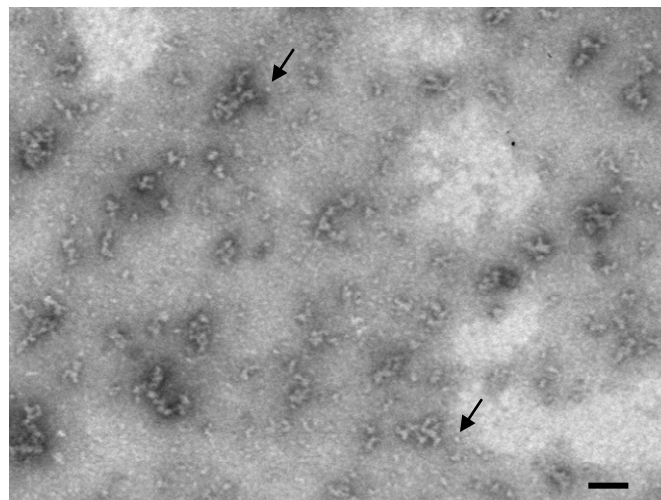


**Figure 3-15. Native gel Western blot analysis of purified scFv.BCL<sub>1</sub>-PVXCP**

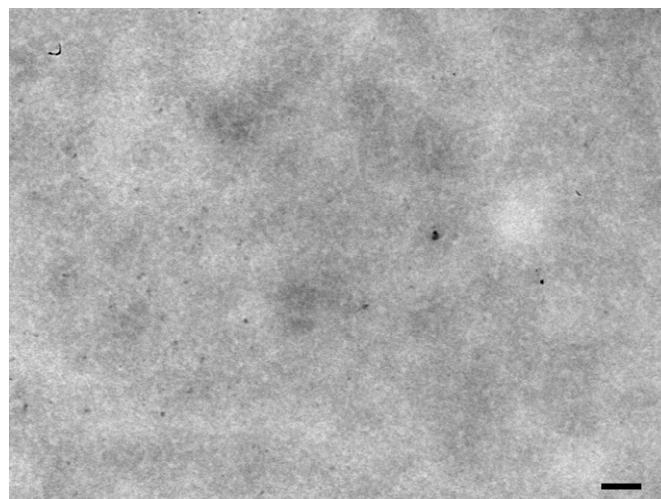
Anti-BCL<sub>1</sub> antibody affinity chromatography-purified scFv.BCL<sub>1</sub>-PVXCP was mixed with native sample buffer (lane 3) or denatured by boiling in SDS sample buffer containing 0.2 M DTT (lane 6) and run on a native protein gel. The proteins were transferred to PVDF membrane using native buffer and detected with anti-PVXCP serum. The protein was analyzed in comparison with native (lane 1) or denatured PVX (lane 4) positive control; and native (lane 2) or denatured (lane 5) 5T33FrC (irrelevant protein) negative control. Full-length Rainbow<sup>TM</sup> molecular weight marker run on the same gel is shown.



Anti-BCL<sub>1</sub>



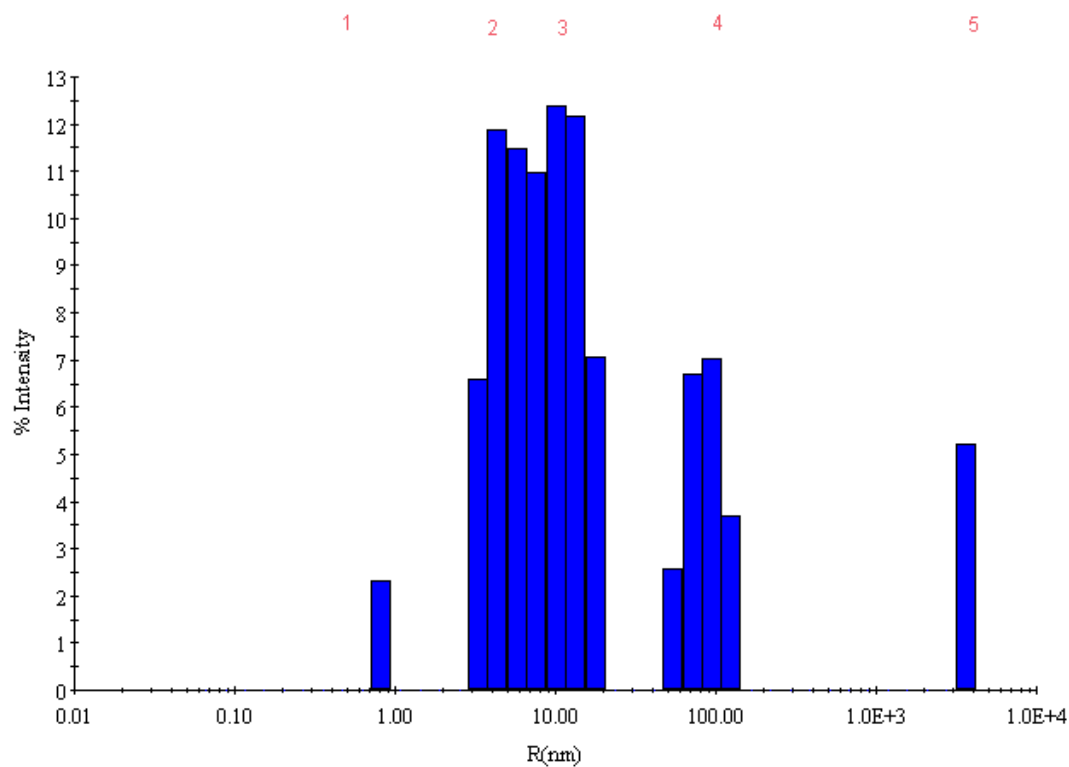
Anti-PVXCP



NMS

**Figure 3-16. ISEM of purified scFv.BCL<sub>1</sub>-PVXCP**

Anti-PVX antibody affinity chromatography-purified scFv.BCL<sub>1</sub>-PVXCP was subjected to ISEM using anti-BCL<sub>1</sub> or anti-PVXCP mouse antisera or serum from a naïve mouse (NMS). Scale bar is 100 nm. Particles approximately 10 nm are indicated with arrows.



Peak number	Radius (nm)	% intensity
1	0.8	2.3
2	5.5	40.9
3	13.1	31.6
4	88	20.0
5	3619.4	5.2

**Figure 3-17. DLS data of purified scFv.BCL<sub>1</sub>-PVXCP**

Graph shows radius (nm) distribution of purified scFv.BCL<sub>1</sub>-PVXCP with red numbers on top of the graph representing peaks of distribution. Percent intensity and radius size of each peak is shown in the table.



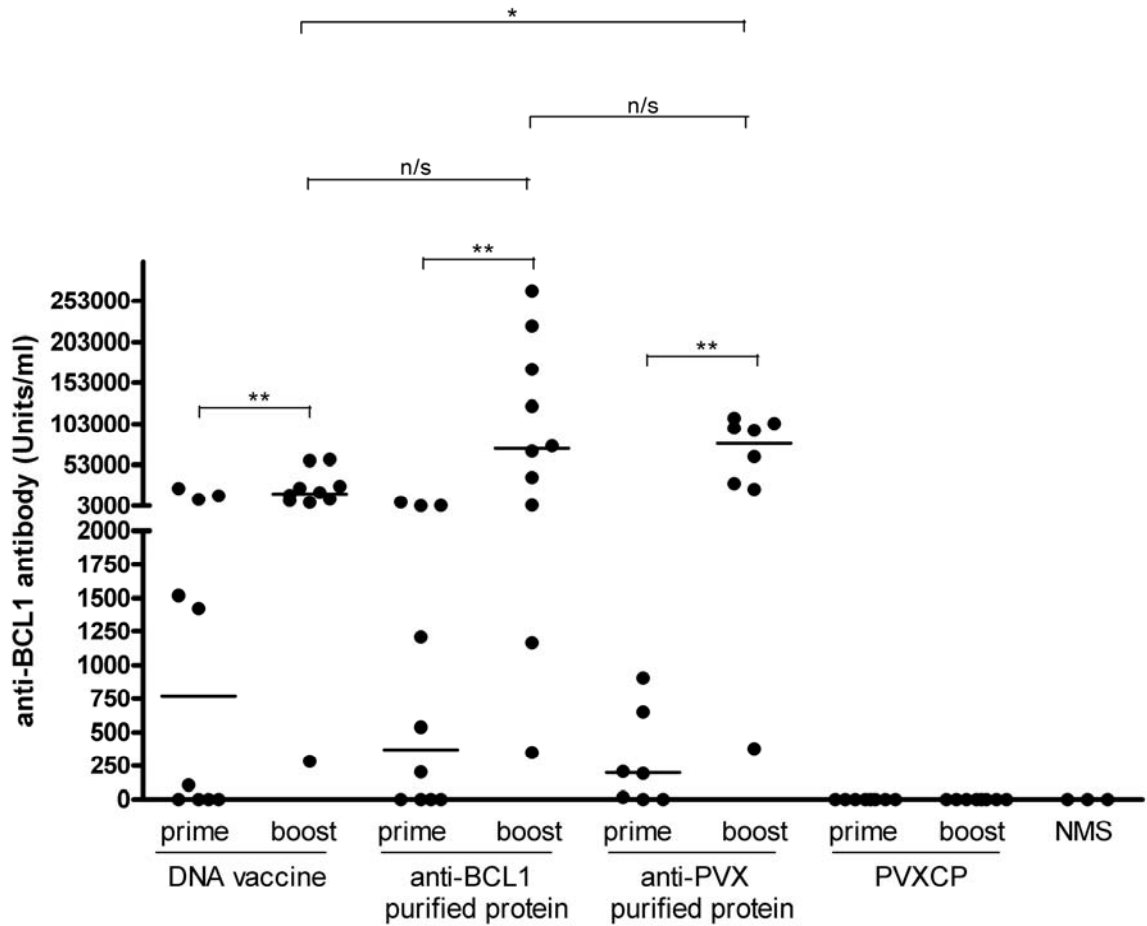


**Figure 3-19. Anti-BCL<sub>1</sub> antibody response after priming/boosting**

Mice were primed with pcDNA3.scFv.BCL<sub>1</sub>-PVXCP (DNA vaccine) or scFv.BCL<sub>1</sub>-PVXCP purified by anti-BCL<sub>1</sub> or anti-PVX antibody affinity chromatography or PVXCP mixed with alum and then boosted on day 35 with the priming material. Antibody levels to BCL<sub>1</sub> were measured on day 21 after priming (prime) and day 14 after boosting (boost). Serum from naïve mice (NMS) was used as a baseline. \*\*: 0.001 < P < 0.005, \*: P < 0.05, n/s: P > 0.05. Each dot represents an individual mouse. Horizontal bars are median values.

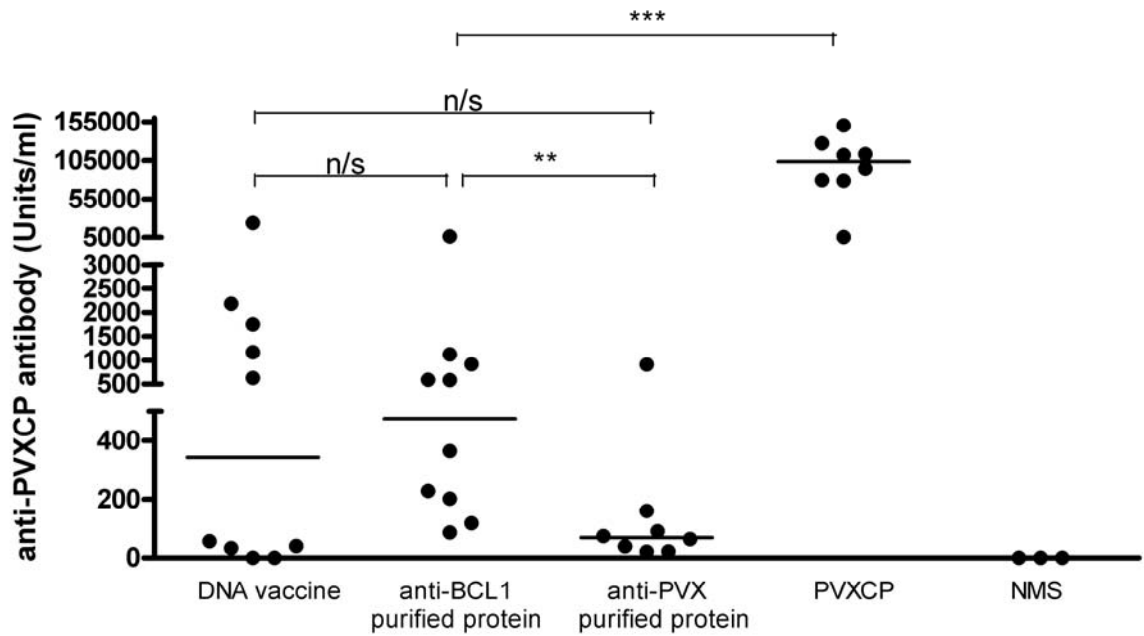


**Figure 3-20. Anti-PVXCP antibody responses after priming**

Mice were injected with pcDNA3.scFv.BCL<sub>1</sub>-PVXCP (DNA vaccine) or scFv.BCL<sub>1</sub>-PVXCP purified by anti-BCL1 or anti-PVX antibody affinity chromatography or PVXCP mixed with alum. Antibody levels to PVXCP were measured on day 21 after injection. Serum from naïve mice (NMS) was used as a baseline. \*\*\*:  $P < 0.001$ , \*\*:  $P < 0.005$ , n/s:  $P > 0.05$ . Each dot represents an individual mouse. Horizontal bars are median values.

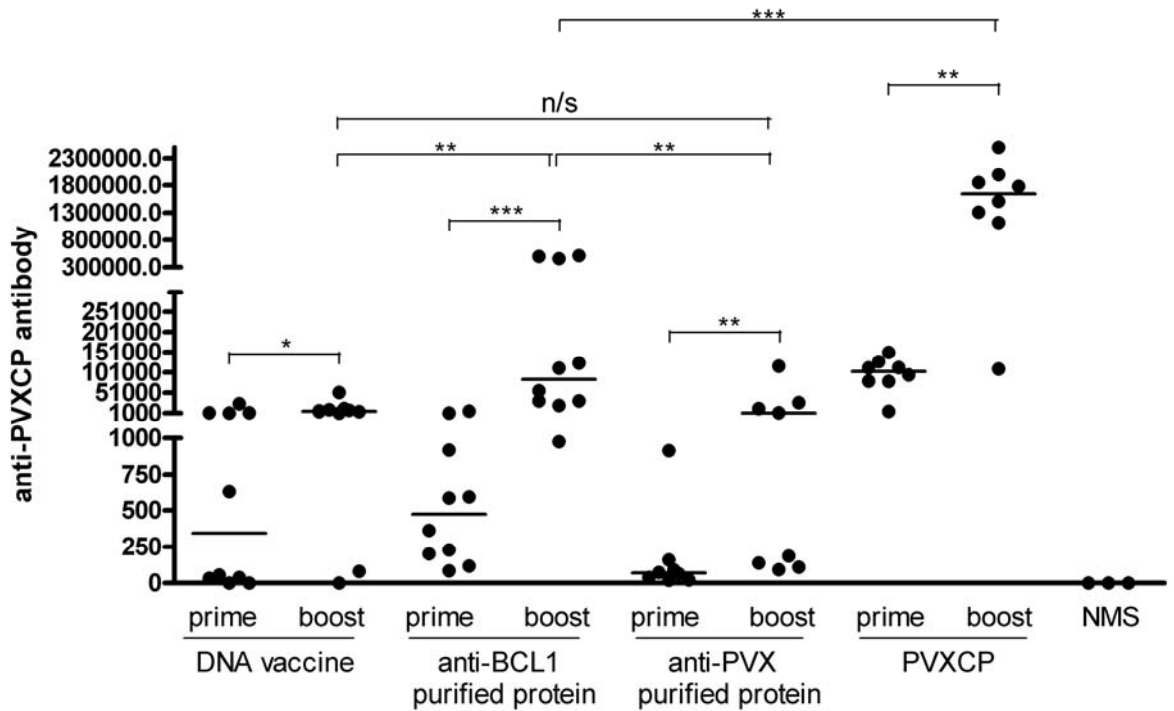
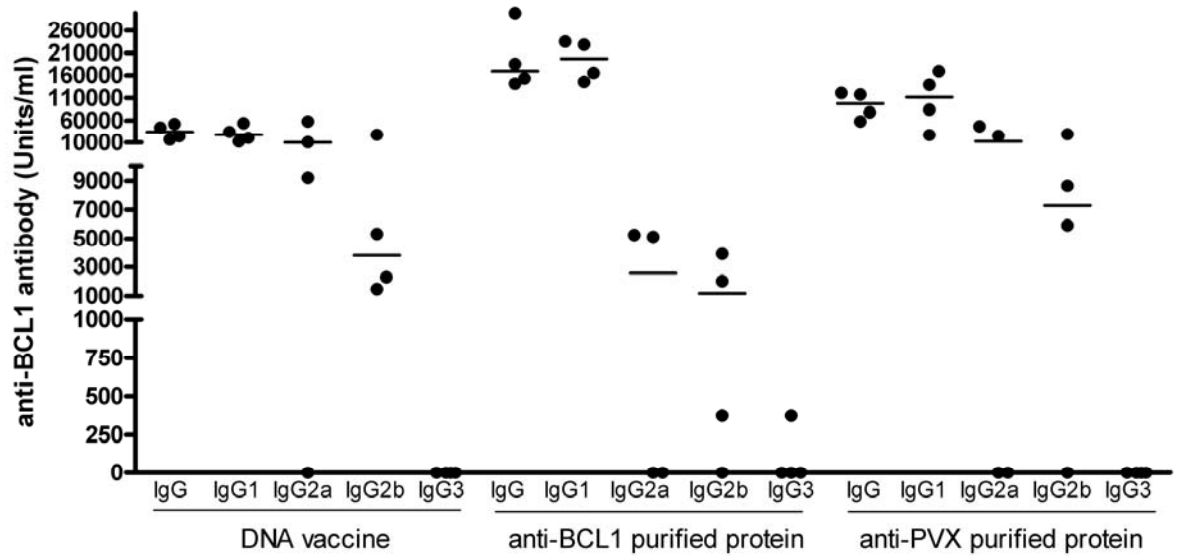


**Figure 3-21. Anti-PVXCP antibody responses after priming/boosting**

Mice were primed with pcDNA3.scFv.BCL<sub>1</sub>-PVXCP (DNA vaccine) or scFv.BCL<sub>1</sub>-PVXCP purified by anti-BCL<sub>1</sub> or anti-PVX antibody affinity chromatography or PVXCP mixed with alum and then boosted on day 35 with the priming material. Antibody levels to PVXCP were measured on day 21 after priming (prime) and day 14 after boosting (boost). Serum from naïve mice (NMS) was used as a baseline. \*\*\*:  $P < 0.0005$ , \*\*:  $0.001 < P < 0.005$ , \*:  $P < 0.05$ , n/s:  $P > 0.05$ . Each dot represents an individual mouse. Horizontal bars are median values.



Vaccine	IgG	IgG1	IgG2a	IgG2b	IgG1/IgG2a	IgG1/IgG2b
DNA vaccine	34,393	27,693	10,085	3,808	2	7
anti-BCL1 purified protein	169,334	196,883	2,567	1,197	76	164
anti-PVX purified protein	97,948	111,638	12,802	7,281	8	15

**Figure 3-22. IgG subclasses of anti-BCL<sub>1</sub> antibody**

After priming/boosting with pcDNA3.scFv.BCL<sub>1</sub>-PVXCP (DNA vaccine) or anti-BCL<sub>1</sub> or anti-PVX purified scFv.BCL<sub>1</sub>-PVXCP mixed with alum, respectively, anti-BCL<sub>1</sub> total IgG, IgG1, IgG2a, IgG2b and IgG3 subclasses from four highest antibody inducing mice in each group were determined. Table shows the median value and the ratio of median values of anti-Id IgG1/IgG2a and IgG1/IgG2b responses in each vaccine groups. Each dot represents an individual mouse. Horizontal bars are median values.

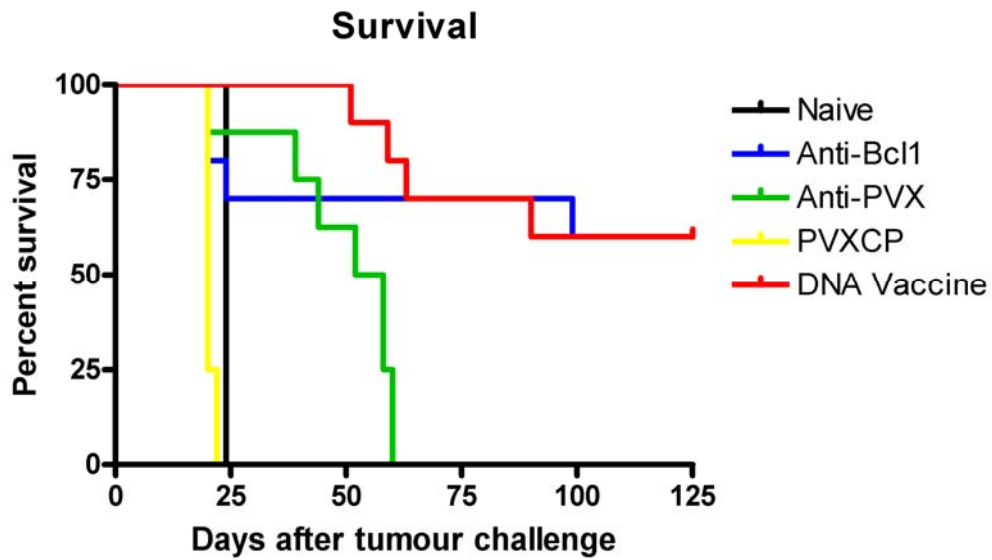


**Figure 3-23. Protection of immunized mice after tumour challenge**

Immunized mice received  $5 \times 10^4$  cells of the BCL<sub>1</sub> tumour at 24 days after boosting. Mice were terminated when splenomegaly was observed and the termination dates were collected. Each line represents survival data from indicated group corresponded to the legend shown on the right hand side of the survival curve.

### 3.3 Summary

ScFv.BCL<sub>1</sub>-PVXCP expression plasmids were constructed to direct the fusion protein into three different compartments of a plant cell; to be produced and to remain in the cytosol, to be secreted as a secretory protein, and to be retained in the ER. By Western blot analysis, the fusion protein targeted for secretion and the fusion protein retained in the ER were expressed at high level; the fusion protein was detected at very low levels when the construct was targeted to the cytosol. The fusion protein obtained from the ER retention construct appeared to remain intact while with the secretory protein construct degradation products were present. Therefore, the construct containing the ER retention signal was chosen for protein expression.

The fusion protein expressed in *Nicotiana* was purified by antibody affinity chromatography using either anti-BCL<sub>1</sub> or anti-PVX antibody. Fusion protein purified from either of the columns was of reasonable purity with the appearance of some degradation products. Their presence was more apparent in the fraction purified using anti-BCL<sub>1</sub> column. The intact fusion protein was detected by a sandwich ELISA with anti-BCL<sub>1</sub> and anti-PVX antibody as well as by Western blot analysis. Anti-BCL<sub>1</sub> antibody column appeared to select for better folded protein as judged by ELISA.

Greater purity was achieved by using size exclusion chromatography. Separation of fusion protein from the smaller products was successful but the yield of fusion protein after the process was too low to use further for vaccine immunogenicity investigation in mice. But this material was later used for vaccine characterisation by DLS.

Based on the ability of PVXCP to aggregate into disk-like structures [136, 210], scFv.BCL<sub>1</sub>-PVXCP was expected to appear in a multimeric form. Multimerisation of the fusion protein was shown by ISEM as the particles of 10 nm and larger were observed. DLS data showed that the majority (70%) of aggregates were 5.5 – 13.1 nm, which corresponded to the size of between half a PVX disk and two disks stuck together.

Anti-BCL<sub>1</sub> and anti-PVX antibody affinity chromatography purified protein vaccine was evaluated in separate groups of mice in comparison with the homologous DNA vaccine positive control and PVXCP negative control. An alum-mixed protein vaccine purified with either of the columns induced antibody to BCL<sub>1</sub> Id similar to the DNA vaccine and the antibody levels were increased by boosting. After boosting, the highest anti-Id antibody levels induced were in the group vaccinated with anti-PVX column-purified protein. The levels were significantly higher than in DNA vaccine group but the difference with the group vaccinated with anti-BCL<sub>1</sub> column-purified protein did not reach statistical significance. With respect to anti-BCL<sub>1</sub> IgG subclasses, both DNA and protein vaccines

induced high level of IgG1, while IgG2a and IgG2b levels were lower than IgG1 levels with ratio of IgG1/IgG2a and IgG1/IgG2b being higher for anti-BCL<sub>1</sub> purified vaccine.

Anti-PVXCP antibody was induced by both DNA and protein vaccines, and the antibody levels were increased by boosting. Anti-BCL<sub>1</sub> purified protein induced higher levels of anti-PVXCP antibody than anti-PVX purified protein and DNA vaccine where the antibody levels were similar.

ScFv.BCL<sub>1</sub>-PVXCP vaccine provided protection against the BCL<sub>1</sub> tumour challenge as both anti-BCL<sub>1</sub> and anti-PVX purified protein vaccinated mice were protected from challenge with the lethal dose of the BCL<sub>1</sub> tumour. Anti-PVX purified protein protected mice significantly with the median survival 55 days compared to 24 days survival in naive mice. Anti-BCL<sub>1</sub> purified protein protected mice better as 60% of mice survived until day 100, the same protection was observed in the DNA vaccine group.

### **3.4 Discussion**

#### **3.4.1 Expression and purification of scFv.BCL<sub>1</sub>-PVXCP**

Among the three scFv.BCL<sub>1</sub>-PVXCP expression constructs, SK-LH, which targets the expressed protein to ER with subsequent retention, appeared to be the successful construct for protein expression. Western blot analysis of protein extracted from the infiltrated leaf revealed that both SK-L and SK-LH constructs were able to direct the expression of scFv.BCL<sub>1</sub>-PVXCP. But only the protein expressed from SK-LH construct appeared to maintain the intact fusion protein. This could be because the protein expressed from SK-LH was directed to and maintained in the ER and therefore it was not subjected to proteolysis in the cytosol. In contrast, SK-B protein production occurred in the cytosol which potentially exposes the protein to degradation by the ubiquitin/proteasome system (reviewed in [211]). In addition, the protein expressed by SK-L was possibly degraded in the vacuole as it was shown that a portion of recombinant protein targeted for a secretory pathway was delivered to the vacuole and degraded [212]. Moreover, the ER of plant cells can tolerate an unusually high accumulation of protein without compromising plant development (reviewed in [211]) and the strategy of retaining protein in the ER has been used for high accumulation of foreign protein in transgenic plants (reviewed in [211]).

In addition, only a small proportion (less than 6 % [213]) of protein retained in the ER contained  $\beta$ (1,2- xylose residues which are normally found in plant secretory proteins [77, 213]. Therefore, when the protein vaccine is administered into mice, the vaccine is unlikely induce antibody to these plant glycans to the level that cause elimination of the protein vaccine in the next administration. Therefore, using SK-LH for targeting of

expressed protein to and subsequently retaining in the ER appeared to be the best strategy for the production of scFv.BCL<sub>1</sub>-PVXCP vaccine.

ScFv.BCL<sub>1</sub>-PVXCP was effectively purified using anti-BCL<sub>1</sub> and anti-PVX affinity columns. Large amounts of protein were obtained, with anti-BCL<sub>1</sub> column giving higher yield than the anti-PVX column. In both protein purification methods the two protein subunits of the fusion protein retained structural integrity as the fusion protein bound to both anti-BCL<sub>1</sub> antibody and anti-PVX antibody. However, the purification process resulted in a certain level of degradation. The protein degradation possibly resulted from released proteases which could be controlled by further optimising proteinase inhibitors or from the extremely high pH of the elution buffer required for separation of the protein from tight-binding antibody on the column.

For characterisation of the fusion protein vaccine *in vitro* I attempted to separate scFv.BCL<sub>1</sub>-PVXCP fusion protein from degraded products by size-exclusion chromatography. The intact scFv.BCL<sub>1</sub>-PVXCP is of higher molecular weight than the degradation products and is also expected to form multimers (the multimerization of the fusion protein was confirmed by ISEM and DLS) and hence will emerge from the column rapidly while the small degraded proteins will need more time to travel through the column medium and will emerge from the column later [214]. Even though the yield of scFv.BCL<sub>1</sub>-PVXCP obtained by size-exclusion chromatography was low, this strategy provided a good way of obtaining high purity protein. Although in this study the protein purified by this method was used only for an *in vitro* assay, the scaling up would be possible if one starts with high amounts of plant material. On the other hand, optimising the affinity chromatography could be another way.

### **3.4.2 Characterization of scFv.BCL<sub>1</sub>-PVXCP fusion protein**

Plant expressed ScFv.BCL<sub>1</sub>-PVXCP fusion protein reacted well with both anti-BCL<sub>1</sub> and anti-PVX antibodies, demonstrating that the protein expressed in plants retained the correct conformation recognised by the antibodies. As shown by many studies, mammalian proteins expressed in plants maintain their biological functions even though the glycosylation patterns, i.e. the generated glycan structures, of plant proteins are different from that of mammalian proteins (reviewed in [175, 178]).

ScFv.BCL<sub>1</sub>-PVXCP was expected to form disks, as it was previously shown that CP of potexvirus appeared to form disks in the absence of viral RNA (reviewed in [210]) as well as CP fusion to scFv was shown to be able to aggregate into a disk-like structure [136]. Aggregation of the fusion protein was studied by three methods; native gel, ISEM and DLS. ScFv.BCL<sub>1</sub>-PVXCP, similarly to PVX particle, showed slower migration on a native

protein gel in comparison to denatured protein, indicating multimerisation. The multimerisation was confirmed by ISEM, as the particles of 10 nm and larger were observed, and by DLS with the majority of the purified protein found to be aggregates of 5.5 -13.1 nm. The DLS estimation would be more reliable because ISEM relies on the trapping of protein by antibody and therefore enhances aggregation hence the differences in estimation of the size of aggregates.

### **3.4.3 Immunogenicity of scFv.BCL<sub>1</sub>-PVXCP vaccine**

Immunogenicity of purified scFv.BCL<sub>1</sub>-PVXCP was studied in the mouse. Alum was the adjuvant of choice since it has long been successfully used in human for antibody induction. After boosting, the protein vaccine purified with either of the columns induced anti-Id antibody close to the levels induced by DNA vaccine. The patterns of IgG isotype expression were also similar. Both protein and DNA vaccines provided protection against the tumour challenge with anti-BCL<sub>1</sub> purified protein inducing protection in mice better than anti-PVX purified protein and protection induced by anti-BCL<sub>1</sub> purified protein was comparable to that induced by DNA vaccine. The result that anti-PVX purified protein protected mice less efficiently than other vaccines in contrast to its ability to induce high anti-Id antibody levels in terms of ELISA values suggests that BCL<sub>1</sub>IgG used as an anti-BCL<sub>1</sub> antibody ligand (coating protein) in ELISA did not reveal levels of protective anti-Id antibody.

As the Th1 response results in IgG2 and IgG3 switching while the Th2 response results in IgG1 switching [215-217], both the fusion protein and DNA vaccines appeared to have a mixed Th1/Th2 response. Studies in aluminum-containing adjuvants showed that this adjuvant predominantly skews T-cell responses towards Th2 [218-219]. Therefore, it is possible that the Th1 response observed, as judged by high levels of IgG2 isotypes, was induced by the vaccines themselves even when the experiments were performed in BALB/c mice known for Th2 bias. High IgG1 levels were not found in DNA vaccine incorporating PVXCP in C57BL/6 mice, where IgG2a was dominant [136]. Additionally, there was a consistency of mixed responses irrespective of means of vaccine delivery (DNA or protein).

In many model systems where isotype-switched variants were studied, IgG2a and IgG2b were more potent in immune function than IgG1 and IgG3 ([220] and reviewed in [51]). However, in our experiment, even though IgG2 levels were lower than IgG1, mice were protected from the lethal dose of tumour. IgG1/IgG2 ratios in the anti-BCL<sub>1</sub> purified vaccine group were higher than the anti-PVX purified vaccine group but the protection by the former vaccine was better. This suggests that IgG2 may not play a crucial role in the

BCL<sub>1</sub> model or the IgG2 levels induced by the vaccines were high enough to mediate protective immunity against the tumour.

The immunoenhancing property of PVXCP in the DNA vaccine was shown previously in other tumour models [136]. PVXCP was shown to provide T-cell help for B cells and it also provides means of multimerisation of the fusion protein. The fusion protein vaccine in a multimeric form would induce higher immunogenicity than the monomeric protein as a multimeric antigen is better in BCR cross-linking thus activating B cells. A multimeric antigen would also be more attractive to DCs (figure 3-24). Another advantage of vaccine production in plants with the retention in the ER is high mannose addition. Plants similarly to mammals add high mannose to the proteins in the ER which is subsequently trimmed in Golgi. However, in plants unlike in mammals ER retention allows large amount of proteins to be accumulated without causing ER stress. These high mannose proteins might cause problems to therapeutic proteins that require correct mammalian-type glycosylation for their biological activity, such as antibody Fc [221]. In contrast, these high mannose glycans may be beneficial for plant derived protein vaccines as they can enhance vaccine internalisation by DC through the mannose receptor (MR) or DC-SIGN on those cells (figure 3-24). BCL<sub>1</sub> scFv has no glycosylation site in contrast to the Ig of human follicular lymphoma cells which contain high mannose at the Ig V region [222]. PVXCP contains a potential N-glycosylation site at the N-terminus (as predicted by NetNGlyc version 1.0 [223]) thus providing an opportunity to add high mannose to the fusion scFv vaccine in plant ER, thereby potentially enhancing vaccine immunogenicity. The question of MR and DC-SIGN binding has now been addressed in our laboratory. Data from binding assay clearly indicates that the fusion protein can bind to MR. The binding to DC-SIGN is being addressed.

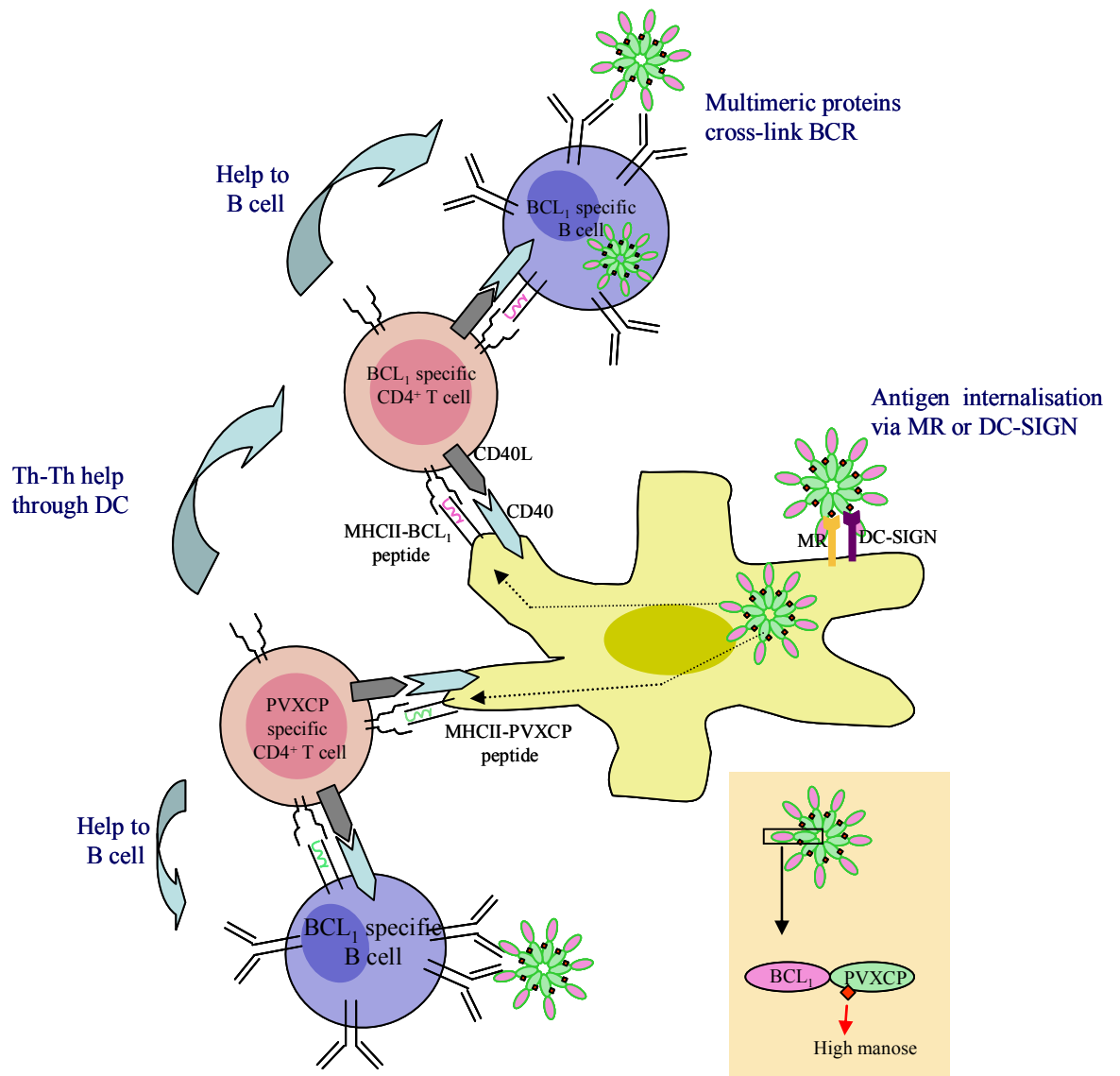


**Figure 3-24. Proposed mechanism of BCL<sub>1</sub>.scFv-PVXCP fusion protein vaccine**

BCL<sub>1</sub>.scFv-PVXCP fusion protein may be able to induce immune responses against BCL<sub>1</sub> lymphoma by three ways. The first mechanism is through T-cell help as provide by the fusion principle. Second, the multimeric form of the fusion protein provides better BCR cross-linking thus better in B-cell activation. Finally, the fusion protein produced in the ER retention manner is expected to contain high mannose and thereby it is able to enhance the ability of DCs to internalise the vaccine via mannose receptor (MR) or DC-SIGN.

## Chapter 4. PVX-based PVP vaccine

### 4.1 Introduction

#### 4.1.1 Plant virus-based vaccines

Plant viruses including PVX have been used as carrier molecules for vaccine preparation. Plant viruses have been genetically modified to display antigenic peptides from infectious diseases on its surface and the resulting chimeric virus particles (CVPs) were able to induce immune responses. PVX CVP displaying the ELDKWA epitope from HIV glycoprotein 41 was able to induce high levels of HIV-1 specific IgG and IgA antibodies when it was injected without addition of adjuvant into mice [170]. PVX CVP displaying the D2 peptide derived from an *S. aureus* fibronectin-binding protein (FnBP) in combination with QS-21 adjuvant induced IgG2a and IgG2b antibodies specific to FnBP in mice and the mouse serum was shown to inhibit the binding of fibronectin to the immobilised FnBP [160]. Recently, the vaccine consisting of PVX displaying a CTL epitope of influenza virus was produced and it showed the ability to activate specific CD8<sup>+</sup> T cells without addition of adjuvant [172].

Data on using plant viruses for vaccines against cancer are limited. The only published study is work of McCormick *et al* (2006) in which CTL epitopes were chemically or genetically fused to TMV. For chemical conjugation, they used a modified TMV particle which contained a single lysine residue on the particle surface [152]. The lysine residue provided a site for conjugation with the model peptide. They showed that both TMV chemically and genetically fused with a tumour-derived T-cell epitope induced IFN- $\gamma$  producing T cells and prolonged survival of tumour challenged mice [151-152].

Very limited data describing the direct effect of plant viruses on the immune system are available. One example is the papaya mosaic virus (PapMV). PapMV was able to activate DCs and macrophages, as determined by up-regulation of the activation markers (CD86 and class II MHC), suggesting that it was recognised by the APCs [224]. It was also shown that PapMV induced T-cell responses as determined by a delayed-type hypersensitivity test. In addition, PapMV induced pro-inflammatory cytokines (TNF- $\alpha$  and IL-6) secreted by macrophages and DCs [224]. The receptors for plant viruses, including PapMV, have not been identified.

PapMV was also presented efficiently to the immune system as an antigen without addition of adjuvant. A single injection of PapMV without added adjuvant was able to induce a long-lasting antibody response [224]. In addition, a lymphocytic choriomeningitis virus (LCMV) CTL epitope fused to PapMV was also correctly processed and induced

specific CTLs [150]. Mice vaccinated with the CVP without addition of adjuvant (which are normally required for peptide vaccination) were protected from the virus infection, suggesting that PapMV has an adjuvant property. In addition, the adjuvanticity of PapMV was shown by its ability to strengthen the antibody response by mixing with antigen with increased protective capacity of the vaccine [224].

#### **4.1.2 APC activation by microbes**

Innate immune cells, including APCs, recognise PAMPs by their PRRs. TLR is the best characterised group of PRR. Each TLR detects different pathogen molecules (reviewed in [225]). TLR1, 2, 4 and 6 are expressed on the cell surface and mainly recognise bacterial products, with TLR4 being the receptor for LPS. TLR3, 7, 8, and 9 localise to intracellular compartments and detect microbial sequences inside those compartments. TLR9 is a receptor for DNA; TLR3 detects double-stranded RNA, and TLR7 detects single-stranded viral RNA (reviewed in [225]). Activation of TLR leads to cell signalling and subsequent expression of many genes including those encoding cytokines and chemokines involved in antimicrobial activity and the inflammatory response. In addition, TLR-activated DCs secrete cytokines that are involved in initiation of an adaptive immune response [226].

DCs are professional APCs which capture and process microbial antigens for presentation to antigen specific T cells. After immature DCs have internalised antigen, their phenotypes are changed; the antigen-capturing molecules disappear and T-cell stimulatory functions are increased (reviewed in [227]). Activated DCs down-regulate chemokine receptor CCR6 expression and increase expression of CCR7 which is required for their migration from peripheral tissues to the draining lymph nodes, where they present antigen to the antigen-specific naïve T cells. DCs process antigens into peptides and present them in forms of the peptide-MHC complexes on the cell surface. Therefore, activated DCs up-regulate expression of class II MHC molecules required for presentation of the extracellular antigens. Many adhesion and costimulatory molecules, such as CD40, CD80, CD86, are also up-regulated to enhance adhesion and signalling required for T-cell activation (reviewed in [227]). In addition, activated DCs secrete cytokines required for T-cell differentiation [226, 228-230].

DCs are generally divided into cDCs which express high level of CD11c and classII MHC and pDCs which express low level of CD11c and classII MHC (reviewed in [231-232]). In the mouse, cDCs in lymphoid tissues have been defined as 5 major subsets according to surface expression of CD4, CD8 $\alpha$ , CD11b and DEC-205 (CD205) markers as shown in table 4-1. In the spleen, 20% of DCs are of the CD4<sup>-</sup>CD8 $\alpha$ <sup>+</sup> phenotype. The

majority of DCs in the spleen are CD8 $\alpha$ <sup>-</sup> and can be further divided into two subsets based on CD4 expression; a major CD8 $\alpha$ <sup>-</sup>CD4<sup>+</sup> subset and a minor CD8 $\alpha$ <sup>-</sup>CD4<sup>-</sup> subset (reviewed in [232]). CD8 $\alpha$ <sup>+</sup> DCs have the ability to induce a Th1 response by secreting high amounts of IL-12 and they are able to cross-prime CD8<sup>+</sup> T cell. In contrast, CD8 $\alpha$ <sup>-</sup> DCs induce Th2 response. The functional differences between CD8 $\alpha$ <sup>-</sup>CD4<sup>+</sup> and CD8 $\alpha$ <sup>-</sup>CD4<sup>-</sup> subsets are currently unknown (reviewed in [233]). Mouse pDCs, similar to their human counterpart, have a unique phenotype, CD11c<sup>lo</sup>CD45RA<sup>hi</sup>B220<sup>+</sup>CD11b<sup>-</sup>MHC-II<sup>lo</sup> [234-237]. Both human and mouse pDCs produce large amount of type I IFNs in response to viral stimulation [238]. Moreover, a newly identified DC lineage, interferon-producing killer DC (IKDC), has also been found in mouse spleen (reviewed in [231]. These IKDCs have a phenotype of NK cells and DCs (CD11c<sup>+</sup>NK1.1<sup>+</sup>B220<sup>+</sup>) [239-240]. Upon activation by various stimuli, IKDCs produce a large amount of IFN- $\gamma$  and kill typical NK target cells and display some antigen-presenting activity [240].

Expression of TLRs is different in DC subsets; pDCs express TLR 7 and 9; CD8 $\alpha$ <sup>+</sup> DCs express TLR 1-3, 6 and 9; CD11b<sup>+</sup> DCs express TLR 1-3, 5-7 and 9. Therefore, DCs will respond to pathogens if they have appropriate TLRs (reviewed in [225]). In addition, cytokine secretion induced by the same ligand is distinct in different DCs. For example, stimulation with CpG induced pDCs to secrete IFN- $\alpha$  but induced DCs to secrete IL-12 [241]. Despite the differences in cytokine secretion by DC subsets, signalling through TLRs generally results in the activation and maturation of all DCs, as determined by enhanced expression of co-stimulatory molecules CD40, CD80 and CD86.

### 4.1.3 Aims

This chapter is focused on determination of the ability of PVX to enhance antibody to linked Id Ig antigen in the BCL<sub>1</sub> tumour model and on investigation of the immuno-activating property of PVX and its ability to activate APCs, especially DCs.

### 4.1.4 Hypotheses

1. The vaccine consisting of BCL<sub>1</sub> IgG linked to PVX induces anti-Id antibody responses and provides protection against lymphoma challenge via activation of linked T-cell help.
2. PVX RNA is involved in immunogenicity of PVX-based PVP vaccine.
3. PVX interacts with DCs and induces DC maturation.

DC subsets	Spleen	Mesenteric lymph nodes	Skin-draining lymph nodes	Thymus
CD8 <sup>+</sup> CD4 <sup>-</sup> CD205 <sup>hi</sup> CD11b <sup>-</sup>	++	+	+	++++
CD8 <sup>-</sup> CD4 <sup>+</sup> CD205 <sup>-</sup> CD11b <sup>+</sup>	++++	+/-	+/-	CD8 <sup>lo/-</sup> CD11b <sup>-</sup> (+)
CD8 <sup>-</sup> CD4 <sup>-</sup> CD205 <sup>-</sup> CD11b <sup>+</sup>	++	+++	++	
CD8 <sup>-</sup> CD4 <sup>-</sup> CD205 <sup>+</sup> CD11b <sup>+</sup>	+/-	++	++	CD8 <sup>lo/-</sup> CD11b <sup>+</sup> (+/-)
CD8 <sup>lo</sup> CD4 <sup>-</sup> CD205 <sup>hi</sup> CD11b <sup>+</sup>	-	+/-	+	

**Table 4-1. DC subsets in mouse lymphoid tissues**

The relative frequency of DC subsets is expressed by the number of '+' symbols : 50-70% (++++), 30-50% (+++), 20-30% (++), 10-20% (+), and <5% (+/-). The five major DC subsets are not all present in the thymus [232].

## 4.2 Results

### 4.2.1 PVX-based vaccine induced antibody response to the attached Id antigen

To examine the ability of PVX to enhance an immune response in the BCL<sub>1</sub> lymphoma model, a plant viral particle (PVP) vaccine consisting of PVX displaying BCL<sub>1</sub> Id antigen on its surface was generated. The PVP vaccine was made by linking BCL<sub>1</sub> IgG (BCL<sub>1</sub> V<sub>H</sub> and V<sub>L</sub> linked to human C<sub>γ1</sub> and C<sub>κ</sub>) to the PVX particle using biotin-streptavidin binding reaction. Biotinylation of the antigen and PVXCP can be achieved through lysine (amino acid with amine side chain) residues on the proteins. This vaccine preparation by linking of biotinylated antigen and viral particles through streptavidin has been used by others. The vaccine was able to induce specific immunity against the antigen [242]. PVXCP contains 11 lysine residues thus providing a good target for biotinylation and Steinmetz *et al* showed that more than one lysine residues in each CP can be modified [243]. PVX N-terminus which is exposed on the virion surface [244] contains one lysine residue [245]. The additional lysine residues in other CP domains may also locate on PVX surface.

BCL<sub>1</sub> IgG used in these experiments was expressed in CHO cells. These CHO cells for BCL<sub>1</sub> IgG expression were provided by Dr C Chan (Cancer Sciences Division, University of Southampton). This strategy was adapted for convenient purification by a protein-A column and also as a general strategy for generating Id tumour antigen as opposed to using material from the tumour. The biotinylated BCL<sub>1</sub> IgG was firstly linked to streptavidin (SA) (3 molecules of IgG to 1 molecule of SA) before attaching to biotinylated PVX to yield PVP vaccine (figure 4-1). The equal amount (μg unit) of BCL<sub>1</sub> IgG and PVX were used and thus provided the ratio of 1 IgG molecule to 6 PVXCP molecules. BCL<sub>1</sub> IgG linked to PVX is called BCL<sub>1</sub>-PVP from now on.

In the initial vaccination experiment, BCL<sub>1</sub>-PVP was tested in comparison with the DNA vaccine. A group of 4 mice was injected with BCL<sub>1</sub>-PVP (containing 20 μg of BCL<sub>1</sub> IgG) or 50 μg of the DNA vaccine or 20 μg of biotinylated PVX (a negative control for BCL<sub>1</sub> vaccination). In an additional group of 3 mice, BCL<sub>1</sub>-PVP vaccine was mixed with alum before injection to evaluate if alum would enhance immunogenicity of the vaccine. Mice were injected with the same material 6 weeks after priming. Mice were bled at 3 weeks after priming and 2 weeks after boosting. Antibody to BCL<sub>1</sub> F(ab')<sub>2</sub> or PVXCP was measured by ELISA. After priming, BCL<sub>1</sub>-PVP vaccine induced significantly higher levels of antibody than the DNA vaccine ( $p = 0.029$ ) (figure 4-2). The antibody levels were enhanced by boosting both in the DNA and the PVP vaccine groups but the levels induced in the PVP group were significantly higher ( $p = 0.029$ ). These data indicate that BCL<sub>1</sub>-PVP vaccine used alone was more potent in inducing antibody responses than DNA vaccine.

Mixing alum with BCL<sub>1</sub>-PVP appeared to induce higher anti-BCL<sub>1</sub> antibody than BCL<sub>1</sub>-PVP alone but the higher levels did not reach statistical significance. Sera from PVX-vaccinated mice and naïve mice did not react to BCL<sub>1</sub> F(ab')<sub>2</sub> as expected, indicating specificity of antibody responses. Anti-PVXCP antibody levels induced by BCL<sub>1</sub>-PVP and BCL<sub>1</sub>-PVP mixed with alum were higher than those induced by DNA vaccine after both priming and boosting. Mice vaccinated with PVX produced anti-PVXCP antibody as expected. Boosting enhanced antibody levels in all groups. Naive mouse serum did not react with PVXCP as expected.

To see if the BCL<sub>1</sub>-PVP vaccine generated protective anti-lymphoma responses, mice were challenged with BCL<sub>1</sub> tumours at day 28 after boosting. Naïve mice and PVX-vaccinated mice died within 24 days after tumour challenge (figure 4-3). All BCL<sub>1</sub> Id vaccines protected mice against the tumour challenge (Logrank test showed significantly different survival in comparison with naïve mice); 50% of mice vaccinated with the DNA vaccine and BCL<sub>1</sub>-PVP vaccine and 1 of 3 mice vaccinated with BCL<sub>1</sub>-PVP mixed with alum survived with good health until day 78 after challenge when they were terminated. There was no significance difference in protection induced among BCL<sub>1</sub> Id vaccine groups. The data indicate that BCL<sub>1</sub>-PVP vaccines induce significant protection against the tumour.

In a second experiment, a group of ten mice was vaccinated with BCL<sub>1</sub>-PVP alongside BCL<sub>1</sub>IgG linked to SA (BCL<sub>1</sub>-SA). Anti-BCL<sub>1</sub> antibody responses induced by BCL<sub>1</sub>-PVP vaccine was significantly higher than the levels induced by BCL<sub>1</sub>-SA ( $p = 0.015$ ) (figure 4-4). This demonstrates immunoenhancing property of PVX particle.

As alum further enhanced antibody responses induced by BCL<sub>1</sub>-PVP vaccine, BCL<sub>1</sub>-PVP (containing 20 µg of BCL<sub>1</sub> IgG) mixed with alum was chosen for the next vaccination experiment with more mice. Figure 4-5 shows the antibody response induced by the PVP ( $n = 6$ ) and the DNA vaccine ( $n = 13$ ). BCL<sub>1</sub>-PVP vaccine induced significantly higher antibody levels than those induced by the DNA vaccine both after priming ( $p = 0.039$ ) and boosting ( $p = 0.016$ ). These data further indicate that BCL<sub>1</sub>-PVP vaccine was more potent in induction of antibody responses than the DNA vaccine. The vaccinated mice were challenged with BCL<sub>1</sub> tumour cells at day 24 after boosting. Both the PVP and the DNA vaccines protected mice from the tumour challenge significantly in comparison to naïve mice which died within 24 days after tumour challenge; 1 of 6 mice vaccinated with the PVP vaccine and 2 of 10 mice vaccinated with the DNA vaccine were healthy until day 114 after challenge when the experiment was terminated (figure 4-6).

To determine whether lower dose of antigen can be used to induce antibody, different amounts of BCL<sub>1</sub>-PVP vaccine were injected into mice. A group of 6 mice was injected with the PVP vaccine containing 1 µg or 2 µg or 5 µg or 10 µg or 20 µg of

BCL<sub>1</sub>IgG. After priming, all BCL<sub>1</sub>-PVP vaccinations induced higher anti-BCL<sub>1</sub> antibody levels than the DNA vaccine with as low as 2 µg being significantly higher ( $p = 0.0043$ ) (figure 4-7); 1 µg of BCL<sub>1</sub>-PVP induced antibody responses lower than other amounts of the vaccine. There was no difference in anti-Id antibody levels among 2 µg, 5 µg, 10 µg and 20 µg groups. After boosting, anti-BCL<sub>1</sub> antibody levels were increased in all groups. Antibody levels induced by the DNA vaccine were lower than those induced by BCL<sub>1</sub>-PVP vaccine groups with as low as 2 µg being significantly higher ( $p = 0.0043$ ). Among the PVP vaccine groups, anti-Id antibody levels were comparable except that 1 µg of BCL<sub>1</sub>-PVP induced antibody responses significantly lower than 2 µg of the vaccine. All groups of BCL<sub>1</sub>-PVP vaccine protected mice from the tumour challenge with no significantly difference and the protection was comparable to the DNA vaccine (figure 4-10). These data showed that as low as 1 µg of BCL<sub>1</sub>-PVP was able to induce anti-Id antibody and provided protection against the tumour challenge.

For anti-PVXCP antibody levels, after priming 1 µg of the vaccine induced lower antibody response than other doses (figure 4-8). There was no difference in anti-PVXCP antibody levels between other doses of the vaccine. After boosting, all groups of mice injected with different doses of the BCL<sub>1</sub>-PVP vaccine produced comparable levels of anti-PVXCP antibody. All BCL<sub>1</sub>-PVP vaccine groups produced higher levels of anti-PVXCP antibody than the DNA vaccine group.

Subclasses of anti-BCL<sub>1</sub> IgG induced by BCL<sub>1</sub>-PVP and the DNA vaccines were determined as they are good indicators of the type of Th response induced by the vaccine as well as the ability of the antibody to engage ADCC. Sera from a group of mice vaccinated with BCL<sub>1</sub>-PVP (containing an amount of 20 µg of BCL<sub>1</sub> IgG) and mice vaccinated with DNA vaccine were tested for anti-BCL<sub>1</sub> IgG1, IgG2a, IgG2b and IgG3 isotypes. All IgG isotypes were detected, with both the DNA and BCL<sub>1</sub>-PVP vaccines induced high level of IgG1 (figure 4-9). Anti-Id IgG2a and IgG2b levels were lower than IgG1 in the BCL<sub>1</sub>-PVP group. In the DNA vaccine group, anti-Id IgG2a levels were induced to the level comparable to IgG1; but IgG2b levels were lower than IgG1. Anti-Id IgG3 were detectable in both the DNA and the PVP vaccine groups but the levels were very low compare to IgG1 levels.

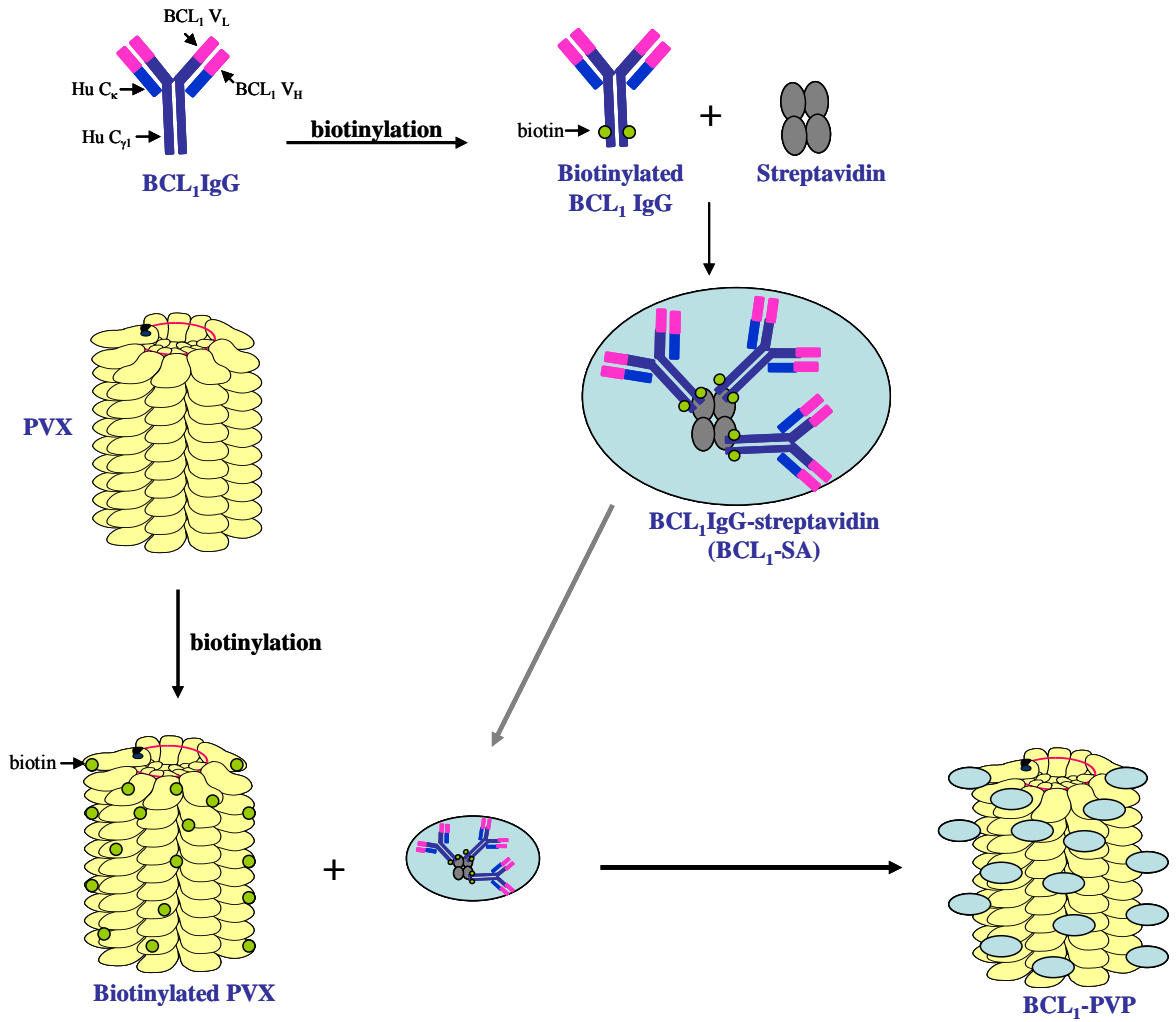


**Figure 4-1. BCL<sub>1</sub>-PVP vaccine design**

BCL<sub>1</sub>IgG and PVX were labelled with biotin. Initially biotinylated BCL<sub>1</sub> IgG was linked to streptavidin (SA) in the ratio of 3 molecules of IgG to 1 molecule of SA thus resulting in BCL<sub>1</sub> IgG-streptavidin (BCL<sub>1</sub>-SA). Then BCL<sub>1</sub>-SA was linked to biotinylated PVX to yield BCL<sub>1</sub>-PVP vaccine.

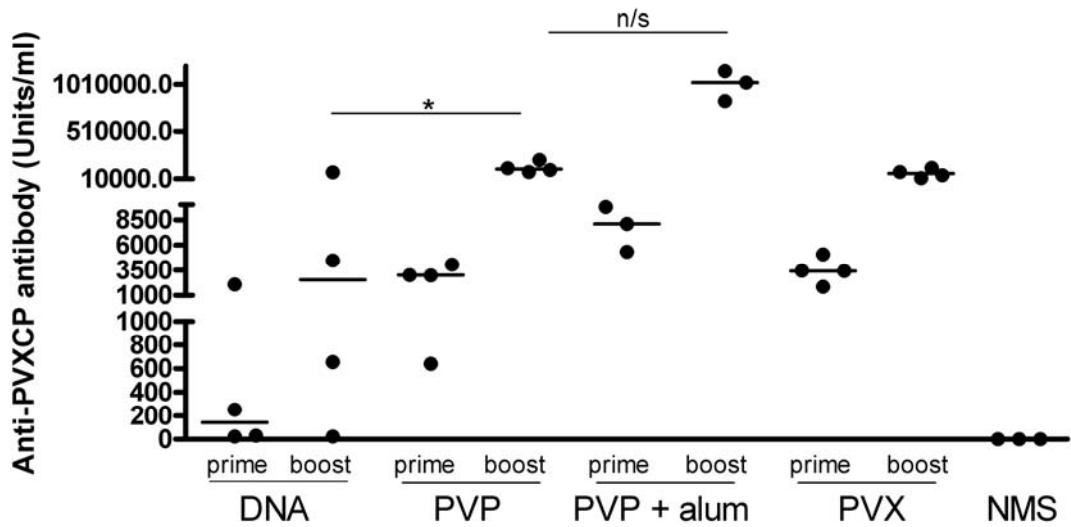
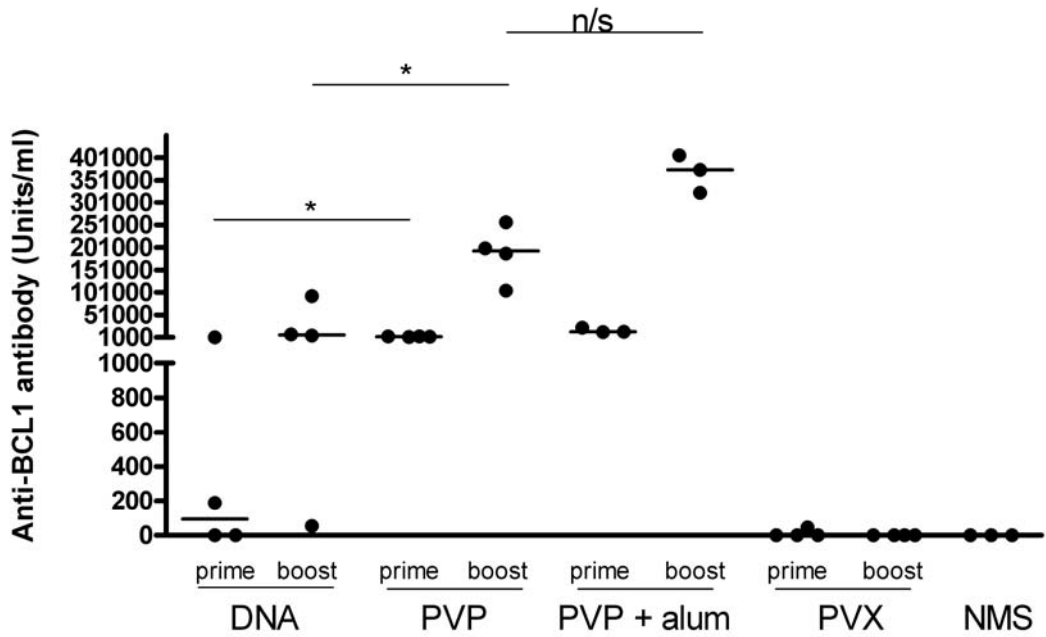


**Figure 4-2. Antibody responses after PVP vaccination**

Mice were primed with pcDNA3.scFv.BCL<sub>1</sub>-PVXCP (DNA vaccine) or BCL<sub>1</sub>-PVP vaccine or BCL<sub>1</sub>-PVP vaccine mixed with alum or PVX as a control and then boosted 6 weeks later with the priming vaccine. Antibody levels to BCL<sub>1</sub> Id (top graph) or PVXCP (bottom graph) were measured on day 21 after priming (prime) and day 14 after boosting (boost). Serum from naïve mice (NMS) was used as a baseline. \*: p < 0.05, n/s: p > 0.05. Each dot represents an individual mouse. Horizontal bars are median values.

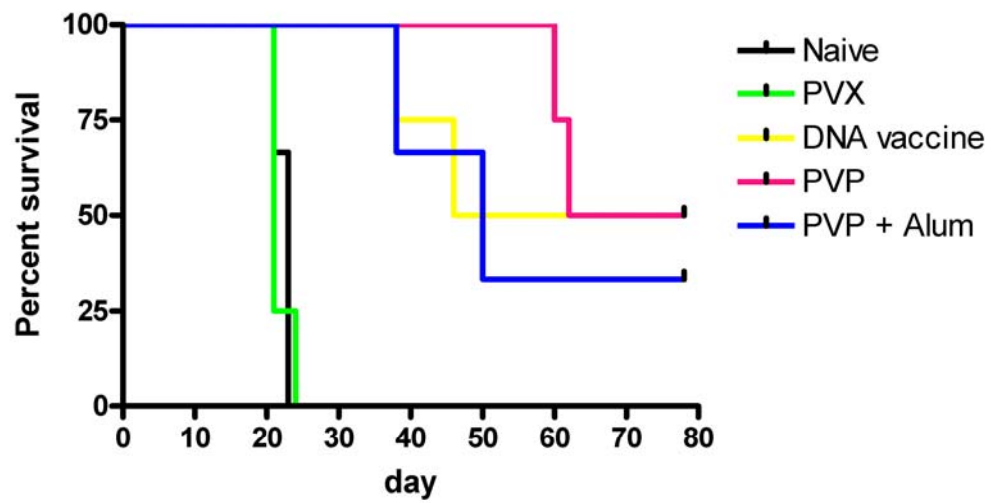


**Figure 4-3. Protection of BCL<sub>1</sub>-PVP-immunised mice**

Mice primed and boosted with indicated vaccines were injected with  $5 \times 10^4$  cells of the BCL<sub>1</sub> tumour at 28 days after boosting. Mice were terminated when splenomegaly was observed and the termination dates were noted. Each line represents survival data of the groups indicated in the legend shown on the right hand side of the survival curve.

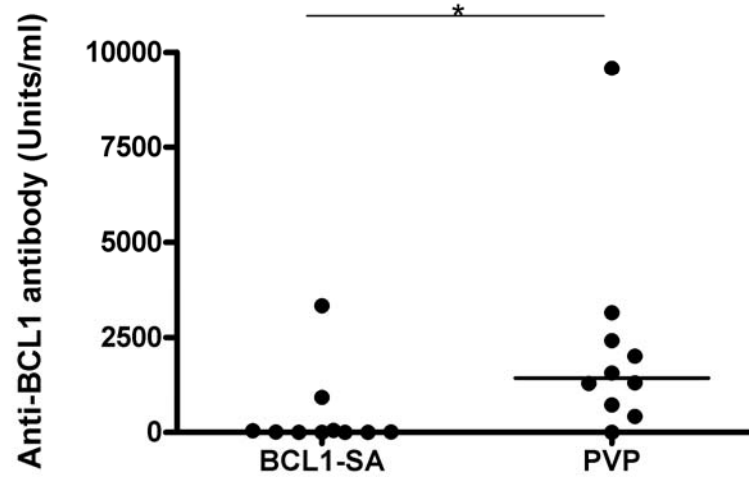


**Figure 4-4. Comparison of anti-BCL<sub>1</sub> antibody responses induced by BCL<sub>1</sub>-PVP vaccine and by Id Ig without linked PVX**

BALB/c mice were injected with PVP vaccine or the same dose (15 µg) of BCL<sub>1</sub>-SA . Blood was collected from tail tip at day 21 after injection. The levels of antibody against BCL<sub>1</sub> F(ab')<sub>2</sub> were determined by ELISA. \*: P < 0.05. Each dot represents an individual mouse. Horizontal bars are median values.

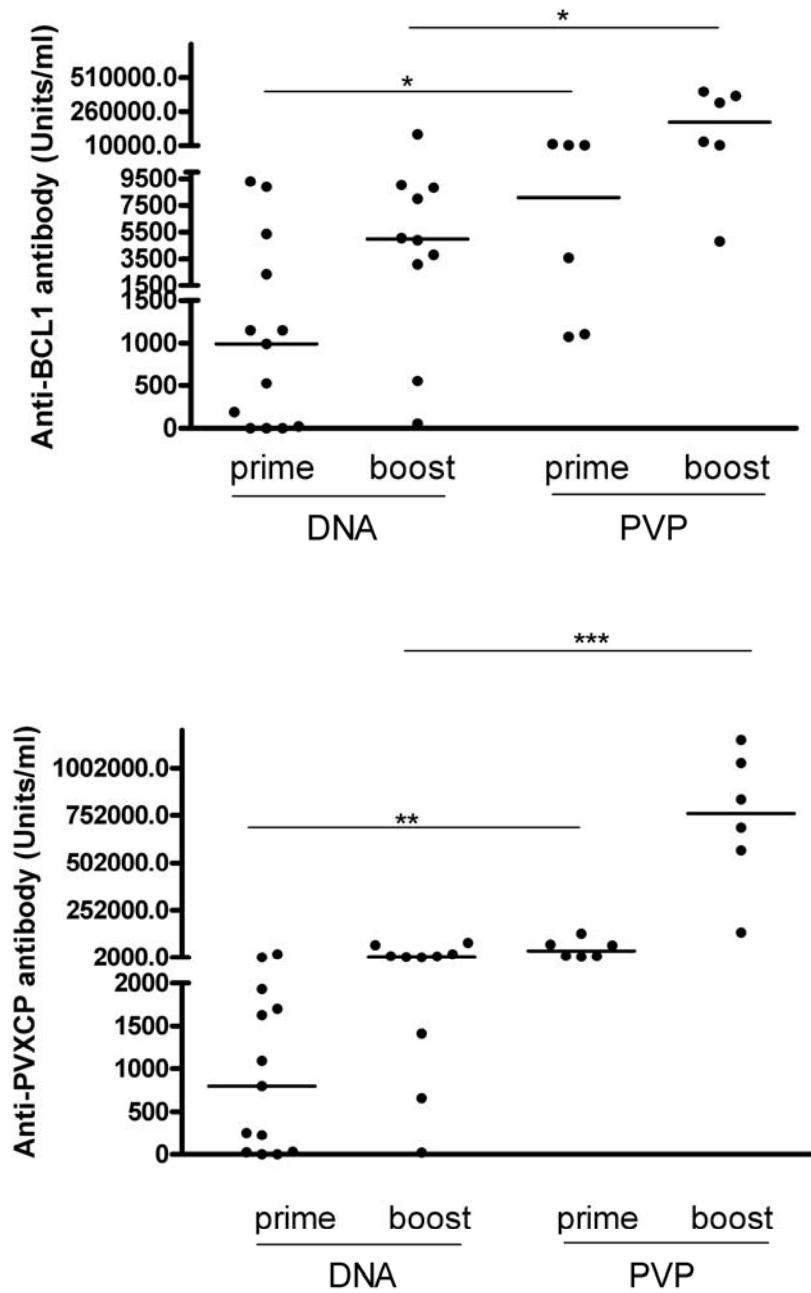


**Figure 4-5. Comparison of antibody responses induced by BCL<sub>1</sub>-PVP and DNA vaccines**

Mice were primed with pcDNA3.scFv.BCL<sub>1</sub>-PVXCP (DNA) or BCL<sub>1</sub>-PVP vaccine mixed with alum (PVP) and then boosted on day 35 with the priming material. Antibody levels to BCL<sub>1</sub> (top graph) or PVXCP (bottom graph) were measured on day 21 after priming (prime) and day 14 after boosting (boost). \*\*\*:  $p < 0.0005$ , \*\*:  $0.001 < p < 0.005$ , \*:  $p < 0.05$ . Each dot represents an individual mouse. Horizontal bars are median values.

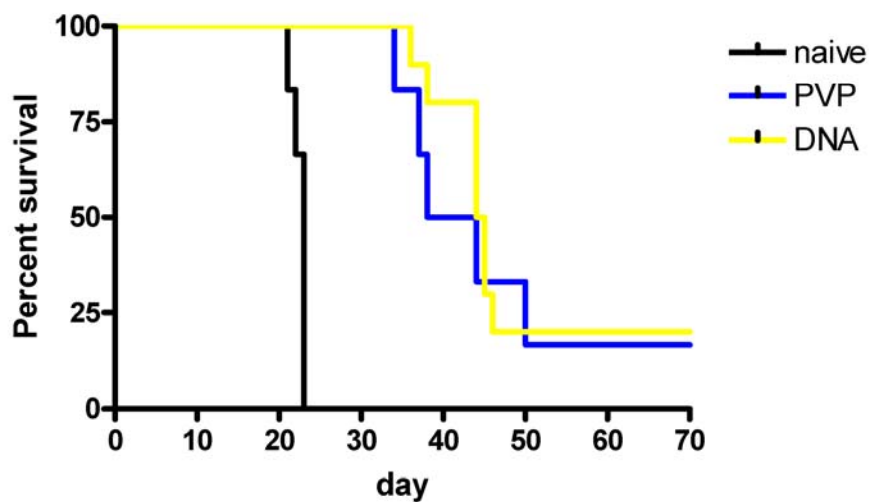


**Figure 4-6. Protection of BCL<sub>1</sub>-PVP and DNA vaccine-immunised mice after tumour challenge**

Immunised mice received  $5 \times 10^4$  BCL<sub>1</sub> tumour cells at day 24 after boosting. Mice were terminated when splenomegaly was observed and the termination dates were collected. Each line represents survival data of the groups indicated in the legend shown on the right hand side of the survival curve.

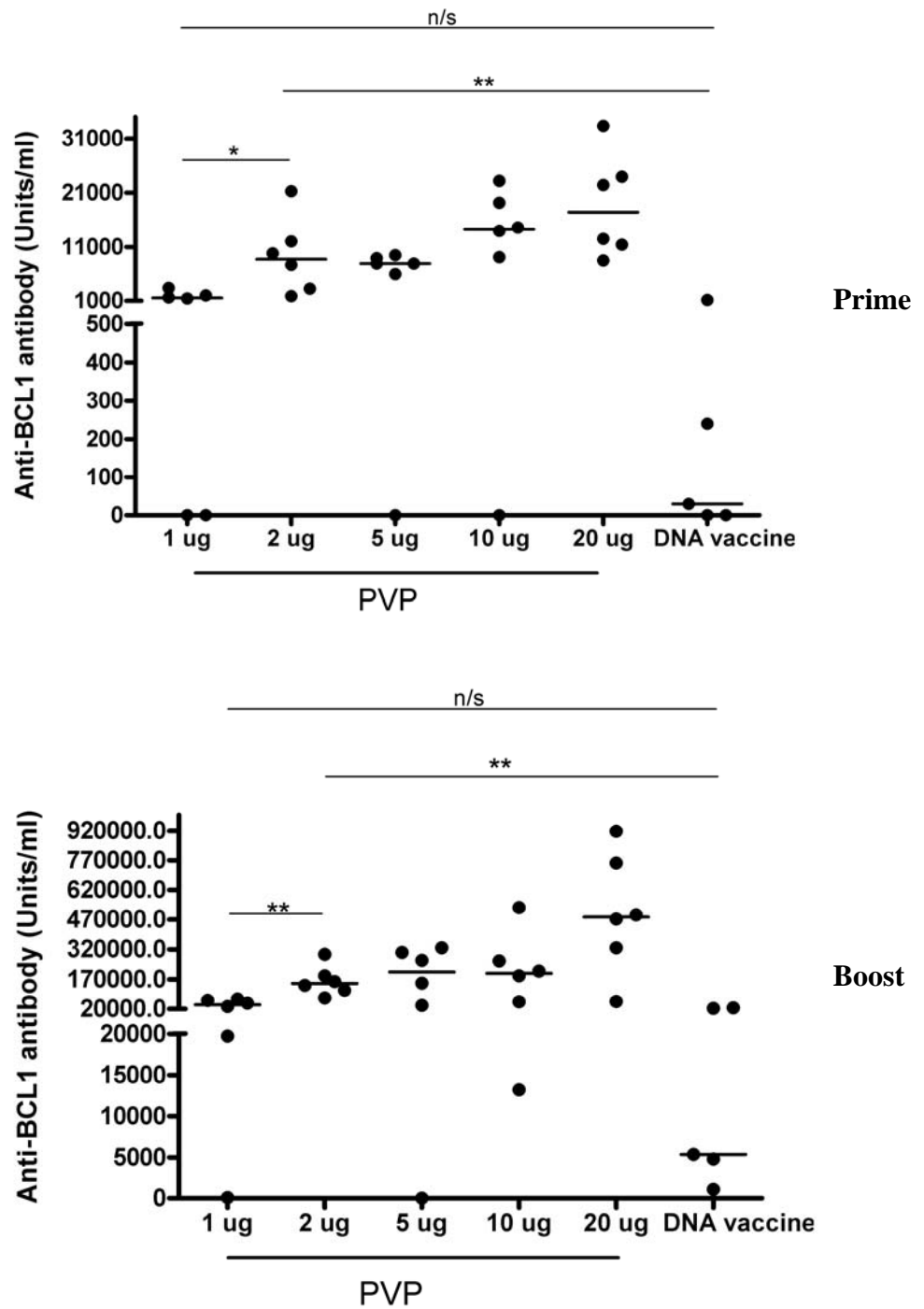


**Figure 4-7. Anti-BCL<sub>1</sub> antibody responses after vaccination with different doses of BCL<sub>1</sub>-PVP**

Mice were primed with pcDNA3.scFv.BCL<sub>1</sub>-PVXCP (DNA vaccine) in comparison to different doses (1 µg, 2 µg, 5 µg, 10 µg and 20 µg of BCL<sub>1</sub> IgG) of BCL<sub>1</sub>-PVP vaccine mixed with alum and then boosted on day 35 with the priming material. Antibody levels to BCL<sub>1</sub> were measured on day 21 after priming (prime) and day 14 after boosting (boost). \*\*: 0.001 < p < 0.005, \*: p < 0.05. Each dot represents an individual mouse. Horizontal bars are median values.

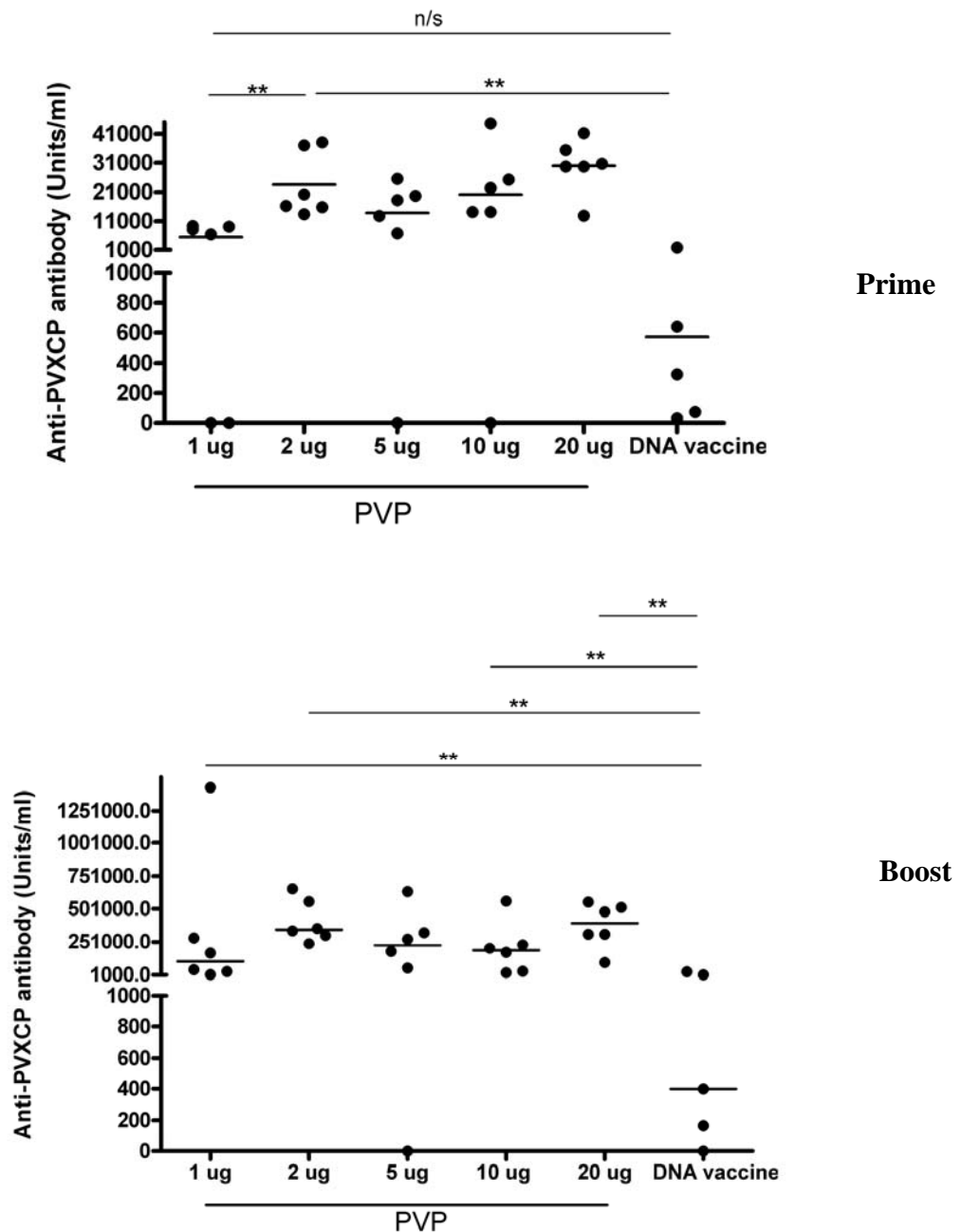
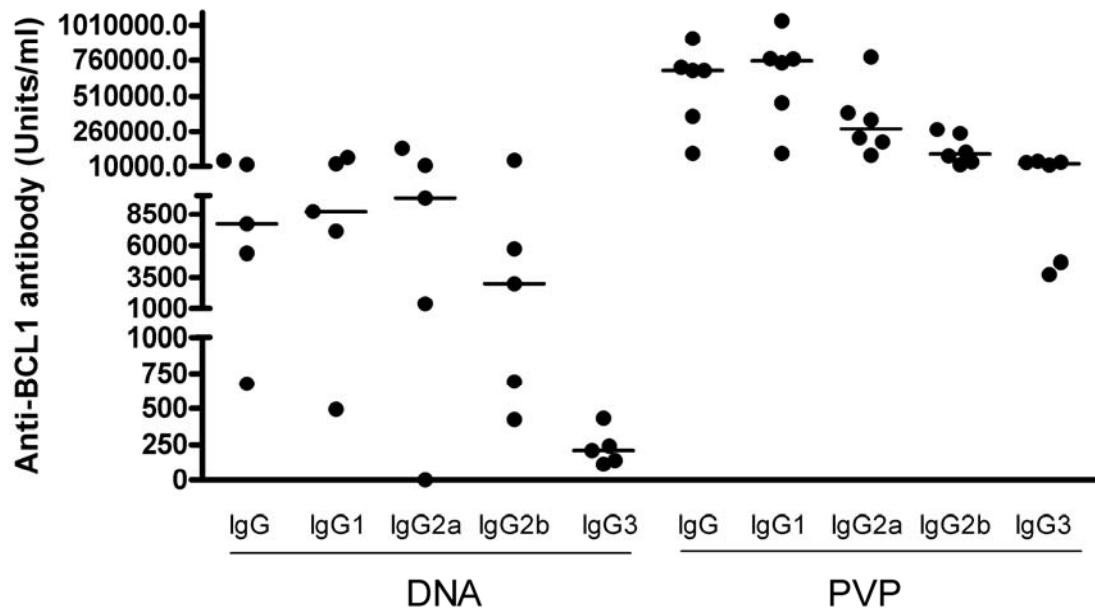


**Figure 4-8. Anti-PVXCP antibody responses after vaccination with different doses of BCL<sub>1</sub>-PVP**

Mice were primed with pcDNA3.scFv.BCL<sub>1</sub>-PVXCP (DNA vaccine) in comparison to different doses (1 µg, 2 µg, 5 µg, 10 µg and 20 µg of BCL<sub>1</sub> IgG) of BCL<sub>1</sub>-PVP vaccine mixed with alum and then boosted on day 35 with the priming material. Antibody levels to PVXCP were measured on day 21 after priming (prime) and day 14 after boosting (boost). \*\*: 0.001 < p < 0.005, \*: p < 0.05. Each dot represents an individual mouse. Horizontal bars are median values.



	IgG	IgG1	IgG2a	IgG2b	IgG3
<b>DNA</b>	7,726	8,728	9,816	2,995	208
<b>PVP</b>	687,485	756,412	279,012	98,143	28,998

	IgG1/IgG2a	IgG1/IgG2b	IgG1/IgG3
<b>DNA</b>	0.89	2.91	41.93
<b>PVP</b>	2.71	7.71	26.08

**Figure 4-9. IgG subclasses of anti-BCL<sub>1</sub> antibody induced by BCL<sub>1</sub>-PVP vaccine**

After priming/boosting with pcDNA3.scFv.BCL<sub>1</sub>-PVXCP (DNA vaccine) or BCL<sub>1</sub>-PVP mixed with alum, anti-BCL<sub>1</sub> total IgG, IgG1, IgG2a, IgG2b and IgG3 subclasses were determined. Tables show the median value of IgG and IgG isotypes and ratio of median values of anti-Id IgG1/IgG2a, IgG1/IgG2b and IgG1/IgG3 responses in each vaccine groups. Each dot represents an individual mouse. Horizontal bars are median values.

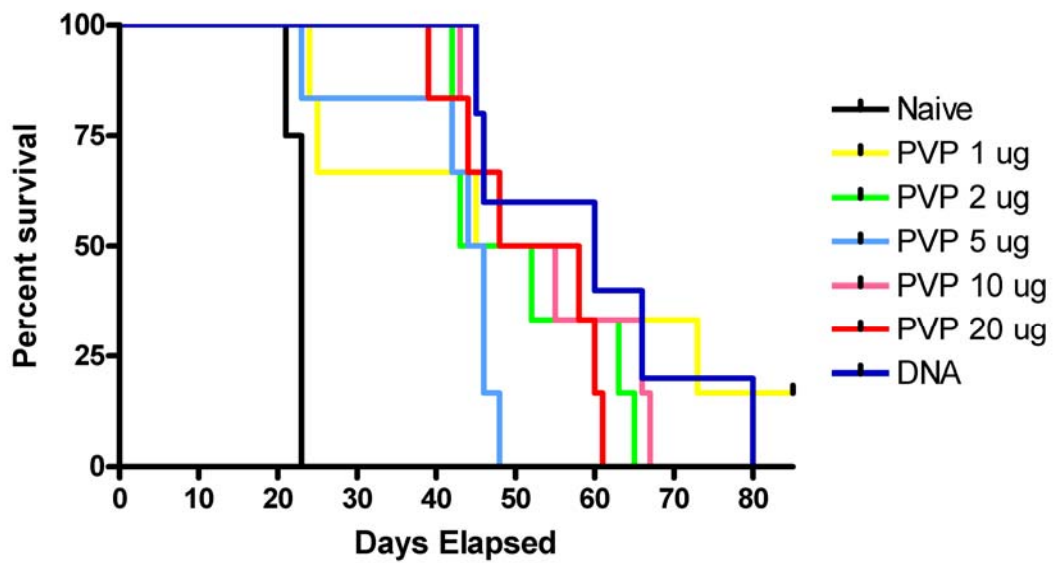


**Figure 4-10. Protection of mice immunised with different doses of BCL<sub>1</sub>-PVP vaccine**

Immunised mice received  $5 \times 10^4$  cells of the BCL<sub>1</sub> tumour at 25 days after boosting. Mice were terminated when splenomegaly was observed and the termination dates were noted. Each line represents survival data of the groups indicated in the legend shown on the right hand side of the survival curve.

#### 4.2.2 Role of PVX RNA in induction of anti-BCL<sub>1</sub> antibody response

To investigate the role of PVX RNA in induction of immunity against the BCL<sub>1</sub> tumour, vaccination was performed using a vaccine containing PVX RNA and compared to the vaccine without the RNA. In order to obtain the vaccine without PVX RNA, BCL<sub>1</sub> IgG linked to SA was linked with biotinylated PVXCP in the same ratio as in BCL<sub>1</sub>-PVP vaccine (6 IgGs to 1 PVXCP molecule) to produce BCL<sub>1</sub> IgG-PVXCP (BCL<sub>1</sub>-CP) vaccine. In vaccination using BCL<sub>1</sub>-CP mixed with PVX RNA, 6 µg RNA per 94 µg PVXCP was used according to the relative amount of (6%) RNA to (94%) CP in the virus particle [246].

A group of 8 mice was injected with BCL<sub>1</sub>-CP or BCL<sub>1</sub>-CP mixed with RNA or BCL<sub>1</sub>-SA. BCL<sub>1</sub>-CP with RNA induced highest level of anti-Id antibody, with the levels significantly higher than BCL<sub>1</sub>-SA group (figure 4-11). The anti-Id levels of BCL<sub>1</sub>-CP group appeared to be higher than BCL<sub>1</sub>-SA group. Taken together, these data suggest the role of RNA together with linked CP in antibody responses, i.e. CP and RNA act synergistically to increase the antibody response.

Since PVX RNA (ssRNA) could activate the immune response through TLR7, the role of PVX RNA was further studied in TLR7 KO mice (Appendix A-2) by Dr N Savelyeva in collaboration with Dr S Diebold (Kings' college, London). The experiment was performed only once so far. In TLR7 KO, injection with either PVX (no adjuvant) or PVXCP mixed with pU21 (TLR7 ligand) did not induce anti-PVXCP antibody response. In wild-type mice or TRIF (adaptor molecule for TLR3 signalling) KO, both antigens induced anti-PVXCP antibody response. These data indicate the role of TLR7, not TLR3, in immunity induced by PVX. PVXCP alone did not induce anti-PVXCP antibody responses in both wild-type and TRIF KO thus further indicating the role of PVX RNA in immune induction.

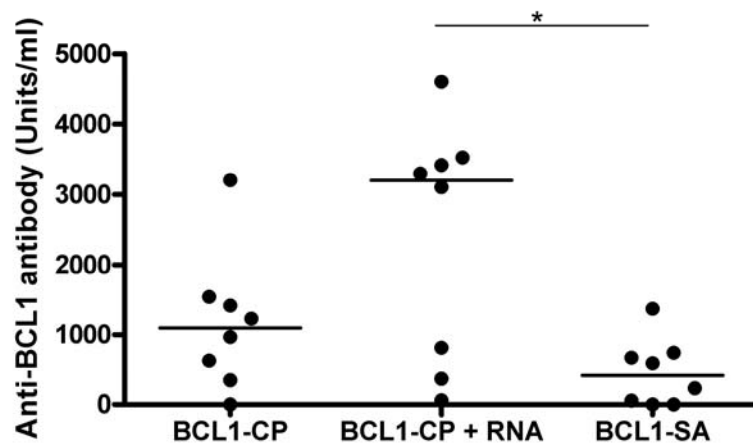


**Figure 4-11. Anti-BCL<sub>1</sub> antibody responses after vaccination with BCL<sub>1</sub>-CP mixed with RNA**

Mice were injected with BCL<sub>1</sub>-CP vaccine or BCL<sub>1</sub>-CP mixed with PVX RNA (BCL<sub>1</sub>-CP + RNA) or BCL<sub>1</sub>-SA. Antibody levels to BCL<sub>1</sub> were measured on day 21 after injection. \*:  $p < 0.05$ . Each dot represents an individual mouse. Horizontal bars are median values.

### 4.2.3 BCL<sub>1</sub>-PVP vaccine induced helper T cell responses

One of the contributions from PVX to immunogenicity of BCL<sub>1</sub>-PVP vaccine would be provision of CD4 T-cell help by CP. Therefore helper responses specific to PVXCP and BCL<sub>1</sub> antigens induced by BCL<sub>1</sub>-PVP vaccine were determined by IFN- $\gamma$ , IL-2 and IL-4 ELISPOT. BCL<sub>1</sub> antigen was included to see if any tumour specific responses were also induced. A group of four mice was vaccinated with BCL<sub>1</sub>-PVP vaccine or the DNA vaccine. Fourteen days after vaccination spleens from vaccinated mice were collected and splenocytes were isolated. Two naïve mice were included as controls. Splenocytes ( $2.5 \times 10^5$  cells per well) were incubated with PVXCP or BCL<sub>1</sub> IgM or ovalbumin (control protein) in plates that were coated with anti-IFN- $\gamma$  or anti-IL-2 or anti-IL-4 antibody for 42 hr before subsequent cytokine detection with an ALP-labelled antibodies. The responses were counted positive if they were at least two times higher than the naïve mouse controls and the control protein.

In response to PVXCP, high number of IFN- $\gamma$  secreting cell spots was detected in BCL<sub>1</sub>-PVP immunised mice (figure 4-12). All four mice vaccinated with the PVP vaccine responded to 40  $\mu$ g/ml of PVXCP with the average of 407 spots/million cells (range between 44 – 785 spots/million cells). All four BCL<sub>1</sub>-PVP vaccinated mice also responded to 4  $\mu$ g/ml of PVXCP although with lower spot number (the average of 273 spots/million cells, ranging between 42 – 534 spots/million cells). Only one mouse with the highest response to PVXCP also responded to BCL<sub>1</sub> IgM (208 spots/million cells). No response was seen to ovalbumin indicating specificity. Responses were much lower in the DNA vaccine group, two of four mice responded to 40  $\mu$ g/ml of PVXCP (53 and 72 spots/million cells) and only one mouse responded to 4  $\mu$ g/ml of PVXCP (70 spots/million cells). None of DNA vaccinated mice responded to BCL<sub>1</sub> IgM.

The BCL<sub>1</sub>-PVP vaccine also induced IL-2. After stimulation of splenocytes with PVXCP high number of IL-2 secreting cell spots were detected by ELISPOT (figure 4-13). Three of four PVP vaccinated mice responded to 40  $\mu$ g/ml of PVXCP with the average of 293 spots/million cells (range between 198 – 370 spots/million cells). Three of four BCL<sub>1</sub>-PVP vaccinated mice also responded to 4  $\mu$ g/ml of PVXCP with the average of 184 spots/million cells (range between 66 - 273 spots/million cells) although the response was lower than to 40  $\mu$ g/ml of PVXCP as expected. In the DNA vaccine group, number of IL-2 secreting cells upon PVXCP stimulation was low; only one mouse responded to 40  $\mu$ g/ml of PVXCP (69 spots/million cells) and one mouse responded to 4  $\mu$ g/ml of PVXCP (28 spots/million cells). Responses to PVXCP were specific as responses to ovalbumin were much lower. Specific response to BCL<sub>1</sub> IgM was not detected in both PVP and DNA

vaccinated mice. In IL-4 ELISPOT, 2 of 4 PVP vaccinated mice were likely to have responded to 40  $\mu\text{g}$  of PVXCP when compare to naïve mice. However, the responses to both antigens were generally non-specific as the levels of responses to ovalbumin control protein were high (figure 4-14).

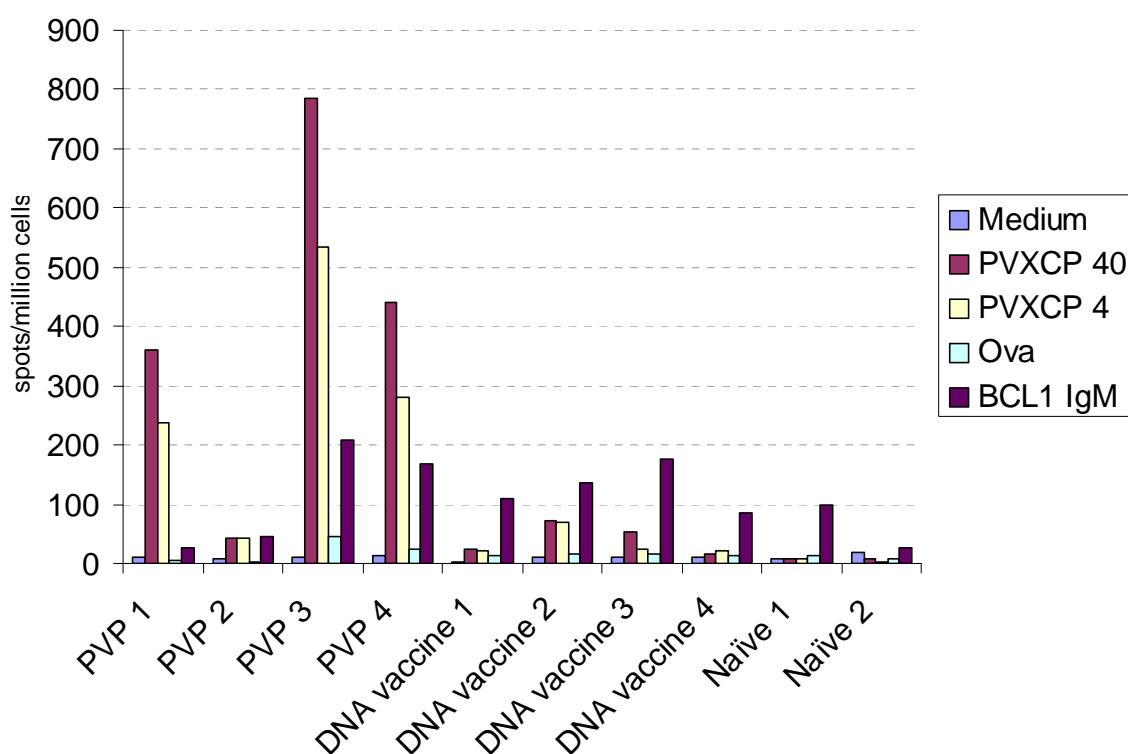


**Figure 4-12. IFN- $\gamma$  ELISPOT**

A group of 4 mice was injected with BCL<sub>1</sub>-PVP mixed with alum (PVP) or DNA vaccine. Spleens were collected at day 14 after injection for ELISPOT assay. Spleens from 2 naïve mice were included as controls. IFN- $\gamma$  producing cells (spots/million cells) were determined after incubation with medium alone or medium containing 40  $\mu\text{g}/\text{ml}$  (PVXCP 40) or 4  $\mu\text{g}/\text{ml}$  of PVXCP (PVXCP 4) or 100  $\mu\text{g}/\text{ml}$  of ovalbumin (Ova) or 60  $\mu\text{g}/\text{ml}$  of BCL<sub>1</sub>IgM (BCL1 IgM).

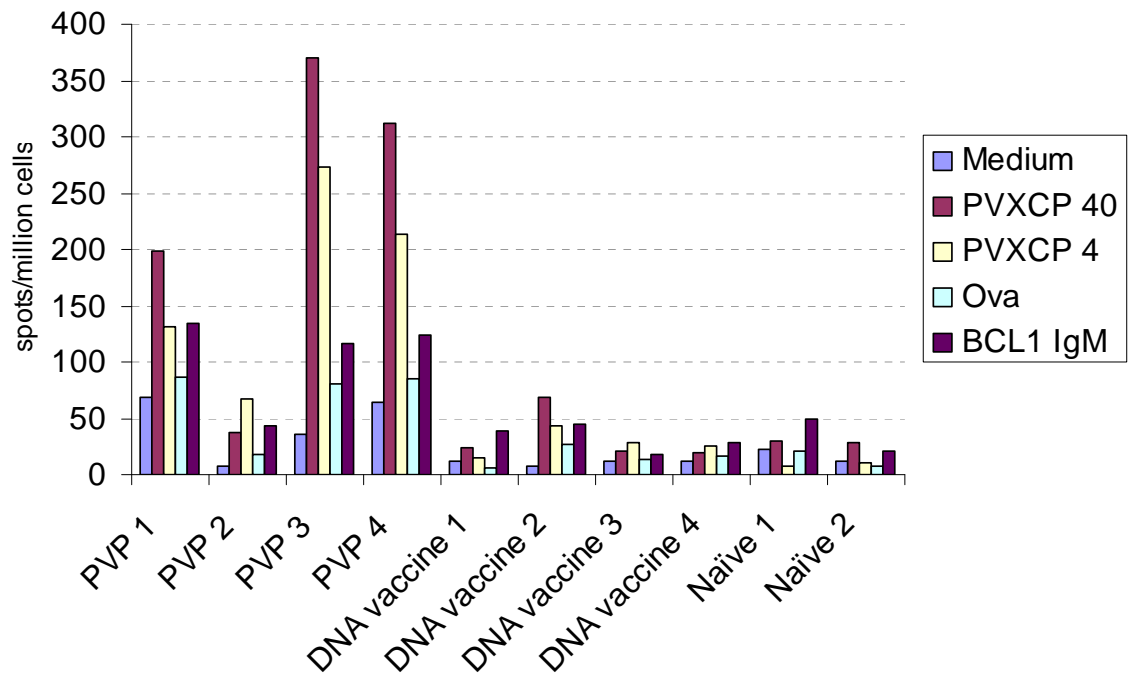


**Figure 4-13. IL-2 ELISPOT**

A group of 4 mice was injected with BCL<sub>1</sub>-PVP mixed with alum (PVP) or DNA vaccine. Spleens were collected at day 14 after injection for ELISPOT assay. Spleens from 2 naïve mice were included as controls. IL-2 producing cells (spots/million cells) were determined after incubation with medium alone or medium containing 40 µg/ml (PVXCP 40) or 4 µg/ml of PVXCP (PVXCP 4) or 100 µg/ml of ovalbumin (Ova) or 60 µg/ml of BCL<sub>1</sub> IgM (BCL1 IgM).

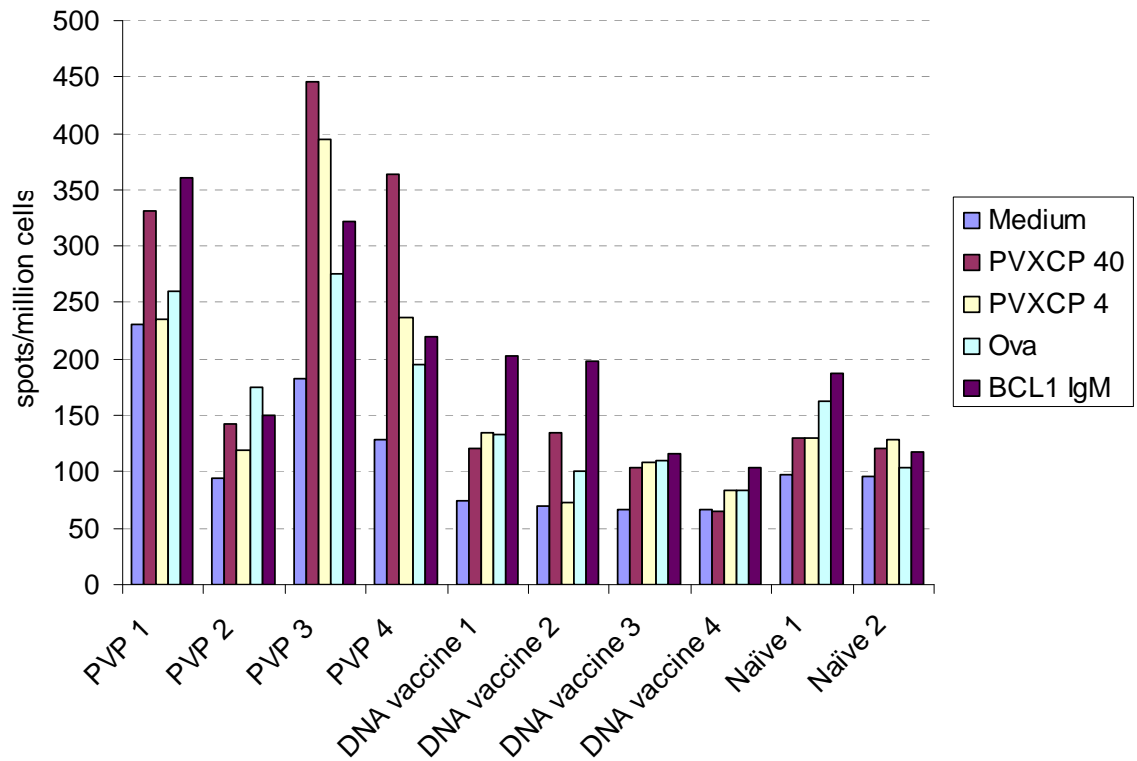


**Figure 4-14. IL-4 ELISPOT**

A group of 4 mice was injected with BCL<sub>1</sub>-PVP mixed with alum (PVP) or DNA vaccine. Spleens were collected at day 14 after injection for ELISPOT assay. Spleens from 2 naïve mice were included as controls. IL-4 producing cells (spots/million cells) were determined after incubation with medium alone or medium containing 40 µg/ml (PVXCP 40) or 4 µg/ml of PVXCP (PVXCP 4) or 100 µg/ml of ovalbumin (Ova) or 60 µg/ml of BCL<sub>1</sub>IgM (BCL1 IgM).

### 4.2.3 Activation of APCs by PVX

To efficiently engage the immune response, a candidate vaccine should be able to activate DCs. Therefore the effect of PVX on DC activation was studied. Activation of DCs by PVX was studied first *in vitro* using bone marrow-derived DCs (BmDCs). BmDCs were incubated with 10 µg/ml of PVX or 1 µg/ml of LPS for 48 h or left untreated and stained with PE-labeled anti-CD11c and APC-labeled anti-CCR7 or anti-CD40 or anti-CD80 or anti-CD86 or FITC-labeled anti-I-A/I-E antibodies. An isotype control was included for each marker. FACS analysis showed that PVX did not up-regulate any of 5 DC activation markers while LPS induced up-regulation of the activation markers as expected. In figure 4-15 the representative plot is shown. The experiments were repeated three times and similar results were obtained (one repeat experiment is shown in the appendix).

In addition, DC cytokines, chemokines and chemokine receptors expression were determined using reverse transcription real time PCR. Upon activation, DCs change the gene expression profiles. It has been shown that some genes such as CCR7, some chemokines (CCL2, CCL4, CCL5, CXCL10) and some cytokines (IL-6, IL-12 and TNF-α) are up-regulated while CCR2 is down-regulated [247-249]. Expression of those genes was therefore determined. BmDCs were incubated for 15 h with 10 µg/ml of PVX or 1 µg/ml of LPS or left untreated. CD11c<sup>+</sup> cells were positively selected from each treatment and subjected to RNA extraction. RNA was reverse-transcribed and analysed by real-time PCR. In PVX treated cells, the expression levels of tested genes were comparable to non-activated cells while the LPS-activated DCs up-regulated expression of CCL2, CCL4, CCL5, CCR7, IL-6, IL-12 and TNF-α and down-regulated expression of CCR2 as expected (figure 4-16). Taken together with surface marker determination, these data indicate that PVX could not activate DCs *in vitro*. Therefore, APC activations by PVX were next evaluated *in vivo*, the method used in mammalian virology.

Initially, binding of PVX to APCs *in vivo* was evaluated using Alexa<sup>®</sup> Fluor 647-conjugated PVX. The labelled PVX (100 µg) was injected into C57BL/6 mouse and the binding of the labeled-PVX to splenic DCs and B cells was examined by FACS analysis. Spleens were collected from mice injected with Alexa Fluor 647-conjugated PVX or saline 2 h after injection. Splenocytes were stained with PE-labeled anti-CD11c or anti-CD19 antibody. FACS analysis of three identical experiments showed that 50 % of CD11c<sup>+</sup> cells and 60 % of CD19<sup>+</sup> cells bound to PVX (figure 4-17). These data indicate that PVX bound to both DCs and B cells.

Activation of DCs by PVX was further determined in comparison with LPS as a positive control. LPS (endotoxin) is a potent DC activator hence its presence in the PVX

preparation might lead to DC activation. Initially, an endotoxin level in the 100 µg of PVX sample, the amount used for DC activation, was measured using LPS as a standard concentration. From the endotoxin test, 100 µg of PVX contained an equivalent of 250 pg of LPS. Although care was taken to purify the virus some levels of endotoxin were always detected and these were due to technology used for PVX infection in plants. To investigate the effect of contaminated endotoxin in DC activation, PVX was injected i.v. into C57BL/6 mice in comparison with 250 pg or 25 µg of LPS or saline. Spleens were collected 20 h after injection. Splenocytes were stained with PE-labeled anti-CD11c antibody and up-regulation of activation markers was determined by using APC-labeled anti-CCR7 or anti-CD40 or anti-CD80 or anti-CD86 or anti-I-A/I-E antibody. An isotype control was included for each marker. FACS analysis showed that PVX induced up-regulation of all 5 DC activation markers at comparable levels to LPS (a representative plot is shown in figure 4-18). In contrast, 250 pg of LPS did not up-regulate DC activation markers similarly to saline (negative control). These data indicate that up-regulation of DC activation markers was by PVX and not the result of the low level of endotoxin contamination. This experiment was performed twice and the results were similar. Results of the repeated experiment are shown in the appendix.

To further investigate the ability of PVX to activate  $CD8\alpha^+$ ,  $CD8\alpha^-CD4^+$  and  $CD8\alpha^-CD4^-$  DC subsets, 20 h activated splenocytes were stained with PE-labeled anti-CD11c antibody, APC-labeled anti-CD8 $\alpha$  antibody, FITC-labeled anti-CD4 antibody and PerCP-Cy5.5-labeled anti-CCR7 or anti-CD40 or anti-CD80 or anti-CD86 or anti-I-A/I-E antibody. An isotype control for each marker was included. FACS analysis showed that PVX up-regulated CCR7, CD40, CD86, and I-A/I-E expression in all DC subsets to the levels comparable to those induced by LPS (a representative plot is shown in figure 4-19). Saline (negative control) did not induce DC activation. CD80 was up-regulated in  $CD8\alpha^-CD4^+$  subset, slightly increased in  $CD8\alpha^-CD4^-$  subset and was not increased in  $CD8\alpha^+CD4^-$  subset. These data indicate that PVX was a potent activator of CD11c $^+$  DC. Similar results were observed in three independent experiments. Results of one of two repeated experiments are shown in the appendix.

Activation of B cells by PVX was initially determined by analysis of CD40, CD86 and I-A/I-E activation markers in comparison with LPS as a positive control (figure 4-20). An isotype control for each marker was included. LPS up-regulated expression of all tested activation markers as expected. However, PVX induced higher expression of CD86 and I-A/I-E, the molecules required for interaction with T cells, but not CD40. The levels of up-regulated CD86 and I-A/I-E induced by PVX were similar to the levels induced by LPS control. Saline did not induce B-cell activation. The high expression of CD86 was

consistent when determined in CD19<sup>+</sup>CD21<sup>+</sup> marginal zone B cells and CD19<sup>+</sup>CD23<sup>+</sup> follicular B cells, indicating that both major splenic B-cell subsets were activated by PVX. The experiment was performed twice independently and both showed similar results. Results of the repeated experiment are shown in the appendix.

Cytokine, chemokine and chemokine receptor gene expression after *in vivo* PVX activation was further evaluated. A group of three mice was injected with 100 µg of PVX or 25 µg of LPS or saline and spleens were collected at 6 hr after injection. DCs were isolated from spleen cells using PE-anti-CD11c and anti-PE microbeads. After isolation, approximately 70% of cells were positive for CD11c. RNA was extracted from isolated cells and reverse-transcribed before the real-time PCR analysis. Mean values of relative gene expression compare to non-treated cells from 3 treated mice are shown in figure 4-21. PVX-activated DCs down-regulated CCR2 expression and up-regulated expression of CCL4, CCL5, CXCL10, CCR7, IL-6, TNF- $\alpha$  and IL-12, these profiles were expected from activated DCs. PVX increased expression of CCL4, CXCL10 and IL-6 in a similar level to LPS. The level of TNF- $\alpha$  expression induced by PVX was higher than that induced by LPS. For IL-12, PVX induced up-regulation of the gene expression but LPS unexpectedly did not induced IL-12 expression. Taken together PVX induced DC maturation as indicated by changing in the cytokine, chemokine and chemokine receptor expression profiles toward mature DC phenotypes.

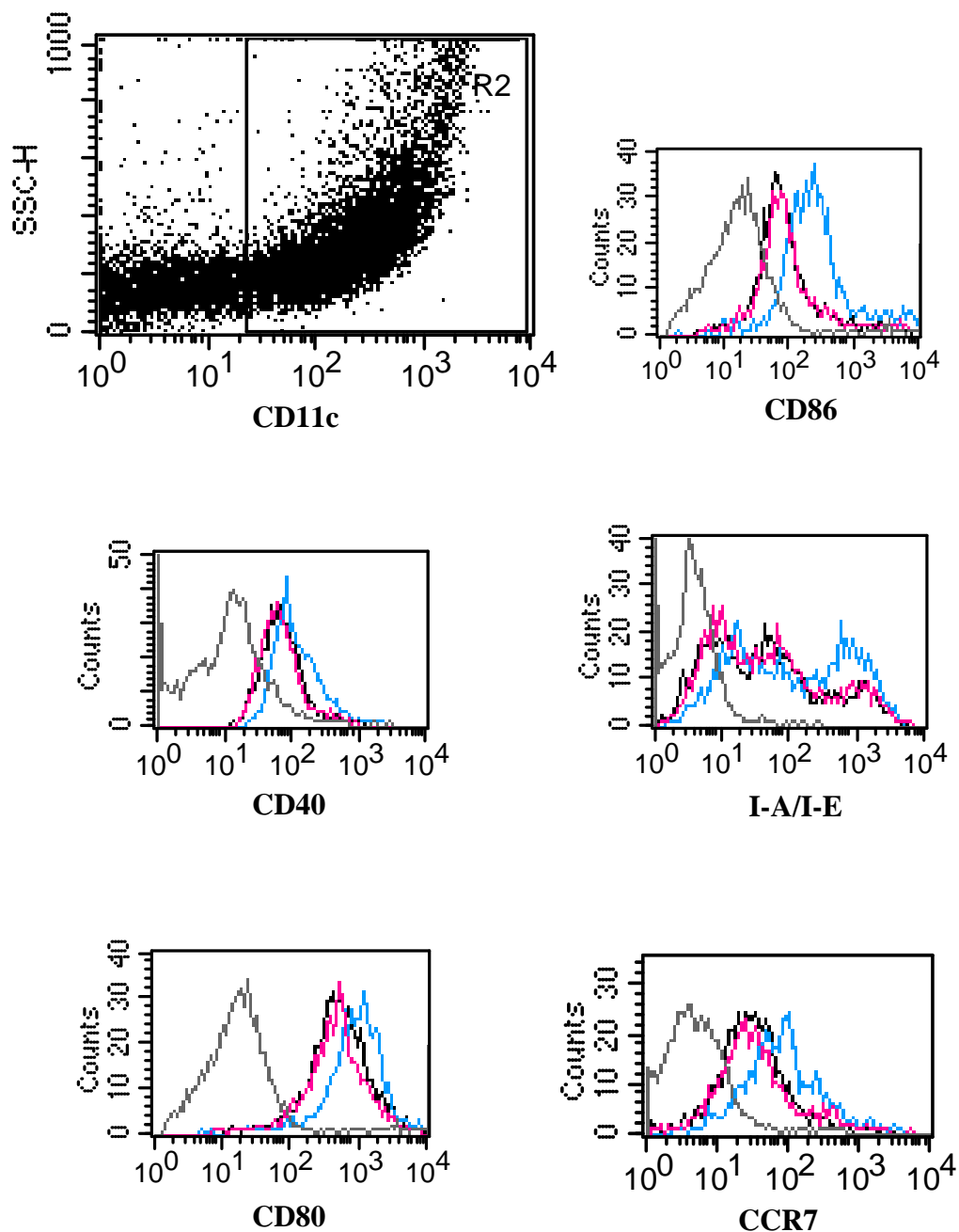


**Figure 4-15. FACS analysis of DC activation *in vitro***

BmDCs were incubated with 10  $\mu$ g of PVX (pink histogram) or 1  $\mu$ g of LPS (blue histogram) for 48 hrs. Cells were stained with PE-labeled anti-CD11c antibody and APC-labeled anti-CCR7 or anti-CD40 or anti-CD80 or anti-CD86 or FITC-labeled anti-I-A/I-E antibody and analyzed by FACSCalibur with the Cell Quest Pro software. Cells were gated for CD11c as shown in the top-left graph. Non-treated control cells are shown in black histogram. Isotype controls are shown in grey histogram. This is a representative plot of three experiments.

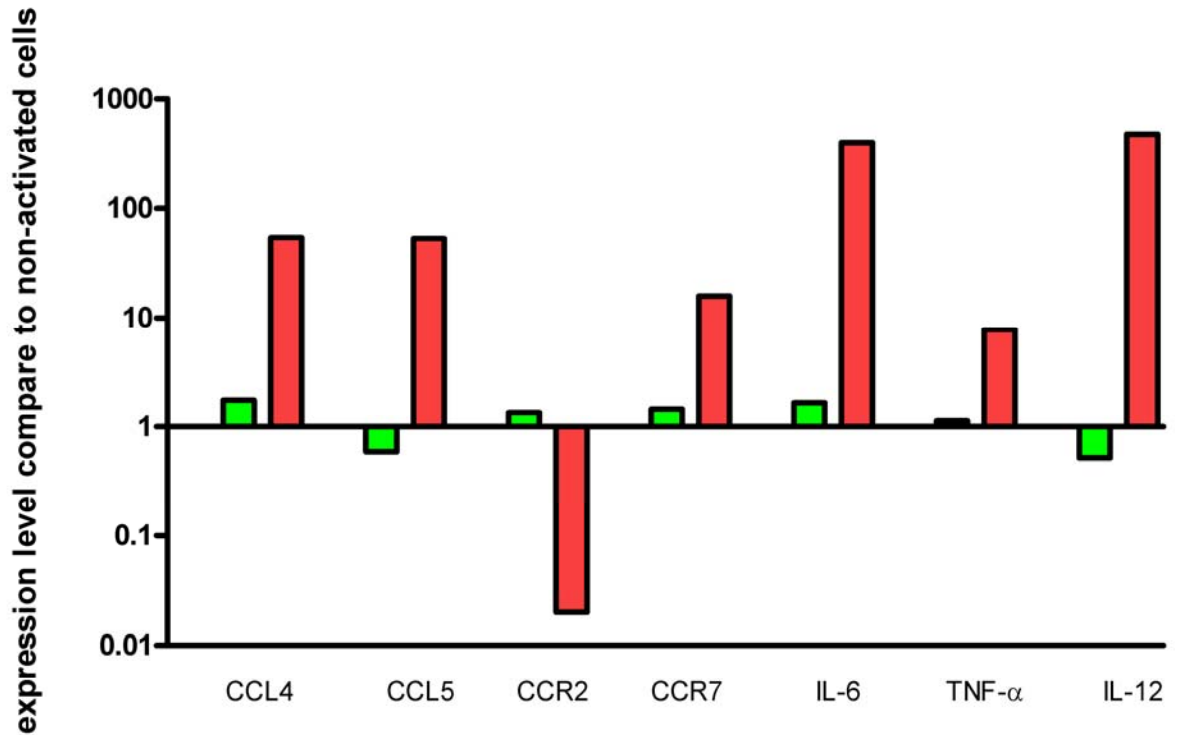
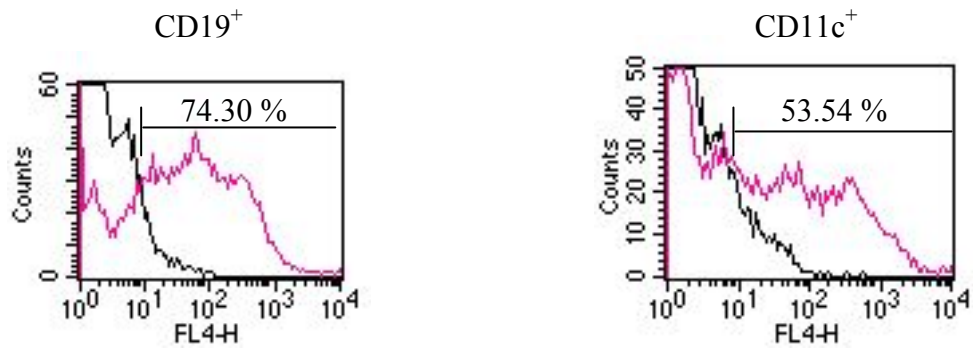


**Figure 4-16. Expression of cytokines, chemokines and chemokine receptors after *in vitro* PVX activation**

BmDCs were incubated in media alone (non-activated cells control) or media containing 10  $\mu\text{g/ml}$  of PVX (green bar) or 1  $\mu\text{g/ml}$  of LPS (orange bar) for 15 hrs. CD11c<sup>+</sup> cells were positively isolated using PE-anti-CD11c antibody following with anti-PE microbead. RNA was extracted from selected cells and reverse-transcribed before analysing with real-time PCR. Relative expression levels to non-activated cells of each tested RNA species (as indicated on X-axis) in activated cells are shown.



	% Alexa Fluor 647-PVX positive	
	CD19+ cells	CD11c+ cells
Experiment 1	74.30	53.54
Experiment 2	63.75	51.17
Experiment 3	56.20	44.62
Mean	64.75	49.78

**Figure 4-17. FACS analysis of PVX binding to B cells and DCs *in vivo***

Alexa Fluor 647-conjugated PVX (pink histogram) or saline (black histogram) was injected into C57BL/6 mouse and the spleen was collected at 2 hrs after injection. Splenocytes were stained with PE-labeled anti-CD11c or anti-CD19 antibody. Alexa Fluor 647 (FL4-H) positive CD11c<sup>+</sup> cells or CD19<sup>+</sup> cells were analyzed by FACSCalibur with the Cell Quest Pro software. The representative plot of three experiments is shown. Percentage of CD11c<sup>+</sup> cells or CD19<sup>+</sup> cells containing Alexa Fluor 647 from three experiments is shown in the table.

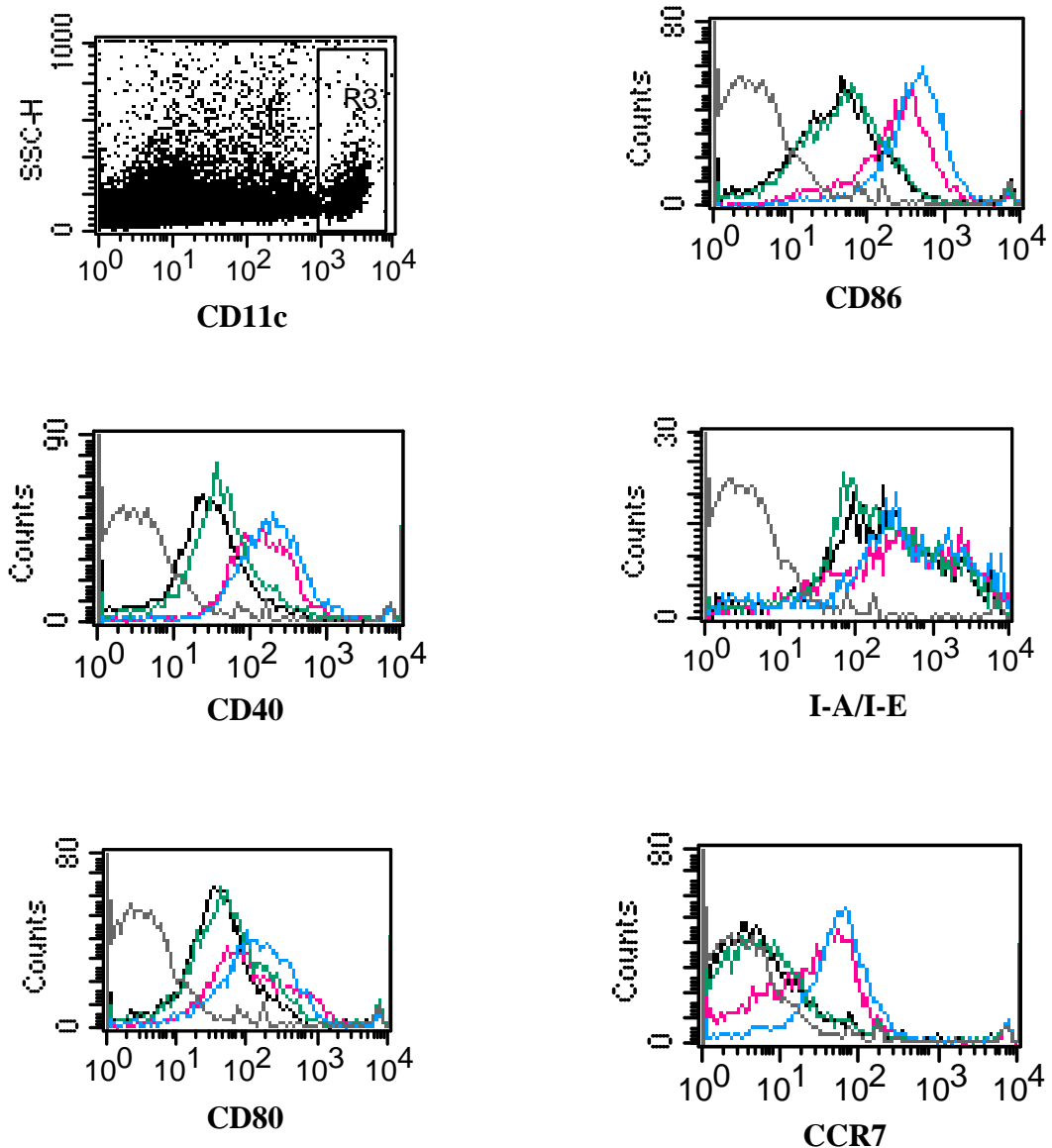


**Figure 4-18.** FACS analysis of the effect of low amounts of LPS in DC activation *in vivo*

100  $\mu$ g of PVX (pink histogram) or 250  $\mu$ g of LPS (green histogram) or 25  $\mu$ g of LPS (blue histogram) or saline (black histogram) was injected into C57BL/6 mouse and spleen was collected at 20 h after injection. Splenocytes were stained with PE-labeled anti-CD11c and APC-labeled anti-CCR7 or anti-CD40 or anti-CD80 or anti-CD86 or anti-I-A/I-E antibodies and analyzed by FACSCalibur with the Cell Quest Pro software. Cells were gated for CD11c as shown in the top-left graph. Isotype controls are shown in grey histogram. This is a representative plot of two experiments.

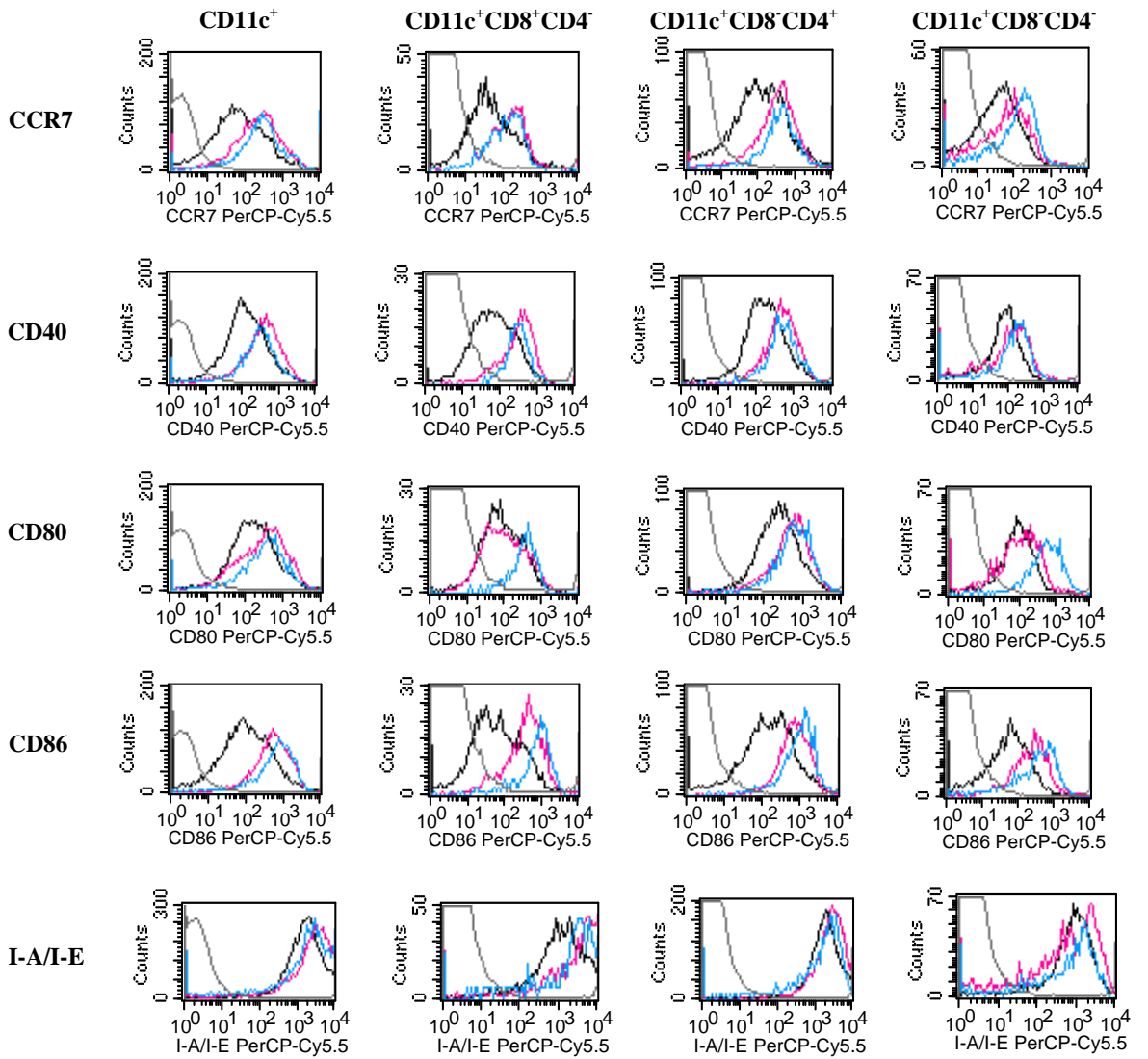
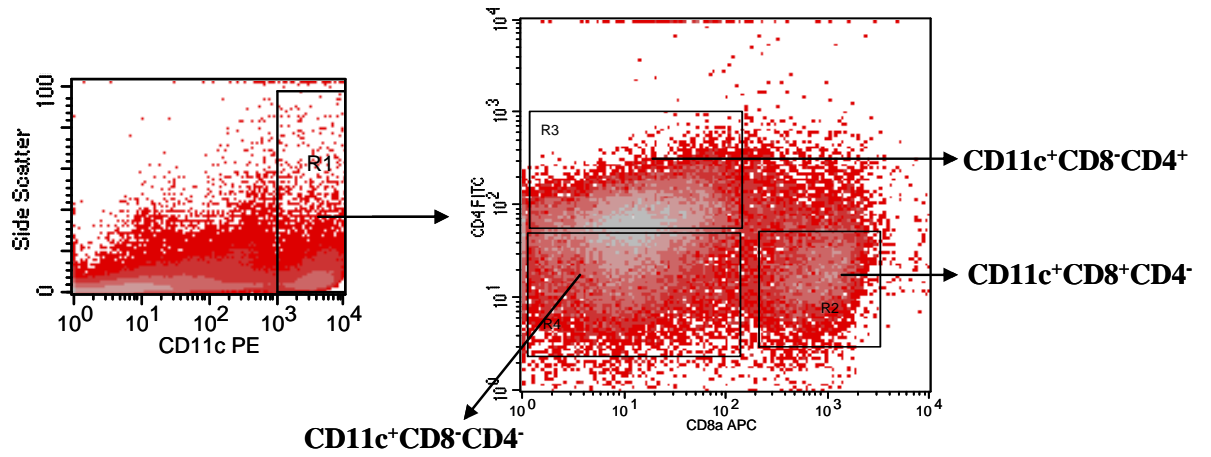


**Figure 4-19. FACS analysis of PVX induced DC activation *in vivo***

100 µg of PVX (pink histogram) or 25 µg of LPS (blue histogram) or saline (black histogram) was injected into C57BL/6 mouse and spleen was collected at 20 hrs after injection. Splenocytes were stained with PE-labeled anti-CD11c, APC-labeled anti-CD8α, FITC-labeled anti-CD4, and PerCP-Cy5.5-labeled anti-CCR7 or anti-CD40 or anti-CD80 or anti-CD86 or anti-I-A/I-E antibodies and analyzed by FACSCalibur with the Cell Quest Pro software. Cells were gated for CD11c as shown in the top-left graph. CD11c gated cells were further divided into CD8<sup>+</sup>CD4<sup>-</sup>, CD8<sup>-</sup>CD4<sup>+</sup> and CD8<sup>-</sup>CD4<sup>-</sup> subsets and each gated subset was further analysed for cell surface markers. Isotype controls are shown in grey histogram. This is a representative plot of three experiments.

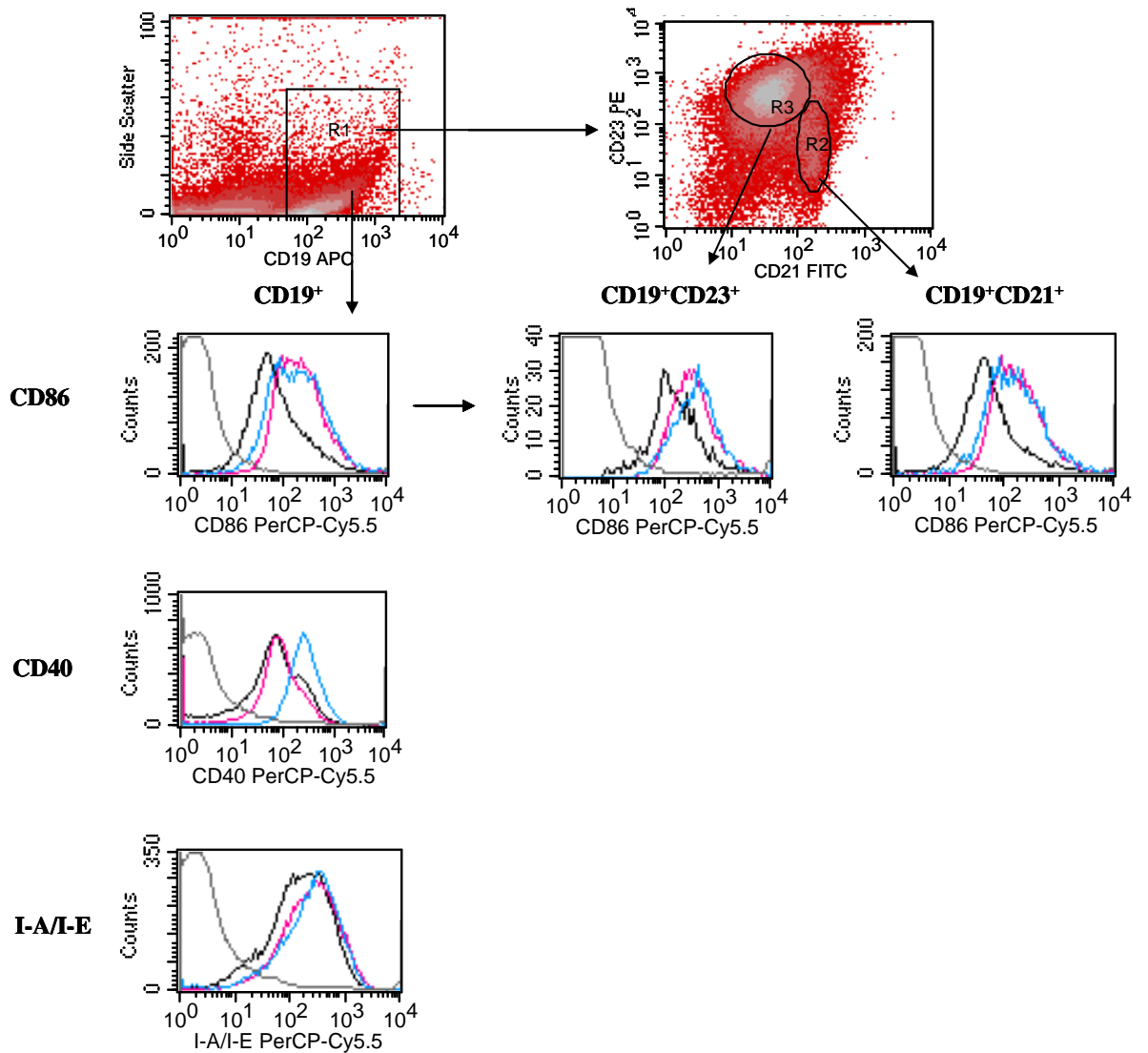


**Figure 4-20. FACS analysis of PVX induced B-cell activation *in vivo***

100  $\mu$ g of PVX (pink histogram) or 25  $\mu$ g of LPS (blue histogram) or saline (black histogram) was injected into C57BL/6 mouse and spleen was collected at 20 hrs after injection. Splenocytes were stained with PE-labeled anti-CD19 and PerCP-Cy5.5-labeled anti-CD40 or I-A/I-E antibodies. Separately, cells were stained with APC-labeled anti-CD19, FITC-labeled anti-CD21, PE-labeled anti-CD23 and PerCP-Cy5.5-labeled anti-CD86 antibodies. Stained cells were analyzed by FACSCalibur with the Cell Quest Pro software. Cells were gated on CD19 as shown in the top-left graph. CD19 gated cells were plotted against CD21 and CD23, gated CD21 and CD23 were further analysed for CD86. Isotype controls are shown in grey histogram. This is a representative plot of two experiments.

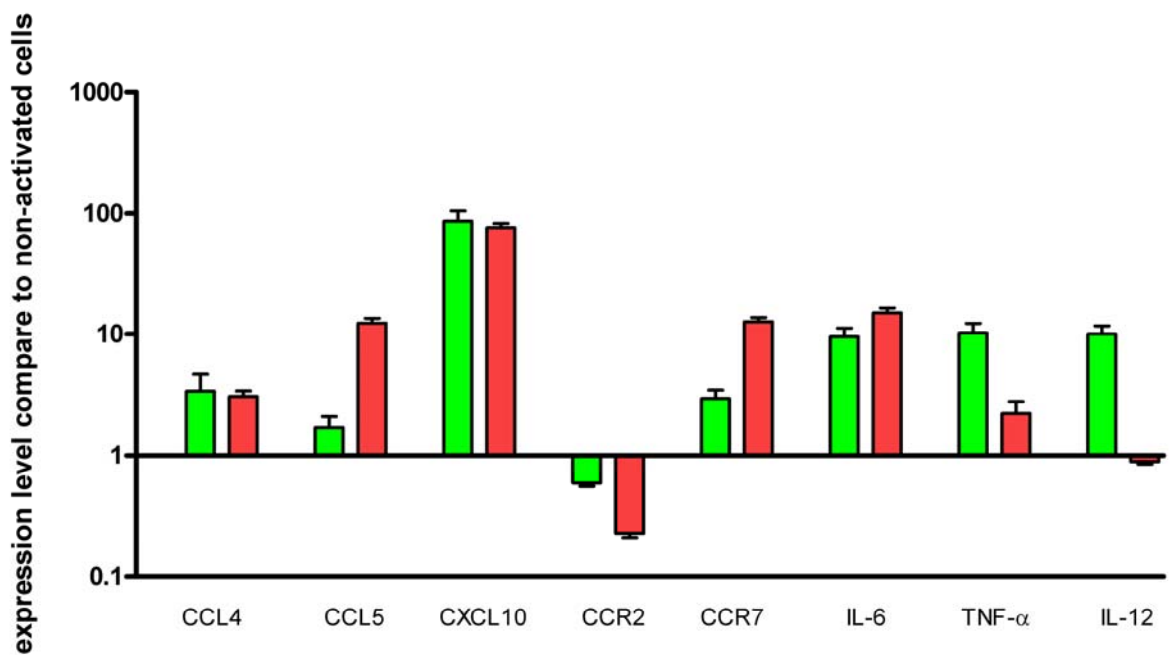


**Figure 4-21. Expression of cytokines, chemokines and chemokine receptors after *in vivo* PVX activation**

A group of three mice was i.v. injected with 100  $\mu$ g PVX (green bar) or 25  $\mu$ g of LPS (orange bar) or saline (non-activated control). Spleens were collected 6 hours after injection. CD11c<sup>+</sup> cells were positively selected using PE-anti-CD11c antibody following with anti-PE microbeads. RNA was extracted from selected cells and reverse-transcribed before analysing with real-time PCR. Relative expression levels to non-activated cells of each tested RNA species (as indicated on X-axis) in activated cells are shown. Each bar represents a mean value of the relative gene expression from three mice.

### 4.3 Summary

To evaluate the ability of PVX to enhance the immune response to the BCL<sub>1</sub> Id of lymphoma, the PVX-based BCL<sub>1</sub>-PVP vaccine displaying BCL<sub>1</sub> antigen was generated by linking BCL<sub>1</sub> IgG to PVX particle via biotin-streptavidin binding. In the initial vaccination experiment, mice were vaccinated with BCL<sub>1</sub>-PVP or BCL<sub>1</sub>-PVP mixed with alum or the DNA vaccine or PVX control. Mice injected with BCL<sub>1</sub>-PVP vaccine generated both anti-Id and anti-PVX antibodies to the levels significantly higher than those induced by the DNA vaccine. Alum appeared to enhance the antibody responses and therefore, BCL<sub>1</sub>-PVP vaccine was mixed with alum in the next vaccination experiments. PVX only induced anti-PVXCP antibody response as expected. In addition, both BCL<sub>1</sub>-PVP vaccine alone and BCL<sub>1</sub>-PVP mixed with alum provided protection against tumour challenge and that was comparable to protection generated by the DNA vaccine. In another experiment, mice were vaccinated with the PVP vaccine in comparison with BCL<sub>1</sub>IgG linked to SA alone, alum was not added in this experiment. The PVP vaccine induced significantly higher anti-Id antibody levels than the vaccine without linked PVX suggesting that linked PVX enhanced antibody responses to the Id Ig.

The next BCL<sub>1</sub>-PVP vaccination with higher number of mice confirmed that the PVP vaccine was superior in induction of anti-Id antibody responses than DNA vaccine and protected mice from tumour challenge similar to DNA vaccine. In the dose response experiment, BCL<sub>1</sub>-PVP vaccine containing 1, 2, 5, 10 and 20 µg of BCL<sub>1</sub> IgG were tested. The anti-Id antibody responses induced by different doses of the vaccine were comparable, with exception that 1 µg of the vaccine induced the lowest anti-Id antibody response which was significantly lower than the responses induced by 2 µg dose. As low as 2 µg of the PVP vaccine induced significantly higher anti-Id antibody responses than DNA vaccine. However, all tested doses were able to protect mice from tumour challenge similar to the DNA vaccine. These data suggest that only 1 µg of the PVP vaccine was able to induce antibody response and protect mice from the tumour challenge. Both BCL<sub>1</sub>-PVP and the DNA vaccines induced all IgG isotypes with IgG1 being dominant, IgG2a was higher than IgG2b. IgG3 was detected but at low level compared to other isotypes.

In order to evaluate the role of PVX RNA in anti-tumour response, BCL<sub>1</sub>IgG was linked to PVXCP (BCL<sub>1</sub>-CP) and the vaccination was performed in the setting of with or without added PVX RNA. BCL<sub>1</sub>IgG linked to streptavidin alone was used as a control. BCL<sub>1</sub>-CP mixed with RNA induced the highest levels of anti-Id antibody after priming; the antibody levels induced by BCL<sub>1</sub>-CP were higher than those induced by BCL<sub>1</sub>-SA; the antibody levels induced by BCL<sub>1</sub>-CP mixed with RNA were significantly higher than those

induced by BCL<sub>1</sub>-SA. This suggests the role of PVX RNA together with the linked CP in induction of antibody responses.

Induction of Th cell responses by BCL<sub>1</sub>-PVP and DNA vaccines was determined by IFN- $\gamma$ , IL-2 and IL-4 ELISPOT. All 4 PVP vaccinated mice generated specific-PVXCP IFN- $\gamma$  secreting cells, the mouse with a highest response also generated BCL<sub>1</sub> IgM-specific IFN- $\gamma$  secreting cells. In the DNA vaccine groups, only 2 of 4 mice produced IFN- $\gamma$  secreting cells specific to PVXCP and none of them responded to BCL<sub>1</sub> IgM. The number of IFN- $\gamma$  secreting cells in the PVP vaccine group was higher than that in the DNA vaccine group. In IL-2 ELISPOT, three of four BCL<sub>1</sub>-PVP vaccinated mice also induced IL-2 secreting cells specific to PVXCP. Only one of four mice vaccinated with the DNA vaccine induced IL-2 secreting cells. The number of IL-2 secreting cells in the PVP vaccine group was higher than that of the DNA vaccine group. None of PVP or DNA vaccinated mice induced IL-2 secreting cells in response to BCL<sub>1</sub> IgM. PVXCP or BCL<sub>1</sub> specific IL-4 secreting cells were detected in both vaccine groups but were not specific because of high levels of responses to ovalbumin protein control. Collectively, the number of helper cells induced by the PVP vaccine was higher than those induced by the DNA vaccine.

Evaluation of PVX ability to activate APCs was initially tested *in vitro*. Incubation of PVX with bmDCs did not result in changing of surface markers or cytokine, chemokine and chemokine receptor gene expression. Therefore, APC activation was further evaluated *in vivo*. *In vivo* PVX bound to both DCs and B cells and it induced up-regulation of activation markers of CD11c<sup>+</sup> DCs and B cells. PVX induced up-regulation of CCR7, CD40, CD80, CD86 and I-A/I-E in all DC CD11c<sup>+</sup> subsets with the exception of CD80 expression in CD8<sup>+</sup> DC subset. In addition, PVX induced up-regulation of CCL4, CCL5, CXCL10, CCR7, IL-6, TNF- $\alpha$  and IL-12 and down-regulation of CCR2. B cells also increased expression of CD86 and I-A/I-E upon PVX activation. These data indicate that DCs and B cells were activated by PVX in comparable manner to LPS.

#### **4.4 Discussion**

It has been shown that antibody plays an important role in anti-lymphoma immunity [138, 148]. Vaccination with the PVP vaccine consisting of PVX particle displaying multiple copies of BCL<sub>1</sub>IgG was able to induce high anti-Id antibody response and the vaccinated mice were protected from tumour challenge. The antibody responses were higher than those induced by the DNA vaccine even when as low as PVP vaccine containing 2  $\mu$ g of BCL<sub>1</sub>IgG was used. Even though PVP vaccine containing 1  $\mu$ g of BCL<sub>1</sub>IgG induced lower anti-Id antibody than other higher doses, it could protect mice against tumour

challenge comparably to DNA vaccine and those high dose of PVP vaccines. The observation that only low level of anti-Id antibody is required for protection was previously noted in BCL<sub>1</sub> DNA vaccine [203].

The superior ability of PVP vaccine to induce high levels of antibody could be explained by the form of antigen multimerisation through aggregation when linked to the viral particle and by immunoenhancing properties of PVX through providing T-cell help and DC activation (figure 4-22). It has long been recognised that antigen density influences the magnitude of an antibody response [250]. Multivalent antigens of HBV and HPV VLP vaccines have been shown to be superior in antibody responses [251-253]. As PVX showed an immunoenhancing property when linked with the BCL<sub>1</sub>IgG, this result implied that one possible reason how PVX enhances the immune response was from the multiple copies of BCL<sub>1</sub> antigen displayed on the surface. Vaccination of BCL<sub>1</sub>IgG linked to monomeric PVXCP in comparison to the vaccine of linked PVX will further reveal the importance of multimerization.

The immunoenhancing property of PVX might come from its RNA. The involvement of the virus RNA was determined by using BCL<sub>1</sub>IgG linked to PVXCP for vaccination with or without purified PVX RNA. The presence of PVX RNA enhanced anti-Id antibody response, thus indicating the role of the RNA in the immune induction. Since PVX RNA is single-stranded therefore it could potentially activate the immune response through TLR7 signalling (figure 4-22) [31, 254-255]. The preliminary experiment done in collaboration with Dr S Diebold showed that PVX could not induce antibody response in TLR7 KO mice while the response was not abolished in TRIF KO and wild-type mice. These data indicate the role of TLR7, but not TLR3 in immunity induced by PVX. This is in contrast to HPV VLP vaccine that activates immune response through TLR4 [256].

The PVP vaccine induced mixed anti-Id IgG isotypes and high levels of IFN- $\gamma$  and IL2 secreting cells. The induction of IFN- $\gamma$  and IL-2 secreting T cells by the PVP vaccine was better than that by the DNA vaccine. Induction of IgG2 and IFN- $\gamma$  secreting T cells indicates that PVP vaccine induced Th1 responses. In addition, PVX activated DCs to up-regulate the expression of IL-12, the cytokine that plays an important role in differentiation and expansion of Th1 cells. Collectively, PVX is able to strongly induce Th1 responses even when the vaccinations were performed in the Th2 biased BALB/c mice. This is in contrast to widely-used KLH-conjugated vaccine, which skews the immune response toward Th2 [257]. Hence PVX offers an effective alternative which can polarise the response to a vaccine toward Th1 as well as Th2 hence engaging a wider immune response.

Mice vaccinated with PVP without added adjuvant produced IgG antibody against Id and PVX. This result suggests that PVX has the ability to enhance immunity

(adjuvanticity) without addition of other adjuvant. This points toward its ability to activate DCs. *In vitro*, PVX did not activate bmDC as judged by unchanged surface markers, cytokines, chemokines and chemokine receptors expression. This is in contrast to the *in vivo* study where PVX appeared to bind to mouse splenic DCs and B cells as shown by FACS analysis as the Alexa<sup>®</sup> Fluor 647-labeled PVX was detected in the CD11c<sup>+</sup> cells and CD19<sup>+</sup> cells. More DC take it up hence more can activate T cells. The large percentage of B cells bound to PVX indicates that the binding was non-specific and why it is so remains unclear at present. The PVX uptake was accompanied by DC and B cell activation as determined by up-regulation of the activation markers. PVX was able to up-regulate expression of the examined activation markers (CCR7, CD40, CD80, CD86 and I-A/I-E) in all 3 DC CD11c<sup>+</sup> subsets with the only exception that the virus did not induce up-regulation of CD80 in CD8<sup>+</sup> subset. These data combined with mixed IgG isotypes induced by the PVP vaccine further suggest that PVX induces both Th1 and Th2 responses since the CD8<sup>+</sup> DCs induce Th1 response and the CD4<sup>+</sup> DCs induce Th2 response. The finding that PVX did not up-regulate CD80 in CD8<sup>+</sup> DCs was similar to the study on vaccinia virus (VACV) where VACV infected CD8<sup>+</sup> DC predominantly expressed CD86 but CD80 was minimally induced and was not required for induction of cellular responses [258].

The reason why PVX did not activate DC *in vitro* but was able to induce DC activation *in vivo* is not identified so far. The explanation might be that *in vitro* DCs representing all DC subsets presented *in vivo* (for example pDC) cannot be generated from bone marrow in the presence of GM-CSF. *In vivo* CD11c<sup>+</sup> DCs activation by PVX may be modulated by other components of the immune system such as macrophages and NK cells. In addition, natural antibody may bind to PVX and enhances PVX uptake by phagocytes including DCs hence leading to DC activation.

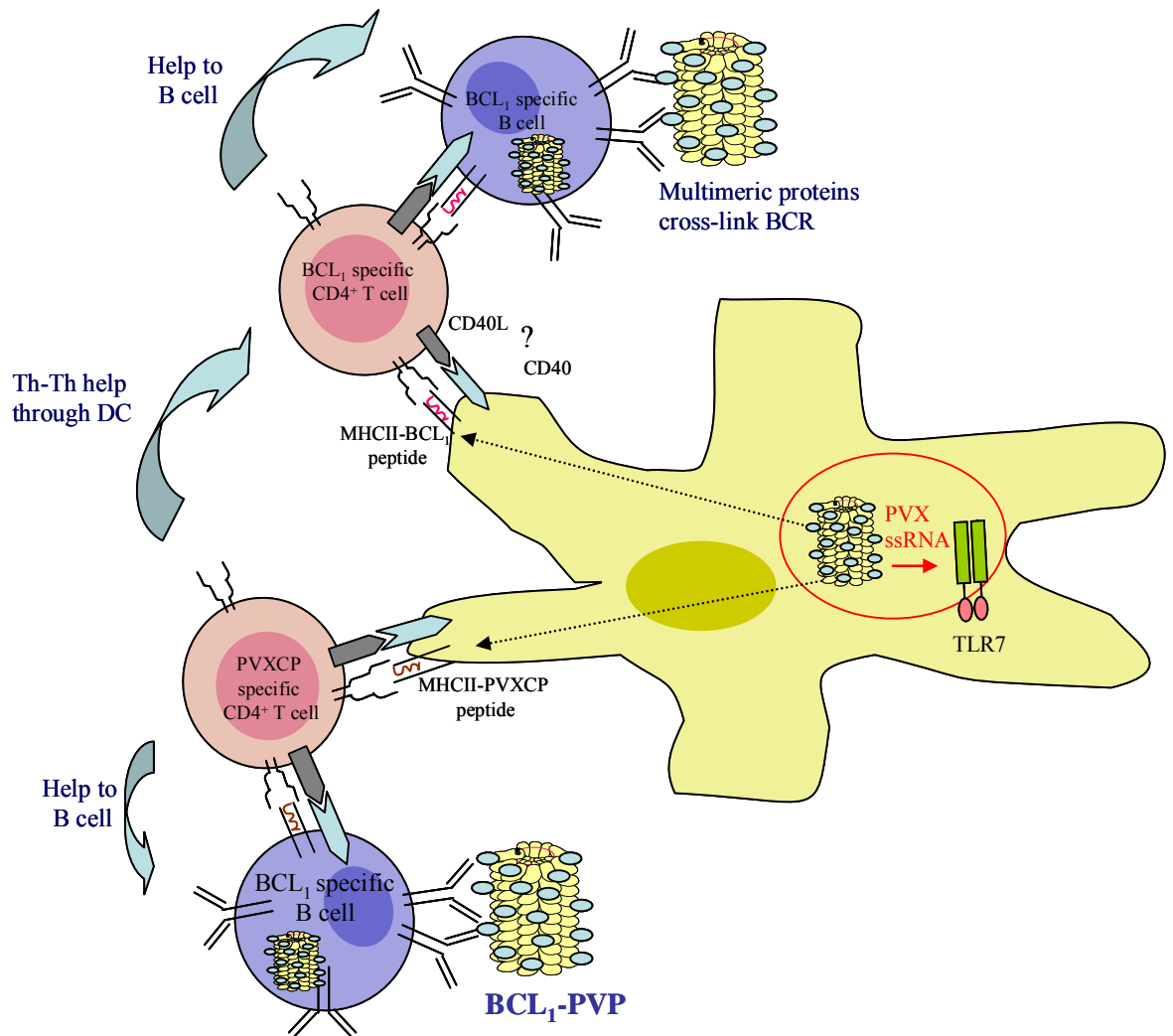


**Figure 4-22. Proposed mechanism of BCL<sub>1</sub>-PVP vaccine**

BCL<sub>1</sub>-PVP vaccine may be able to induce immune responses against BCL<sub>1</sub> lymphoma by three ways. The first mechanism is through T-cell help as provide by the fusion principle. Second, multimeric form of the fusion protein provides better BCR cross-linking thus better in B-cell activation. Finally, PVX RNA within the vaccine is able to activate DCs through TLR7 signalling.

## Chapter 5. Expression of PVX CVP vaccine in plants

### 5.1 Introduction

#### 5.1.1 Expression of CVP vaccine with genetically fused antigen on the surface

To date, there are no data using PVX to display tumour antigens, even though the virus has been used widely to display various sizes of peptides and proteins. Previously, chimeric PVX displaying microbial peptides of up to 38 amino acids [160, 170-171] or proteins ranging from 27 – 46 kDa have been successfully produced in plants [167-169]. While the production of PVX with a fused peptide is straightforward, the production of PVX with a large fused protein required the presence of free CP for viral particle assembly. Without unmodified CP the virion structure is unstable. This CP can be released when FMDV2A linker is inserted between the protein of interest and the CP sequences. The CVPs displaying microbial peptides were shown to be able to induce antibodies in animal model [160, 170]. However, the immunogenicity of CVP displaying a large antigen has not been studied.

Another plant virus, TMV displaying T-cell epitope was produced in plants and was shown to induce specific immune responses in a mouse model [151]. Mice vaccinated with the TMV displaying SIINFEKL ovalbumin (Ova) peptide, in combination with CpG, produced peptide specific IFN- $\gamma$  secreting cells resulting in protection from EG.7-Ova tumour challenge [151]. In addition, TMV was further used to display the p15e B16 murine melanoma epitope and the CVP provided protection against the tumour [151].

#### 5.1.2 pgR107 vector

Expression vector pgR107 (GenBank: AY297842.1) is a Ti vector based on the pGreen vector. The vector provides benefits of *A. tumefaciens* Ti plasmid to transfer the gene of interest to the plant genome [259]. Vector pgR107 contains the PVX genome in place of the T-DNA between the RB and LB, a strong constitutive 35S-promoter driving the synthesis of a PVX infectious transcript in plants, and the kanamycin resistant gene as a selection marker (figure 5-1). *In vitro* recombinant pgR107 can be manipulated in *E. coli* and the recombinant plasmid is transferred by electroporation into *Agrobacterium* GV3101 strain, or other suitable strain, containing a helper plasmid bearing *vir* genes and another plasmid bearing *repA* gene necessary for pgR107 replication.

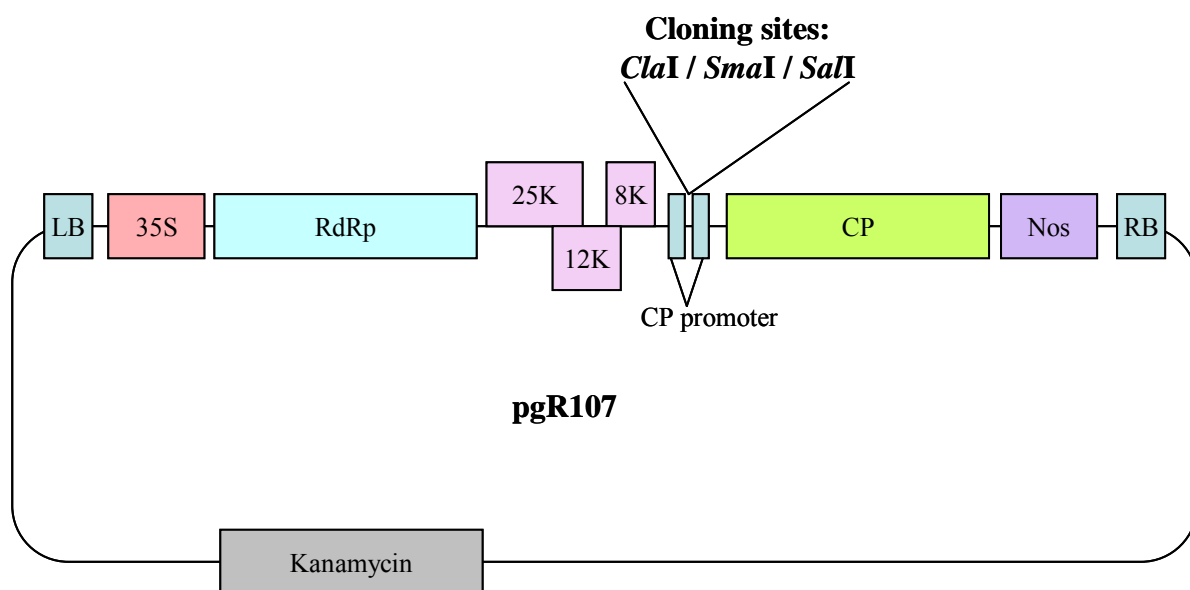


**Figure 5-1. Schematic diagram of pgR107 vector**

LB and RB represent left and right border of *Agrobacterium* T-DNA, respectively. *35S*: the 35S RNA promoter; *RdRp*: the virus RNA-dependent RNA polymerase gene; *25 K*, *12 K* and *8K*: Movement protein genes; *CP*: the PVX coat protein gene; *Nos*: the transcriptional terminator of the nopaline synthase gene of *Agrobacterium tumefaciens*.

### **5.1.3 PVX infection by pgR107**

The *Agrobacterium* containing pgR107 vector is used to inoculate *N. benthamiana* host plants. The PVX nucleic acid with the fused foreign gene is transferred to the plant nucleus and integrated into the plant genome. The DNA transfer mediated by *Agrobacterium* is described in details previously in chapter 3. The virus genes are replicated and expressed by the host cell nuclear transcription and subsequent processing machinery [260]. This process alters the host cell's metabolism resulting in biochemical and physiological changes. Alterations in the infected host plant start in the inoculated cells, spread to the surrounding tissues and may finally affect the whole plant [246]. If a virus is not confined to the site of inoculation, it will spread from cell to cell within the leaf (local infection). Eventually the virus may reach the vascular system, usually the phloem, and spread through the entire plant, this causes the so-called systemic infection. The infection symptoms include reduction in plant size, discolouration and necrosis of the infected tissue [246].

Similar symptoms have been observed during infections with CVP with attached epitopes or larger fragments.

### **5.1.4 Aims**

In this section, the aim of the project is to determine the feasibility of expression of the PVX CVP displaying BCL<sub>1</sub> Id scFv of BCL<sub>1</sub> lymphoma in plants. The CVP is expected to assemble in plants and be able to purify from the plant tissue.

### **5.1.5 Hypotheses**

1. The PVX CVP vaccine with genetically fused scFv.BCL<sub>1</sub> can be produced in plants.
2. The CVPs can be purified using established PVX purification method.

## 5.2. Results

### 5.2.1 Construction of BCL<sub>1</sub>2APVX

In order to produce assembled PVX particles displaying the 28 kDa BCL<sub>1</sub> scFv, insertion of FMDV2A between scFv and PVXCP sequence was required to produce a mixed population of fusion proteins and free CPs (figure 5-2). The FMDV2A-PVXCP was amplified by PCR and replaced PVXCP sequence of pcDNA3.scFv.BCL<sub>1</sub>-PVXCP, resulting in pcDNA3.scFv.BCL<sub>1</sub>-2A-PVXCP. The new constructed plasmid was transformed into *E.coli*, positive scFv.BCL<sub>1</sub>-2A-PVXCP clones were screened by PCR using cloning primers (figure 5-3A.) and subjected to DNA sequence analysis. The correct gene in pcDNA3 was used for subcloning into pgR107 vector. The PCR colony screening showed clones with the correct insert size of 1.5 kb (figure 5- 3B.). The PCR screened clone with the correct sequence confirmed by DNA sequencing analysis was further transferred to *Agrobacterium* for subsequent plant infiltration.

### 5.2.2 *In vitro* transcription/translation (IVTT)

The functionality of FMDV2A was initially tested by IVTT. Apart of the production of the fusion protein, the presence of FMDV2A sequence between the two protein sequences would provide other 2 protein fragments; one is the fragment upstream of 2A sequence fused with 2A, and another is the fragment downstream of 2A [166-167, 261]. Therefore, scFv.BCL<sub>1</sub>-2A-PVXCP sequence was expected to generate 3 protein fragments, 50 kDa fusion protein, 28 kDa fragment of scFv.BCL<sub>1</sub>-2A and 25 kDa CP. The result of pcDNA3.scFv.BCL<sub>1</sub>-2A-PVXCP IVTT showed 2 protein fragments (figure 5-4). The larger product size corresponded to the predicted molecular weight of BCL<sub>1</sub>2APVX fusion protein. The other IVTT product was approximately 30 kDa which could result from a pool of scFv.BCL<sub>1</sub>-2A and CP fragments migrating to the same position on the gel. The proportion of the small fragment was higher than that of the large protein. Collectively, the FMDV2A was functional in the context of the fusion protein. The pcDNA3.5T33PVX and pcDNA3.scFv.BCL<sub>1</sub>-PVXCP were used as positive controls for IVTT and the expected fusion proteins size of 50 kDa were observed for both plasmids with some fainter bands present. The fusion protein product from scFv.BCL<sub>1</sub>-2A-PVXCP construct was slightly larger than the protein produced from the scFv.BCL<sub>1</sub>-PVXCP construct as expected, because of the addition of the 2A sequence. The IVTT reaction without addition of a plasmid template was utilized as a negative control with no protein products observed as expected.

### **5.2.3 scFv.BCL<sub>1</sub>-2A-PVXCP expression in Cos-7 cells**

The expression of the scFv.BCL<sub>1</sub>-2A-PVXCP fusion protein was initially evaluated in Cos-7 cell. Cos-7 cells were transfected with pcDNA3.scFv.BCL<sub>1</sub>-2A-PVXCP, in parallel with pcDNA3.FrC or pcDNA3.scFv.BCL<sub>1</sub>-PVXCP as controls. After 48 hours, intracellular and secreted proteins were analyzed by Western blot analysis with anti-PVXCP mouse antiserum. The scFv.BCL<sub>1</sub>-2A-PVXCP fusion proteins from both PVXCP constructs were detected in both cell lysates and culture media. As expected, the fusion protein from pcDNA3.scFv.BCL<sub>1</sub>-2A-PVXCP was slightly larger than that of pcDNA3.scFv.BCL<sub>1</sub>-PVXCP as a result of the insertion of the FMDV2A sequence (figure 5-5). Proteins in culture medium appeared to be larger than protein inside the cells. This might be caused by higher levels of glycosylation of secreted proteins than that of immature proteins inside the cells. For pcDNA3.scFv.BCL<sub>1</sub>-2A-PVXCP construct, the expected 25 kDa PVXCP protein released because of FMDV2A sequence presence was not detected. Proteins extracted from pcDNA3.FrC transfected cells were used as a negative control for Western blot analysis and they did not react with anti-PVXCP antibody as expected.

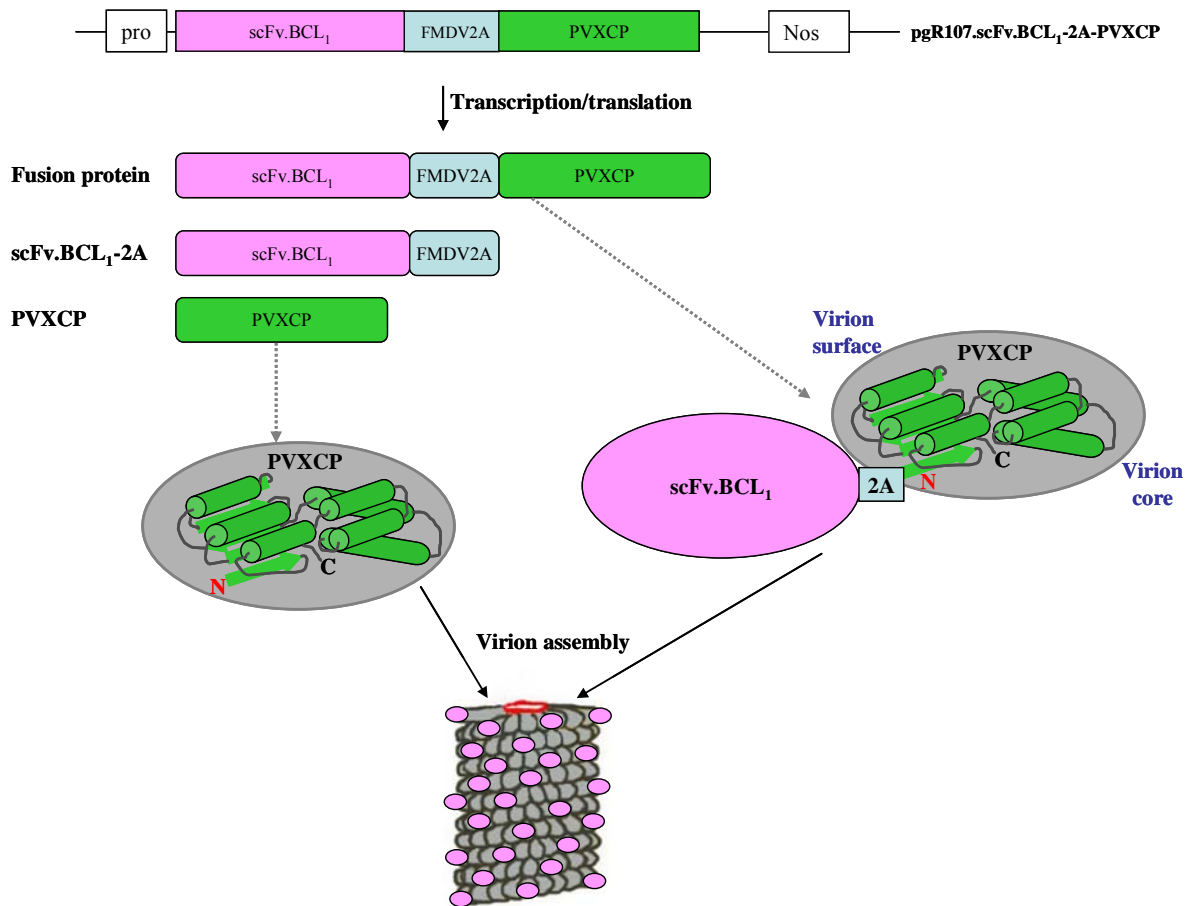


**Figure 5-2. Construction of BCL<sub>1</sub>2APVX**

In order to produce assembled BCL<sub>1</sub>2APVX, FMDV2A was inserted between scFV.BCL<sub>1</sub> C-terminus and PVXCP N-terminus. FMDV2A mediates production of mixed population of fusion proteins and free PVXCPs which is required for virion assembly. After transcription, scFV.BCL<sub>1</sub>-FMDV2A-PVXCP mRNAs undergo translation with three protein populations produced by FMDV2A function; scFV.BCL<sub>1</sub>-FMDV2A-PVXCP (fusion protein), scFV.BCL<sub>1</sub>-FMDV2A and free PVXCPs. In plants, scFV.BCL<sub>1</sub>-FMDV2A-PVXCPs and PVXCPs together with PVX RNA assemble into virus particle. As N-terminus of PVXCP is on the virion surface, fused scFv.BCL<sub>1</sub> is displayed on the CVP surface.

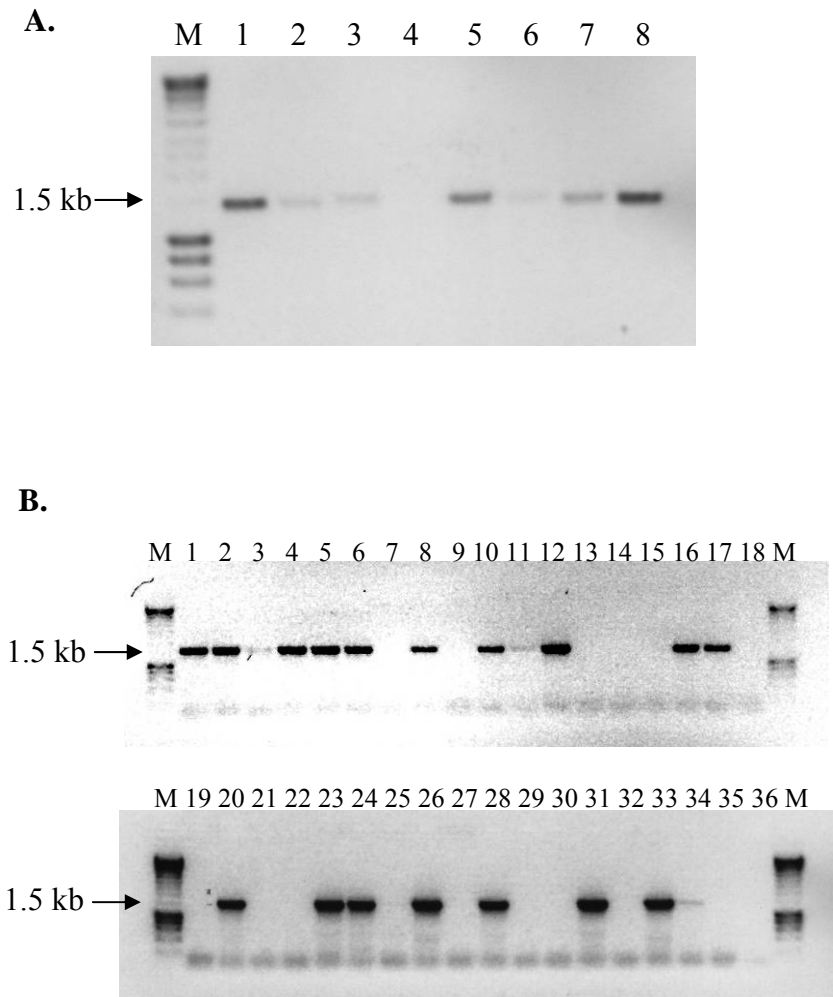


**Figure 5-3. PCR screening for scFv.BCL<sub>1</sub>-2A-PVXCP positive clones**

Positive bacterial colonies containing pcDNA3.scFv.BCL<sub>1</sub>-2A-PVXCP (A.) or pgR107.scFv.BCL<sub>1</sub>-2A-PVXCP (B.) were PCR screened using the cloning primers. Numbers represent each colony screened by PCR. The expected insert size is 1.5 kb.

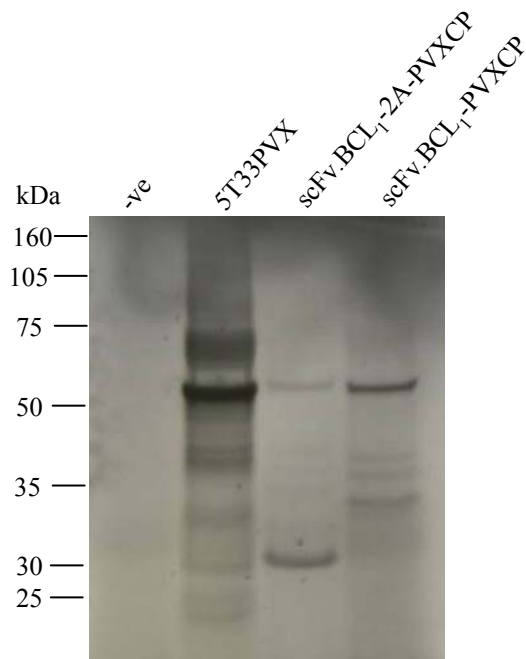


**Figure 5-4. *In vitro* transcription/translation (IVTT) of pcDNA3.scFv.BCL<sub>1</sub>-2A-PVXCP**

pcDNA3.scFv.BCL<sub>1</sub>-2A-PVXCP was transcribed and translated *in vitro* and compared with no-plasmid negative control (-ve), pcDNA3.5T33PVX and pcDNA3.scFv.BCL<sub>1</sub>-PVXCP. Protein size markers are indicated.

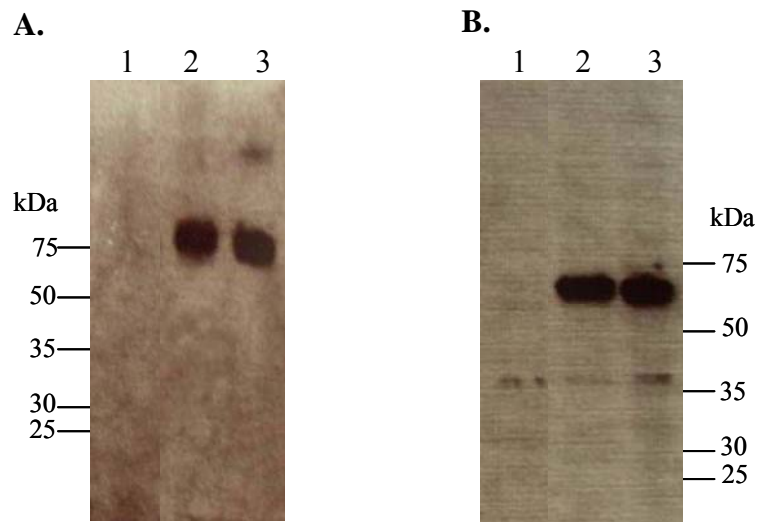


**Figure 5-5. Western blot analysis of transfected Cos-7 cells**

Cos-7 cells were transfected with pcDNA3.FrC (1), pcDNA3.scFv.BCL<sub>1</sub>-2A-PVXCP (2), or pcDNA3.scFv.BCL<sub>1</sub>-PVXCP (3). The proteins secreted into the medium (A.) or remained inside the cells (B.) were analysed by Western blot analysis with anti-PVXCP mouse antiserum. The protein size markers are indicated.

## 5.2.4 Propagation of BCL<sub>1</sub>2APVX in plants

### 5.2.4.1 BCL<sub>1</sub>2APVX infection

After scFv.BCL<sub>1</sub>-2A-PVXCP fusion protein expression was evaluated by IVTT and in Cos-7 cells, the scFv.BCL<sub>1</sub>-2A-PVXCP sequence was then transferred to *N. benthamiana* host plants by infiltration with *Agrobacterium* containing pgR107.scFv.BCL<sub>1</sub>-2A-PVXCP. The CVP resulted from pgR107.scFv.BCL<sub>1</sub>-2A-PVXCP vector is called BCL<sub>1</sub>2APVX from now on. The ability of BCL<sub>1</sub>2APVX to infect the host plant was monitored by observing the symptoms of viral infection in comparison with wild-type PVX infection of pgR107 agroinfiltrated plants. Eight days post-infiltration (p.i.) both pgR107.scFv.BCL<sub>1</sub>-2A-PVXCP and pgR107 infiltrated plants showed primary systemic symptoms (the symptoms initially appear on the non-infiltrated tissues) such as leaf mottling and growth retardation in comparison with the control healthy plants (figure 5-6 and 5-7), indicating that BCL<sub>1</sub>2APVX was able to move both locally and systemically. At this stage, the symptoms of BCL<sub>1</sub>2APVX infection were milder than that of the wild-type infection. However, at 20 days p.i., all the leaves of pgR107.scFv.BCL<sub>1</sub>-2A-PVXCP infiltrated plants were infected, while the pgR107 infiltrated plants had some symptom-free leaves (figure 5-8). In addition, at this stage the recombinant virus appeared to have damaged the infected tissue more than the wild-type virus did.

The presence of the recombinant viral RNA in the infected tissue was assessed by RT-PCR using the cloning primers. The fusion gene was detected in all BCL<sub>1</sub>2APVX infected tissue, i.e. the infiltrated leaf; the primary and the secondary systemic infected leaf (figure 5-9). As expected, RNA extracted from a healthy plant or pgR107 infected tissue was not amplified by these primers (figure 5-9). The RT reaction without the reverse transcriptase enzyme was carried out as a control for DNA contamination and the result showed no amplified product from this control (figure 5-9). In order to confirm the correct scFv.BCL<sub>1</sub> sequence in the CVP, the RNA from 2 weeks p.i. systemically infected tissue was amplified using pgR107seqf and PVX REV primers (table 2-1). This primers pair amplifies the fragment starting from 100 bp upstream of BCL<sub>1</sub>. This PCR product was subjected to DNA sequence analysis and the correct BCL<sub>1</sub> sequence was confirmed, demonstrating that the correct scFv.BCL<sub>1</sub> sequence was maintained during infection.

The expression of the scFv.BCL<sub>1</sub>-2A-PVXCP at protein level was subsequently confirmed by Western blot analysis with anti-PVXCP mouse antiserum. In BCL<sub>1</sub>2APVX infected plants, both fusion scFv.BCL<sub>1</sub>-2A-PVXCP and free PVXCP were detected in both an infiltrated leaf and a systemically infected leaf as expected (figure 5-10). Free CP from the BCL<sub>1</sub>2APVX infected tissue migrated to the same position as CP from the wild-type infected tissue. In addition, protein of 40 kDa also reacted with the antibody. This protein

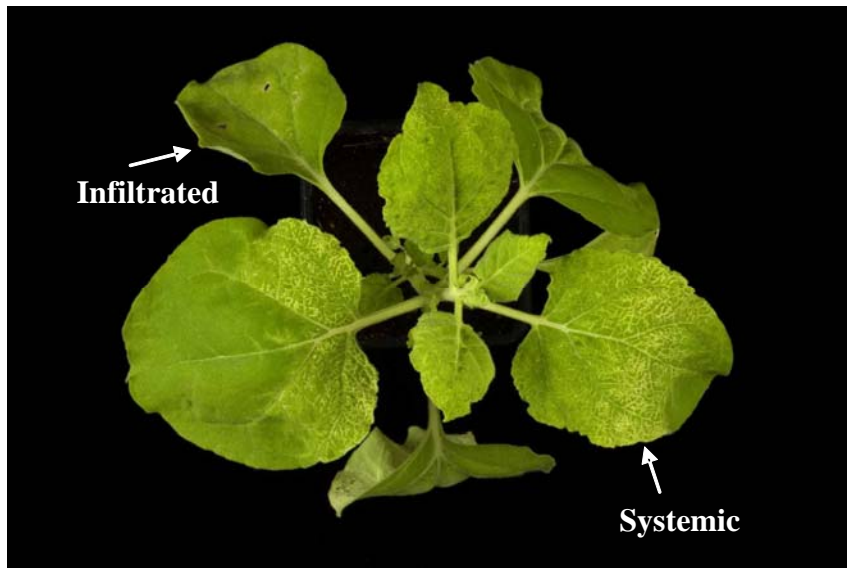
may be a degraded product of the fusion protein. Protein extracted from a healthy plant was used as a negative control and it did not react to the antibody. Taken together the results of sequencing and Western blot analysis demonstrated that BCL<sub>1</sub>2APVX was present in all infected tissues and therefore the infected tissues were further subjected to virus purification.



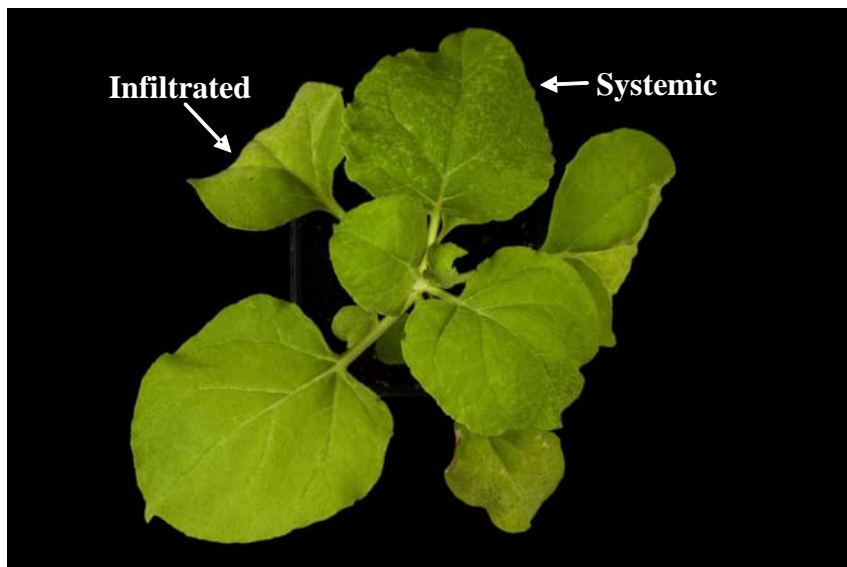
**Figure 5-6. Symptoms of plants inoculated with either pgR107 or pgR107.scFv.BCL<sub>1</sub>-2A-PVXCP**

As observed on day 8 and day 20 post inoculation (p.i.), pgR107 inoculated plant (PVX) and pgR107.scFv.BCL<sub>1</sub>-2A-PVXCP inoculated plant (BCL<sub>1</sub>2APVX) showed growth retardation compare to a healthy non-infected plant (WT).

**8 DAYS**



**PVX**



**BCL<sub>1</sub>2APVX**

**Figure 5-7. Symptoms of plants inoculated with either pgR107 or pgR107.scFv.BCL<sub>1</sub>-2A-PVXCP on day 8 post inoculation**

On day 8 p.i pgR107 (PVX) and pgR107.scFv.BCL<sub>1</sub>-2A-PVXCP (BCL<sub>1</sub>2APVX) inoculated plants showed systemic infection at the upper leaves

20 DAYS



PVX



BCL<sub>1</sub>2APVX

**Figure 5-8. Symptoms of plants inoculated with either pgR107 or pgR107.scFv.BCL<sub>1</sub>-2A-PVXCP on day 20 post inoculation**

On day 20 p.i. both pgR107 (PVX) and pgR107.scFv.BCL<sub>1</sub>-2A-PVXCP (BCL<sub>1</sub>2APVX) inoculated plants showed secondary systemic infection in which pgR107 inoculated plant had some symptom-free leaves.

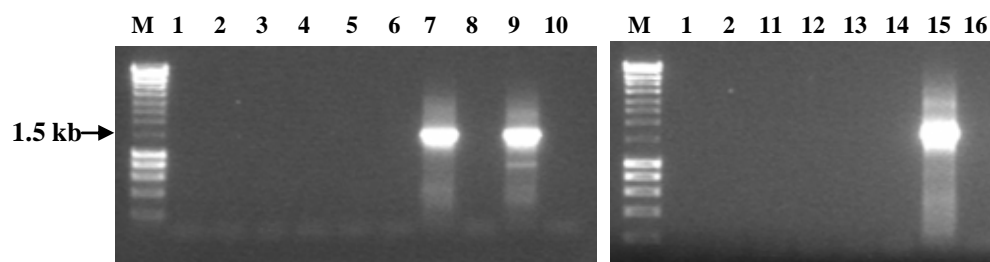


**Figure 5-9. RT-PCR detection of BCL<sub>1</sub>-2A-PVXCP in infected leaves**

RNA was extracted from a healthy leaf (lane 1 and 2); pgR107 infiltrated leaf (lane 3 and 4), primary systemic infected leaf (lane 5 and 6), no symptom leaf (lane 11 and 12), secondary systemic infected leaf (lane 13 and 14); pgR107.scFv.BCL<sub>1</sub>-2A-PVXCP infiltrated leaf (lane 7 and 8), primary systemic infected leaf (lane 9 and 10), and secondary systemic infected leaf (lane 15 and 16). The extracted RNA was amplified by RT-PCR using cloning primers. In each RNA samples, the RT reaction without reverse transcriptase control was carried out (lane 2, 4, 6, 8, 10, 12, 14, and 16).

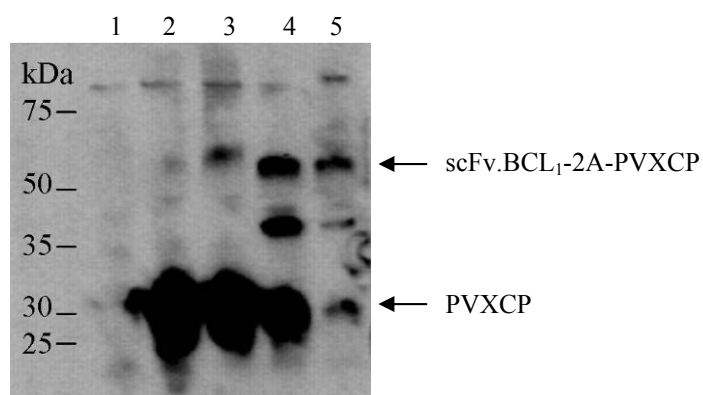


**Figure 5-10. Western blot analysis of PVXCP**

Total protein extracts from healthy leaf (lane 1), pgR107 infiltrated leaf (lane 2), PVX systemic infected leaf (lane 3), pgR107.scFv.BCL<sub>1</sub>-2A-PVXCP infiltrated leaf (lane 4), and BCL<sub>1</sub>2APVX systemic infected leaf (lane 5) were separated on 4-12% gradient NuPage gel and transferred to PVDF membrane. The membrane was probed with anti-PVXCP mouse antiserum. Protein size markers are indicated.

#### 5.2.4.2 BCL<sub>1</sub>2APVX purification

BCL<sub>1</sub>2APVX was purified from 2 weeks p.i. infected leaves. At the beginning, the CVP was purified using the established double-PEG precipitation method for the wild-type PVX purification. Briefly, the virus was extracted with NaBr buffer and clarified with chloroform before precipitation with PEG and NaCl. The pellet was resuspended in NaBr buffer and the insoluble material was eliminated by centrifugation. The virus was precipitated again with PEG and subsequently solubilized in NaBr buffer. However, neither spectrophotometry nor Western blot analysis showed the presence of viral particles in the pellet.

In another purification experiment, the presence of CVPs in the pellets or supernatants during the purification process (figure 5-11) was investigated by Western blot analysis with anti-PVXCP mouse antiserum to determine where CVPs were lost. Neither PVXCP nor the fusion protein was detected in the pellet of chloroform clarification step (figure 5-12A, lane 3B). After PEG precipitation, the remaining supernatant (figure 5-12A, lane 5A) did not contain the proteins, suggesting that CVPs were not lost at this stage. Pellet of PEG precipitation was solubilized in NaBr buffer and subsequently the insoluble protein was eliminated by centrifugation. The clarified supernatant was expected to contain high amount of soluble CVP for further purified by second-PEG precipitation. However, the supernatant contained a small amount of the fusion protein and CP (figure 5-12A, lane 7A) while the large amount of the proteins was found in the clarified pellet (figure 5-12A, lane 7B). The pellet contained large amount of plant proteins as observed by Coomassie-stained SDS-PAGE (figure 5-12B, lane 7B). Since the low amount of CVPs remained in the clarified supernatant, subsequent PEG precipitation resulted in low amount of purified CVPs (figure 5-12A, lane 9B). Therefore, it appeared that CVPs could not be purified by the conventional method as it was poorly solubilized and co-precipitated with the plant proteins after the first PEG precipitation.

The purification method was then modified in several ways. Initially, in order to improve solubility of the CVPs in the PEG-precipitated suspension, 1-2 % Triton X-100 or 1-2%  $\beta$ -mercaptoethanol was added. However, addition of these chemicals did not result in successful CVP solubilisation, as a large amount of CVPs was still detected in the clarified pellet.

Since CVPs were co-precipitated with plant proteins when the resuspended PEG precipitation product was clarified by centrifugation, this clarification step was then skipped and CVPs were further purified by ultracentrifugation (UC) or another round of PEG precipitation. The presence of CVP in pellets and supernatants during purification processes (figure 5-13) was detected by Western blot analysis with anti-PVXCP mouse antiserum.

The CVPs were detected in the extract of infected tissue (figure 5-14A, lane 1) and in the chloroform-clarified solution (figure 5-14A, lane 3A). CVPs were precipitated with PEG and then resuspended in half the starting extract volume of NaBr buffer. Post PEG precipitation the remaining solution did not contain CVP (figure 5-14A, lane 5A). CVP proteins were detected in the resuspended PEG pellet (figure 5-14A, lane 5B) and the resuspended PEG-precipitation product was further purified by ultracentrifugation (UC) through a 30% sucrose cushion or via another round of PEG precipitation. Following UC, both the fusion protein and PVXCP were detected in the resuspended UC pellet (figure 5-14A, lane 7B) but not in the remaining supernatant (figure 5-14A, lane 7A). In contrast, from the same starting material, only the fusion protein was detected in the second PEG precipitation product (figure 5-14A, lane 9D) with the remaining solution not containing the proteins (figure 5-14A, lane 9C). From Coomassie-stained SDS-PAGE, most of plant endogenous proteins were eliminated by UC (figure 5-14B, lane 7B) and second PEG (figure 5-14B, lane 9D).

Transmission electron microscopy (TEM) was employed to assess the structural integrity of the purified viral particles. TEM imaging showed that only the UC-purified product contained viral particles (figure 5-15). The CVP structure was similar to that of PVX wild-type. In addition, the CVP contained scFv.BCL<sub>1</sub> on its surface as it was detected by gold- labeled anti-BCL<sub>1</sub> mouse antiserum. In contrast, the wild-type PVX was not labelled by immunogold as it did not react with the antibody. Although some assembled viral particles were found, the most of the UC product was large aggregate. Only large aggregates and no CVPs were observed in the second PEG-purified product (figure 5-15).

Occasionally, a large amount of viral particles was obtained from the double PEG precipitation method, but the particles incorporated only PVXCP with no fusion protein present (figure 5-16). Therefore, the anti-BCL<sub>1</sub> antibody affinity chromatography for BCL<sub>1</sub>2APVX purification was employed to isolate only BCL<sub>1</sub> scFv bearing particles. After affinity chromatography, both fusion protein and CP were detected, by Western blot analysis using anti-PVXCP mouse antiserum, in the purified product (figure 5-17A) with most of plant endogenous proteins were eliminated as observed by Coomassie-stained SDS-PAGE (figure 5-17B). By observation using TEM, the purified sample contained mostly aggregates with appearance of some CVPs (figure 5-17C). Taken together with the TEM observation of UC and PEG purified product, low amount of CVPs could be purified from the infected plant tissue.

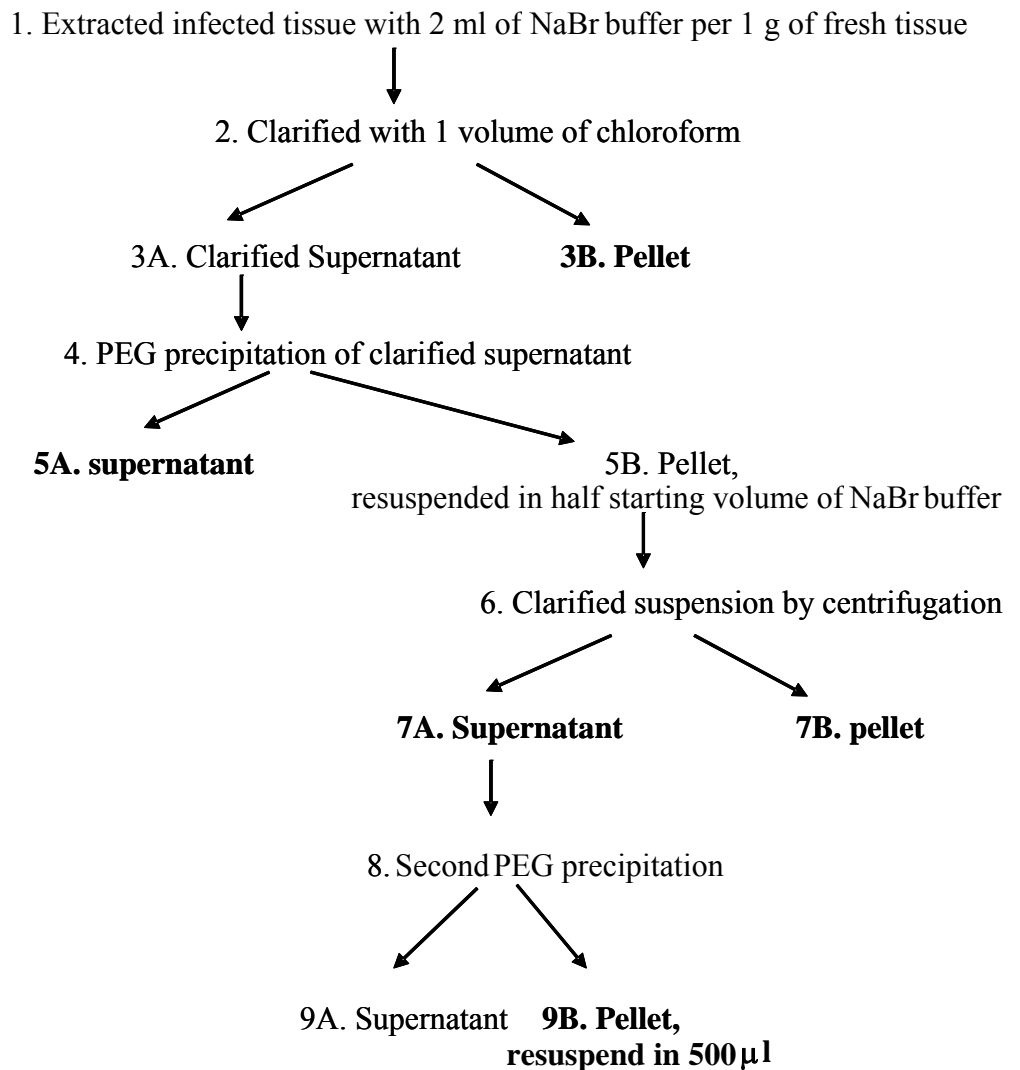


**Figure 5-11. Diagram of PVX purification method**

Initially, BCL<sub>1</sub>2APVX purification was carried out following the established PVX purification method. Some pellets or supernatants (in bold characters) were analyzed by Western blot analysis as shown in figure 5-12.

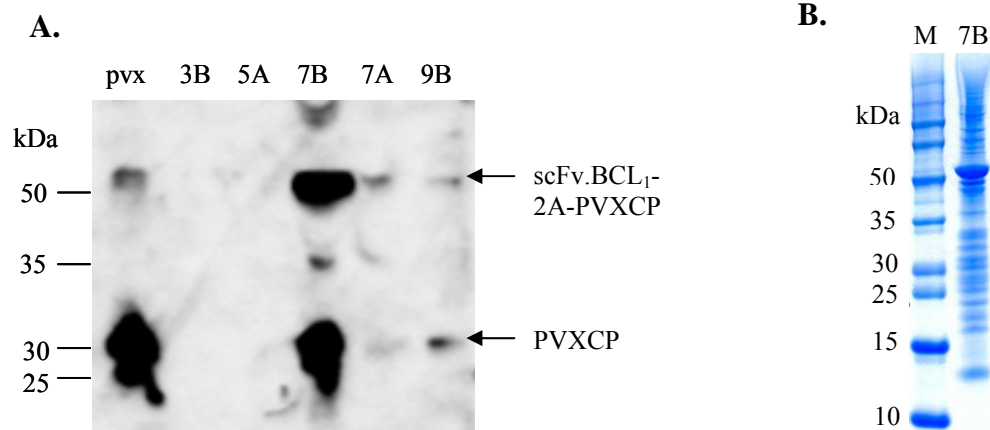


**Figure 5-12. Detection of BCL<sub>1</sub>2APVX in various samples obtained from established purification method**

BCL<sub>1</sub>2APVX was purified by using an established method for wild-type PVX purification as in the diagram shown in figure 5-11. The pellets and supernatants in some steps were analyzed by Western blot analysis using anti-PVXCP mouse antiserum (A.). The samples were the pellet of chloroform clarification (lane 3B), the supernatant of first PEG precipitation (lane 5A), the pellet of first PEG-precipitated suspension clarification (lane 7B), a clarified supernatant (lane 7A), and a resuspended final PEG precipitate (lane 9B). Wild-type PVX was used as a positive control for Western blot. The pellet of clarification step after first PEG precipitation (7B) was further analyzed by Coomassie-stained SDS-PAGE (B.). Protein size markers are indicated.

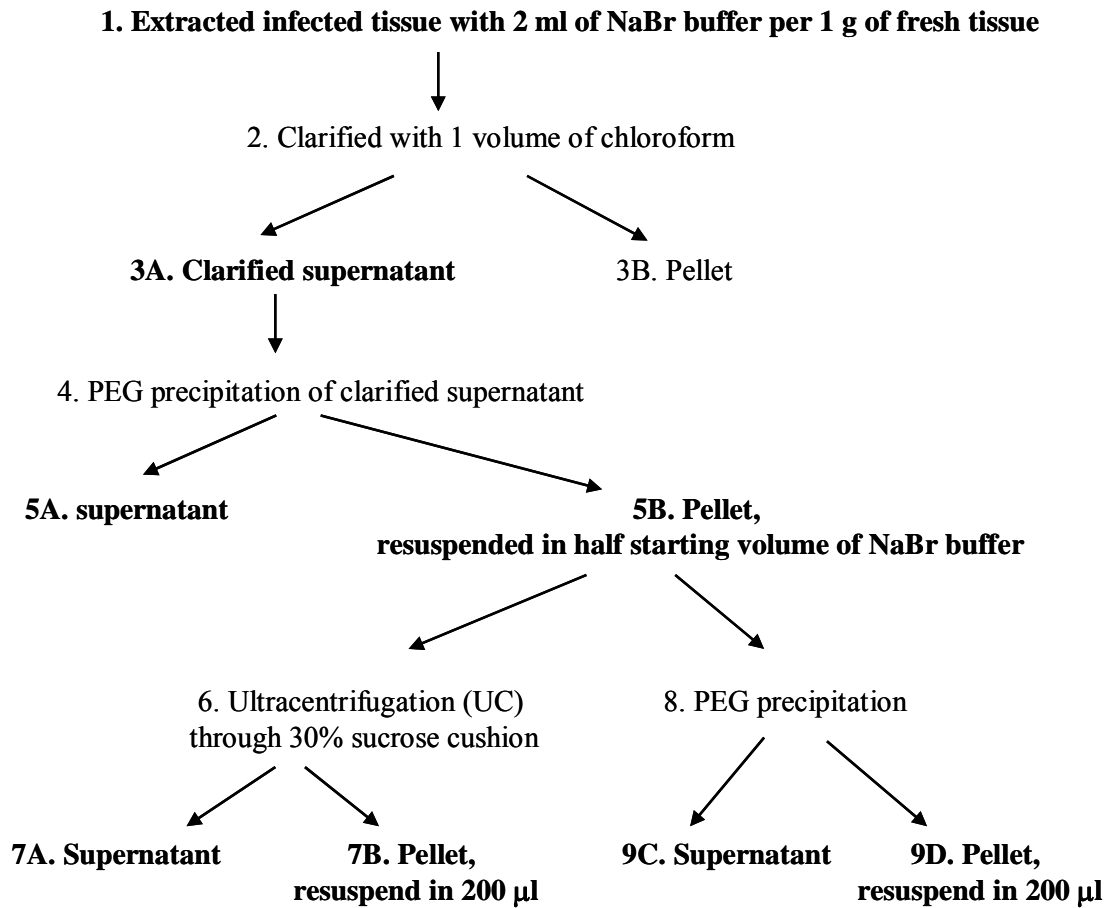


**Figure 5-13. Diagram of modified BCL<sub>1</sub>2APVX purification method**

BCL<sub>1</sub>2APVX purification method was modified from the established PVX purification protocol. Some of pellets or supernatants (in bold characters) were analyzed by Western blot analysis as shown in figure 5-14.

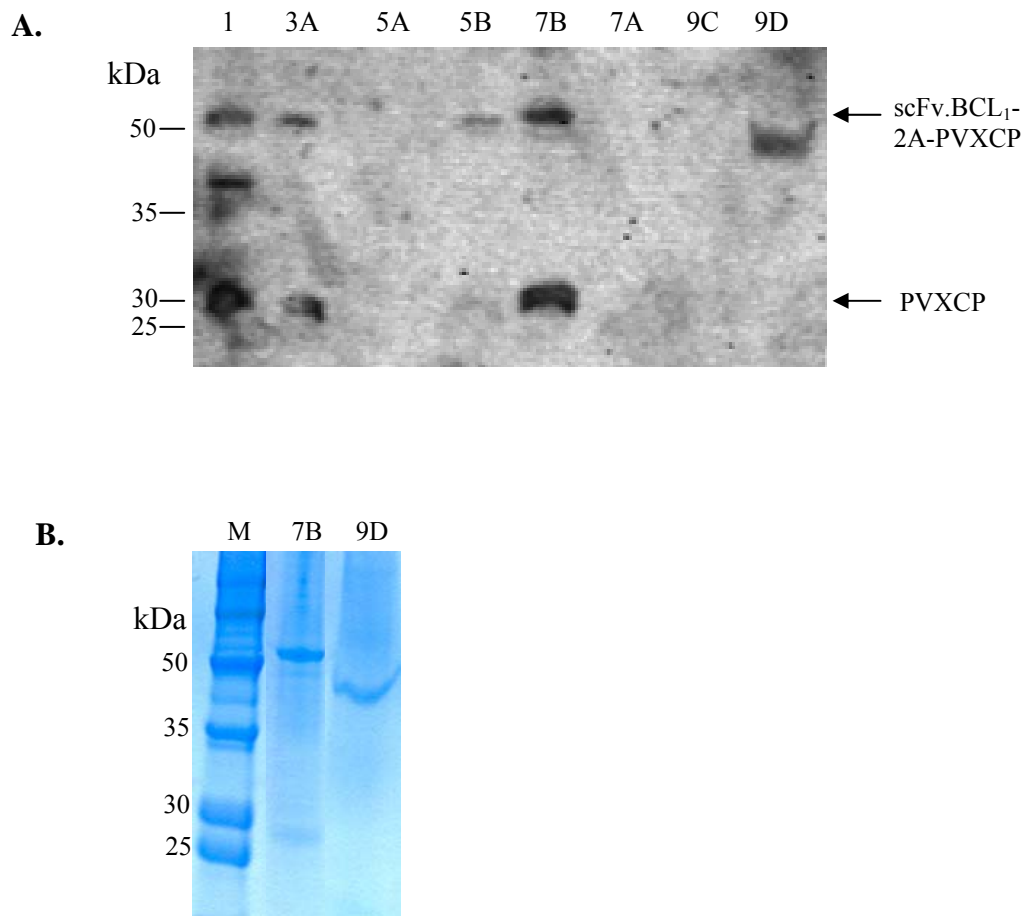


**Figure 5-14. Detection of BCL<sub>1</sub>2APVX in various samples obtained from modified purification method**

BCL<sub>1</sub>2APVX was purified using the method modified from the established protocol as the diagram shown in figure 5-13. The pellets and supernatants in some steps were analyzed by Western blot analysis using anti-PVXCP mouse antiserum (A.). The samples were infected tissue extract (lane 1), clarified supernatant (lane 3A), the supernatant of the first PEG precipitation (lane 5A), the first PEG-precipitated suspension (lane 5B), the supernatant of UC (lane 7A), resuspended UC pellet (lane 7B), supernatant of final PEG precipitation (lane 9C), and resuspended final PEG precipitate (lane 9B). The virus purified by UC (7B) or PEG precipitation (9D) was further analyzed by Coomassie-stained SDS-PAGE (B.). Protein size markers are indicated.

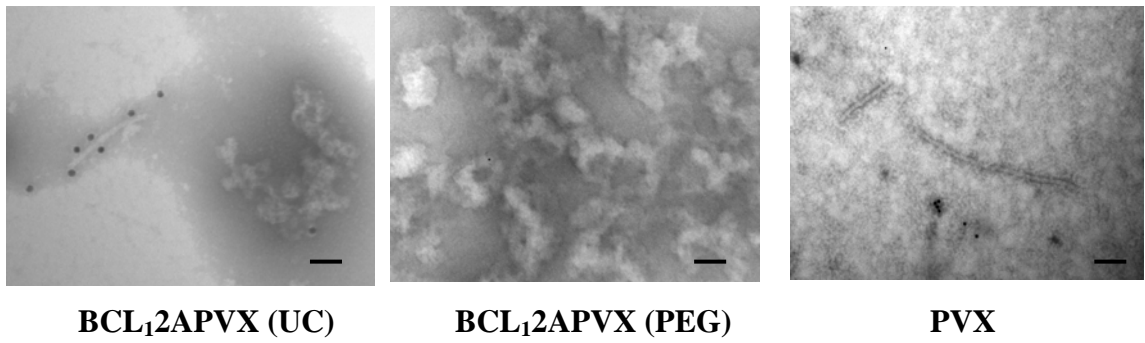


**Figure 5-15. TEM images of purified products**

After purification of BCL<sub>1</sub>2APVX by UC or PEG, the purified product was analysed by TEM in comparison with the wild-type PVX. BCL<sub>1</sub> scFv was probed with anti-BCL<sub>1</sub> mouse antiserum and detected with gold-conjugated anti-mouse IgG. The scale bar is 100 nm.

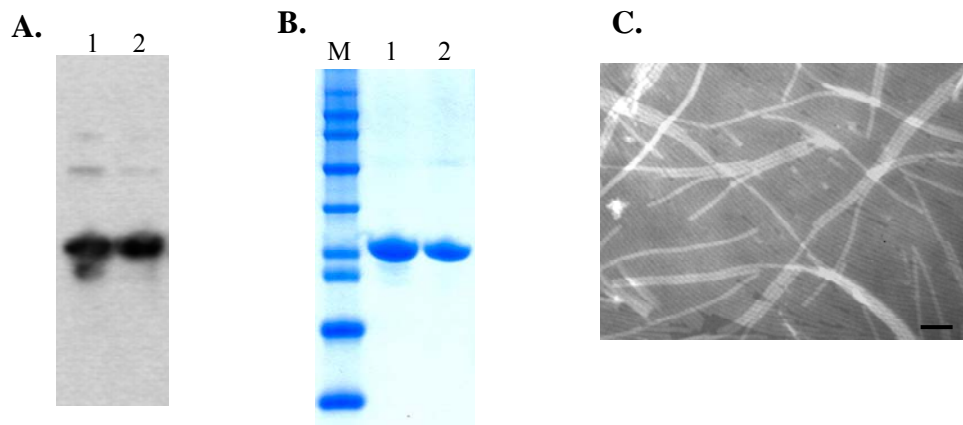


**Figure 5-16. Virus particles purified from pgR107.scFv.BCL<sub>1</sub>-2A-PVXCP infected plants incorporated free CPs**

Virus particles (lane 2) purified from pgR107.scFv.BCL<sub>1</sub>-2A-PVXCP infected plant was analyzed by Western blot with anti-PVXCP mouse antiserum (A.) and Coomassie-stained SDS-PAGE (B.) in comparison with wild-type PVX (lane 1). The virus particles were observed using TEM (C), the scale bar is 100 nm.

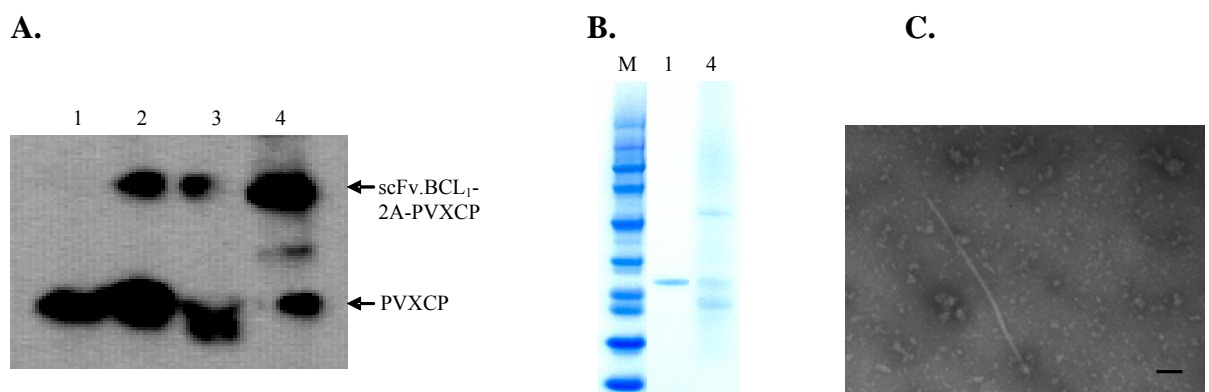


**Figure 5-17. BCL<sub>1</sub>2APVX purified by anti-BCL<sub>1</sub> antibody affinity chromatography**

The presence of BCL<sub>1</sub>2APVX was determined by Western blot analysis (A.) in plant extract (lane 2), clarified plant extract (lane 3), and anti-BCL<sub>1</sub> antibody affinity chromatography purified product (lane 4) in comparison with wild-type PVX (lane 1). The purified product was checked by protein gel electrophoresis (B.) and TEM (C.). In the TEM image (C.), the scale bar is 100 nm.

### 5.3 Summary

Initially, DNA construct for expression of PVX CVP displaying scFv.BCL<sub>1</sub> contained scFv.BCL<sub>1</sub> linked to FMDV2A followed with PVXCP sequence. The scFv.BCL<sub>1</sub>-2A-PVXCP fusion sequence was inserted into pcDNA3 and pgR107 for expression in mammalian cells and in plants, respectively. FMDV2A was included for production of scFv.BCL<sub>1</sub>-2A-PVXCP fusion proteins and free PVXCPs to enable assembly of the CVP. Expression of the fusion proteins was initially tested *in vitro* and in Cos-7 cells using pcDNA3.scFv.BCL<sub>1</sub>-2A-PVXCP. By the IVTT method, protein of the size scFv.BCL<sub>1</sub>-2A-PVXCP and another smaller protein band predicted to be a mixture of scFv.BCL<sub>1</sub> and PVXCP were detected. In Cos-7 cells, the fusion protein, but not free PVXCP, was detected by Western blot analysis with anti-PVXCP mouse antiserum.

As the fusion protein expression was confirmed by IVTT and Cos-7 cells, the fusion protein gene sequence was further introduced into plant expression system using pgR107 vector with scFv.BCL<sub>1</sub>-2A-PVXCP and agrobacterial gene transfer. Plants agroinfiltrated with pgR107.scFv.BCL<sub>1</sub>-2A-PVXCP exhibited symptoms of local and systemic viral infection, suggesting the production of CVP from the expression plasmid. Systemic infection by BCL<sub>1</sub>2APVX was slower than wild type PVX infection (from pgR107 agroinfiltration control) but once the infection was established the BCL<sub>1</sub>2APVX infection was more aggressive than PVX infection. The propagation of BCL<sub>1</sub>2APVX CVP in host plants was confirmed by RT-PCR and Western blot analysis; scFv.BCL<sub>1</sub>-2A-PVXCP RNA and protein were detected in both infiltrated and systemic infected tissue.

CVP was initially purified using the established double-PEG precipitation method for the wild-type PVX purification. However, the CVP could not be purified by this method. The CVP appeared to be poorly solubilised and co-precipitated with the plant proteins when the first PEG precipitation product was clarified by centrifugation. The presence of 1-2% of Triton-X 100 or  $\beta$ -mercaptoethanol in the buffer used to resuspend PEG precipitation product did not improve CVP solubility. As the CVP precipitated by centrifugation, the clarification of first PEG precipitation product was then skipped and the CVP was further purified by UC through 30% sucrose cushion or second PEG precipitation. Both UC and second PEG methods eliminated most of plant proteins. By UC method, both fusion protein and PVXCP were detected by SDS-PAGE and Western blot analysis. However, by second PEG method, only fusion protein was detected. Observation by TEM revealed that large protein aggregates were observed from samples purified by both UC and PEG and some virus particles were obtained from UC method but not from PEG method;. The CVP purified by UC contained scFv.BCL<sub>1</sub> on the surface as detected by gold-labeled anti-BCL<sub>1</sub> mouse antiserum.

A large amount of virus particles was obtained from double PEG precipitation method occasionally. However, the particles incorporated PVXCP only; the fusion protein was not detected in these particles. This observation resulted in turning to a purification method that would select only particles containing fusion protein. The anti-BCL<sub>1</sub> antibody affinity chromatography was therefore employed to serve this purpose. After affinity chromatography, both fusion protein and PVXCP were detected by Western blot analysis and most of plant proteins were eliminated as determined by SDS-PAGE. From TEM, the purified product composed of protein aggregates with some CVPs detected. Collectively, low amount of CVPs could be obtained from the infected plant tissue.

#### **5.4 Discussion**

BCL<sub>1</sub> scFv is a large polypeptide with a size comparable to PVXCP. It was shown that the proteins of 27-46 kDa fused to PVXCP would successfully assemble into viral particles in the presence of some free PVXCPs [167-169]. The FMDV2A linker was therefore inserted between BCL<sub>1</sub> scFv and PVXCP sequence with the aim of producing scFv.BCL<sub>1</sub>-2A-PVXCP fusion proteins and free PVXCPs. To evaluate that the FMDV2A linker will not compromise the structural integrity of both components and to evaluate its functionality, the linker was initially used in a DNA construct and compared with previously available scFv.BCL<sub>1</sub>-PVXCP DNA vaccine. The IVTT results showed that the protein size corresponding to PVXCP or scFv.BCL<sub>1</sub>-FMDV2A was detected only in the DNA vaccine with FMDV2A linker but not in the construct without the linker. The proportion of the smaller product was higher than that of the fusion protein, as was shown by another study [166]. Cos-7 cells transfected with the DNA vaccine containing FMDV2A linker expressed and secreted the fusion protein, indicating that the protein was successfully folded. Free PVXCP protein was not detected in both the cell lysate and the cell supernatant, indicating that the 2A functioned in IVTT but not in Cos-7 cells. However, subsequently Western blot analysis of protein extracted from BCL<sub>1</sub>2APVX infected plants showed that both fusion protein and free PVXCP were produced in the host plant. These data indicated that the FMDV2A was functional.

After infiltrating plants with pgR107.scFv.BCL<sub>1</sub>-2A-PVXCP, BCL<sub>1</sub>2APVX was able to infect host plants both locally and systemically indicating that the CVP was assembled. It also maintained the correct BCL<sub>1</sub> scFv sequence as analyzed by DNA sequencing after RT-PCR of the viral RNA purified from systemic infected leaves. Subsequently, the CVP in the plant tissue was subjected for purification. The established method for PVX purification could not be used to purify the CVP. It appeared that the CVP

may have co-precipitated with the plant proteins as the CVP proteins (fusion protein and CP) were detected in the centrifugation step aimed to eliminate the plant proteins from first PEG precipitation product. This may be the result of the presence of cysteine residues on BCL<sub>1</sub> scFv sequence. BCL<sub>1</sub> scFv contains cysteine residues which required for disulfide bond formation and subsequent correct protein conformation. It is therefore possible that cysteine residues also react with the plant proteins containing cysteine, resulting in binding of the CVP proteins to the plant materials. In an attempt to purify the CVP, that centrifugation step was therefore skipped and the CVP was further isolated from the first PEG precipitation product by UC or second PEG. The CVP proteins could be detected by both Coomassie-stained SDS-PAGE and Western blot analysis but only low amount of CVPs was obtained from UC method and not from PEG method. This low amount of CVP was also found after purification using anti-BCL<sub>1</sub> antibody affinity chromatography.

As low amount of CVP was obtained, it implies that low amount of CVP being assembled into virion in the host plants. In the observation of infection symptoms, BCL<sub>1</sub>2APVX appeared to infect host plant slower than PVX. The slow progress of infection suggests that the CVP met difficulty to propagate into particle with the fusion protein. This difficulty may be resulted from the nature of BCL<sub>1</sub> scFv which contains cysteine residues. In TMV, the presence of cysteine residues in the foreign protein fused to the virus CP caused virus morphology and stability changes [262]. These changes may also apply to BCL<sub>1</sub>2APVX and result in low amount of recombinant virus being assembled into viral particles.

## Chapter 6. General conclusion

### 6.1 Main findings

#### 6.1.1 Fusion protein vaccine

Tumour antigens are generally weakly immunogenic therefore, it is important to present these antigens in a suitable context to achieve appropriate stimulation of the immune system. These self-tumour antigens either do not elicit appropriate T-cell help or can also be subject to tolerogenic pressure such as regulatory T cells. There have been significant efforts to improve the immunogenicity of tumour antigens. They include targeting antigens to DC [263-265], co-injection or incorporation with cytokines and chemokines [266-267], combining delivery with bacterial and viral pathogens [268], conjugating to immunogenic molecules such as KLH [117, 138, 140, 142] and DNA vaccines [134-135]. Our laboratory has been developing a DNA fusion vaccine approach. This strategy links the weak tumour antigen to an immunogenic molecule derived from human or plant pathogen in order to engage the non-deleted pathogen-specific Th-cell repertoire. This together with the immunostimulatory nature of the plasmid DNA backbone redirects CD4<sup>+</sup> T cells to provide help to tumour-specific B cells, cytotoxic T cells and tumour-specific Th cells. Together with FrC derived from tetanus toxin PVXCP has proven to be an excellent fusion partner to include into fusion DNA vaccines [136]. This DNA vaccine design induced protective antibody and T-cell responses in mouse lymphoma and myeloma models. I have now extended these principles to the design of two novel vaccines incorporating the immunoenhancing molecule, PVXCP, to induce antibody responses in the BCL<sub>1</sub> lymphoma model. One vaccine was Id scFv fused to PVXCP and expressed as a fusion protein in plants and the other vaccine was the Id attached to the whole PVX particle either by biotin-SA linkage or genetic fusion.

I chose the plant expression system due to many advantages it offers, such as high biomass, ease of scale up, cost-effectiveness and low risk of contamination [173-174, 269-271]. Recently a number of viral vector systems have become available which allow the very efficient expression of proteins in plants [146, 182, 194, 272]. I have used the novel HyperTrans (HT) expression system based on the deleted version of CPMV vector. This powerful expression system allows the accumulation of a high yield of protein without producing viral particles, thus reducing the risk to the environment [182]. This vector has now been used for expression of several proteins in plants [194]. ScFv.BCL<sub>1</sub>-PVXCP expression plasmids were constructed to direct the fusion protein into three different compartments of a plant cell; to the cytosol, to be secreted as a secretory protein, or to be

retained in the ER. Of the three the ER-targeted construct yielded the highest expression with minimal degradation. This was in keeping with the data obtained by Sainsbury and Lomonossoff using the same vector for expression of 2G12 anti-HIV antibody [194]. Retention of the antibody in the ER provided the highest yield of the antibody per fresh leave tissue. Therefore, targeting to the ER when using the HT system appears to be beneficial for obtaining high yields of expressed protein. The most common strategy with other viral expression systems has been to direct the expression into secretory pathway and no comparison with direction to other cellular compartments has been made [146, 185].

Evaluation of immunogenicity in mice clearly showed that plant-expressed fusion protein induced anti-Id antibody responses and provided protection against the lymphoma at similar levels to the DNA vaccine. Previous studies expressed tumour-derived Id either in the form of scFv or whole Id Ig molecule alone without fusion to immunogenic sequences [138, 140-142, 185]. A subsequent conjugation step was then required to link KLH to the tumour-derived protein; the aim being to augment T-cell help. Expression of fusion protein vaccines, rather than the Id protein alone, provides the opportunity to bypass the subsequent conjugation step as T-cell help will already be incorporated into the protein vaccine product. From the manufacturing point of view, a fusion protein strategy offers a single unit immunogenic vaccine, thereby reducing manufacturing time and eliminating additional vaccine characterisation steps. I have also confirmed that the nature of CP provides additional advantages to this fusion protein vaccine design since it allows the protein to aggregate into disk-like particles with a size of between 5 and 18 units of the fusion protein product.

Targeting the fusion protein to the ER retains the protein with high mannose glycans [221] and this may compromise the function of some proteins, for example, preventing binding of antibody to Fc receptor. However, for expression of immunogens, the presence of these glycans can be beneficial and potentially enhance immunogenicity through targeting to the mannose receptor (MR) and DC-SIGN on APCs [1, 273]. Targeting antigens through MR has been shown to enhance antibody responses [274]. BCL<sub>1</sub> scFv-PVXCP fusion protein can acquire high mannose through a potential N-glycosylation site on the PVXCP portion, thereby potentially enhancing the vaccine immunogenicity. In experiments performed after I completed my experimental work, it was demonstrated the fusion protein was able to bind MR in an *in vitro* binding assay (Shipton and Savelyeva, personal communication). Furthermore analysis of sugars by HPLC, performed by our collaborators (Sainsbury and Lomonossoff, personal communication), also showed the presence of high mannose glycans in several ER expressed proteins. However, whether there is a role for this binding in enhancing vaccine immunogenicity *in vivo* remains to be seen. MR KO

mice are available and evaluation of antibody responses in these mice will answer this question. Another advantage of ER targeting for expression of immunogens is to avoid the addition of fucose and xylose as terminal glycans through processing pathways in the Golgi. These could cause allergic reactions as well as cause vaccine neutralisation following subsequent administrations [221, 275].

For Id vaccines in particular, ER-targeting gives the additional advantage of incorporating a high mannose into V genes in a similar fashion to cells of follicular lymphoma [222] thereby making plant expression systems particularly attractive. This has not been appreciated previously. In a study conducted by Large Scale Biology Corp.(Vacaville, CA), which used the TMV-based transient vector for expression of Id scFv from patients with lymphoma the expression was directed for secretion [146]. Similarly, ICON genetics (Halle, Germany) is currently evaluating the immunogenicity of plant-expressed whole Id Ig in a Phase I clinical trial using magnICON viral vector system, with direction of protein expression into the secretory pathway ([272] and V. Klimyuk, personal communication). Our findings can potentially improve immunogenicity of Id vaccines.

### **6.1.2 BCL<sub>1</sub> PVP vaccine**

I have explored the use of the whole PVX particle as a multivalent antigen delivery system for Id tumour antigen with the aim of antibody induction. To evaluate the ability of PVX to enhance the immune response to the BCL<sub>1</sub> Id of the lymphoma, the PVX-based BCL<sub>1</sub>-PVP vaccine displaying BCL<sub>1</sub> antigen was generated by linking BCL<sub>1</sub> IgG to PVX particles via biotin-SA binding to CP. Mice injected with BCL<sub>1</sub>-PVP vaccine without an adjuvant generated significantly higher anti-Id antibody than the DNA vaccine. These antibody levels were enhanced by addition of alum adjuvant with as low as 1 µg of PVX-linked BCL<sub>1</sub> Id Ig inducing antibody at the level sufficient to protect mice from the tumour. The superior ability of PVP vaccine to induce high levels of antibody could be explained by antigen multimerisation through aggregation when linked to the viral particle and by immunoenhancing properties of PVX through providing T-cell help and DC activation. It has long been recognized that antigen density influences the magnitude of an antibody response [250]. Multivalent antigens of HBV and HPV VLP vaccines have been shown to be superior in antibody responses [251-253]. As PVX showed an immunoenhancing property when linked with the BCL<sub>1</sub>IgG, this result implied that one possible reason why PVX enhanced the immune response was from the multiple copies of BCL<sub>1</sub> antigen displayed on the surface. A comparison of vaccination with BCL<sub>1</sub>IgG linked to monomeric PVXCP or linked to PVX will further reveal the importance of multimerization.

BCL<sub>1</sub>-PVP induced IFN- $\gamma$  and IL-2 secreting T cells as judged by ELISPOT with a much higher number of helper cells induced by the PVP vaccine than by the DNA vaccine indicating that the vaccine was superior in Th activation. Together with the induction of IgG2 isotypes the induction of IFN- $\gamma$  Th cells indicate that the vaccine was able to induce a strong Th1 response.

Mice vaccinated with PVP without added adjuvant generated IgG antibody against both Id and PVX. This evidence points to its ability to act as an adjuvant and activate DC. *In vivo* PVX bound to both DCs and B cells and induced up-regulation of activation markers on all CD11c<sup>+</sup> DC subsets and B cells. Furthermore, PVX induced up-regulation of inflammatory cytokines including IL-12 consistent with the activation of Th1 responses.

Since PVX contains single stranded (ss) RNA we hypothesised that it might play a role in activating the immune system through engagement of TLR7. And indeed the presence of PVX RNA enhanced anti-Id antibody responses indicating a role in immune induction. Furthermore, data recently obtained in TLR7KO mice through collaboration with Dr S. Diebold's laboratory, clearly showed that PVX RNA acts as a ligand for TLR7 (N. Savelyeva and S. Diebold, unpublished data). Hence, in addition to being an excellent multivalent carrier for a non-immunogenic tumour antigen, PVX also provides an additional advantage by activating the immune system through TLR7 triggering by ssRNA.

PVX is also easy and cheap to purify. One mg of PVX can be easily purified from one gram of PVX-infected plant tissues. To obtain PVX, the whole process, including growing host plants, growing *Agrobacterium* containing pGR107 for PVX expression, agroinfiltration, maintenance of host plant and PVX purification should be very cheap (estimated to be less than £10 per mg of PVX). Due to very well established purification methods there is little variation between purified batches of PVX, making it easy to qualify. Therefore, PVX is an excellent candidate for a carrier molecule in vaccine production for comparison with the widely used carrier molecule, KLH. Furthermore, the source of keyhole limpet is unsustainable as its population has decreased. In the future the manufacturers will need to develop keyhole limpet mariculture. However, one of the KLH isoforms (KLH1) is known to be lost when the keyhole limpet is cultured in captivity [276].

### **6.1.3 BCL<sub>1</sub> CVP vaccine**

The third approach I took was to generate a PVX-based vaccine where the Id antigen was genetically linked to the virus. Initially, a DNA construct for expression of PVX CVP displaying scFv.BCL<sub>1</sub> was assembled. It contained scFv.BCL<sub>1</sub> linked to FMDV2A followed with PVXCP sequence. FMDV2A was included for production of scFv.BCL<sub>1</sub>-2A-PVXCP fusion proteins and free PVXCPs to enable assembly of the CVP as

previously reported [167-169]. The fusion protein gene sequence was further introduced into a plant expression system using the pgR107 vector with incorporated scFv.BCL<sub>1</sub>-2A-PVXCP and agrobacterial gene transfer. Plants agroinfiltrated with pgR107.scFv.BCL<sub>1</sub>-2A-PVXCP exhibited symptoms of a local and a systemic viral infection, suggesting the production of CVP from the expression plasmid. Systemic infection by BCL<sub>1</sub>2APVX was slower than the wild type PVX infection (from pgR107 agroinfiltration control) but once the infection was established the BCL<sub>1</sub>2APVX infection was more aggressive than PVX infection. The presence of BCL<sub>1</sub>2APVX CVP in host plants was confirmed by RT-PCR and Western blot analysis; scFv.BCL<sub>1</sub>-2A-PVXCP RNA and protein were detected in both infiltrated and systemically infected tissues. Despite extensive attempts to purify CVP using methods described by others I did not yield sufficient amounts of chimeric virus to allow me to perform studies in mice. The number of studies which reported the use of this strategy is very limited. In fact all published studies on the immunogenicity of chimeric PVX only used small peptides or fragments [170-172]. This probably indicates that although a few succeeded in fusing whole proteins [167-169] or large fragments [160] to PVX genetically through the use of FMDV2A genetic fusion probably works better for small peptides. This is because free CP is not required and hence the virion assembly occurs in a more controlled manner.

## 6.2 Optimisation

Plant-made scFv.BCL<sub>1</sub>-PVXCP fusion vaccine showed the ability to induce anti-Id antibody and provide protection against the BCL<sub>1</sub> lymphoma. Direction of vaccine expression to the ER has proven to be optimal for plant expression when it's driven by the HT system. Although affinity chromatography provided a good way of purifying the fusion vaccine in large quantities some impurities and degradation products were present. For human vaccination, the vaccine needs to be highly pure. Further improvement of purification procedure can be achieved by further optimising the elution conditions to prevent degradation of the fusion protein. I showed that highly pure protein can be obtained by size exclusion. Even though the yield of scFv.BCL<sub>1</sub>-PVXCP obtained by size-exclusion chromatography was low, this strategy could be applied in industrial scale production where the starting material is plentiful. The addition of an affinity tag such as His-tag to the fusion protein could be another way to improve the purification procedure. This strategy was previously used by Large Scale Biology Corp in their clinical trial [146].

BCL<sub>1</sub> PVP vaccine induced a potent antibody response and protection against the BCL<sub>1</sub> tumour. The only drawback of this vaccine is the relative complexity of its

preparation. Both the antigen and PVX are needed to be expressed separately then purified and then linked together. The vaccine subunits were linked together using biotin-streptavidin binding. The levels of biotinylation vary and that may affect the vaccine assembly. If an IgG molecule contains too many biotin molecules, all four biotin moieties on streptavidin may be occupied before incubation with biotinylated PVX and therefore, the antigen would not be linked to PVX. This problem can be solved by optimisation of the biotinylation reaction for each protein antigen, i.e. to optimise concentration of biotin, concentration of protein to be biotinylated and the molar ratio of biotin to protein. The alternative is to genetically link antigen to streptavidin. GFP fused to streptavidin was produced in plants using the TMV vector and the GFP-streptavidin tetramer was able to bind to biotinylated TMV [277]. Using this strategy, it could be possible to reduce variability in linking antigen and PVX.

BCL<sub>1</sub> CVP could not be purified in the amount required for vaccination even though the CVPs with scFv.BCL<sub>1</sub> on its surface were produced in plants. This may be because of low amounts of CVP assembled in harvested plant tissues. Isolation of CVP from plants may be optimised by evaluation of the infection stage and identifying the location where CVP assembles best before CVP purification. Another approach to improve CVP accumulation is to avoid using the FMDV2A sequence in the linker. The presence of FMDV2A in scFv.BCL<sub>1</sub>-PVXCP gives three types of polypeptides; the fusion protein scFv.BCL<sub>1</sub>-2A-PVXCP, as well as the individual subunits scFv.BCL<sub>1</sub>-2A and PVXCP. Since FMDV2A-mediated ribosomal skipping is random, the concentration of the subunits may be too high thereby preventing incorporation of the fusion protein into CVP. Agroinfiltration with a combination of the two plasmids, one plasmid for the scFv.BCL<sub>1</sub>-PVXCP expression and another plasmid for PVXCP expression, may help. This will keep a required mixed population of the fusion protein and free CP for CVP assembly and eliminate the non-required protein scFv.BCL<sub>1</sub>-2A.

### **6.3 Future use**

ScFv.BCL<sub>1</sub>-PVXCP fusion protein vaccine can be expressed at high levels in plants in only 7 days using the vector of the HT system. As the fusion protein vaccine can induce anti-tumour immunity in comparable levels to the DNA vaccine, it's a good alternative candidate vaccine for DNA vaccine non-responders or for use in patients who reject electroporation, the strategy proved to be efficient for DNA vaccine delivery [137]. Delivery of the protein vaccine is simple and does not require complex devices as it can be given subcutaneously with a needle injection. A big advantage of scFv.BCL<sub>1</sub>-PVXCP is

that it is a single unit vaccine and can be obtained in one production step. Direction of the expression to the ER gives the additional advantage of adding a high mannose glycan to the glycosylation site in CP thereby incorporating a danger signal. For Id vaccines in particular, ER-targeting gives the additional advantage of incorporating a high mannose into V genes in a similar fashion to lymphoma cells thereby making plant expression systems particularly attractive. This fusion vaccine design can be utilised for other tumour antigens and antigens derived from pathogens.

As the PVP vaccine is a very potent vaccine for induction of antibody responses, PVX-based vaccine design will be beneficial for induction of antibody-mediated anti-tumour immunity. Tumours expressing Her2/Neu antigen can be controlled by anti-Her2/Neu monoclonal antibody (herceptin) in humans with breast cancer. Antibodies induced by the DNA vaccine encoding Her2 (Neu) are also protective in mouse models of a mammary carcinoma [278]. In addition, IgG2 antibody isotypes associated with a Th1 response have been shown to be important for protection against the Balb-NeuT spontaneous mammary carcinoma [279]. Including PVX as a carrier molecule in a Her2/Neu vaccine could induce high anti-Her2/Neu antibody responses and therefore is a good candidate vaccine against this target. Her2 may be expressed in plants to reduce the cost of antigen production and then linked to PVX using biotin-SA as in the PVP vaccine. The activation of a strong Th1 skewed immune response also means that this vaccine design could be potentially used to induce anti-tumour CTL responses. In addition to large protein-PVX linking, the antigenic peptides from Her2 antigen may be displayed on PVX CVP particles as short peptides carrying CVP can be easily purified from the infected tissues [170, 172].

In a large scale production, plants will be grown in contained conditions such as greenhouses to avoid environmental release of viral particles or Agrobacterium used for expression vector delivery [271]. The first registration (2006) for a plant-derived poultry vaccine against Newcastle disease, produced in tobacco cells within sealed and sterile containers, was granted to Dow AgroSciences company by the USDA Centre for Veterinary Biologics [269]. Tobacco has been the plant of choice in commercial production of recombinant proteins in transgenic plants since it provides high biomass yields, plentiful seed production as well as efficient, well-established methods of gene transfer and expression [269]. Recently, commercial production of recombinant proteins by transient expression using a viral vector has been developed. Kentucky Bioprocessing (KBP), USA, has developed GENEWARE<sup>®</sup>, the TMV-based transient expression system [280]. Using this technology the company now offers production and purification of plant-made proteins. Another plant-virus based technology developed by ICON Genetics (Germany),

‘magnICON’, has been used to produce hepatitis B core antigen, Norwalk virus capsid protein, and plague antigens F1 and V at levels of up to 1-2 mg per g fresh weight leaf of *N. Benthamiana* [269]. These examples of industrial plant-made protein production indicate that scaling up of PVXCP fusion vaccine production would be possible. We have set up collaboration with ICON Genetics to further explore our findings and to enable large-scale manufacturing for clinical use.

## Appendix

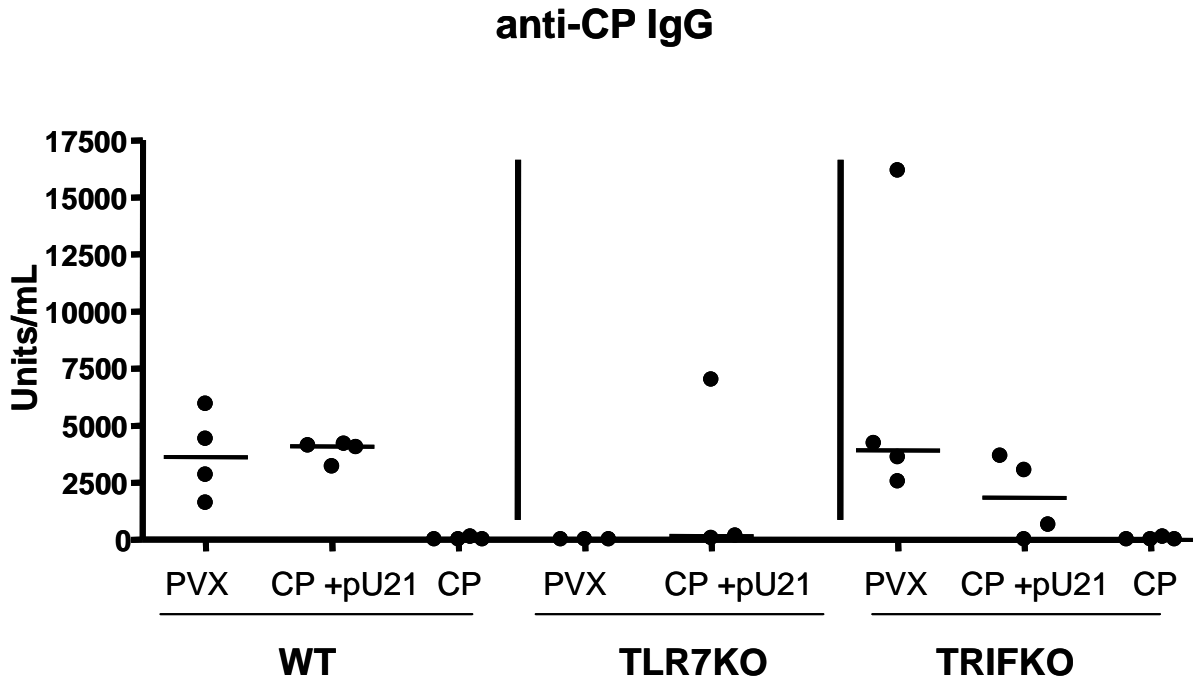


**Figure A-1. Induction of anti-PVXCP antibody response by PVX/CP in TLR-7 knockout mice**

A group of three TLR7 knockout mice (TLR7KO) was injected with 15  $\mu$ g of PVX or PVXCP mixed with pU21 (CP + pU21). A control group of four C57/Blk mice or four TRIF knockout mice (TRIFKO) was injected with the same amount of either PVX or PVXCP (CP) or PVXCP mixed with pU21. Antibody levels to PVXCP were measured on day 21 after injection. Each dot represents an individual mouse. Horizontal bars are median values.

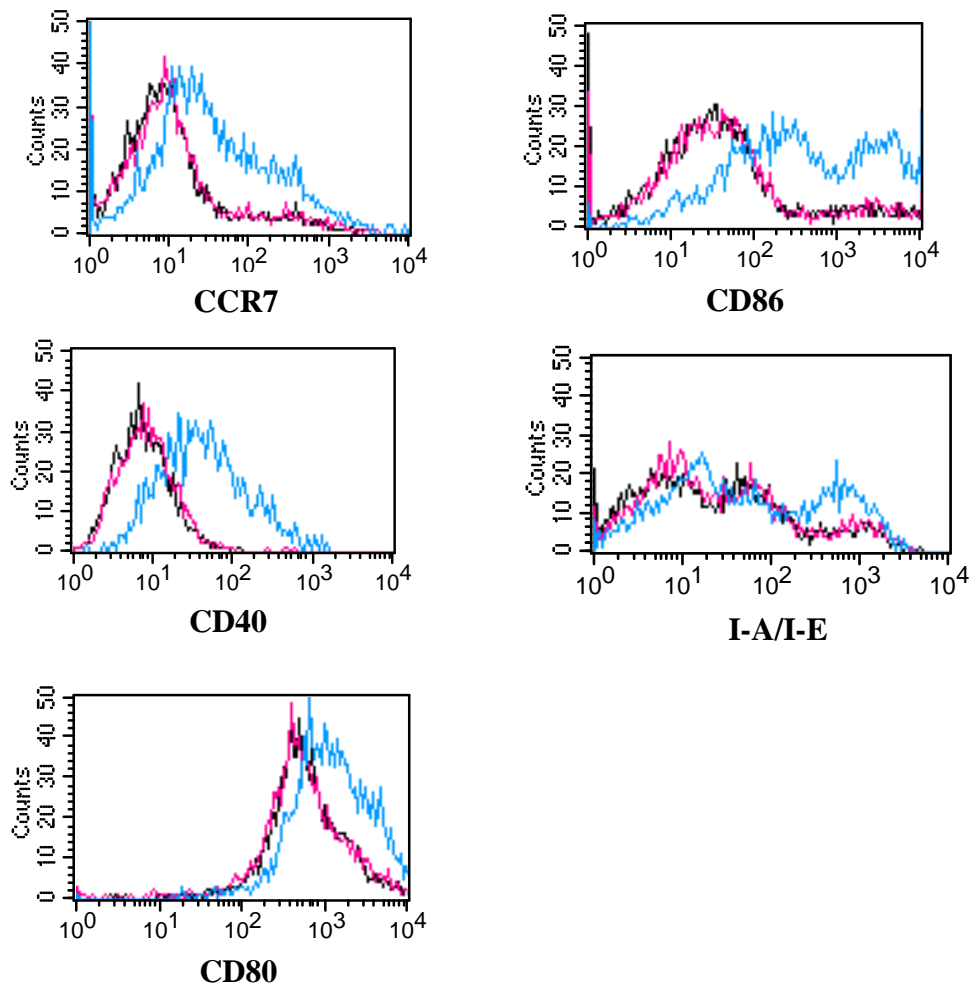


**Figure A-2. Repeat experiment of FACS analysis of DC activation *in vitro***

BMDCs were incubated with 10 μg of PVX (pink histogram) or 1 μg of LPS (blue histogram) for 48 hrs. Cells were stained with PE-labeled anti-CD11c antibody and APC-labeled anti-CCR7 or anti-CD40 or anti-CD80 or anti-CD86 or FITC-labeled anti-I-A/I-E antibody and analyzed by FACSCalibur with the Cell Quest Pro software. Non-treated control cells are shown in black histogram. One of three experiments is shown in chapter 4 (figure 4-15). This is a plot of one of two repeat experiments.

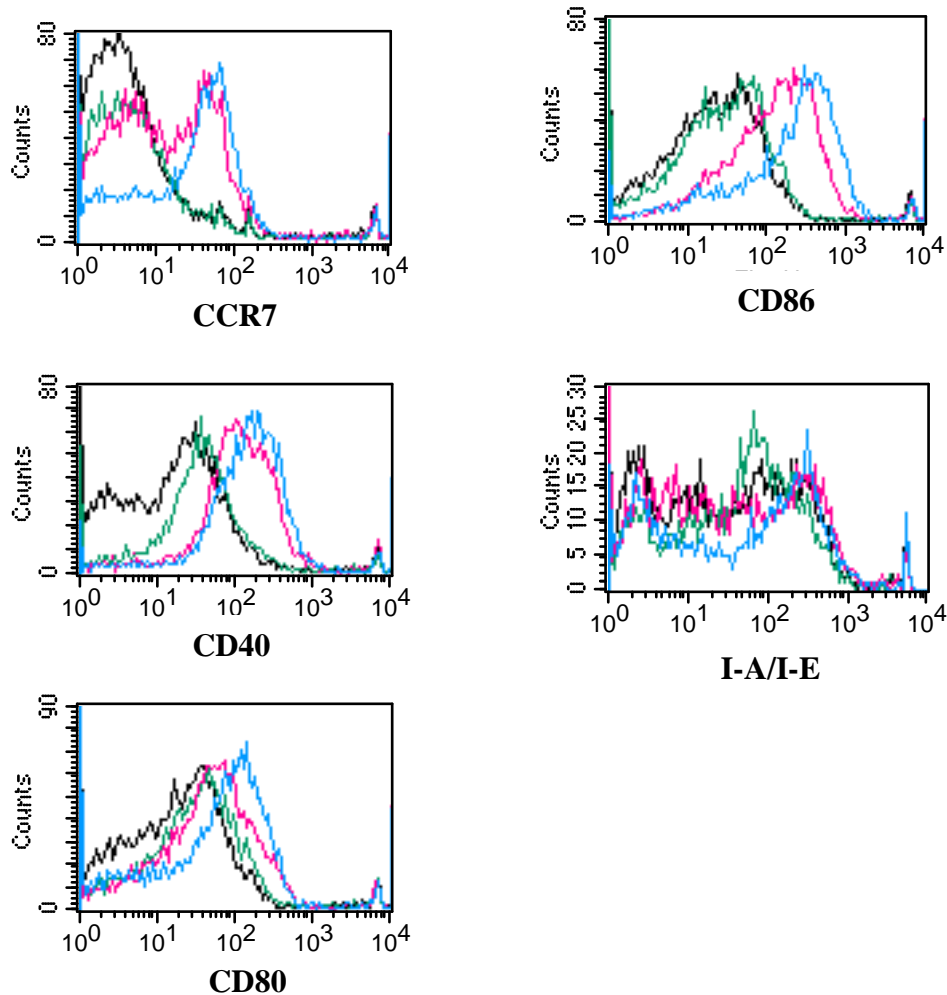


**Figure A-3. Repeat experiment of FACS analysis of the effect of low amounts of LPS in DC activation *in vivo***

100  $\mu$ g of PVX (pink histogram) or 250 pg of LPS (green histogram) or 25  $\mu$ g of LPS (blue histogram) or saline (black histogram) was injected into C57BL/6 mouse and the spleen was collected at 20 h after injection. Splenocytes were stained with PE-labeled anti-CD11c and APC-labeled anti-CCR7 or anti-CD40 or anti-CD80 or anti-CD86 or anti-I-A/I-E antibodies and analyzed by FACSCalibur with the Cell Quest Pro software. One of two experiments is shown in chapter 4 (figure 4-18). This is a plot of the repeat experiment.

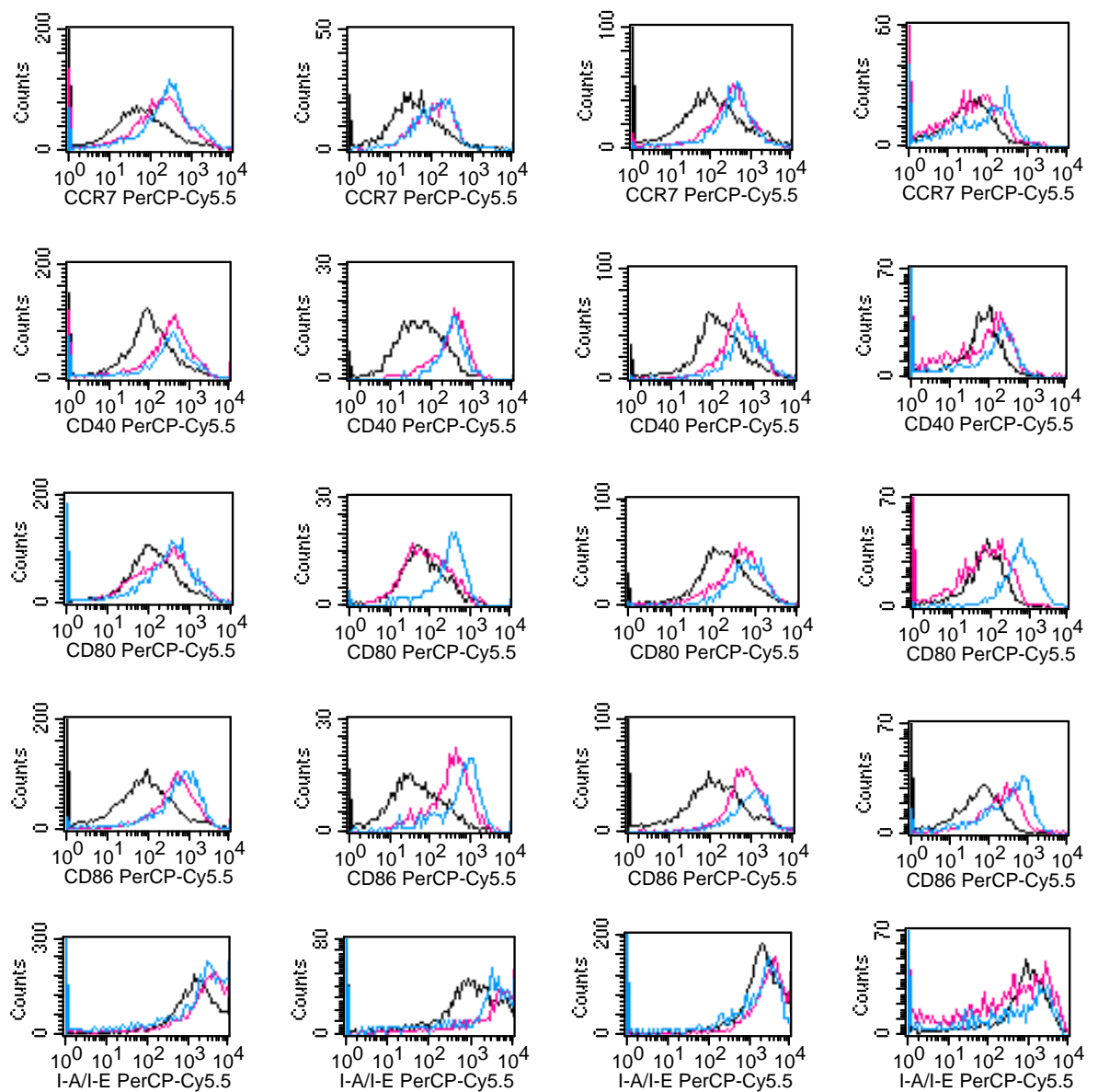


**Figure A-4. Repeat experiment of FACS analysis of PVX induced DC activation *in vivo***

100  $\mu$ g of PVX (pink histogram) or 25  $\mu$ g of LPS (blue histogram) or saline (black histogram) was injected into C57BL/6 mouse and spleen was collected at 20 hrs after injection. Splenocytes were stained with PE-labeled anti-CD11c, APC-labeled anti-CD8 $\alpha$ , FITC-labeled anti-CD4, and PerCP-Cy5.5-labeled anti-CCR7 or anti-CD40 or anti-CD80 or anti-CD86 or anti-I-A/I-E antibodies and analyzed by FACSCalibur with the Cell Quest Pro software. Cells were gated for CD11c as shown in the top-left graph. One of three experiments is shown in chapter 4 (figure 4-19). This is a plot of one of two repeat experiments.

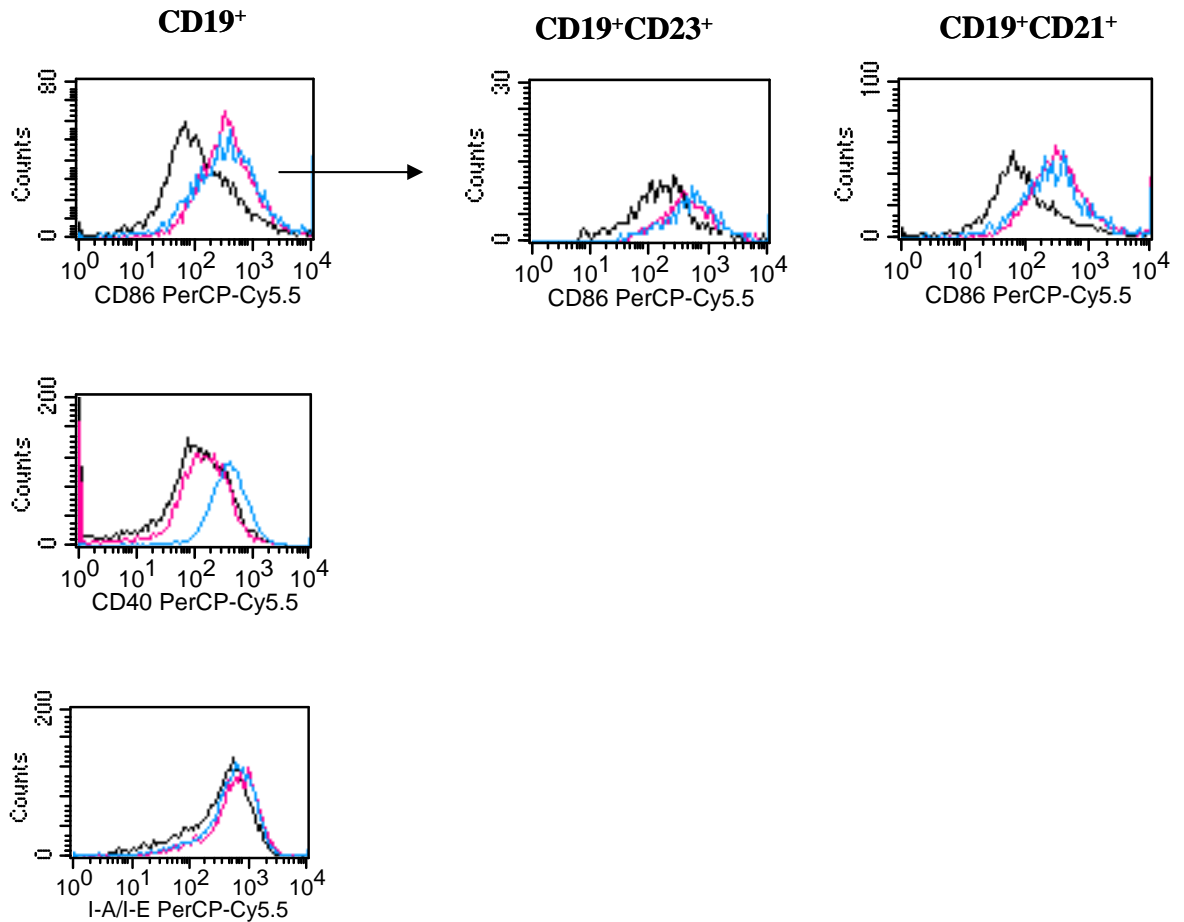


**Figure A-5. Repeat experiment of FACS analysis of PVX induced B-cell activation *in vivo***

100  $\mu$ g of PVX (pink histogram) or 25  $\mu$ g of LPS (blue histogram) or saline (black histogram) was injected into C57BL/6 mouse and spleen was collected at 20 hrs after injection. Splenocytes were stained with PE-labeled anti-CD19 and PerCP-Cy5.5-labeled anti-CD40 or I-A/I-E antibodies. Separately, cells were stained with APC-labeled anti-CD19, FITC-labeled anti-CD21, PE-labeled anti-CD23 and PerCP-Cy5.5-labeled anti-CD86 antibodies. Stained cells were analyzed by FACSCalibur with the Cell Quest Pro software. One of two experiments is shown in chapter 4 (figure 4-20). This is a plot of the repeat experiment.

	relative expression levels			
	PVX		LPS	
	mean	SD	mean	SD
<b>CCL4</b>	3.41	2.20	3.08	0.60
<b>CCL5</b>	1.69	0.68	12.32	2.07
<b>CXCL10</b>	86.17	32.60	76.31	11.03
<b>CCR2</b>	0.59	0.06	0.23	0.03
<b>CCR7</b>	2.96	0.90	12.68	1.81
<b>IL-6</b>	9.46	3.03	15.03	2.46
<b>TNF</b>	10.24	3.46	2.22	0.99
<b>IL-12</b>	9.97	2.94	0.89	0.07

**Table A-1. Expression of cytokines, chemokines and chemokine receptors after in vivo PVX activation**

A group of three mice was i.v. injected with 100 µg PVX or 25 µg of LPS or saline (non-activated control). Splens were collected 6 hours after injection. CD11c<sup>+</sup> cells were positively selected using PE-anti-CD11c antibody following with anti-PE microbeads. RNA was extracted from selected cells and reverse-transcribed before analysing with real-time PCR. Mean and standard deviation (SD) values of relative expression levels to non-activated cells from three mice are shown.

## References

1. Gazi, U. and L. Martinez-Pomares, *Influence of the mannose receptor in host immune responses*. Immunobiology, 2009. **214**(7): p. 554-61.
2. Swiggard, W.J., et al., *DEC-205, a 205-kDa protein abundant on mouse dendritic cells and thymic epithelium that is detected by the monoclonal antibody NLDC-145: purification, characterization, and N-terminal amino acid sequence*. Cell Immunol, 1995. **165**(2): p. 302-11.
3. Jiang, W., et al., *The receptor DEC-205 expressed by dendritic cells and thymic epithelial cells is involved in antigen processing*. Nature, 1995. **375**(6527): p. 151-5.
4. den Dunnen, J., S.I. Gringhuis, and T.B. Geijtenbeek, *Innate signaling by the C-type lectin DC-SIGN dictates immune responses*. Cancer Immunol Immunother, 2009. **58**(7): p. 1149-57.
5. Svajger, U., et al., *C-type lectin DC-SIGN: An adhesion, signalling and antigen-uptake molecule that guides dendritic cells in immunity*. Cell Signal, 2010.
6. van Kooyk, Y., *C-type lectins on dendritic cells: key modulators for the induction of immune responses*. Biochem Soc Trans, 2008. **36**(Pt 6): p. 1478-81.
7. Koppel, E.A., et al., *Distinct functions of DC-SIGN and its homologues L-SIGN (DC-SIGNR) and mSIGNR1 in pathogen recognition and immune regulation*. Cell Microbiol, 2005. **7**(2): p. 157-65.
8. Fernandes-Alnemri, T., et al., *AIM2 activates the inflammasome and cell death in response to cytoplasmic DNA*. Nature, 2009. **458**(7237): p. 509-13.
9. Burckstummer, T., et al., *An orthogonal proteomic-genomic screen identifies AIM2 as a cytoplasmic DNA sensor for the inflammasome*. Nat Immunol, 2009. **10**(3): p. 266-72.
10. Hornung, V. and E. Latz, *Intracellular DNA recognition*. Nat Rev Immunol, 2010. **10**(2): p. 123-30.
11. Barr, T.A., et al., *TLR-mediated stimulation of APC: Distinct cytokine responses of B cells and dendritic cells*. Eur J Immunol, 2007. **37**(11): p. 3040-53.
12. Nauseef, W.M., *How human neutrophils kill and degrade microbes: an integrated view*. Immunol Rev, 2007. **219**: p. 88-102.
13. Nicola, A.M., A. Casadevall, and D.L. Goldman, *Fungal killing by mammalian phagocytic cells*. Curr Opin Microbiol, 2008. **11**(4): p. 313-7.
14. Houchins, J.P., et al., *DNA sequence analysis of NKG2, a family of related cDNA clones encoding type II integral membrane proteins on human natural killer cells*. J Exp Med, 1991. **173**(4): p. 1017-20.
15. Ogasawara, K. and L.L. Lanier, *NKG2D in NK and T cell-mediated immunity*. J Clin Immunol, 2005. **25**(6): p. 534-40.
16. Hirano, T., *Interleukin 6 and its receptor: ten years later*. Int Rev Immunol, 1998. **16**(3-4): p. 249-84.
17. Chorro, L., et al., *Langerhans cell (LC) proliferation mediates neonatal development, homeostasis, and inflammation-associated expansion of the epidermal LC network*. J Exp Med, 2009. **206**(13): p. 3089-100.
18. Geissmann, F., et al., *Development of monocytes, macrophages, and dendritic cells*. Science, 2010. **327**(5966): p. 656-61.
19. Coquerelle, C. and M. Moser, *Are dendritic cells central to regulatory T cell function?* Immunol Lett, 2008. **119**(1-2): p. 12-6.
20. Kindt, T.J., Goldsby, R.A., Osborne, B.A., *Immunology*. 2007, Sara Tenney: New York.
21. Abbas, A.K., Lichtman, A.H., Pillai, S., *Cellular and molecular immunology*. updated 6th ed. ed. 2010: Saunders Elsevier.
22. Diebold, S., *Innate recognition of viruses*. Immunol Lett, 2010. **128**(1): p. 17-20.

23. Hovanessian, A.G., *On the discovery of interferon-inducible, double-stranded RNA activated enzymes: the 2'-5'oligoadenylate synthetases and the protein kinase PKR*. Cytokine Growth Factor Rev, 2007. **18**(5-6): p. 351-61.
24. Takeuchi, O. and S. Akira, *MDA5/RIG-I and virus recognition*. Curr Opin Immunol, 2008. **20**(1): p. 17-22.
25. Takeda, K., T. Kaisho, and S. Akira, *Toll-like receptors*. Annu Rev Immunol, 2003. **21**: p. 335-76.
26. Takeuchi, O., et al., *Differential roles of TLR2 and TLR4 in recognition of gram-negative and gram-positive bacterial cell wall components*. Immunity, 1999. **11**(4): p. 443-51.
27. Alexopoulou, L., et al., *Recognition of double-stranded RNA and activation of NF-kappaB by Toll-like receptor 3*. Nature, 2001. **413**(6857): p. 732-8.
28. Sugiyama, T., et al., *Immunoadjuvant effects of polyadenylic:polyuridylic acids through TLR3 and TLR7*. Int Immunol, 2008. **20**(1): p. 1-9.
29. Poltorak, A., et al., *Defective LPS signaling in C3H/HeJ and C57BL/10ScCr mice: mutations in Tlr4 gene*. Science, 1998. **282**(5396): p. 2085-8.
30. Qureshi, S.T., et al., *Endotoxin-tolerant mice have mutations in Toll-like receptor 4 (Tlr4)*. J Exp Med, 1999. **189**(4): p. 615-25.
31. Diebold, S.S., et al., *Innate antiviral responses by means of TLR7-mediated recognition of single-stranded RNA*. Science, 2004. **303**(5663): p. 1529-31.
32. Heil, F., et al., *Species-specific recognition of single-stranded RNA via toll-like receptor 7 and 8*. Science, 2004. **303**(5663): p. 1526-9.
33. Hemmi, H., et al., *A Toll-like receptor recognizes bacterial DNA*. Nature, 2000. **408**(6813): p. 740-5.
34. Haas, T., et al., *The DNA sugar backbone 2' deoxyribose determines toll-like receptor 9 activation*. Immunity, 2008. **28**(3): p. 315-23.
35. Wagner, H., *The sweetness of the DNA backbone drives Toll-like receptor 9*. Curr Opin Immunol, 2008. **20**(4): p. 396-400.
36. Yarovinsky, F., et al., *TLR11 activation of dendritic cells by a protozoan profilin-like protein*. Science, 2005. **308**(5728): p. 1626-9.
37. Shortman, K. and W.R. Heath, *The CD8+ dendritic cell subset*. Immunol Rev, 2010. **234**(1): p. 18-31.
38. Kurts, C., B.W. Robinson, and P.A. Knolle, *Cross-priming in health and disease*. Nat Rev Immunol, 2010. **10**(6): p. 403-14.
39. Allan, R.S., et al., *Migratory dendritic cells transfer antigen to a lymph node-resident dendritic cell population for efficient CTL priming*. Immunity, 2006. **25**(1): p. 153-62.
40. Backer, R., et al., *Effective collaboration between marginal metallophilic macrophages and CD8+ dendritic cells in the generation of cytotoxic T cells*. Proc Natl Acad Sci U S A, 2010. **107**(1): p. 216-21.
41. Giodini, A. and M.L. Albert, *A whodunit: an appointment with death*. Curr Opin Immunol, 2010. **22**(1): p. 94-108.
42. Rodriguez, A., et al., *Selective transport of internalized antigens to the cytosol for MHC class I presentation in dendritic cells*. Nat Cell Biol, 1999. **1**(6): p. 362-8.
43. Guermonprez, P., et al., *ER-phagosome fusion defines an MHC class I cross-presentation compartment in dendritic cells*. Nature, 2003. **425**(6956): p. 397-402.
44. Lizee, G., et al., *Control of dendritic cell cross-presentation by the major histocompatibility complex class I cytoplasmic domain*. Nat Immunol, 2003. **4**(11): p. 1065-73.
45. Basha, G., et al., *MHC class I endosomal and lysosomal trafficking coincides with exogenous antigen loading in dendritic cells*. PLoS One, 2008. **3**(9): p. e3247.
46. Casola, S., *Control of peripheral B-cell development*. Curr Opin Immunol, 2007. **19**(2): p. 143-9.
47. Hardy, R.R., *B-1 B cell development*. J Immunol, 2006. **177**(5): p. 2749-54.

48. Batista, F.D. and N.E. Harwood, *The who, how and where of antigen presentation to B cells*. Nat Rev Immunol, 2009. **9**(1): p. 15-27.
49. Nimmerjahn, F. and J.V. Ravetch, *Fcγ receptors as regulators of immune responses*. Nat Rev Immunol, 2008. **8**(1): p. 34-47.
50. Glennie, M.J., et al., *Mechanisms of killing by anti-CD20 monoclonal antibodies*. Mol Immunol, 2007. **44**(16): p. 3823-37.
51. Nimmerjahn, F. and J.V. Ravetch, *Fcγ receptors: old friends and new family members*. Immunity, 2006. **24**(1): p. 19-28.
52. Cartron, G., et al., *From the bench to the bedside: ways to improve rituximab efficacy*. Blood, 2004. **104**(9): p. 2635-42.
53. Groselj-Grenc, M., et al., *Neutrophil and monocyte CD64 indexes, lipopolysaccharide-binding protein, procalcitonin and C-reactive protein in sepsis of critically ill neonates and children*. Intensive Care Med, 2009. **35**(11): p. 1950-8.
54. Zhu, J. and W.E. Paul, *CD4 T cells: fates, functions, and faults*. Blood, 2008. **112**(5): p. 1557-69.
55. Coffman, R.L., et al., *Antibody to interleukin-5 inhibits helminth-induced eosinophilia in mice*. Science, 1989. **245**(4915): p. 308-10.
56. Fazilleau, N., et al., *Follicular helper T cells: lineage and location*. Immunity, 2009. **30**(3): p. 324-35.
57. McHeyzer-Williams, L.J., et al., *Follicular helper T cells as cognate regulators of B cell immunity*. Curr Opin Immunol, 2009. **21**(3): p. 266-73.
58. Yu, D., et al., *Lineage specification and heterogeneity of T follicular helper cells*. Curr Opin Immunol, 2009. **21**(6): p. 619-25.
59. Jin, D., et al., *The inflammatory Th 17 subset in immunity against self and non-self antigens*. Autoimmunity, 2008. **41**(2): p. 154-62.
60. Sakaguchi, S., et al., *Regulatory T cells: how do they suppress immune responses?* Int Immunol, 2009. **21**(10): p. 1105-11.
61. Hoves, S., J.A. Trapani, and I. Voskoboinik, *The battlefield of perforin/granzyme cell death pathways*. J Leukoc Biol, 2010. **87**(2): p. 237-43.
62. Meresse, B. and N. Cerf-Bennussan, *Innate T cell responses in human gut*. Semin Immunol, 2009. **21**(3): p. 121-9.
63. Godfrey, D.I., et al., *NKT cells: facts, functions and fallacies*. Immunol Today, 2000. **21**(11): p. 573-83.
64. Godfrey, D.I., S. Stankovic, and A.G. Baxter, *Raising the NKT cell family*. Nat Immunol, 2010. **11**(3): p. 197-206.
65. Treiner, E., et al., *Selection of evolutionarily conserved mucosal-associated invariant T cells by MRI*. Nature, 2003. **422**(6928): p. 164-9.
66. Huang, S., et al., *MRI uses an endocytic pathway to activate mucosal-associated invariant T cells*. J Exp Med, 2008. **205**(5): p. 1201-11.
67. Vardiman, J.W., *The World Health Organization (WHO) classification of tumors of the hematopoietic and lymphoid tissues: An overview with emphasis on the myeloid neoplasms*. Chem Biol Interact, 2009.
68. CRUK. *Cancer in the UK*. 2009; [http://info.cancerresearchuk.org/prod\\_consump/groups/cr\\_common/@nre/@sta/documents/generalcontent/018070.pdf](http://info.cancerresearchuk.org/prod_consump/groups/cr_common/@nre/@sta/documents/generalcontent/018070.pdf). Available from: [http://info.cancerresearchuk.org/prod\\_consump/groups/cr\\_common/@nre/@sta/documents/generalcontent/018070.pdf](http://info.cancerresearchuk.org/prod_consump/groups/cr_common/@nre/@sta/documents/generalcontent/018070.pdf).
69. Ottensmeier, C., *The classification of lymphomas and leukemias*. Chem Biol Interact, 2001. **135-136**: p. 653-64.
70. Larson, M.L. and P. Venugopal, *Clofarabine: a new treatment option for patients with acute myeloid leukemia*. Expert Opin Pharmacother, 2009. **10**(8): p. 1353-7.
71. Abbott, B.L., *Chronic lymphocytic leukemia: recent advances in diagnosis and treatment*. Oncologist, 2006. **11**(1): p. 21-30.

72. Janssens, A., M. Boogaerts, and G. Verhoef, *Development of fludarabine formulations in the treatment of chronic lymphocytic leukemia*. Drug Des Devel Ther, 2009. **3**: p. 241-52.
73. Huynh, E., D. Sigal, and A. Saven, *Cladribine in the treatment of hairy cell leukemia: initial and subsequent results*. Leuk Lymphoma, 2009. **50 Suppl 1**: p. 12-7.
74. Janusch, M., et al., *The hand-foot syndrome--a frequent secondary manifestation in antineoplastic chemotherapy*. Eur J Dermatol, 2006. **16**(5): p. 494-9.
75. Fausel, C., *Targeted chronic myeloid leukemia therapy: Seeking a cure*. Am J Health Syst Pharm, 2007. **64**(24 Suppl 15): p. S9-15.
76. Faderl, S., et al., *The biology of chronic myeloid leukemia*. N Engl J Med, 1999. **341**(3): p. 164-72.
77. Ramirez, P. and J.F. DiPersio, *Therapy options in imatinib failures*. Oncologist, 2008. **13**(4): p. 424-34.
78. Deininger, M.W., et al., *Practical management of patients with chronic myeloid leukemia receiving imatinib*. J Clin Oncol, 2003. **21**(8): p. 1637-47.
79. Jabbour, E., J. Cortes, and H. Kantarjian, *Dasatinib for the treatment of Philadelphia chromosome-positive leukaemias*. Expert Opin Investig Drugs, 2007. **16**(5): p. 679-87.
80. Winter, M.C. and B.W. Hancock, *Ten years of rituximab in NHL*. Expert Opin Drug Saf, 2009. **8**(2): p. 223-35.
81. Weng, W.K., et al., *Clinical outcome of lymphoma patients after idiotype vaccination is correlated with humoral immune response and immunoglobulin G Fc receptor genotype*. J Clin Oncol, 2004. **22**(23): p. 4717-24.
82. Weng, W.K. and R. Levy, *Two immunoglobulin G fragment C receptor polymorphisms independently predict response to rituximab in patients with follicular lymphoma*. J Clin Oncol, 2003. **21**(21): p. 3940-7.
83. Cartron, G., et al., *Therapeutic activity of humanized anti-CD20 monoclonal antibody and polymorphism in IgG Fc receptor FcgammaRIIIa gene*. Blood, 2002. **99**(3): p. 754-8.
84. Selenko, N., et al., *Cross-priming of cytotoxic T cells promoted by apoptosis-inducing tumor cell reactive antibodies?* J Clin Immunol, 2002. **22**(3): p. 124-30.
85. van Meerten, T. and A. Hagenbeek, *CD20-targeted therapy: a breakthrough in the treatment of non-Hodgkin's lymphoma*. Neth J Med, 2009. **67**(7): p. 251-9.
86. Peipp, M. and T. Valerius, *Bispecific antibodies targeting cancer cells*. Biochem Soc Trans, 2002. **30**(4): p. 507-11.
87. Molhoj, M., et al., *CD19-/CD3-bispecific antibody of the BiTE class is far superior to tandem diabody with respect to redirected tumor cell lysis*. Mol Immunol, 2007. **44**(8): p. 1935-43.
88. Lee, S.T., et al., *BiovaxID: a personalized therapeutic cancer vaccine for non-Hodgkin's lymphoma*. Expert Opin Biol Ther, 2007. **7**(1): p. 113-22.
89. Stanley, M., *Prevention strategies against the human papillomavirus: the effectiveness of vaccination*. Gynecol Oncol, 2007. **107**(2 Suppl 1): p. S19-23.
90. Lowy, D.R. and J.T. Schiller, *Prophylactic human papillomavirus vaccines*. J Clin Invest, 2006. **116**(5): p. 1167-73.
91. Stevenson, F.K., J. Rice, and D. Zhu, *Tumor vaccines*. Adv Immunol, 2004. **82**: p. 49-103.
92. Srinivasan, R. and J.D. Wolchok, *Tumor antigens for cancer immunotherapy: therapeutic potential of xenogeneic DNA vaccines*. J Transl Med, 2004. **2**(1): p. 12.
93. Robbins, P.F., et al., *A mutated beta-catenin gene encodes a melanoma-specific antigen recognized by tumor infiltrating lymphocytes*. J Exp Med, 1996. **183**(3): p. 1185-92.
94. Wang, R.F., et al., *Cloning genes encoding MHC class II-restricted antigens: mutated CDC27 as a tumor antigen*. Science, 1999. **284**(5418): p. 1351-4.

95. Rosenberg, S.A., et al., *Identification of the genes encoding cancer antigens: implications for cancer immunotherapy*. Adv Cancer Res, 1996. **70**: p. 145-77.
96. Clynes, R.A., et al., *Inhibitory Fc receptors modulate in vivo cytotoxicity against tumor targets*. Nat Med, 2000. **6**(4): p. 443-6.
97. Wang, R.F., *Human tumor antigens: implications for cancer vaccine development*. J Mol Med, 1999. **77**(9): p. 640-55.
98. Boon, T., et al., *Tumor antigens recognized by T lymphocytes*. Annu Rev Immunol, 1994. **12**: p. 337-65.
99. Van den Eynde, B.J. and P. van der Bruggen, *T cell defined tumor antigens*. Curr Opin Immunol, 1997. **9**(5): p. 684-93.
100. Guinn, B.A., et al., *Humoral detection of leukaemia-associated antigens in presentation acute myeloid leukaemia*. Biochem Biophys Res Commun, 2005. **335**(4): p. 1293-304.
101. Cooper, C.D., et al., *PASDI, a DLBCL-associated cancer testis antigen and candidate for lymphoma immunotherapy*. Leukemia, 2006. **20**(12): p. 2172-4.
102. Sahota, S.S., et al., *PASDI is a potential multiple myeloma-associated antigen*. Blood, 2006. **108**(12): p. 3953-5.
103. Magarian-Blander, J., et al., *Intercellular and intracellular events following the MHC-unrestricted TCR recognition of a tumor-specific peptide epitope on the epithelial antigen MUC1*. J Immunol, 1998. **160**(7): p. 3111-20.
104. Galon, J., et al., *Type, density, and location of immune cells within human colorectal tumors predict clinical outcome*. Science, 2006. **313**(5795): p. 1960-4.
105. Laghi, L., et al., *CD3+ cells at the invasive margin of deeply invading (pT3-T4) colorectal cancer and risk of post-surgical metastasis: a longitudinal study*. Lancet Oncol, 2009. **10**(9): p. 877-84.
106. Swann, J.B. and M.J. Smyth, *Immune surveillance of tumors*. J Clin Invest, 2007. **117**(5): p. 1137-46.
107. Dougan, M. and G. Dranoff, *Immune therapy for cancer*. Annu Rev Immunol, 2009. **27**: p. 83-117.
108. Curiel, T.J., *Tregs and rethinking cancer immunotherapy*. J Clin Invest, 2007. **117**(5): p. 1167-74.
109. Campoli, M., C.C. Chang, and S. Ferrone, *HLA class I antigen loss, tumor immune escape and immune selection*. Vaccine, 2002. **20 Suppl 4**: p. A40-5.
110. Frey, A.B. and N. Monu, *Signaling defects in anti-tumor T cells*. Immunol Rev, 2008. **222**: p. 192-205.
111. Serafini, P., I. Borrello, and V. Bronte, *Myeloid suppressor cells in cancer: recruitment, phenotype, properties, and mechanisms of immune suppression*. Semin Cancer Biol, 2006. **16**(1): p. 53-65.
112. Marigo, I., et al., *Tumor-induced tolerance and immune suppression by myeloid derived suppressor cells*. Immunol Rev, 2008. **222**: p. 162-79.
113. Maloney, D.G., et al., *Phase I clinical trial using escalating single-dose infusion of chimeric anti-CD20 monoclonal antibody (IDEC-C2B8) in patients with recurrent B-cell lymphoma*. Blood, 1994. **84**(8): p. 2457-66.
114. Yeon, C.H. and M.D. Pegram, *Anti-erbB-2 antibody trastuzumab in the treatment of HER2-amplified breast cancer*. Invest New Drugs, 2005. **23**(5): p. 391-409.
115. Hsu, F.J., et al., *Tumor-specific idiotype vaccines in the treatment of patients with B-cell lymphoma--long-term results of a clinical trial*. Blood, 1997. **89**(9): p. 3129-35.
116. Renard, V., et al., *HER-2 DNA and protein vaccines containing potent Th cell epitopes induce distinct protective and therapeutic antitumor responses in HER-2 transgenic mice*. J Immunol, 2003. **171**(3): p. 1588-95.
117. Bendandi, M., et al., *Complete molecular remissions induced by patient-specific vaccination plus granulocyte-monocyte colony-stimulating factor against lymphoma*. Nat Med, 1999. **5**(10): p. 1171-7.

118. Vuist, W.M., R. Levy, and D.G. Maloney, *Lymphoma regression induced by monoclonal anti-idiotypic antibodies correlates with their ability to induce Ig signal transduction and is not prevented by tumor expression of high levels of bcl-2 protein*. *Blood*, 1994. **83**(4): p. 899-906.
119. Zhu, D., et al., *Acquisition of potential N-glycosylation sites in the immunoglobulin variable region by somatic mutation is a distinctive feature of follicular lymphoma*. *Blood*, 2002. **99**(7): p. 2562-8.
120. Marchand, M., et al., *Tumor regressions observed in patients with metastatic melanoma treated with an antigenic peptide encoded by gene MAGE-3 and presented by HLA-A1*. *Int J Cancer*, 1999. **80**(2): p. 219-30.
121. van der Burg, S.H., et al., *Improved peptide vaccine strategies, creating synthetic artificial infections to maximize immune efficacy*. *Adv Drug Deliv Rev*, 2006. **58**(8): p. 916-30.
122. Petrovsky, N. and J.C. Aguilar, *Vaccine adjuvants: current state and future trends*. *Immunol Cell Biol*, 2004. **82**(5): p. 488-96.
123. Aguilar, J.C. and E.G. Rodriguez, *Vaccine adjuvants revisited*. *Vaccine*, 2007. **25**(19): p. 3752-62.
124. Schubert, C., *Illuminating alum*. *Nat Med*, 2009. **15**(9): p. 985.
125. Hamid, O., et al., *Alum with interleukin-12 augments immunity to a melanoma peptide vaccine: correlation with time to relapse in patients with resected high-risk disease*. *Clin Cancer Res*, 2007. **13**(1): p. 215-22.
126. Kool, M., et al., *Alum adjuvant boosts adaptive immunity by inducing uric acid and activating inflammatory dendritic cells*. *J Exp Med*, 2008. **205**(4): p. 869-82.
127. Martinon, F., et al., *Gout-associated uric acid crystals activate the NALP3 inflammasome*. *Nature*, 2006. **440**(7081): p. 237-41.
128. Eisenbarth, S.C., et al., *Crucial role for the Nalp3 inflammasome in the immunostimulatory properties of aluminium adjuvants*. *Nature*, 2008. **453**(7198): p. 1122-6.
129. De Gregorio, E., E. Tritto, and R. Rappuoli, *Alum adjuvant activity: unraveling a century old mystery*. *Eur J Immunol*, 2008. **38**(8): p. 2068-71.
130. Franchi, L. and G. Nunez, *The Nlrp3 inflammasome is critical for aluminium hydroxide-mediated IL-1beta secretion but dispensable for adjuvant activity*. *Eur J Immunol*, 2008. **38**(8): p. 2085-9.
131. McKee, A.S., et al., *Alum induces innate immune responses through macrophage and mast cell sensors, but these sensors are not required for alum to act as an adjuvant for specific immunity*. *J Immunol*, 2009. **183**(7): p. 4403-14.
132. Wang, F., et al., *Phase I trial of a MART-1 peptide vaccine with incomplete Freund's adjuvant for resected high-risk melanoma*. *Clin Cancer Res*, 1999. **5**(10): p. 2756-65.
133. Stills, H.F., Jr., *Adjuvants and antibody production: dispelling the myths associated with Freund's complete and other adjuvants*. *ILAR J*, 2005. **46**(3): p. 280-93.
134. Rice, J., C.H. Ottensmeier, and F.K. Stevenson, *DNA vaccines: precision tools for activating effective immunity against cancer*. *Nat Rev Cancer*, 2008. **8**(2): p. 108-20.
135. Stevenson, F.K., C.H. Ottensmeier, and J. Rice, *DNA vaccines against cancer come of age*. *Curr Opin Immunol*, 2010. **22**(2): p. 264-70.
136. Savelyeva, N., et al., *Plant viral genes in DNA idiotype vaccines activate linked CD4+ T-cell mediated immunity against B-cell malignancies*. *Nat Biotechnol*, 2001. **19**(8): p. 760-4.
137. Buchan, S., et al., *Electroporation as a "prime/boost" strategy for naked DNA vaccination against a tumor antigen*. *J Immunol*, 2005. **174**(10): p. 6292-8.
138. George, A.J., A.L. Tutt, and F.K. Stevenson, *Anti-idiotypic mechanisms involved in suppression of a mouse B cell lymphoma, BCL1*. *J Immunol*, 1987. **138**(2): p. 628-34.

139. Sugai, S., et al., *Protective and cellular immune responses to idiotypic determinants on cells from a spontaneous lymphoma of NZB-NZW F1 mice*. J Exp Med, 1974. **140**(6): p. 1547-58.
140. Campbell, M.J., et al., *Idiotype vaccination against murine B cell lymphoma. Humoral and cellular responses elicited by tumor-derived immunoglobulin M and its molecular subunits*. J Immunol, 1987. **139**(8): p. 2825-33.
141. Campbell, M.J., et al., *Idiotype vaccination against murine B cell lymphoma. Humoral and cellular requirements for the full expression of antitumor immunity*. J Immunol, 1990. **145**(3): p. 1029-36.
142. Kaminski, M.S., et al., *Idiotype vaccination against murine B cell lymphoma. Inhibition of tumor immunity by free idiotype protein*. J Immunol, 1987. **138**(4): p. 1289-96.
143. George, A.J., et al., *Idiotypic vaccination as a treatment for a B cell lymphoma*. J Immunol, 1988. **141**(6): p. 2168-74.
144. Houot, R. and R. Levy, *Vaccines for lymphomas: idiotype vaccines and beyond*. Blood Rev, 2009. **23**(3): p. 137-42.
145. Savelyeva, N., et al., *Inhibition of a vaccine-induced anti-tumor B cell response by soluble protein antigen in the absence of continuing T cell help*. Proc Natl Acad Sci U S A, 2005. **102**(31): p. 10987-92.
146. McCormick, A.A., et al., *Plant-produced idiotype vaccines for the treatment of non-Hodgkin's lymphoma: safety and immunogenicity in a phase I clinical study*. Proc Natl Acad Sci U S A, 2008. **105**(29): p. 10131-6.
147. de Cerio, A.L. and S. Inoges, *Future of idiotypic vaccination for B-cell lymphoma*. Expert Rev Vaccines, 2009. **8**(1): p. 43-50.
148. Ai, W.Z., et al., *Anti-idiotype antibody response after vaccination correlates with better overall survival in follicular lymphoma*. Blood, 2009. **113**(23): p. 5743-6.
149. Porta, C. and G.P. Lomonosoff, *Scope for using plant viruses to present epitopes from animal pathogens*. Rev Med Virol, 1998. **8**(1): p. 25-41.
150. Lacasse, P., et al., *Novel plant virus-based vaccine induces protective cytotoxic T-lymphocyte-mediated antiviral immunity through dendritic cell maturation*. J Virol, 2008. **82**(2): p. 785-94.
151. McCormick, A.A., et al., *TMV-peptide fusion vaccines induce cell-mediated immune responses and tumor protection in two murine models*. Vaccine, 2006. **24**(40-41): p. 6414-23.
152. McCormick, A.A., et al., *Chemical conjugate TMV-peptide bivalent fusion vaccines improve cellular immunity and tumor protection*. Bioconjug Chem, 2006. **17**(5): p. 1330-8.
153. Takamatsu, N., et al., *Production of enkephalin in tobacco protoplasts using tobacco mosaic virus RNA vector*. FEBS Lett, 1990. **269**(1): p. 73-6.
154. Fitchen, J., R.N. Beachy, and M.B. Hein, *Plant virus expressing hybrid coat protein with added murine epitope elicits autoantibody response*. Vaccine, 1995. **13**(12): p. 1051-7.
155. Koo, M., et al., *Protective immunity against murine hepatitis virus (MHV) induced by intranasal or subcutaneous administration of hybrids of tobacco mosaic virus that carries an MHV epitope*. Proc Natl Acad Sci U S A, 1999. **96**(14): p. 7774-9.
156. Brennan, F.R., T.D. Jones, and W.D. Hamilton, *Cowpea mosaic virus as a vaccine carrier of heterologous antigens*. Mol Biotechnol, 2001. **17**(1): p. 15-26.
157. Dalsgaard, K., et al., *Plant-derived vaccine protects target animals against a viral disease*. Nat Biotechnol, 1997. **15**(3): p. 248-52.
158. Langeveld, J.P., et al., *Inactivated recombinant plant virus protects dogs from a lethal challenge with canine parvovirus*. Vaccine, 2001. **19**(27): p. 3661-70.
159. Nicholas, B.L., et al., *Characterization of the immune response to canine parvovirus induced by vaccination with chimaeric plant viruses*. Vaccine, 2002. **20**(21-22): p. 2727-34.

160. Brennan, F.R., et al., *Immunogenicity of peptides derived from a fibronectin-binding protein of S. aureus expressed on two different plant viruses*. Vaccine, 1999. **17**(15-16): p. 1846-57.
161. Buchen-Osmond, C. *International committee on taxonomy of viruses*. <http://www.ncbi.nlm.nih.gov/ICTVdb/index.htm> 2002.
162. Huisman, M.J., et al., *The complete nucleotide sequence of potato virus X and its homologies at the amino acid level with various plus-stranded RNA viruses*. J Gen Virol, 1988. **69** ( Pt 8): p. 1789-98.
163. Baratova, L.A., et al., *The topography of the surface of potato virus X: tritium planigraphy and immunological analysis*. J Gen Virol, 1992. **73** ( Pt 2): p. 229-35.
164. Lecours, K., et al., *Purification and biochemical characterization of a monomeric form of papaya mosaic potexvirus coat protein*. Protein Expr Purif, 2006. **47**(1): p. 273-80.
165. Tremblay, M.H., et al., *Effect of mutations K97A and E128A on RNA binding and self assembly of papaya mosaic potexvirus coat protein*. FEBS J, 2006. **273**(1): p. 14-25.
166. Donnelly, M.L., et al., *Analysis of the aphthovirus 2A/2B polyprotein 'cleavage' mechanism indicates not a proteolytic reaction, but a novel translational effect: a putative ribosomal 'skip'*. J Gen Virol, 2001. **82**(Pt 5): p. 1013-25.
167. Cruz, S.S., et al., *Assembly and movement of a plant virus carrying a green fluorescent protein overcoat*. Proc Natl Acad Sci U S A, 1996. **93**(13): p. 6286-90.
168. O'Brien, G.J., et al., *Rotavirus VP6 expressed by PVX vectors in Nicotiana benthamiana coats PVX rods and also assembles into viruslike particles*. Virology, 2000. **270**(2): p. 444-53.
169. Smolenska, L., et al., *Production of a functional single chain antibody attached to the surface of a plant virus*. FEBS Lett, 1998. **441**(3): p. 379-82.
170. Marusic, C., et al., *Chimeric plant virus particles as immunogens for inducing murine and human immune responses against human immunodeficiency virus type 1*. J Virol, 2001. **75**(18): p. 8434-9.
171. Uhde, K., R. Fischer, and U. Commandeur, *Expression of multiple foreign epitopes presented as synthetic antigens on the surface of Potato virus X particles*. Arch Virol, 2005. **150**(2): p. 327-40.
172. Lico, C., et al., *Plant-produced potato virus X chimeric particles displaying an influenza virus-derived peptide activate specific CD8+ T cells in mice*. Vaccine, 2009. **27**(37): p. 5069-76.
173. Fischer, R. and N. Emans, *Molecular farming of pharmaceutical proteins*. Transgenic Res, 2000. **9**(4-5): p. 279-99; discussion 277.
174. Yin, J., et al., *Select what you need: a comparative evaluation of the advantages and limitations of frequently used expression systems for foreign genes*. J Biotechnol, 2007. **127**(3): p. 335-47.
175. Ko, K. and H. Koprowski, *Plant biopharming of monoclonal antibodies*. Virus Res, 2005. **111**(1): p. 93-100.
176. Mechtcheriakova, I.A., et al., *The use of viral vectors to produce hepatitis B virus core particles in plants*. J Virol Methods, 2006. **131**(1): p. 10-5.
177. Ma, J.K., et al., *Antibody processing and engineering in plants, and new strategies for vaccine production*. Vaccine, 2005. **23**(15): p. 1814-8.
178. Yusibov, V., et al., *The potential of plant virus vectors for vaccine production*. Drugs R D, 2006. **7**(4): p. 203-17.
179. Lico, C., Q. Chen, and L. Santi, *Viral vectors for production of recombinant proteins in plants*. J Cell Physiol, 2008. **216**(2): p. 366-77.
180. Giritch, A., et al., *Rapid high-yield expression of full-size IgG antibodies in plants coinfecting with noncompeting viral vectors*. Proc Natl Acad Sci U S A, 2006. **103**(40): p. 14701-6.

181. Liu, L., et al., *Cowpea mosaic virus-based systems for the production of antigens and antibodies in plants*. Vaccine, 2005. **23**(15): p. 1788-92.
182. Sainsbury, F. and G.P. Lomonossoff, *Extremely high-level and rapid transient protein production in plants without the use of viral replication*. Plant Physiol, 2008. **148**(3): p. 1212-8.
183. Franconi, R., et al., *Plant-derived human papillomavirus 16 E7 oncoprotein induces immune response and specific tumor protection*. Cancer Res, 2002. **62**(13): p. 3654-8.
184. Alamillo, J.M., et al., *Use of virus vectors for the expression in plants of active full-length and single chain anti-coronavirus antibodies*. Biotechnol J, 2006. **1**(10): p. 1103-11.
185. McCormick, A.A., et al., *Rapid production of specific vaccines for lymphoma by expression of the tumor-derived single-chain Fv epitopes in tobacco plants*. Proc Natl Acad Sci U S A, 1999. **96**(2): p. 703-8.
186. Wigdorovitz, A., et al., *Protection of mice against challenge with foot and mouth disease virus (FMDV) by immunization with foliar extracts from plants infected with recombinant tobacco mosaic virus expressing the FMDV structural protein VP1*. Virology, 1999. **264**(1): p. 85-91.
187. Krebitz, M., et al., *Rapid production of the major birch pollen allergen Bet v 1 in Nicotiana benthamiana plants and its immunological in vitro and in vivo characterization*. FASEB J, 2000. **14**(10): p. 1279-88.
188. Santi, L., et al., *An efficient plant viral expression system generating orally immunogenic Norwalk virus-like particles*. Vaccine, 2008. **26**(15): p. 1846-54.
189. Kohl, T., et al., *Plant-produced cottontail rabbit papillomavirus L1 protein protects against tumor challenge: a proof-of-concept study*. Clin Vaccine Immunol, 2006. **13**(8): p. 845-53.
190. Webster, D.E., et al., *Production and characterization of an orally immunogenic Plasmodium antigen in plants using a virus-based expression system*. Plant Biotechnol J, 2009. **7**(9): p. 846-55.
191. McCormick, A.A., et al., *Individualized human scFv vaccines produced in plants: humoral anti-idiotypic responses in vaccinated mice confirm relevance to the tumor Ig*. J Immunol Methods, 2003. **278**(1-2): p. 95-104.
192. Roggero, P., et al., *The expression of a single-chain Fv antibody fragment in different plant hosts and tissues by using Potato virus X as a vector*. Protein Expr Purif, 2001. **22**(1): p. 70-4.
193. Zelada, A.M., et al., *Expression of tuberculosis antigen ESAT-6 in Nicotiana tabacum using a potato virus X-based vector*. Tuberculosis (Edinb), 2006. **86**(3-4): p. 263-7.
194. Sainsbury, F., E.C. Thuenemann, and G.P. Lomonossoff, *pEAQ: versatile expression vectors for easy and quick transient expression of heterologous proteins in plants*. Plant Biotechnol J, 2009. **7**(7): p. 682-93.
195. Krolick, K.A., et al., *Murine B cell leukemia (BCL1): organ distribution and kinetics of growth as determined by fluorescence analysis with an anti-idiotypic antibody*. J Immunol, 1979. **123**(5): p. 1928-35.
196. Muirhead, M.J., et al., *BCL1, a murine model of prolymphocytic leukemia. I. Effect of splenectomy on growth kinetics and organ distribution*. Am J Pathol, 1981. **105**(3): p. 295-305.
197. Knapp, M.R., et al., *Characterization of a spontaneous murine B cell leukemia (BCL1). I. Cell surface expression of IgM, IgD, Ia, and FcR*. J Immunol, 1979. **123**(3): p. 992-9.
198. Krolick, K.A., et al., *In vivo therapy of a murine B cell tumor (BCL1) using antibody-ricin A chain immunotoxins*. J Exp Med, 1982. **155**(6): p. 1797-809.

199. Tutt, A.L., et al., *Monoclonal antibody therapy of B cell lymphoma: signaling activity on tumor cells appears more important than recruitment of effectors*. J Immunol, 1998. **161**(6): p. 3176-85.
200. Hawkins, R.E., et al., *Idiotypic vaccination against human B-cell lymphoma. Rescue of variable region gene sequences from biopsy material for assembly as single-chain Fv personal vaccines*. Blood, 1994. **83**(11): p. 3279-88.
201. King, C.A., et al., *DNA vaccines with single-chain Fv fused to fragment C of tetanus toxin induce protective immunity against lymphoma and myeloma*. Nat Med, 1998. **4**(11): p. 1281-6.
202. Benvenuti, F., O.R. Burrone, and D.G. Efremov, *Anti-idiotypic DNA vaccines for lymphoma immunotherapy require the presence of both variable region genes for tumor protection*. Gene Ther, 2000. **7**(7): p. 605-11.
203. Cesco-Gaspere, M., F. Benvenuti, and O.R. Burrone, *BCL1 lymphoma protection induced by idio type DNA vaccination is entirely dependent on anti-idiotypic antibodies*. Cancer Immunol Immunother, 2005. **54**(4): p. 351-8.
204. Canizares, M.C., et al., *A bipartite system for the constitutive and inducible expression of high levels of foreign proteins in plants*. Plant Biotechnol J, 2006. **4**(2): p. 183-93.
205. Valentine, L., *Agrobacterium tumefaciens and the plant: the David and Goliath of modern genetics*. Plant Physiol, 2003. **133**(3): p. 948-55.
206. Gelvin, S.B., *Agricultural biotechnology: gene exchange by design*. Nature, 2005. **433**(7026): p. 583-4.
207. Lee, L.Y. and S.B. Gelvin, *T-DNA binary vectors and systems*. Plant Physiol, 2008. **146**(2): p. 325-32.
208. Hellens, R., P. Mullineaux, and H. Klee, *Technical Focus: a guide to Agrobacterium binary Ti vectors*. Trends Plant Sci, 2000. **5**(10): p. 446-51.
209. Philo, J.S., *Is any measurement method optimal for all aggregate sizes and types?* AAPS J, 2006. **8**(3): p. E564-71.
210. Verchot-Lubicz, J., C.M. Ye, and D. Bamunusinghe, *Molecular biology of potexviruses: recent advances*. J Gen Virol, 2007. **88**(Pt 6): p. 1643-55.
211. Vitale, A. and E. Pedrazzini, *Recombinant pharmaceuticals from plants: the plant endomembrane system as bioreactor*. Mol Interv, 2005. **5**(4): p. 216-25.
212. Frigerio, L., et al., *Assembly, secretion, and vacuolar delivery of a hybrid immunoglobulin in plants*. Plant Physiol, 2000. **123**(4): p. 1483-94.
213. Ko, K., et al., *Function and glycosylation of plant-derived antiviral monoclonal antibody*. Proc Natl Acad Sci U S A, 2003. **100**(13): p. 8013-8.
214. Ricker, R.D. and L.A. Sandoval, *Fast, reproducible size-exclusion chromatography of biological macromolecules*. J Chromatogr A, 1996. **743**(1): p. 43-50.
215. Finkelman, F.D., et al., *Lymphokine control of in vivo immunoglobulin isotype selection*. Annu Rev Immunol, 1990. **8**: p. 303-33.
216. Stavnezer, J., *Regulation of antibody production and class switching by TGF-beta*. J Immunol, 1995. **155**(4): p. 1647-51.
217. Mosmann, T.R. and R.L. Coffman, *TH1 and TH2 cells: different patterns of lymphokine secretion lead to different functional properties*. Annu Rev Immunol, 1989. **7**: p. 145-73.
218. Brewer, J.M., et al., *Neither interleukin-6 nor signalling via tumour necrosis factor receptor-1 contribute to the adjuvant activity of Alum and Freund's adjuvant*. Immunology, 1998. **93**(1): p. 41-8.
219. Brewer, J.M., et al., *Aluminium hydroxide adjuvant initiates strong antigen-specific Th2 responses in the absence of IL-4- or IL-13-mediated signaling*. J Immunol, 1999. **163**(12): p. 6448-54.
220. Nimmerjahn, F. and J.V. Ravetch, *Divergent immunoglobulin g subclass activity through selective Fc receptor binding*. Science, 2005. **310**(5753): p. 1510-2.

221. Saint-Jore-Dupas, C., L. Faye, and V. Gomord, *From planta to pharma with glycosylation in the toolbox*. Trends Biotechnol, 2007. **25**(7): p. 317-23.
222. McCann, K.J., et al., *Remarkable selective glycosylation of the immunoglobulin variable region in follicular lymphoma*. Mol Immunol, 2008. **45**(6): p. 1567-72.
223. Gupta, R., Jung, E., Brunak, S. *Prediction of N-glycosylation site in human proteins*. 2004; Available from: <http://www.cbs.dtu.dk/services/NetNGlyc/>.
224. Acosta-Ramirez, E., et al., *Translating innate response into long-lasting antibody response by the intrinsic antigen-adjuvant properties of papaya mosaic virus*. Immunology, 2008. **124**(2): p. 186-97.
225. Iwasaki, A. and R. Medzhitov, *Toll-like receptor control of the adaptive immune responses*. Nat Immunol, 2004. **5**(10): p. 987-95.
226. Trinchieri, G., *Interleukin-12 and the regulation of innate resistance and adaptive immunity*. Nat Rev Immunol, 2003. **3**(2): p. 133-46.
227. Banchereau, J. and R.M. Steinman, *Dendritic cells and the control of immunity*. Nature, 1998. **392**(6673): p. 245-52.
228. Redecke, V., et al., *Cutting edge: activation of Toll-like receptor 2 induces a Th2 immune response and promotes experimental asthma*. J Immunol, 2004. **172**(5): p. 2739-43.
229. Agrawal, S., et al., *Cutting edge: different Toll-like receptor agonists instruct dendritic cells to induce distinct Th responses via differential modulation of extracellular signal-regulated kinase-mitogen-activated protein kinase and c-Fos*. J Immunol, 2003. **171**(10): p. 4984-9.
230. Eisenbarth, S.C., et al., *Lipopolysaccharide-enhanced, toll-like receptor 4-dependent T helper cell type 2 responses to inhaled antigen*. J Exp Med, 2002. **196**(12): p. 1645-51.
231. Wu, L. and Y.J. Liu, *Development of dendritic-cell lineages*. Immunity, 2007. **26**(6): p. 741-50.
232. Wu, L. and A. Dakic, *Development of dendritic cell system*. Cell Mol Immunol, 2004. **1**(2): p. 112-8.
233. Liu, Y.J., *Dendritic cell subsets and lineages, and their functions in innate and adaptive immunity*. Cell, 2001. **106**(3): p. 259-62.
234. O'Keeffe, M., et al., *Mouse plasmacytoid cells: long-lived cells, heterogeneous in surface phenotype and function, that differentiate into CD8(+) dendritic cells only after microbial stimulus*. J Exp Med, 2002. **196**(10): p. 1307-19.
235. Nakano, H., M. Yanagita, and M.D. Gunn, *CD11c(+)B220(+)Gr-1(+) cells in mouse lymph nodes and spleen display characteristics of plasmacytoid dendritic cells*. J Exp Med, 2001. **194**(8): p. 1171-8.
236. Asselin-Paturel, C., et al., *Mouse type I IFN-producing cells are immature APCs with plasmacytoid morphology*. Nat Immunol, 2001. **2**(12): p. 1144-50.
237. Bjorck, P., *Isolation and characterization of plasmacytoid dendritic cells from Flt3 ligand and granulocyte-macrophage colony-stimulating factor-treated mice*. Blood, 2001. **98**(13): p. 3520-6.
238. Hochrein, H., M. O'Keeffe, and H. Wagner, *Human and mouse plasmacytoid dendritic cells*. Hum Immunol, 2002. **63**(12): p. 1103-10.
239. Taieb, J., et al., *A novel dendritic cell subset involved in tumor immunosurveillance*. Nat Med, 2006. **12**(2): p. 214-9.
240. Chan, C.W., et al., *Interferon-producing killer dendritic cells provide a link between innate and adaptive immunity*. Nat Med, 2006. **12**(2): p. 207-13.
241. Hemmi, H., et al., *The roles of Toll-like receptor 9, MyD88, and DNA-dependent protein kinase catalytic subunit in the effects of two distinct CpG DNAs on dendritic cell subsets*. J Immunol, 2003. **170**(6): p. 3059-64.
242. Chackerian, B., M.R. Durfee, and J.T. Schiller, *Virus-like display of a neo-self antigen reverses B cell anergy in a B cell receptor transgenic mouse model*. J Immunol, 2008. **180**(9): p. 5816-25.

243. Steinmetz, N.F., et al., *Potato virus X as a novel platform for potential biomedical applications*. Nano Lett, 2010. **10**(1): p. 305-12.
244. Nemykh, M.A., et al., *One more probable structural transition in potato virus X virions and a revised model of the virus coat protein structure*. Virology, 2008. **373**(1): p. 61-71.
245. Baratova, L.A., et al., *N-Terminal segment of potato virus X coat protein subunits is glycosylated and mediates formation of a bound water shell on the virion surface*. Eur J Biochem, 2004. **271**(15): p. 3136-45.
246. Walkey, D.G.A., *Applied plant virology*.-2nd ed. Second ed. 1991, London: Chapman and Hall.
247. Jin, P., et al., *Molecular signatures of maturing dendritic cells: implications for testing the quality of dendritic cell therapies*. J Transl Med, 2010. **8**: p. 4.
248. Neves, B.M., et al., *Differential roles of PI3-Kinase, MAPKs and NF-kappaB on the manipulation of dendritic cell T(h)1/T(h)2 cytokine/chemokine polarizing profile*. Mol Immunol, 2009. **46**(13): p. 2481-92.
249. Chen, Z., et al., *Analysis of the gene expression profiles of immature versus mature bone marrow-derived dendritic cells using DNA arrays*. Biochem Biophys Res Commun, 2002. **290**(1): p. 66-72.
250. Dintzis, H.M., R.Z. Dintzis, and B. Vogelstein, *Molecular determinants of immunogenicity: the immunon model of immune response*. Proc Natl Acad Sci U S A, 1976. **73**(10): p. 3671-5.
251. Sominskaya, I., et al., *Construction and immunological evaluation of multivalent hepatitis B virus (HBV) core virus-like particles carrying HBV and HCV epitopes*. Clin Vaccine Immunol, 2010. **17**(6): p. 1027-33.
252. Jagu, S., et al., *Vaccination with multimeric L2 fusion protein and LI VLP or capsomeres to broaden protection against HPV infection*. Vaccine, 2010.
253. Schiller, J.T. and D.R. Lowy, *Papillomavirus-like particle vaccines*. J Natl Cancer Inst Monogr, 2001(28): p. 50-4.
254. Schwarz, K., et al., *Role of Toll-like receptors in costimulating cytotoxic T cell responses*. Eur J Immunol, 2003. **33**(6): p. 1465-70.
255. Lund, J.M., et al., *Recognition of single-stranded RNA viruses by Toll-like receptor 7*. Proc Natl Acad Sci U S A, 2004. **101**(15): p. 5598-603.
256. Yan, M., et al., *Activation of dendritic cells by human papillomavirus-like particles through TLR4 and NF-kappaB-mediated signalling, moderated by TGF-beta*. Immunol Cell Biol, 2005. **83**(1): p. 83-91.
257. Kwak, L.W., et al., *Vaccination with syngeneic, lymphoma-derived immunoglobulin idiotype combined with granulocyte/macrophage colony-stimulating factor primes mice for a protective T-cell response*. Proc Natl Acad Sci U S A, 1996. **93**(20): p. 10972-7.
258. Salek-Ardakani, S., et al., *Preferential use of B7.2 and not B7.1 in priming of vaccinia virus-specific CD8 T cells*. J Immunol, 2009. **182**(5): p. 2909-18.
259. Zhou, X.-F., Peng-Da Ma, Ren-Hou Wang, Bo Liu and Xing-Zhi Wang, *A Novel Approach to Functional Analysis of the Ribulose Bisphosphate Carboxylase Small Subunit Gene by Agrobacterium-Mediated Gene silencing*. Journal of Integrative Plant Biology, 2006. **48**(10): p. 8.
260. Hull, R., *Matthews' Plant Virology*. 2004, London: Elsevier Academic Press.
261. Ryan, M.D. and J. Drew, *Foot-and-mouth disease virus 2A oligopeptide mediated cleavage of an artificial polyprotein*. EMBO J, 1994. **13**(4): p. 928-33.
262. Li, Q., et al., *Morphology and stability changes of recombinant TMV particles caused by a cysteine residue in the foreign peptide fused to the coat protein*. J Virol Methods, 2007. **140**(1-2): p. 212-7.
263. Xie, J., et al., *Antitumor effects of murine bone marrow-derived dendritic cells infected with xenogeneic livin alpha recombinant adenoviral vectors against Lewis lung carcinoma*. Lung Cancer, 2010. **68**(3): p. 338-45.

264. Youlin, K., Xiaodong, W., Xiuheng, L., Hengchen, Z., Zhiyuan, C., Batao, J., Hui, C., *Anti-tumor immune response induced by dendritic cells transduced with truncated PSMA IRES4-1BBL recombinant adenoviruses*. *Cancer Lett*, 2010. **293**: p. 9.
265. Wieckowski, E., et al., *Type-1 polarized dendritic cells loaded with apoptotic prostate cancer cells are potent inducers of CD8(+) T cells against prostate cancer cells and defined prostate cancer-specific epitopes*. *Prostate*, 2010.
266. Berzofsky, J.A., et al., *Progress on new vaccine strategies for the immunotherapy and prevention of cancer*. *J Clin Invest*, 2004. **113**(11): p. 1515-25.
267. Waldmann, T.A., *Effective cancer therapy through immunomodulation*. *Annu Rev Med*, 2006. **57**: p. 65-81.
268. Fraser, C.K., et al., *Inducing both cellular and humoral immunity following a rational prime-boost immunisation regimen incorporating recombinant ovine atadenovirus and fowlpox virus*. *Clin Vaccine Immunol*, 2010.
269. Sparrow, P.A., et al., *Pharma-Planta: road testing the developing regulatory guidelines for plant-made pharmaceuticals*. *Transgenic Res*, 2007. **16**(2): p. 147-61.
270. Ma, J.K., et al., *Plant-derived pharmaceuticals--the road forward*. *Trends Plant Sci*, 2005. **10**(12): p. 580-5.
271. Daniell, H., et al., *Plant-made vaccine antigens and biopharmaceuticals*. *Trends Plant Sci*, 2009. **14**(12): p. 669-79.
272. Bendandi, M., et al., *Rapid, high-yield production in plants of individualized idiotype vaccines for non-Hodgkin's lymphoma*. *Ann Oncol*, 2010.
273. Svajger, U., et al., *C-type lectin DC-SIGN: an adhesion, signalling and antigen-uptake molecule that guides dendritic cells in immunity*. *Cell Signal*, 2010. **22**(10): p. 1397-405.
274. He, L.Z., et al., *Antigenic targeting of the human mannose receptor induces tumor immunity*. *J Immunol*, 2007. **178**(10): p. 6259-67.
275. Gomord, V., et al., *Biopharmaceutical production in plants: problems, solutions and opportunities*. *Trends Biotechnol*, 2005. **23**(11): p. 559-65.
276. Oakes, F.R., et al., *The effect of captivity and diet on KLH isoform ratios in Megathura crenulata*. *Comp Biochem Physiol A Mol Integr Physiol*, 2004. **138**(2): p. 169-73.
277. Smith, M.L., et al., *Modified tobacco mosaic virus particles as scaffolds for display of protein antigens for vaccine applications*. *Virology*, 2006. **348**(2): p. 475-88.
278. Quaglino, E., et al., *A better immune reaction to ErbB-2 tumors is elicited in mice by DNA vaccines encoding rat/human chimeric proteins*. *Cancer Res*, 2010. **70**(7): p. 2604-12.
279. Aurisicchio, L., et al., *Treatment of mammary carcinomas in HER-2 transgenic mice through combination of genetic vaccine and an agonist of Toll-like receptor 9*. *Clin Cancer Res*, 2009. **15**(5): p. 1575-84.
280. KBP, K. 2008; Available from: <http://www.kbpllc.com/GENEWARE/tabid/86/Default.aspx>.